

INVESTIGATION OF
OXYGEN-RICH MATERIALS
AND
THE CRYSTAL STRUCTURE OF
ISOCYANIC ACID



Thomas Reith

DISSERTATION ZUR ERLANGUNG DES DOKTORGRADES
DER FAKULTÄT FÜR CHEMIE UND PHARMAZIE
DER LUDWIG-MAXIMILIANS-UNIVERSITÄT MÜNCHEN

INVESTIGATION OF
OXYGEN-RICH MATERIALS
AND
THE CRYSTAL STRUCTURE OF
ISOCYANIC ACID

Thomas Reith

aus Augsburg, Deutschland

2018

Erklärung

Diese Dissertation wurde im Sinne von § 7 der Promotionsordnung vom 28. November 2011 von Herrn Prof. Dr. Thomas M. Klapötke betreut.

EIDESSTATTLICHE VERSICHERUNG

Diese Dissertation wurde eigenständig und ohne unerlaubte Hilfe erarbeitet.

München, den 08.08.2018

Thomas Reith

Dissertation eingereicht am	24.05.2018
1. Gutachter:	Prof. Dr. Thomas M. Klapötke
2. Gutachter:	Prof. Dr. Konstantin Karaghiosoff
Mündliche Prüfung am	19.07.2018

MEINER GELIEBTEN FAMILIE

UND IM GEDENKEN

AN MEINE MUTTER

MARIA REITH

* 24.10.1960

† 29.03.2009

Danksagung

Mein Dank gilt anforderster Stelle meinem Doktorvater Herrn Prof. Dr. Thomas M. Klapötke für die Aufnahme in seinen Arbeitskreis, die interessante Themenstellung und das entgegebengebrachte Vertrauen, sowie die Unterstützung und Freiheiten meiner Forschungsarbeiten. Ein besonderer Dank gilt auch der uneingeschränkten finanziellen Unterstützung und die Möglichkeiten, meine Ergebnisse auf internationalen Konferenzen vorzustellen.

Herrn Prof. Dr. Konstantin Karaghiosoff danke ich für die freundliche Übernahme des Zweitgutachtens dieser Dissertation. Darüber hinaus gilt mein besonderer Dank der Einführung und Einarbeitung in die faszinierende Welt der Kristallographie, sowie seinem unerschütterlichen Optimismus.

Der Prüfungskommision, bestehend aus Herrn Prof. Dr. Thomas M. Klapötke, Herrn Prof. Dr. Konstantin Karaghiosoff, Herrn Prof. Dr. Franz Bracher, Herrn Prof. Dr. Wolfgang Beck, Herrn Prof. Dr. Jürgen Evers und Herrn Prof. Dr. Ingo-Peter Lorenz möchte ich für Ihre Zeit und die Bereitschaft zur Bildung der Kommision danken.

Herrn Dr. Burkhard Krumm danke ich für das schnelle und problemlose Messen von NMR Proben, sowie die fachkundige Hilfe beim Auswerten der NMR Spektren. Des Weiteren gilt mein Dank der fortwährenden Unterstützung und der akribischen Korrektur jeglicher Schriftstücke.

Herrn Dr. Jörg Stierstorfer gilt mein Dank für Hilfestellungen und Anregungen jeder Art sowie der teambildenden Maßnahmen für den Arbeitskreis unter welchen vor allem der Sieg der Campusmeisterschaft in Erinnerung bleiben wird.

Herrn Prof. Dr. Jürgen Evers danke ich für die Einarbeitung und die Hilfe im Zusammenhang mit der Strukturaufklärung der Isocyansäure, sowie seiner Begeisterung für die Wissenschaft und den vielen unterhaltsamen Geschichten rund um die Entwicklung der Chemie.

Frau Irene Scheckenbach und Ihrem berühmten Sinn für Organisatorisches gilt mein besonderer Dank. Die Unterstützung in bürokratischen Angelegenheiten, die allzeit gute Laune und der unerschütterliche Einsatz für das Tierwohl werden mir in Erinnerung bleiben.

Dr. Quirin J. Axthammer möchte ich besonders für die ansteckende Begeisterung für die Chemie der hochenergetischen Materialien und die Einführung in die Thematik und den Arbeitskreis danken.

Dem gesamten Arbeitskreis möchte ich für die stets positive und freundschaftliche Atmosphäre danken. Besonderer Dank gilt dabei meinen Laborkollegen aus D3.100, Dr. Quirin Axthammer, Dr. Regina Scharf, Dr. Carolin Pflüger, Cornelia C. Unger und Teresa Küblböck. Ebenso möchte ich mich bei der gesamten Prag-Truppe Johann Glück, Ivan Gospodinov, Marcel Holler, Cornelia Unger, Teresa Küblböck, Anne Friedrichs und meinem Suite-Partner Marc Bölter bedanken.

Im Besonderen möchte ich Cornelia C. Unger und Teresa Küblböck für die Korrektur dieser Arbeit und die enge Zusammenarbeit und Unterstützung im Labor danken. Durch den großartigen Rückhalt, die vielen fachlichen, weltanschaulichen und sonstigen Diskussionen, Metal- und Rockplaylists und einem unfassbaren Vorrat an Schokolade kann ich mir keine besseren Laborkollegen vorstellen.

Meinem Arbeitskreiskollegen Jörn Martens aus dem ersten Stock möchte ich für die vielen Problemlösungen in den Bereichen Kristallographie und IT, den interessanten und manchmal erschreckenden Anekdoten und den gemeinsamen Nächten beim Kristallmessen danken.

Ein besonderer Dank geht auch an meine Bacheloranden und Praktikanten Sebastian Schrader, Simon Graßl, Nicolas Müller, Fabian Heck und Florian Trauner, die alle mit viel Engagement einen erheblichen Beitrag zu dieser Arbeit geleistet haben.

Allen meinen Freunden, ob aus Egenhofen, dem Universitätsumfeld oder aus noch älteren Zeiten möchte ich für unerschütterliche Unterstützung und notwendige Ablenkung während all der Jahre danken.

Nicht zuletzt geht mein Dank an meine Familie, im Besonderen an meine Eltern Maria und Walter und meinen Bruder Michi, sowie meiner Partnerin Sarah, welche dieses Studium und diese Dissertation durch ihre unaufhörliche Unterstützung und Liebe erst ermöglicht haben. Vielen Dank für Alles!

TABLE OF CONTENTS

I General Introduction	1
1 Definition and Classification of Energetic Materials	1
2 Rocket Propellant Systems	4
3 New Oxidizers for Solid Rocket Propellants	6
4 Objective Target	11
5 References	13
II Summary and Conclusion	15
III Results and Discussion	27
1 Organic Nitrates Derived from TRIS	29
1.1 Abstract	30
1.2 Introduction	30
1.3 Results and Discussion	31
1.3.1 Synthesis	31
1.3.2 NMR and Vibrational Spectroscopy	32
1.3.3 Single Crystal Structure Analysis	33
1.3.4 Thermal Stabilities and Energetic Properties	39
1.4 Conclusion	42
1.5 Experimental Section	42
1.5.1 General Information	42
1.5.2 X-ray Crystallography	43
1.5.3 Computational Details	43
1.5.4 Synthesis	43
1.6 References	47
1.7 Supporting Information	49
2 Ionic Nitrates Derived from Dihydrazides	55
2.1 Abstract	56
2.2 Introduction	56
2.3 Results and Discussion	57
2.3.1 Synthesis	57
2.3.2 NMR Spectroscopy	58
2.3.3 Single Crystal Structure Analysis	59

2.3.4 Thermal Stabilities and Energetic Properties.....	63
2.4 Conclusion.....	65
2.5 Experimental Section.....	65
2.5.1 General Information.....	65
2.5.2 X-ray Crystallography.....	66
2.5.3 Computational Details.....	66
2.5.4 Synthesis.....	67
2.6 References.....	73
3 Polynitrocaramates Derived from Nitromethane.....	75
3.1 Abstract.....	76
3.2 Introduction.....	76
3.3 Results and Discussion.....	77
3.3.1 Synthesis.....	77
3.3.2 NMR Spectroscopy.....	78
3.3.3 Single Crystal Structure Analysis.....	80
3.3.4 Thermal Stabilities and Energetic Properties.....	85
3.4 Conclusion.....	87
3.5 Experimental Section.....	87
3.5.1 General Information.....	87
3.5.2 X-ray Crystallography.....	88
3.5.3 Computational Details.....	88
3.5.4 Synthesis.....	88
3.6 References.....	93
4 Silicon Analogues of Neo-Pentane Derivatives.....	95
4.1 Abstract.....	96
4.2 Introduction.....	96
4.3 Results and Discussion.....	97
4.3.1 Synthesis.....	97
4.3.2 NMR and Vibrational Spectroscopy.....	98
4.3.3 Single Crystal Structure Analysis.....	100
4.3.4 Thermal Stabilities and Energetic Properties.....	106
4.4 Conclusion.....	109
4.5 Experimental Section.....	110
4.5.1 General Information.....	110
4.5.2 X-ray Crystallography.....	110
4.5.3 Computational Details.....	111
4.5.4 Synthesis.....	111
4.6 References.....	118

5 N-Trinitroalkyl Substituted Azoles	121
5.1 Abstract	122
5.2 Introduction	122
5.3 Results and Discussion	123
5.3.1 Synthesis	123
5.3.2 NMR and Vibrational Spectroscopy	124
5.3.3 Single Crystal Structure Analysis	124
5.3.4 Thermal Stabilities and Energetic Properties	126
5.4 Conclusion	127
5.5 Experimental Section	128
5.5.1 General Information	128
5.5.2 X-ray Crystallography	128
5.5.3 Synthesis	129
5.6 References	131
5.7 Supporting Information	133
6 N-Dinitrated Oxamides	143
6.1 Abstract	144
6.2 Introduction	144
6.3 Results and Discussion	145
6.3.1 Synthesis	145
6.3.2 NMR and Vibrational Spectroscopy	147
6.3.3 Single Crystal Structure Analysis	149
6.3.4 Thermal Stabilities and Energetic Properties	150
6.4 Conclusion	152
6.5 Experimental Section	153
6.5.1 General Information	153
6.5.2 X-ray Crystallography	153
6.5.3 Computational Details	153
6.5.4 Synthesis	154
6.6 References	158
7 Molecular Structure of Isocyanic Acid	161
7.1 Abstract	162
7.2 Introduction	162
7.3 Experimental Section	163
7.3.1 General Information	163
7.3.2 X-ray Crystallography	163
7.3.3 Density Functional Theory (DFT) Calculations	164
7.4 Results and Discussion	165

7.4.1 X-Ray Diffraction Results.....	165
7.4.2 DFT Results.....	166
7.4.3 Group–Subgroup Relations.....	166
7.4.4 Crystal Chemical Properties.....	168
7.5 Conclusion.....	171
7.6 References.....	173
IV Appendix.....	175

I General Introduction

1 Definition and Classification of Energetic Materials

Energetic materials are commonly defined as compounds or mixtures of substances, which derive their energy from a chemical reaction. These materials contain both the fuel and the oxidizer and decompose readily under release of enormous volumes of gaseous products and large amounts of energy. Energetic materials do not need external reaction partners, and can be initiated by several means, such as thermal, mechanical or electrostatic ignition sources. Energetic materials can be classified into primary explosives, secondary explosives, propellants and pyrotechnics according to their energetic performance and purpose (Figure I.1). Next to these main branches several subgroups of energetic materials exist, like polymer-bonded explosives, sensitizers and energetic binders.^[1]

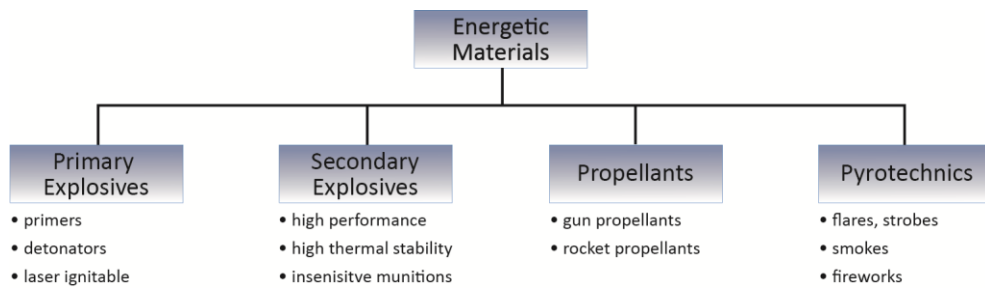


Figure I.1: Schematic classification of energetic materials.^[1]

Primary Explosives typically possess a high sensitivity towards mechanical, thermal or electrostatic stimulation, which allows for a feasible and reliable initiation. In combination with a fast deflagration to detonation transition, primary explosives develop a propagating shockwave to initiate less sensitive energetic materials, such as booster charges, main charges and propellants. Concerning the physical and energetic properties, the impact and friction sensitivity of primary explosives is usually less than 4 J and 10 N, respectively, and the detonation velocity ranges between 3500 and 5500 m s⁻¹. Typical representatives of this group are lead azide (LA) and lead styphnate (LS). However, these substances contain toxic heavy metal cations and therefore do not satisfy today's requirements. To avoid harm to human health and pollution of the surroundings, recent research of primary explosives focuses on more environmentally benign compounds. Some examples of these modern alternatives are the dipotassium salt of dinitraminobistetrazole (K₂DNABT) and the copper containing DBX-1 (Figure I.2).^[1-3]

I General Introduction

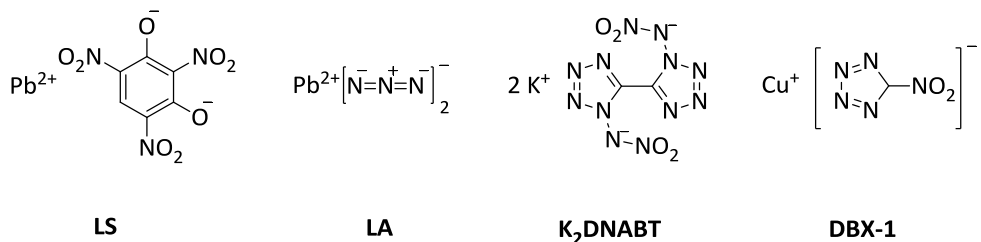


Figure I.2: Molecular structures of typical primary explosives: lead styphnate (LS), lead azide (LA), dipotassium 1,1'-dinitramino-5,5'-bistetrazolate (K₂DNABT) and copper(I) 5-nitrotetrazolate (DBX-1).

Secondary Explosives or High Explosives are generally less sensitive toward impact and friction compared to primary explosives, but also show significantly increased energetic performances concerning heat of explosion, detonation pressure and detonation velocity (approximately 7000–9500 m s⁻¹). In order to get initiated reasonably, they require the heat or shockwave generated by primary explosives. Modern secondary explosives are tailored to achieve for example higher performances, lower sensitivities or less environmental impact. At present, the most employed secondary explosives are the organic nitrate pentaerythritol tetranitrate (PETN) and the cyclic nitramines hexogen (RDX) and octogen (HMX). The next levels regarding the pure performance are highly condensed cage structures like CL-20 and octanitrocubane (ONC). These compounds show promising theoretical and experimental detonation values, however inefficient synthesis pathways and compatibility issues are major drawbacks at present. For highly thermal stable explosives, compounds like TATB and LLM-105 were designed decomposition temperatures over 350 °C; their stabilization is gained by a clever conjugation of nitro and amino groups. Currently the investigation of environmentally benign secondary explosives is a major objective, with the tetrazole based TKX-50 serving as popular example (Figure I.3).^[1, 4-5]

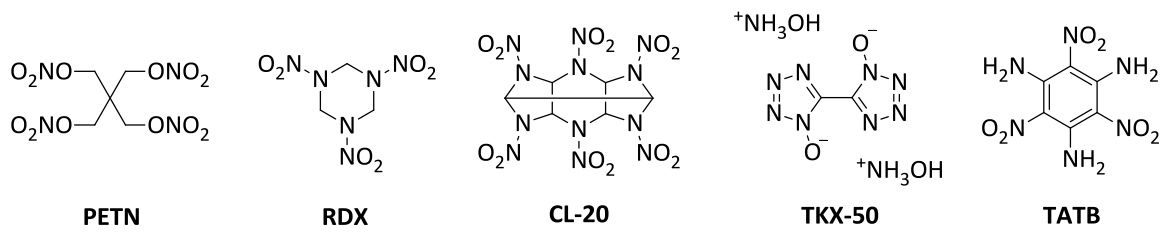


Figure I.3: Molecular structures of typical secondary explosives: pentaerythritol tetranitrate (PETN), hexogen (RDX), hexanitrohexaazaisowurtzitane (CL-20), bis(hydroxylammonium) 5,5'-bis(tetrazolate-1N-oxide) (TKX-50) and triaminotnitrobenzol (TATB).

Pyrotechnics in general are designed to produce a special effect such as heat, light, sound, gas or smoke as well as combinations of these. Usually, pyrotechnic mixtures consist of an oxidizer/fuel pair and several other additives to generate the intended effect. The field of application ranges from signal flares, smoke generators or delay compositions in the military sector to civilian-used night and daylight fireworks. The exothermal redox reaction in pyrotechnics is usually much slower compared to primary and secondary explosives. On the contrary to detonating secondary explosives, the purpose is a consistent burning behavior, which creates a continually effect over a specific period of time. Next to increasing the performance and operational capability, one important approach in pyrotechnics research is to create environmentally harmless compositions. One strategy for nontoxic pyrotechnics is the replacement of heavy metal-containing light emitters utilizing barium or strontium salts and further avoiding halogen depending systems. Therefore, greener alternatives are tested, such as lithium salts as atomic red emitters and substituting ammonium perchlorate with modern oxidizing agents (Figure I.4).^[6]

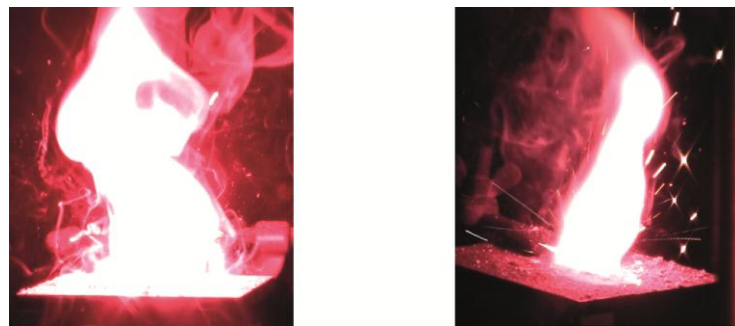


Figure I.4: Comparison of red flares containing harmful strontium and chlorinated materials (left) and environmentally benign composition featuring lithium and halogen-free substitutes (right).

Propellants characteristically show a controlled and smooth combustion behavior. Their main purpose is to transfer the enormous amount of hot gases produced by combustion into a predefined thrust. Propellants are distinguished into two major fields: gun propellants and rocket propellants. Gun propellants, or propellant charges, usually work with superior burning rates and higher pressures up to 4000 bar in the combustion chamber to accelerate projectiles. Depending on the task, gun propellants consist of single, double or triple base compositions. Starting from convenient nitrocellulose (NC) as main ingredient in single base propellants, the addition of nitroglycerin (NG) to form double base propellants enhances the energetic performance. Disadvantages of these mixtures, such as the heat induced erosion and possible appearances of muzzle flashes, can be suppressed by the addition of nitroguanidine (NQ, Figure I.5). These triple base

I General Introduction

propellants are inferior to double base propellants in terms of performance, but lower combustion temperatures and reduced material stress increase the repair interval drastically. This is particularly important for massive weapon systems like large caliber tanks and heavy NAVY canons. In contrast to gun propellants, which accelerate a separate projectile, the rocket propellants are part of the propulsion systems of missiles or rockets.^[1]

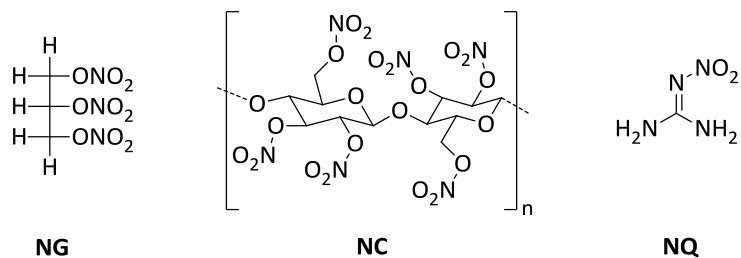


Figure I.5: Molecular structures of compounds in single, double and triple base gun propellants: nitroglycerin (NG), nitrocellulose (NC) and nitroguanidine (NQ).

2 Rocket Propellant Systems

The main purpose of rocket propellants is the acceleration of missiles or rockets. In rocket engines, the propulsion system generates enormous amounts of hot gases in the combustion chamber. These are ejected through a specifically designed nozzle in order to generate thrust, which accelerates the rocket or missile. To measure the effectiveness of different propellant compositions, the most important performance parameter is the specific impulse I_{sp} . It is defined as the change in the impulse delivered per mass unit of the consumed propellant m and can be expressed by the following equation:^[1]

$$I_{\text{sp}} = \frac{\bar{F} \times t_b}{m} \quad . \quad (1)$$

In this equation the impulse (force x time) is described as the average thrust \bar{F} multiplied with the combustion time t_b . The specific impulse is therefore directly connected to the generated thrust of a propulsion system and can be determined in case the propellant mass flow rate is known. The unit of the specific impulse is either " m s^{-1} " or "s", depending on whether the propellant's weight or mass is chosen, differing by the dimensioned constant of standard gravity of the earth g ($g_n = 9.81 \text{ m s}^{-2}$). Furthermore, the specific impulse is proportional to the square root of the ratio of the temperature in the combustion chamber T_c and the average molecular mass of the combustion products M :^[11]

$$I_{sp} \propto \sqrt{\frac{T_c}{M}} . \quad (2)$$

As a consequence satisfying specific impulses can be achieved with a high combustion temperature of the propellant composition or designing the average mass of the combustion products as low as possible. With regards to practical application, increasing the specific impulse by 20 s approximately doubles the maximum payload of a rocket or missile.^[1]

Present rocket propellant systems can be categorized into liquid and solid propellants. The liquid propellants may be further divided into mono- and bipropellants. Monopropellants are liquid endothermic substances, e.g. hydrazine or hydrogen peroxide, which are decomposed catalytically into gaseous products. Monopropellants usually can be stored for long periods, but their performance and the generated thrust is substandard. Bipropellants consist of two separately stored liquids, which are injected simultaneously in the combustion chamber. Usually one liquid acts as fuel and the second one is a potent oxidizer. If both liquids react spontaneously (reaction delay < 20 ms) the reaction mixture is labeled hypergolic. Most applied hypergolic mixtures consist of hydrazine derivatives as fuels which react with nitric acid or dinitrogen tetroxide. However, each of these substances is hazardous and toxic to the environment and human health. Alternatively, environmentally benign alternatives such as the combustion of liquid hydrogen with liquid oxygen require handling at very low temperatures, and therefore are called cryogenic systems. Despite these drawbacks, liquid propellants are generally capable of generating very high specific impulses and can be controlled conveniently.^[1]

Solid rocket propellant systems can be divided into the homogenous double-base propellants and the heterogeneous composite propellants. In accordance with gun propellants, double-base propellants for rocket engines consist of nitrocellulose and proportionate amounts of nitroglycerin. The heterogeneous composite propellants comprise a crystalline oxidizer, a metal-containing fuel and a polymeric binder. The crystalline oxidizer, most commonly ammonium perchlorate (AP), provides enough oxygen for the exhaustive combustion of the fuel and the binder. The fuel, usually aluminum, generates high amounts of heat by an extraordinary exothermic oxidation reaction. The polymeric binder is necessary to tailor the mechanical properties and supplementary acts as additional fuel. If required, several additives are added to the composite in form of specialized binders, catalysts or burn rate modifiers. To enhance the performance of solid rocket propellant systems, several variations and substitutions are under investigation.

I General Introduction

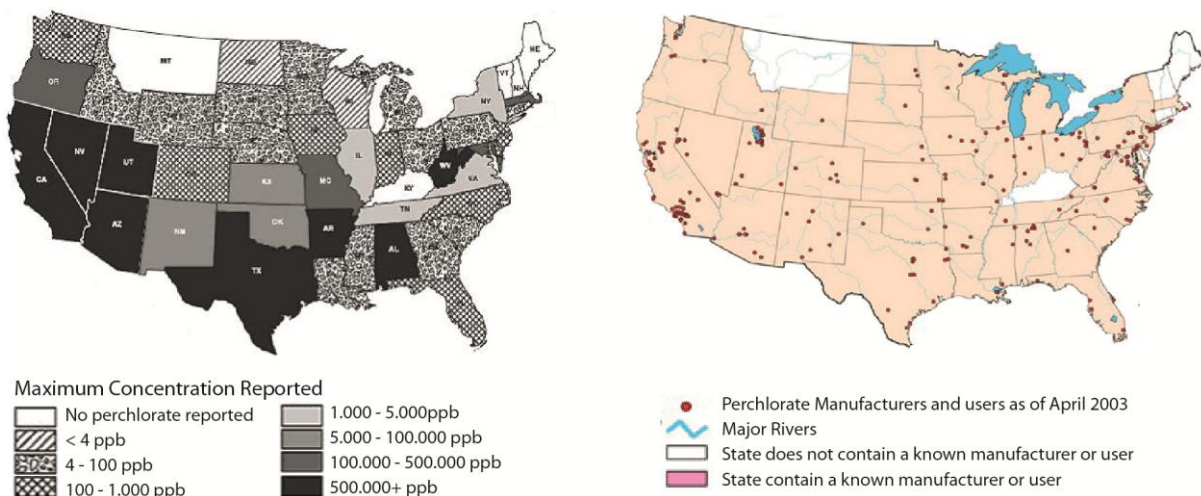
Alternative fuels, such as aluminum hydride AlH_3 or higher silanes (e.g. Si_5H_{10}), increase the calculated specific impulse significantly, but are more expensive and particularly more difficult to handle. Energetic binders, like the azide-containing GAP (Glycidyl Azide Polymer) or the nitrate-based poly-GLY (poly Glycidyl Nitrate), enhance the overall performance at the cost of higher expenses, compatibility problems and insufficient mechanical properties.^[1]

3 New Oxidizers for Solid Rocket Propellants

At present, essentially all solid propellant rocket boosters are based on ammonium perchlorate containing compositions. Regarding potential oxidizers, ammonium perchlorate has several advantages. Its production is simple and scalable with commercially accessible starting materials, it exhibits a very high oxygen balance and is resistant against mechanical stimuli. Further it is stable up to 240 °C and compatible with most propellant systems. Nevertheless, ammonium perchlorate features various hazardous drawbacks. Next to problems with slow cook-off tests^[7] resulting in cracks and cavities in the composite, and autocatalytic decomposition reactions at lower temperatures (150–300 °C),^[8] ammonium perchlorate has acute negative effects on the biotic and abiotic environment. During combustion, huge amounts of chlorinated combustion products, mainly hydrochloric acid, are ejected into the atmosphere provoking environmental issues and contribute to destruction of the ozone layer. Furthermore, the formation of hydrochloric acid generates visible and detectable expulsions leading to tactical disadvantages.^[1, 9]

However, the perchlorate anion itself is considerably the biggest concern. Its manifold application in munitions, pyrotechnics and automotive technologies in combination with the high solubility, chemical stability and persistence caused a widely distributed contamination of surface and ground water systems.^[10-11] Ammonium perchlorate is classified as a potential endocrine disruptive chemical, which interferes with the natural thyroid function on organism-level. The perchlorate anion is a potent inhibitor of the thyroid sodium iodide symporter, essentially blocking the iodine transport, eventually affecting the thyroid hormone synthesis. This is especially critical for normal growth and development in fetuses, children and young children. Furthermore, perchlorate is presumed to be mutagenic and carcinogenic as well as being toxic on repeated doses.^[1, 11-12]

For the United States alone, the cost for remediation of surface and ground water is estimated to be several billion dollars.^[10] Water supplies serving 5 to 17 million Americans contain perchlorates, while the critical levels of concentration seem to interfere with the distribution of perchlorate manufacturers (Figure I.6).^[10, 12-13] Consequently the US Environmental Protection Agency (EPA) developed nationwide rules limiting the amount of perchlorates allowed in drinking water, with a chronic oral reference dose of 0.7 µg per kilogram per day.^[11] Numerous states have established enforceable standards for drinking water concentration of perchlorates, such as Massachusetts with 2 µg L⁻¹. Following this action, EPA is announcing a public peer review meeting with independent experts. Gathering more information, the agency will take the next appropriate steps under the Safe Drinking Water Act.^[11, 14]



In 2006, the European Union established the REACH regulation (Registration, Evaluation, Authorization and Restriction of Chemicals). In order to evaluate the potential impact of chemical substances on both human health and the environment, REACH implemented several rules for the interaction with chemicals. Any chemical that is manufactured or imported in certain quantities or develops a certain hazardous potential has to be registered and will further be evaluated. Ammonium perchlorate is already registered since 2011 at REACH with an estimated annually production of 1000 t to 10000 t per year.^[15] Respecting the function of an endocrine disruptor, ammonium perchlorate was listed in the Community Rolling Action Plan (CoRAP) by the Public Activities Coordination Tool (PACT), which coordinates the evaluation of concerning substances.^[16-17] Ammonium perchlorate, together with sodium perchlorate, was thoroughly investigated by the member state Germany and the finished evaluation report was published in 2016.^[18]

I General Introduction

Ammonium perchlorate was originally selected to clarify concerns about the endocrine disruption in the environment, its wide dispersive use, and several harmful effects to human health, including endocrine disruption, carcinogenicity and thyroid toxicity. Even though the hazardous impact on the human health was not confirmed in the considered studies, the endocrine mode of action in the environment and its following adverse effects were definitely proven. In their final conclusion, the CoRAP report suggests follow up regulations at EU level. Based on the hazardous intrinsic properties of perchlorate, a SVHC (Substance of Very High Concern) identification of perchlorate salts seems to be well substantiated and would affect the future production or import of perchlorates, according to the report.^[15] Once a substance is included as SVHC in REACH's Annex XIV list, follow-up regulations on EU level affecting labeling, transport and production/import limits are conceivable.^[15]

Several alternatives were developed and investigated in the last decades to replace ammonium perchlorate due to its toxicity and potential regulatory issues. These new high energy dense oxidizers (HEDOs) have to fulfill various requirements, which are classified as follows:^[1]

- high oxygen content $\Omega_{\text{CO}} > 25 \text{ \%}$
- high density close to $\rho = 2 \text{ g cm}^{-3}$
- high thermal stability $T_{\text{dec}} > 150 \text{ }^{\circ}\text{C}$
- low sensitivity $IS, FS < \text{PETN (IS 4 J, FS 80 N)}$
- low vapor pressure
- compatibility with fuel and binders
- high enthalpy of formation
- convenient synthesis with minimum number of steps
- economic starting materials

The oxygen balance Ω_{CO_2} or Ω_{CO} , assuming the formation of carbon dioxide and carbon monoxide respectively, represents the probably most important parameter of high energy dense oxidizers. It defines the relative amount of oxygen provided or needed during the combustion of energetic materials without external sources of oxygen. The oxygen balance is normalized to the molecular weight M of a substance and should be as high as possible for potential oxidizers. The oxygen balance Ω_{CO} for compounds with the empirical formula $\text{C}_a\text{H}_b\text{N}_c\text{O}_d$ can be calculated by the following equation:^[1]

$$\Omega_{CO} = \frac{\left[d - a - \left(\frac{b}{2}\right)\right] \times 1600}{M} . \quad (3)$$

To obtain the equation for the oxygen balance assuming the formation of carbon dioxide Ω_{CO_2} the number of carbons a simply has to be doubled in formula 3.

Some of the most promising candidates in the development of oxidizers are the ionic substances ammonium nitrate, ammonium dinitramide and hydrazinium nitroformate (Figure I.7).^[1]

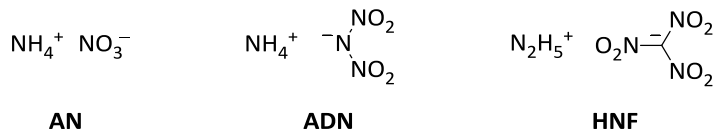


Figure I.7: Molecular structure of typical ionic oxidizers: ammonium nitrate (AN), ammonium dinitramide (ADN) and hydrazinium nitroformate (HNF).

Unfortunately their application as oxidizers is limited, as each of those salts has their unique drawbacks. Ammonium nitrate is readily available and rather eco-friendly, but suffers from hygroscopicity issues, its low thermal stability and multiple phase transitions.^[1] Hydrazinium nitroformate was shown to be too sensitive in terms of impact and friction and its thermal decomposition starts already at 128 °C. Furthermore, it requires hydrazine for production, which itself is extraordinary toxic and might be released under thermal stress or alkaline conditions.^[19] Ammonium dinitramide is currently intensively investigated in several propellant compositions, as it is environmentally benign, halogen-free and develops great performance values.^[20-21] However there are still numerous disadvantages that have to be solved, such as the low thermal stability, the costly synthesis and the compatibility with established binder systems.^[20-21] Another variety of potential replacements was developed around trinitroethyl based energetic compounds, such as bistrinitroethyl oxalate (BTNEO), tristrinitroethyl formate (TNEF) and trinitroethyl nitrocarbamate (TNENC, Figure I.8).^[1, 22-25] These substances feature high oxygen balances, reasonable decomposition temperatures and promising performance data in composite mixtures. Their major drawback is the common precursor trinitroethanol.

I General Introduction

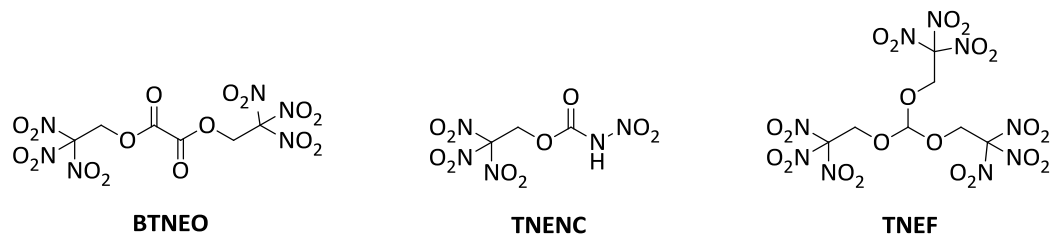


Figure I.8: Molecular structure of typical covalent oxidizers: bis(2,2,2-trinitroethyl) oxalate (BTNEO), 2,2,2-trinitroethyl nitrocarbamate (TNENC) and tris(2,2,2-trinitroethyl) formate (TNEF).

Although a vast number of compounds based on trinitroethanol were developed in the past, the substance or its starting material potassium nitroformate, respectively an aqueous nitroform solution, are not commercially available in larger scales.^[1] There are several synthetic pathways to obtain nitroform and its potassium salt, such as the exhaustive oxidation of isopropanol, acetone or acetic anhydride in white fuming nitric acid, the nitration and multistep hydrolysis of barbituric acid or the catalyzed nitration of acetylene. In the recent past, further synthetic routes were investigated to obtain the crucial starting material, but all of them have substantial disadvantages, either based on economical, ecological or safety issues.^[1]

Altogether ammonium perchlorate is still the most important and most commonly applied oxidizer for composite propellants. Further research is absolutely necessary to find a suitable replacement for AP in order to avoid its hazardous and dangerous properties.

4 Objective Target

The objective of this thesis is the synthesis and characterization of new environmentally benign high energy dense oxidizers. The intention is to find oxygen-rich molecules and their application as possible replacements for ammonium perchlorate in solid rocket composite propellants. The investigated compounds were designed to combine several requirements, such as excellent energetic performance, suitable chemical and physical properties and an economically reasonable synthesis. In this thesis, three major approaches were investigated to accomplish the objective target.

Nitrates are well-known and commonly used energetic materials with numerous applications, such as pentaerythritol tetranitrate, nitrocellulose, nitroglycerin and ammonium nitrate.^[1] The aim was to find suitable, readily available starting materials for synthesis of unknown organic nitrates in order to obtain oxidizers with suitable energetic parameters and an economic synthesis.

Nitrocarbamates are intensively investigated in the last decade.^[25-26] The promising energetic performances of compounds such as trinitroethyl nitrocarbamate and pentaerythritol tetranitrocarbamate demonstrate the high potential of the nitrocarbamate moiety. In general, nitrocarbamates can be obtained straightforward by the nitration of their carbamate precursors, which are easily accessible by the reaction of alcohols with the synthetically valuable reagent chlorosulfonyl isocyanate (CSI).^[27] Regarding nitrocarbamates, the objective is to form advanced energetic materials from readily available starting materials. Additionally the stabilizing properties of the nitrocarbamate group in contrast to organic nitrates were examined further.

Trinitroethanol is one of the most promising and most investigated starting materials in the research for HEDOs.^[1, 23-25] By the combination with different energetic groups, a vast number of energetic materials are known. Frequently, the trinitroethyl moiety is added at the very last synthetic step towards new energetic materials. This highlights its feasible combination with energetic groups that require very harsh synthetic conditions, such as nitrated amides. The objective is to synthesize and characterize new energetic oxidizers, which are based on the trinitroethyl building block.

Along with the synthesis of new high energy dense oxidizers, investigation of the crystal structure of isocyanic acid is a major objective target.^[28-29] Isocyanic acid (HNCO), also as the parent molecule of the important reagent CSI for these studies, is already known since 1830 and plays important roles in the study of isosterism, development of life and astrophysical media. However, a convenient structure of its crystalline state is still missing.

I General Introduction

The difficulties with this objective comprise the low melting point of isocyanic acid, its instability^[30] including polymerization, and to grow suitable single crystals at very low temperatures under the exclusion of moisture.

The main part of this thesis consists of seven chapters integrated in the RESULTS AND DISCUSSION section. The seven chapters are enclosed research projects serving the superior objective targets. Each chapter consists of an abstract, introduction, discussion of the research results, conclusion and experimental details on its own. In order to combine the investigations and results, the final development is detailed in the CONCLUSION section.

5 References

- [1] T. M. Klapötke, *Chemistry of High-Energy Materials*, 4th ed., De Gruyter, Berlin, 2015.
- [2] D. Fischer, T. M. Klapötke, J. Stierstorfer, *Angew. Chem. Int. Ed.* **2014**, *53*, 8172–8175.
- [3] J. W. Fronabarger, M. D. Williams, W. B. Sanborn, J. G. Bragg, D. A. Parrish, M. Bichay, *Propellants, Explos., Pyrotech.* **2011**, *36*, 541–550.
- [4] P. E. Eaton, M. X. Zhang, R. Gilardi, N. Gelber, S. Iyer, R. Surapaneni, *Propellants, Explos., Pyrotech.* **2002**, *27*, 1–6.
- [5] N. Fischer, D. Fischer, T. M. Klapötke, D. G. Piercey, J. Stierstorfer, *J. Mater. Chem.* **2012**, *22*, 20418–20422.
- [6] J. Glück, T. M. Klapötke, M. Rusan, J. J. Sabatini, J. Stierstorfer, *Angew. Chem. Int. Ed.* **2017**, *56*, 16507–16509.
- [7] W. H. Beck, *Combust. Flame* **1987**, *70*, 171–190.
- [8] D. Majda, A. Korobov, U. Filek, B. Sulikowski, P. Midgley, D. Vowles, J. Klinowski, *Chem. Phys. Lett.* **2008**, *454*, 233–236.
- [9] A. M. Mebel, M. C. Lin, K. Morokuma, C. F. Melius, *J. Phys. Chem.* **1995**, *99*, 6842–6848.
- [10] P. Waldmann, *The Wall Street Journal, Perchlorate Runoff Flows To Water Supply of Millions*, New York **2002**.
- [11] EPA.gov – United States Environmental Protection Agency, Technical Fact Sheet - Perchlorate, EPA 505-F-14-003 01.2014, accessed 04.2018.
- [12] C. M. Steinmaus, *Curr. Environ. Health Rep.* **2016**, *3*, 136–143.
- [13] N. Bardiya, J.-H. Bae, *Microbio. Res.* **2011**, *166*, 237–254.
- [14] EPA.gov – United States Environmental Protection Agency, EPA-HQ-OW-2009-0297, Drinking Water Contaminants – Standards and Regulations, accessed 04.2018
- [15] ECHA – European Chemicals Agency, <https://echa.europa.eu/substance-information/-/substanceinfo/100.029.305>, accessed 04.2018
- [16] ECHA – European Chemicals Agency, <https://echa.europa.eu/information-on-chemicals/evaluation/community-rolling-action-plan/corap-table/-/dislist/details/0b0236e1807e9ab1>, accessed 04.2018
- [17] ECHA – European Chemicals Agency, <https://echa.europa.eu/pact>, accessed 04.2018
- [18] ECHA – European Chemicals Agency, <https://echa.europa.eu/documents/10162/5a24f238-6d61-4d67-948d-eba568e9d9ea>, accessed 04.2018
- [19] H. F. R. Schoeyer, A. J. Schnorhk, P. A. O. G. Korting, P. P. J. van Lit, J. M. Mul, G. M. H. J. L. Gadiot, J. J. Meulenbrugge, *J. Propul. Power* **1995**, *11*, 856–869.
- [20] J. Cui, J. Han, J. Wang, R. Huang, *J. Chem. Eng. Data* **2010**, *55*, 3229–3234.
- [21] E. Landsem, T. L. Jensen, F. K. Hansen, E. Unneberg, T. E. Kristensen, *Propellants, Explos., Pyrotechn.* **2012**, *37*, 691–698.

I General Introduction

- [22] Q. J. Axthammer, T. M. Klapötke, B. Krumm, R. Moll, S. F. Rest, *Z. Anorg. Allg. Chem.* **2014**, *640*, 76–83.
- [23] T. M. Klapötke, B. Krumm, R. Scharf, *Eur. J. Inorg. Chem.* **2016**, 3086–3093.
- [24] T. M. Klapötke, B. Krumm, R. Moll, S. F. Rest, *Z. Anorg. Allg. Chem.* **2011**, *637*, 2103–2110.
- [25] Q. J. Axthammer, B. Krumm, T. M. Klapötke, *J. Org. Chem.* **2015**, 6329–6335.
- [26] Q. J. Axthammer, B. Krumm, T. M. Klapötke, *Eur. J. Org. Chem.* **2015**, 723–729.
- [27] D. N. Dhar, P. Dhar, *The Chemistry of Chlorosulfonyl Isocyanate*, World Scientific, Singapore **2002**.
- [28] H. Jones, R. G. Shoolery, D. M. Yost, *J. Chem. Phys.* **1950**, *18*, 990–991.
- [29] G. Herzberg, C. Reid, *Disc. Faraday Soc.* **1950**, *9*, 92–99.
- [30] G. Fischer, J. Geith, T. M. Klapötke, B. Krumm, *Z. Naturforsch. B* **2002**, *57*, 19–24.

II Summary and Conclusion

With the objective to replace ammonium perchlorate (AP) as oxidizer in composite propellants, various novel energetic materials were synthesized, thoroughly characterized and comprehensively investigated in the course of this thesis. The examined compounds were designed to fulfill several requirements for high energy dense oxidizers (HEDOs), such as positive oxygen balances Ω_{CO} , sufficient thermal stabilities T_{dec} and high specific impulses I_s .

The synthesis of organic nitrates and nitrocarbamates was achieved by successful introduction of oxygen-rich moieties to economically reasonable starting materials. To further enhance the oxygen balance, the valuable starting material trinitromethane was employed to construct oxidizers containing the trinitroethyl group. Most of the designed compounds possess a positive oxygen balance in combination with satisfactory thermal and mechanical stabilities, and were therefore classified as HEDOs, which could have potential use as environmentally benign replacements for AP.

Furthermore, a success of this thesis was the determination of the crystal structure of isocyanic acid, HNCO. Growing crystals of isocyanic acid suitable for single crystal X-ray diffraction is a tedious and challenging task. By isolation of pure HNCO in sealed glass capillaries and repeatedly regrowing crystals inside, after several attempts satisfactory crystals were obtained.

Organic and Ionic Nitrates

The first two chapters of this thesis focus on the synthesis and investigation of nitrates, appearing either as covalent organic compounds or ionic salts. The starting materials of these compounds were chosen with respect to economic and ecologic issues. The organic nitrates were developed from the commercially available precursor tris(hydroxymethyl) aminomethane (TRIS), which finds application in biochemical buffer systems. While nitration of pure TRIS has shown to form very sensitive and unstable organic nitrates, clever transformations led to five interesting precursors. Subsequent nitration of these compounds yielded the corresponding organic nitrates, such as **S1** and **S2**, in satisfying yields (45 – 72 %) and high purity (Figure II.1).

II Summary and Conclusion

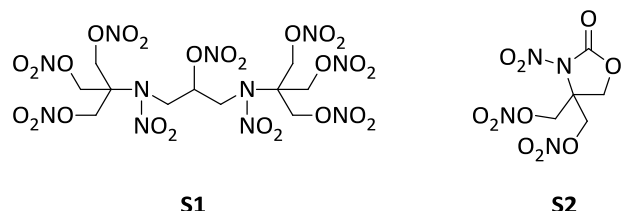


Figure II.1: Molecular structure of the organic nitrates *N,N'*-bis[tris(nitratomethyl)methyl]-1,3-dinitramino-2-nitratopropane (**S1**) and 5-nitro-4,4-bis(nitratomethyl)oxazolidone (**S2**).

Nitrate **S1** showed superior performance compared to the common nitrate PETN regarding the detonation velocity and pressure. Compound **S2**, which includes a cyclic nitrocarbamate unit, resembled PETN in terms of thermal stability and performance data, and is particularly less sensitive to friction and impact. Each investigated nitrate possessed an oxygen content of at least 55 % and a positive oxygen balance Ω_{CO} , and therefore their capability as oxidizers were examined. The most promising nitrates reached 274 s in combination with aluminum, and 256 s upon the addition of large amounts of binder, which is close to the performance of AP with I_{sp} (AP/Al/binder) = 261 s. All synthesized nitrates were thoroughly characterized and their structures could be determined by X-ray single crystal diffraction (Figure II.2).

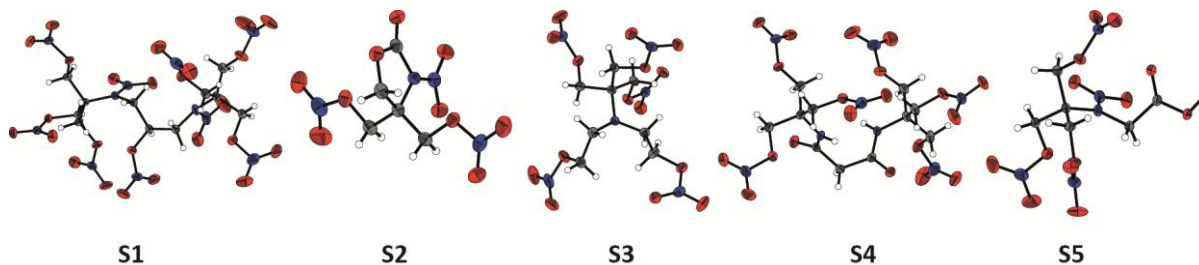


Figure II.2: Crystal structures of five organic nitrates derived from nitromethane. 5-Nitro-4,4-bis(nitratomethyl)oxazolidone (**S1**), *N,N'*-bis(tris(nitratomethyl)methyl)-1,3-dinitramino-2-nitropropane (**S2**), bis(2-nitroethyl)amino-tris(nitratomethyl)methane (**S3**), *N,N'*-bis(tris(nitratomethyl)methyl)malonamide (**S4**) and *N*-(tris(nitratomethyl)methyl)nitramino glycine (**S5**).

To further improve the thermal stability of nitrate-based compounds, a series of ionic nitrates were synthesized. Based on hydrazides and their ability to form stable nitrate salts, the ionic compounds **S6**, **S7** and **S8** were designed and examined (Figure II.3).

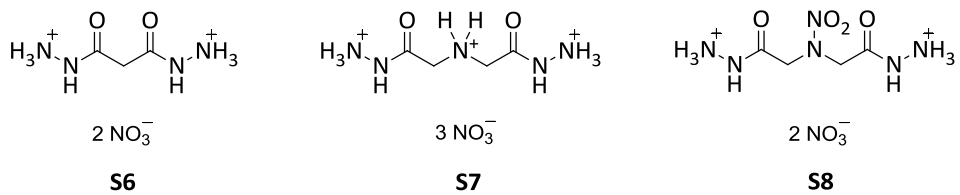
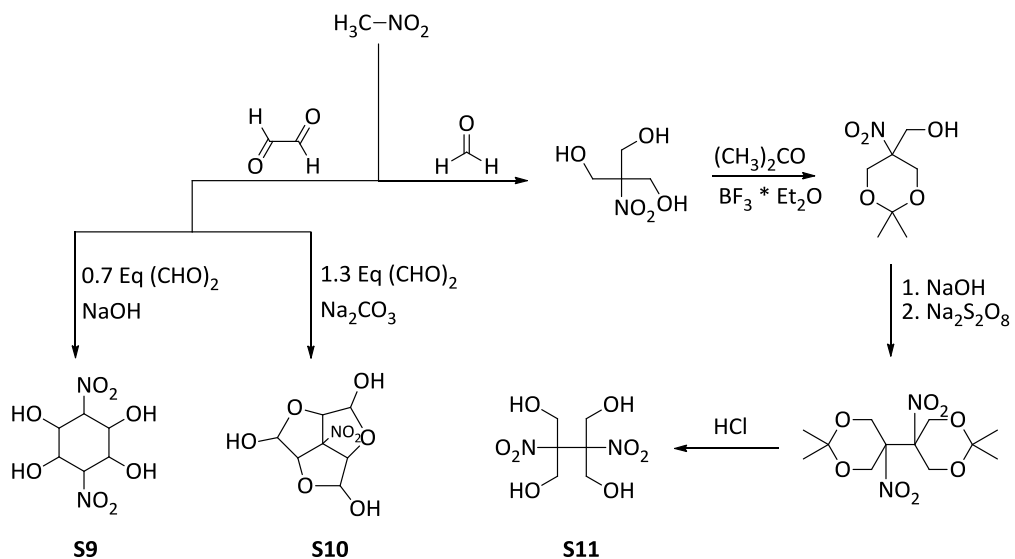


Figure II.3: Molecular structure of the ionic nitrates malonyl dihydrazinium dinitrate (**S6**), ammoniumdiacetyl dihydrazinium trinitrate (**S7**) and nitraminodiacetyl dihydrazinium dinitrate (**S8**).

Developed from the readily available starting materials malonic acid diethyl ester and iminodiacetic acid, these energetic salts were produced in short reaction routes combining high yields with fast work-ups. Despite their hygroscopicity, these ionic nitrates show interesting physical properties, e.g. their low sensitivities towards impact and friction. Particularly the energetic salt **S6** shows a very high decomposition temperature of 266 °C. Furthermore the corresponding chlorides were synthesized in high yields and could embody valuable precursors for forthcoming metathesis reactions.

Nitrocarbamates

The following two chapters 3 and 4 focused on nitrocarbamates for potential use as high energy dense oxidizers primarily and for use as energetic materials in general. Several new nitrocarbamates were synthesized from polyalcohol precursors **S9–S11**, which were developed from condensation reactions of easily accessible nitromethane with aqueous formaldehyde or glyoxal solutions (Scheme II.1).



Scheme II.1: Synthesis of the nitro and polynitro alcohols **S9–S11**.

II Summary and Conclusion

Utilizing the reactive reagent chlorosulfonyl isocyanate (CSI), the syntheses of carbamates originating from alcohol precursors worked smoothly and reliable in high yields. The final nitration gave access to three new energetic nitrocarbamates: the cyclic (**S12**), polycyclic (**S13**) and acyclic (**S14**) compounds combine a nitrated backbone with nitrocarbamate units, resulting in insensitive and oxygen-rich molecules (Figure II.4).

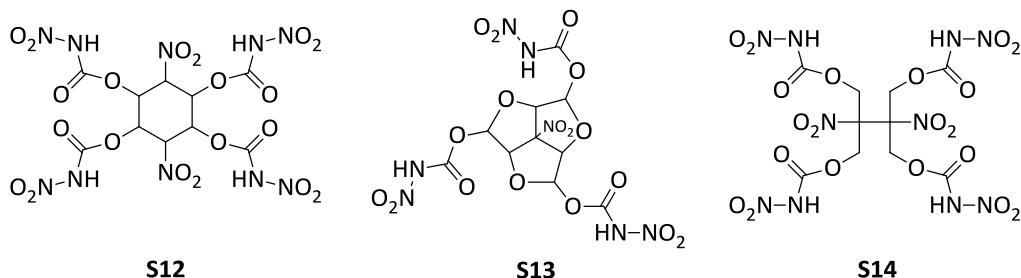


Figure II.4: Molecular structure of the nitrocarbamates 1,4-dideoxy-1,4-dinitro-*neo*-inositol tetranitrocarbamate (**S12**), 6b-nitrohexahydro-2H-1,3,5-trioxacyclopenta[cd]-pentalene-2,4,6-triol trinitrocarbamate (**S13**) and 2,3-bis(hydroxymethyl)-2,3-dinitro-1,4-butanediol tetranitrocarbamate (**S14**).

Particularly compound **S14** showed superior stability towards impact (25 J) and friction (360 N), while still presenting promising performance data, such as a remarkably high density (1.89 g cm^{-3}) and a detonation velocity (8298 m s^{-1}) in the range of frequently deployed secondary explosives. In terms of AP replacements, the nitrocarbamates reached decent theoretical specific impulses in a composite mixture with 15 % aluminum ($I_{\text{sp}} = 240\text{--}246 \text{ s}$). By the addition of further 14 % binder, the oxygen balance is no longer sufficient for an exhaustive oxidation, which led to reduced specific impulses in the final composites.

The stabilizing properties of the nitrocarbamate unit and its comparative insensitivity were further investigated. Observing the distinctly different stabilities of pentaerythritol tetranitrate (PETN, **S15**) and its silicon-based derivative sila-PETN (**S16**), the silicon analogue sila-PETNC (**S18**) of pentaerythritol tetranitrocarbamate (PETNC, **S17**) was synthesized and compared to its related compounds (Figure II.5).

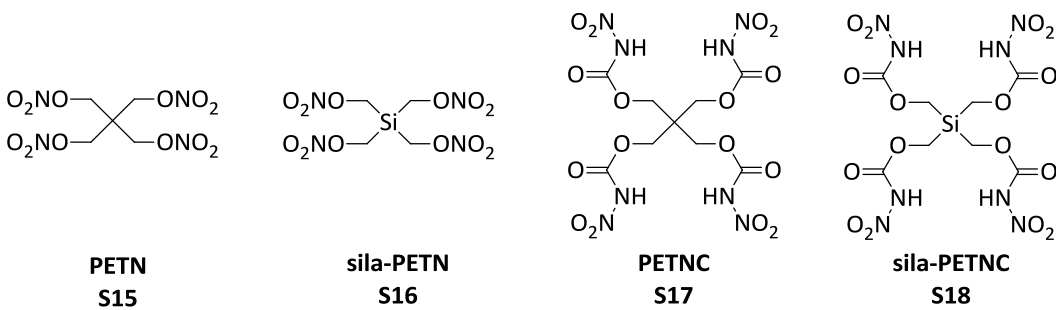


Figure II.5: Molecular structures of PETN (S15), sila-PETN (S16), PETNC (S17) and sila-PETNC (S18).

Next to similar silicon based nitrocarbamates, the tetravalent sila-PETNC (S18) was thoroughly characterized and its properties were examined. The synthesis originated from the reactive starting material silicon tetrachloride, which was subsequently converted into the corresponding chloromethyl-, acetoxyethyl- and hydroxymethylsilane. Further reaction with chlorosulfonyl isocyanate (CSI) and nitration in concentrated nitric acid yielded the target product in high purity. Suitable single crystals for X-ray diffraction measurements were obtained from a slow crystallization from acetone, revealing the crystal structure of sila-PETNC (Figure II.6). Its tetragonal space group $P\bar{4}2_1c$ is shared with its carbon relative PETNC S17.

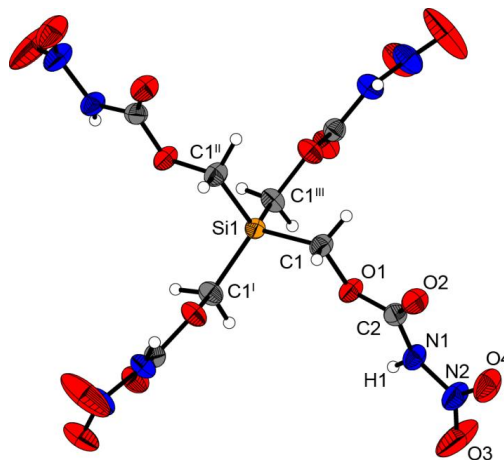


Figure II.6: Crystal structure of tetrakis(nitrocarbamoylmethyl)silane (sila-PETNC, S18).

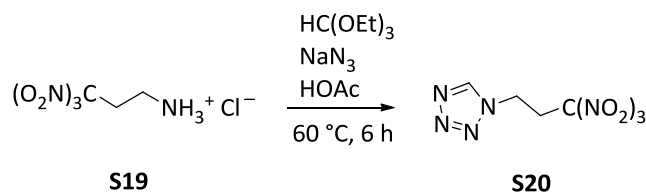
Regarding the energetic parameters, materials combining silicon with the nitrocarbamate unit were substantially less sensitive compared to silicon-based nitrates or azides. In this study, sila-PETNC showed an impact sensitivity of 3 J and a friction sensitivity of 240 N, and therefore an extraordinary higher stability towards outer stimuli. In comparison, sila-PETN was classified too sensitive for safe isolation of the pure material, especially the determination of its sensitivities. At the same time, sila-PETNC is superior to its carbon relative PETNC in

II Summary and Conclusion

terms of the heat of explosion. The higher heat of explosion as well as the higher temperature in the combustion chamber was expected, as the concept of silicon based energetic materials relies heavily on the outstanding exothermal oxidation reaction of silicon forming silicon dioxide. Nonetheless, the energetic performance is inferior in direct comparison with PETNC and PETN, mainly attributed to the lower density and the lower molecular heat of formation.

Oxidizers Developed From Trinitromethane

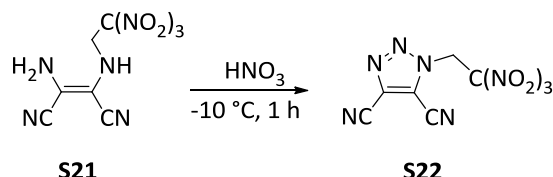
With respect to synthesize and characterize new HEDOs, the following chapters 5 and 6 focus on the oxygen-rich trinitroalkyl unit as building block. In this work, two novel *N*-substituted azoles, one tetrazole and one triazole, were synthesized via cyclization. Both heterocyclic materials contain a trinitroalkyl building block and were thoroughly characterized. *1N*-Trinitropropyl tetrazole (**S20**) was prepared by the reaction of trinitropropylammonium chloride (**S19**) with sodium azide and triethyl orthoformate, leading to the first isolated *N*-substituted trinitroalkyl tetrazole (Scheme II.2).



Scheme II.2: Synthesis of 1*N*-trinitropropyl tetrazole (**S20**) from trinitropropylammonium chloride (**S19**).

Determination of the physical and energetic properties revealed a positive heat of formation for the heterocyclic compound **S20** and a detonation velocity of almost 8400 m s⁻¹.

4,5-Dicyano-1*N*-(trinitroethyl)-1,2,3-triazole (**S22**) was obtained by nitration of a precursor (**S21**) consisting of diaminomaleonitrile and trinitroethanol in concentrated nitric acid (Scheme II.3). The triazole was formed by a reaction mechanism with the nitrosonium ion, which is known to be present in concentrated nitric acid.



Scheme II.3: Synthesis of 4,5-dicyano-1*N*-(trinitroethyl)-1,2,3-triazole (**S22**) from amino-(trinitroethylamino)maleonitrile (**S21**).

Suitable single crystals for X-ray diffraction measurements could be obtained for both azoles and their structures were determined (Figure II.7).

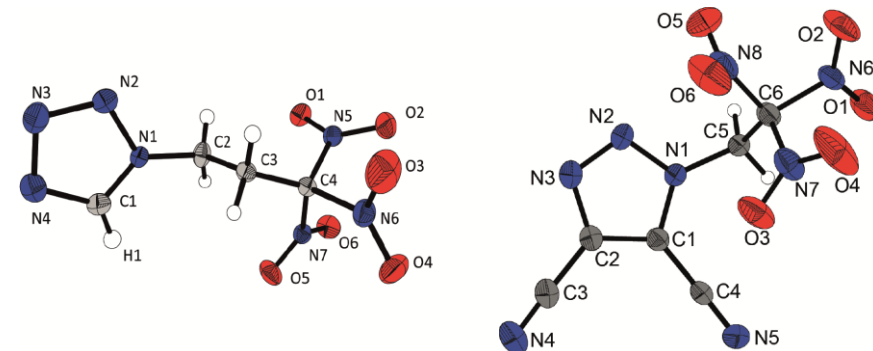
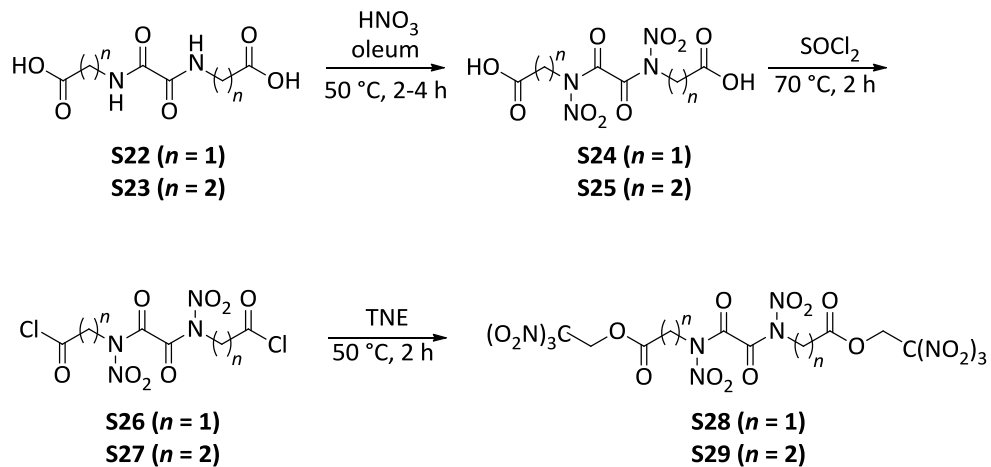


Figure II.7: Crystal structures of the trinitroalkyl substituted azoles **S20** (left) and **S22** (right).

Both compounds crystallized in closely related monoclinic space groups ($P2_1/c$ and $P2_1/n$) and showed the typical propeller-like structure of the trinitroalkyl unit.

Alongside substituted azoles, the trinitroethyl unit was combined with *N*-nitrated oxamides in order to synthesize HEDOs. Several derivates of dinitroxamides were derived from the readily available starting materials diethyl oxalate and the amino acids glycine and β -alanine. The nitration of the oxamide precursors **S22/S23** to the nitroxamides **S24/S25** was accomplished in a mixture of oleum and concentrated nitric acid supported by gentle heating (Scheme II.4).

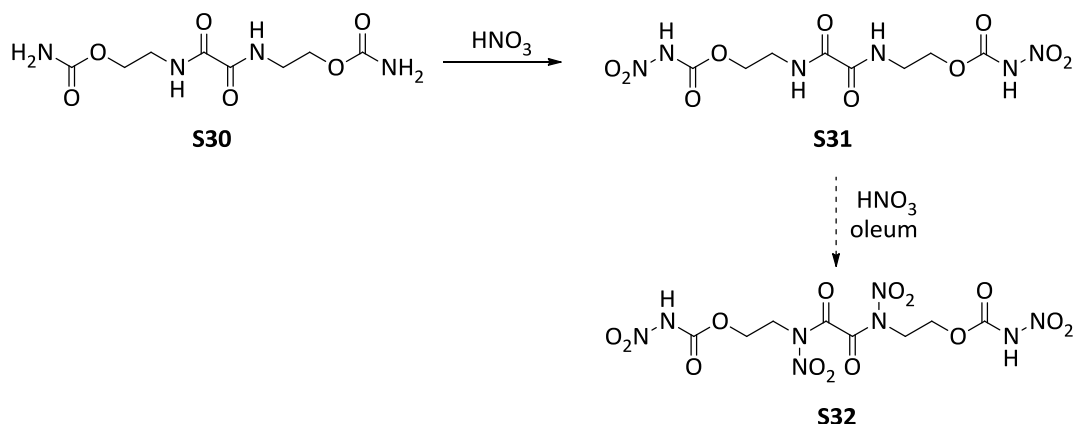


Scheme II.4: Synthesis of the TNE-ester **S29** starting from the condensation-based precursor **S23**. The nitration to the nitroxamides **S24/S25** was accomplished with a mixture of oleum and concentrated nitric acid.

II Summary and Conclusion

Following the harsh nitration conditions, the trinitroethyl unit was incorporated into the β -alanine based dinitroxamide (**S25**) by the reaction of an acid chloride intermediate (**S27**) with trinitroethanol (TNE), giving access to the target ester **S29**. It was not possible to isolate the acid chloride **S26** of the glycine based compound utilizing different chlorinating agents (SOCl_2 , $\text{C}_2\text{O}_2\text{Cl}_2$, PCl_5). Neither did the direct conversion of carbonic acid **S24** with trinitroethanol supported by sulfuric acid yield the desired ester **S28**.

Furthermore, a reaction path starting with diethyl oxalate and ethanolamine yielded a nitrocarbamate derivative **S31**, which was obtained by the conversion into the carbamate **S30** and follow-up nitration. The second, more violent nitration to the dinitroxamide derivative **S32** seems manageable, but no pure product was isolable so far (Scheme II.5).



Scheme II.5: Synthesis of the nitrocarbamate **S31** through nitration of the carbamate **S30**.

The isolation of the nitroxamide **S32** is still in progress.

The first target ester **S29**, based on β -alanine and trinitroethanol, already shows a detonation velocity of over 8000 m s^{-1} and a theoretical specific impulse of $I_{\text{sp}} = 255 \text{ s}$ in a mixture with 15 % aluminum. The desired glycine-based derivative **S28** is supposed to be superior to the β -alanine-based ester **S29**. The oxygen balance is distinctly positive ($\Omega_{\text{CO}} (\mathbf{S29}) = 9.9 \text{ \%}$ vs. $\Omega_{\text{CO}} (\mathbf{S28}) = 20.6 \text{ \%}$), and combined with a lower molecular weight and a probably 10 % higher density, the new ester **S28** should then reach promising propulsion parameters.

Outlook on High Energy Dense Oxidizers

In this thesis, several molecules containing nitro, nitrate and nitrocarbamate units were synthesized, characterized and investigated. Possessing a positive oxygen balance Ω_{CO} , these high energy dense oxidizers (HEDOs) were designed to replace ammonium perchlorate in solid propellant compositions for rocket and missile engines. Although other molecules achieved higher specific impulses, the combination of thermal and mechanical stability, economic synthesis and performance data determine the following three materials as most promising alternatives to ammonium perchlorate (Table II.1):

Table II.1: Molecular Structure and energetic performance data of 5-nitro-4,4-bis(nitromethyl)oxazolidone (**S2**), 2,3-bis(hydroxymethyl)-2,3-dinitro-1,4-butanediol tetranitrocarbamate (**S14**) and bis(carboxyethyl)dinitroxamide bis(2,2,2-trinitroethyl)ester (**S29**).

	S2	S14	S29
^[a] ρ [g cm ⁻³]	1.84	1.89	1.75
^[b] T_{dec} [°C]	160	172	159
^[c] Ω_{CO} [%]	11.3	10.8	9.9
^[d] V_{det} [m s ⁻¹]	8102	8333	8025
^[d] p_{det} [kbar]	284	301	278
^[e] $I_{sp \text{ (max)}}$ [s]	248	245	254

[a] Density at room temperature. [b] Onset decomposition point T_{dec} from DTA measurements. [c] Oxygen balance assuming formation of CO. [d] Predicted detonation velocity and detonation pressure with the program package EXPLO5 (V.6.03). [e] Specific impulse I_{sp} of optimized compositions with aluminum and binder (polybutadiene acrylic acid, polybutadiene acrylonitrile and bisphenol A ether) using the EXPLO5 (Version 6.03) program package (70 kbar, isobaric combustion, equilibrium to throat and frozen to exit).

The energetic performance of compositions containing these oxidizers were optimized with aluminum contents between 10 and 20 % and binder contents of 14, 7 and 3.5 % in the mixture and compared to the optimized composition of AP ($I_{sp} = 261$ s, 71 % oxidizer, 15 % aluminum and 14 % binder).

The best performance for the nitrate **S2** of $I_{sp} = 248$ s was calculated for a composite with 76.5 % oxidizer, 20 % aluminum and 3.5 % binder. Although those values are decent, it is difficult to achieve sufficient oxygen balances on nitrate-based materials. Further, organic

II Summary and Conclusion

nitrates suffer from low thermal decomposition temperatures and high sensitivities towards impact and friction as shown in chapter 1.

The highest specific impulse for the nitrocarbamate **S14** of $I_{sp} = 245$ s was calculated for a composite with 76.5 % oxidizer, 20 % aluminum and 3.5 % binder. This material was designed in accordance to the promising performance of trinitroethyl nitrocarbamate (**TNENC**, $I_{sp} = 261$ s), which achieved specific impulses on the level of AP, but relies heavily on the costly starting material nitroform. In terms of economic aspect, replacing nitroform with its lower substituted derivative nitromethane is far superior to utilizing nitroform itself. In the future, nitrocarbamates derived from dinitromethyl containing alcohols may excel in both, economic synthesis and energetic performance.

The best performance for the TNE-ester **S29** of $I_{sp} = 254$ s was calculated for a composite with 71.6 % oxidizer, 15 % aluminum and 3.5 % binder. With an optimized mixture, the performance is already close to the benchmark of AP ($I_{sp} = 261$ s). The glycine-based derivative **S28** ($n=1$) possesses a better oxygen balance and probably a significantly higher density and should reach superior specific impulses in the range of AP.

Even though the low density and hygroscopicity may limit the practical application of the hydrazide based dinitrates **S6–S8**, the knowledge gained upon their study could lead to potential high performing materials. Unknown dinitrates of the hydrazides **S33** and **S34** (Figure II.8) may be synthetically accessible in an economic reasonable pathway, could develop high densities and thermal stabilities, and posses positive oxygen balances.

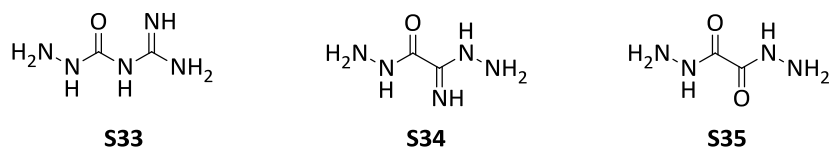


Figure II.8: Molecular Structure of *N*-(aminoiminomethyl)-hydrazinecarboxamide (**S33**), oxalamidrazone hydrazide (**S34**) and oxalyl dihydrazide (**S35**).

Furthermore, the bis-dinitramide salts of **S33**, **S34** and oxalyl dihydrazide **S35** should show superior performance data compared to the dinitrates, but might show low thermal decomposition temperatures and increased sensitivities.

The Crystal Structure of Isocyanic Acid

The last chapter describes the crystal structure of isocyanic acid, HNCO. The pure substance was prepared by the reaction of potassium cyanate and stearic acid in a thoroughly dried glass reactor (Figure II.9). The resulting gaseous HNCO was condensed in a capillary cooled with liquid nitrogen, which was subsequently sealed. The solidified isocyanic acid was recrystallized *in situ* in the capillary through several heating and cooling cycles.



Figure II.9: Glass reactor and setup for the isolation of isocyanic acid (left). X-ray diffraction measurement of the single crystalline HNCO sample (right).

The crystalline material was measured repeatedly to check the diffraction pattern until a suitable crystal was obtained. The structure was determined at 123 K and additional measurements were performed between 100 K and its melting point (~ 187 K) over 24 h. In all cases only slightly varying lattice parameters in agreement with the structure determination were recorded. The investigated structure of HNCO crystallized in the orthorhombic acentric space group $Pca2_1$ with four formula units in the unit cell and a density of 1.61 g cm^{-3} . To help with assigning the hydrogen atoms and particularize the C/N/O positions in the crystal structure, the determination was supported with DFT calculations. Concerning its crystal structure, isocyanic acid forms intermolecular hydrogen bonds N–H \cdots N with nitrogen as proton acceptor, although oxygen is the more electronegative element. The hydrogen bonds arrange in one-dimensional zigzag chains, defining the structure of HNCO in the solid state (Figure II.10). The acentric space group $Pca2_1$ allows for two polar structures for isocyanic acid, which were probably obtained evenly by the condensation and recrystallization procedure. Both can be interchanged by reflection with a mirror and differ by the z parameters for the positions of N and O, respectively.

II Summary and Conclusion

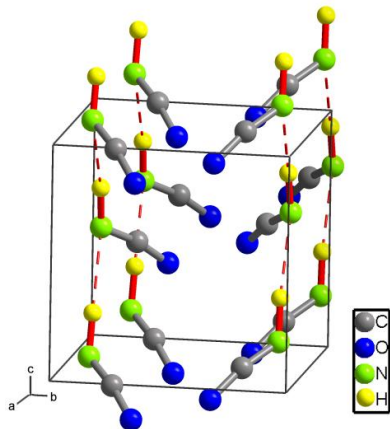


Figure II.10: View along [001] for the polar structure of HNCO in $Pca2_1$. Red dotted lines represent $N-H\cdots N$ hydrogen bonds.

Interestingly, the lattice parameters of orthorhombic HNCO, the imide of carbon dioxide (CO_2), are pseudo-cubic and deviate only very slightly from the lattice parameters of cubic CO_2 . Moreover, the space groups of carbon dioxide ($P2_1/a\bar{3}$) and of isocyanic acid ($Pca2_1$) correlate in a group-subgroup relation. Reducing the symmetry of the cubic space group specifically leads to the non-isomeric orthorhombic subgroup $Pcab$ in a first transformation step. A second transformation with further reduced symmetry leads to the orthorhombic space group of HNCO with the mentioned two polar structures.

III Results and Discussion

- 1 Organic Nitrates Derived from TRIS
- 2 Ionic Nitrates Derived from Dihydrazides
- 3 Polynitrocarbamates Derived from Nitromethane
- 4 Silicon Analogues of Neo-Pentane Derivatives
- 5 *N*-Trinitroalkyl Substituted Azoles
- 6 *N*-Dinitrated Oxamides
- 7 Molecular Structure of Isocyanic Acid

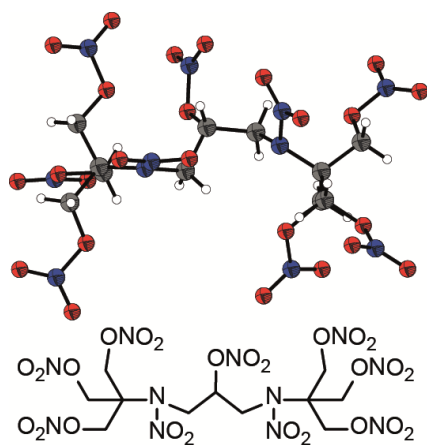
1 Organic Nitrates Derived from TRIS

POLYFUNCTIONAL ENERGETIC NITRATES DERIVED FROM TRIS(HYDROXYMETHYL)AMINOMETHANE (TRIS)

Thomas M. Klapötke, Burkhard Krumm, and Thomas Reith

as published in

European Journal of Organic Chemistry 2017, 3666–3673



1.1 Abstract

A variety of new energetic compounds were synthesized with the tris(hydroxymethyl)aminomethane (TRIS) moiety as building block. The new nitrates were fully characterized, including multinuclear NMR spectroscopy, vibrational analysis, mass spectrometry, differential scanning calorimetry and elemental analysis. The structure of each compound was confirmed using single crystal X-ray diffraction. The energies of formation were calculated with the GAUSSIAN program package and the detonation parameters were predicted using the EXPLO5 computer code. Due to the positive oxygen balance (Ω_{CO}) of the presented compounds, their performance data as oxidizers were compared to the common oxidizer ammonium perchlorate.

1.2 Introduction

As early as the discovery of nitroglycerine in 1847 and its application as main component in Alfred Nobel's dynamite, organic nitrates play a major role in the field of energetic materials (Figure 1.1).¹ The economic starting materials, a facile synthesis and the compatibility with many other energetic or additive compounds make them an important class for both military and commercial use.² With the synthesis of pentaerythritol tetranitrate (nitropenta, PETN), one of the most used secondary explosives was invented in 1894.³ PETN is a powerful high explosive with a high brisance, satisfactory stability and simple synthesis. However, some kind of drawback is found in the relatively high sensitivity on impact and friction, which usually is countered with phlegmatization or uses in mixtures (Semtex-1A, pentolite).³ Another example for the wide use of nitrates in energetic chemistry is nitrocellulose (NC). NC represents one of the oldest and most used energetic materials. It is used in multiple areas of application, such as main component in modern gun and rocket propellants, plasticizer for sensitive explosives and several civil utilizations.¹⁻³

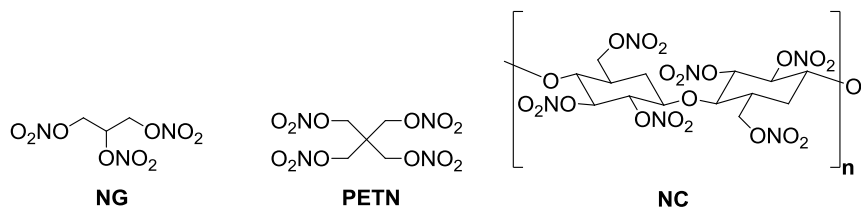


Figure 1.1: Nitroglycerin (NG), pentaerythritol tetranitrate (PETN) and nitrocellulose (NC).

Explosives based on nitrates are one of the oldest classes of energetic materials. Still they are amongst the most powerful explosives known and excel in a wide field of applications.^{1b, 3} Their variety ranges from primary and secondary explosives, plasticizers, oxidizers as well as gun and rocket propellants. Known and new energetic nitrates are still under investigation, e.g. triethylene glycol dinitrate (TEGDN) as alternative to nitroglycerine (NG) in formulations or 1,2-propanediol dinitrate (PDDN) as high energy monopropellant.² The combination of nitrates with other energetic functional groups leads to interesting results. The 2,3-bis(hydroxymethyl)-2,3-dinitro-1,4-butanediol tetranitrate (NEST-1), a relatively new energetic nitrate containing aliphatic nitro groups, combines a low melting point with promising performance data to give a new melt-castable explosive (Figure 1.2).⁴

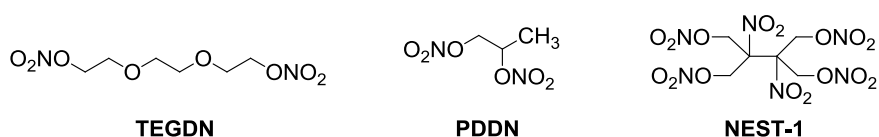


Figure 1.2: Energetic nitrates TEGDN, PDDN and NEST-1 are currently investigated for several applications.

Our previous study of combining nitrate with nitramine groups resulted in an irregular behavior towards impact sensitivity.⁵ Based on these results and preliminary studies of an oxalyl amide, *N,N'*-bis(tris(nitratomethyl)methyl)oxamide,⁶ our point of interest was the synthesis of further new energetic nitrates, which originate on the easily available tris(hydroxymethyl)aminomethane (TRIS) molecule, and further to study their properties.

1.3 Results and Discussion

1.3.1 Synthesis

The well-known and commercially available polyalcohol precursors, TRIS (tris(hydroxymethyl)aminomethane), BISTRIS (bis(2-hydroxyethyl)amino-tris(hydroxymethyl)methane), and TRICINE (N-(tris(hydroxymethyl)methyl)glycine), were used as starting materials for the synthesis of new energetic nitrates. The direct nitration of BISTRIS in a mixture of glacial acetic acid, acetic anhydride and white fuming nitric acid, yielded bis(2-nitrotoethyl)amino-tris(nitratomethyl)methane (**1**) in moderate yields. Treatment of TRIS with diethyl malonate in refluxing methanol resulted in the formation of *N,N'*-bis(tris(hydroxymethyl)methyl)malonamide,⁷ which upon nitration in white fuming nitric acid resulted in the formation of *N,N'*-bis(tris(nitroto-methyl)methyl)malonamide (**2**). TRICINE was nitrated in pure white fuming nitric acid, and the aqueous work-up gave the nitrate

1 Organic Nitrates Derived from TRIS

N-(tris(nitratomethyl)methyl)nitramino glycine (**3**) as a pure compound without further purification. When TRIS is reacted with epichlorohydrin in boiling ethanol, *N,N'*-(tris(hydroxymethyl)methyl)-1,3-diammonium-2-propanol dichloride was obtained.⁸ Further nitration furnished *N,N'*-(tris(nitratomethyl)methyl)-1,3-dinitramino-2-nitratopropane (**4**) as pure compound (Figure 1.3).

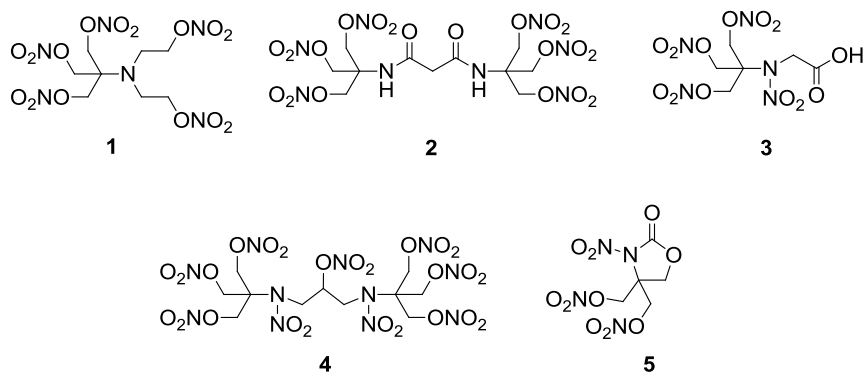
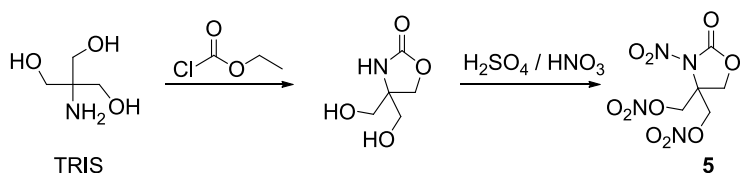


Figure 1.3: New energetic nitrates **1–5** based on TRIS.

The heterocyclic nitrate 5-nitro-4,4-bis(nitratomethyl)-oxazolidone (**5**) was first synthesized in 1944, but none of its physical or energetic properties were determined nor described.⁹ Starting from TRIS, a cyclization with ethyl chloroformate was achieved and the cyclic compound 4,4-dimethyloloxazolidone was obtained. The intermediate diol was nitrated in mixed acid and recrystallized from methanol to yield the nitrate **5** with a cyclic nitrocarbamate unit in good yield (Scheme 1.1).



Scheme 1.1: Synthesis of the nitrated oxazolidone **5**.

All nitrates are colorless solids and can be recrystallized for purification. For compounds **2**, **3**, **4** and **5** the pure material is readily obtained from aqueous work-up after nitration.

1.3.2 NMR and Vibrational Spectroscopy

Regarding the ¹H NMR spectra of the non-cyclic energetic nitrates **1–4**, the nitrated building block of the former TRIS moiety shows the nitratomethyl resonances *CH*₂ signals in the narrow range of 5.27–4.92 ppm. While those resonances for **1–3** appear as sharp singlets, in case of **4** however, due to sterical crowding the methylene groups are split into two separate resonances

at 5.145 and 5.142 ppm. For the cyclic compound **5**, the two methylene groups of the nitratomethyl groups form AB spin systems and appear as two doublets at 5.40 ppm and 5.20 ppm.

In the $^{13}\text{C}\{^1\text{H}\}$ NMR spectra of **2** and **3** the resonances of the carbonyl groups are found identically at 168.6 ppm and that of the nitrocarbamate unit in **5** is found at 146.3 ppm. The resonances of the methylene groups of the former TRIS unit are found in the range of 71.8–69.7 ppm for all compounds **1–5**. The neighboring quaternary carbon $\text{C}(\text{CH}_2)_3\text{R}$ is shifted to 66.6–62.5 ppm with the exception of **2**, which appears at 57.3 ppm. In this case, the high field shift originates from the neighboring electron donating amide function.

In the ^{14}N NMR spectra the resonances of the nitrate ONO_2 units appear in the typical range of nitric acid and their organic derivatives from –48 to –45 ppm.¹⁰ Compound **1** shows a second resonance for the ethylene-bridged nitrate groups at –42 ppm. The NO_2 resonances of the nitramine units of compound **3** and **4** appear at –34 ppm and –32 ppm. The NO_2 group of the cyclic nitrocarbamate moiety of **5** is found at –51 ppm. The resonances of the nitramine nitrogen atoms, as well as those of the amide nitrogen atoms, are not detected due to broadness.

In the vibrational spectra compounds **1–5** show the typical shifts for nitrate groups. The asymmetric stretching vibrations $\nu_{\text{as}}(\text{NO}_2)$ of the nitrato groups occur between 1660–1615 cm^{-1} and can be observed as strong signals. The symmetric vibrations $\nu_{\text{s}}(\text{NO}_2)$ are as expected between 1285–1270 cm^{-1} and split up for secondary alkyl nitrates. Each of the nitrates shows a broad signal in this range, in case of **4** the expected “doublet” is visible as a shoulder (1294 cm^{-1}) next to the broad signal at 1273 cm^{-1} . The N–O wagging vibrations are located at 760–755 cm^{-1} , while the deformation vibrations are found in the range of 720–695 cm^{-1} .

For compounds **2** and **3** additional absorptions are found above 3000 cm^{-1} for the amide $\nu(\text{NH})$ and carboxylic acid $\nu(\text{OH})$ groups, respectively. The nitramine stretching vibrations of compound **3** and **4** appear in the range of 1585–1530 cm^{-1} and 1315–1260 cm^{-1} , which partially overlap with the symmetric stretching vibration $\nu_{\text{s}}(\text{NO}_2)$ of the nitrate units.

1.3.3 Single Crystal Structure Analysis

Solvent free single crystals suitable for structure determination were obtained for **1–5**, and the measurements were recorded between 123–173 K (Table 1.1).

1 Organic Nitrates Derived from TRIS

Table 1.1: Crystal data, details of the structure determinations and refinement of **1–5**.

	1	2	3	4	5
formula	$\text{C}_8\text{H}_{14}\text{N}_6\text{O}_{15}$	$\text{C}_{11}\text{H}_{16}\text{N}_8\text{O}_{20}$	$\text{C}_6\text{H}_9\text{N}_5\text{O}_{13}$	$\text{C}_{11}\text{H}_{17}\text{N}_{11}\text{O}_{25}$	$\text{C}_5\text{H}_6\text{N}_4\text{O}_{10}$
<i>FW</i> [g mol ⁻¹]	434.23	580.29	359.16	703.31	282.12
<i>T</i> [K]	123	123	123	148	173
λ [Å]	0.71073	0.71073	0.71073	0.71073	0.71073
crystal system	triclinic	monoclinic	monoclinic	monoclinic	monoclinic
space group	<i>P</i> –1	<i>P</i> 2 ₁ / <i>n</i>	<i>P</i> 2 ₁ / <i>c</i>	<i>C</i> 2/ <i>c</i>	<i>P</i> 2 ₁ / <i>c</i>
crystal size [mm]	0.40 x 0.40 x 0.40	0.40 x 0.32 x 0.32	0.4 x 0.21 x 0.04	0.1 x 0.1 x 0.02	0.4 x 0.18 x 0.04
crystal habit	colorless block	colorless block	colorless platelet	colorless platelet	colorless block
<i>a</i> [Å]	8.514(7)	9.516(3)	14.690(6)	51.214(13)	10.8221(10)
<i>b</i> [Å]	9.094(5)	18.668(6)	7.217(2)	6.853(2)	6.8962(5)
<i>c</i> [Å]	12.743(8)	12.934(4)	13.364(5)	14.561(4)	13.9313(11)
α [deg]	102.652(5)	90	90	90	90
β [deg]	100.336(6)	101.853(3)	108.086(4)	95.021(9)	105.392(8)
γ [deg]	114.808(7)	90	90	90	90
<i>V</i> [Å ³]	831.8(10)	2248.7(12)	1346.8(12)	5091(4)	1002.42(15)
<i>Z</i>	2	4	4	8	4
$\rho_{\text{calc.}}$ [g cm ⁻³]	1.734	1.714	1.771	1.835	1.869
μ	0.170	0.168	0.177	0.183	0.185
<i>F</i> (000)	448	1192	736	2880	576
2 Θ range [deg]	4.30 – 27.50	4.44 – 31.78	4.18 – 30.21	2.81 – 26.37	4.24 – 26.37
index ranges	$-11 \leq h \leq 8$ $-11 \leq k \leq 11$ $-16 \leq l \leq 16$	$-11 \leq h \leq 11$ $-21 \leq k \leq 23$ $-12 \leq l \leq 16$	$-20 \leq h \leq 20$ $-10 \leq k \leq 10$ $-18 \leq l \leq 18$	$-64 \leq h \leq 64$ $-8 \leq k \leq 8$ $-18 \leq l \leq 18$	$-13 \leq h \leq 13$ $-8 \leq k \leq 7$ $-16 \leq l \leq 17$
reflections collected	7095	18373	12131	25181	8214
reflections unique	3800	4558	3729	5218	2038
parameters	318	516	253	492	196
GooF	1.067	1.028	1.047	1.076	1.023
R_1 / w R_2 [$I > 2\sigma(I)$]	0.0358 / 0.0748	0.0312 / 0.0724	0.0366 / 0.0785	0.0405 / 0.1024	0.0476 / 0.0966
R_1 / w R_2 (all data)	0.0486 / 0.0846	0.0388 / 0.0772	0.0564 / 0.0886	0.0521 / 0.1098	0.0855 / 0.1156
max / min residual electron density [Å ⁻³]	–0.217 / 0.319	–0.241 / 0.280	–0.246 / 0.413	–0.397 / 0.417	–0.272 / 0.255
CCDC	1538330	1538332	1538333	1538334	1538331

Single crystals of bis(2-nitroethoxy)amino-tris(nitratomethyl) methane (**1**) were obtained from boiling ethanol. It crystallizes as big colorless blocks in the triclinic space group *P*–1 with two formula units per unit cell and a density of 1.734 g cm^{–3} at 173 K (Figure 1.4).

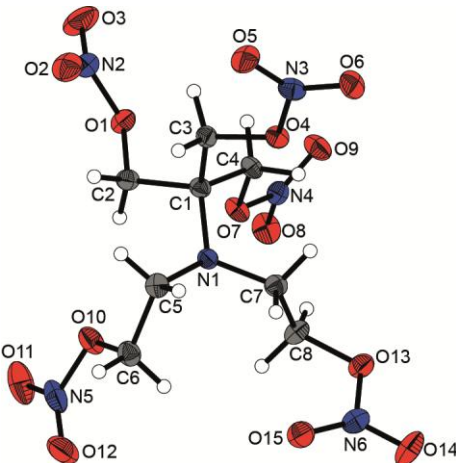


Figure 1.4: X-ray molecular structure of bis(2-nitroethoxy)amino-tris(nitratomethyl) methane (**1**). Selected atom distances (Å) and angles (deg.): N1–C1 1.465(2), O1–N2 1.414(2), N2–O2 1.198(2), N2–O3 1.202(2), C1–N1–C5 116.2(1), C1–N1–C7 119.0(1), C5–N1–C7 113.0(1), N1–C7–C8–O13 –173.9(1), N1–C5–C6–O10 –66.7(2).

The molecules are connected by non-classical hydrogen bonds between the methylene groups as proton donors and nitrate oxygen atoms as proton acceptors. For example, such contacts exist between C4–H6 with O11 (atom distances C–O 3.36 Å, H–O 2.42 Å, bond angle C–H–O 164.1 °), as well as between C3–H4 with O3.¹¹

Suitable single crystals of the nitrated malonamide **2** were obtained from methanol. It crystallizes in the monoclinic space group *P*2₁/n with four formula units per unit cell and a density of 1.714 g cm^{–3} at 173 K (Figure 1.5). Both carbonyl groups in **2** point directly in the opposite direction of each other, creating the maximum distance between the oxygen atoms O1 and O11. Additionally, both carbonyl oxygen atoms are aligned to the protons H1 and H2 in the center of the molecule structure, demonstrated by the torsion angles O11–C7–C1–H1 (–2.1 °) and O1–C2–C1–H2 (–10.5 °). The C2–N1 (C7–N5) atom distance (1.34 Å) is located between a single (1.47 Å) and double bond (1.27 Å), which indicates a strong double bond character of the amide moiety originating from the nitrogen lone pair. This is also supported by the short N–H atom distances (0.79 Å and 0.84 Å).

1 Organic Nitrates Derived from TRIS

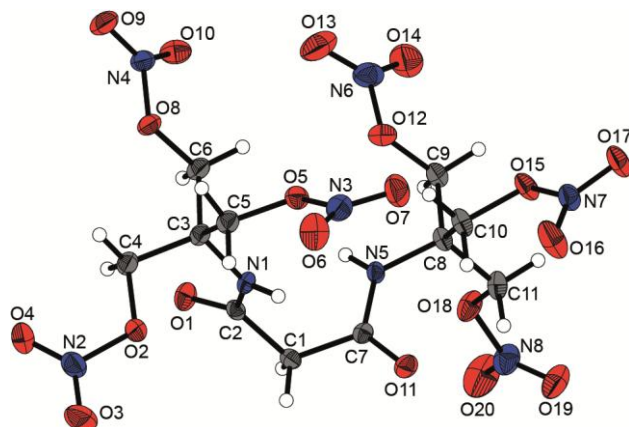


Figure 1.5: X-ray molecular structure of *N,N'*-bis(tris(nitratomethyl)methyl)-malonamide (2). Selected atom distances (Å) and angles (deg.): C2–N1 1.341(2), C2–O1 1.228(2), N1–H3 0.792(2), N5–H10 0.836(2), O2–N2 1.401(2), N2–O3 1.202(2), N2–O4 1.201(2), C2–C1–C7 114.7(1), H1–C1–H2 107.1(1), C3–N1–C2—O1 0.1 (2), C3–N1–C2–C1 –179.8(1), O11–C7–C1–H1 2.1(10), O1–C2–C1–H2 10.5(10).

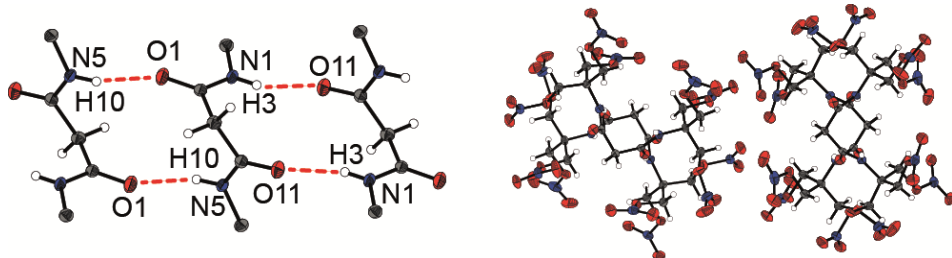


Figure 1.6: Left: Intermolecular hydrogen bonds between the amide groups of compound 2. Right: Column-type structure of compound 2 along the crystallographic axis *a*.

The strongest intermolecular hydrogen bonds are located between the amide moieties (atom distances N5···O1 2.80 Å, H10···O1 2.01 Å, bond angle N5–H10···O1 158.9 °). Both amide units of the same molecule are connected to four amide units of two neighboring molecules. In this constellation, the amide groups of the central molecule act as proton donor and acceptor at the same time. Since both carbonyl oxygen atoms are aligned in the opposite directions, two molecules are facing each other with one amide group as donor and one amide group as acceptor, respectively. This configuration of intermolecular hydrogen bonds leads to a column-type structure, which is visible along the crystallographic axis *a* (Figure 1.6).

Single crystals from the nitrated glycine **3** were obtained from aqueous work-up by slow evaporation at room temperature. The *N*-(tris(nitratomethyl)methyl)nitramino glycine (**3**) crystallizes in the monoclinic space group *P2₁/c* with four molecules per unit cell and a density of 1.77 g cm⁻³ at 173 K (Figure 1.7).

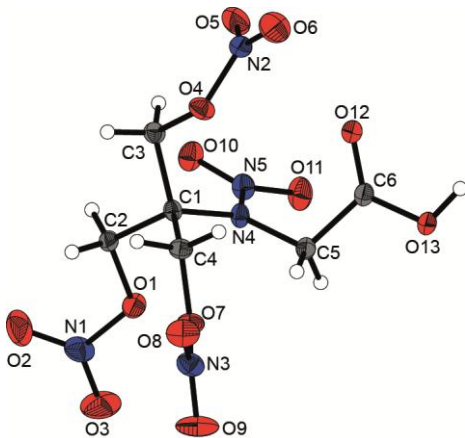


Figure 1.7: X-ray molecular structure of *N*-(tris(nitratomethyl)methyl)nitramino glycine (**3**). Selected atom distances (Å) and angles (deg.): C1–N4 1.485(2), N4–N5 1.365(2), N5–O10 1.230(2), N5–O11 1.232(2), C6–O12 1.216(2), C6–O13 1.304(2), O13–H9 0.921(2), C6–O13–H9 108.2(1), C1–N4–N5–O10 1.3(1), C1–N4–N5–O11 –178.9(1), C1–C3–O4–N2 124.6(1), C1–C4–O7–N3 –173.2(1), C1–C2–O1–N1 164.2(1).

In the crystal structure the nitramine group arranges in trans position to the tris(nitratomethyl)methyl moiety. Strong hydrogen bonding occurs between two carboxylic acid functionalities and leads to dimers of compound **3** in the solid state (Figure 1.8). The atom distance O12–O13 along the hydrogen bond is 2.61 Å with a hydrogen-acceptor distance H9···O12 of 1.69 Å and a bond angle O–H···O of 175.5 °.

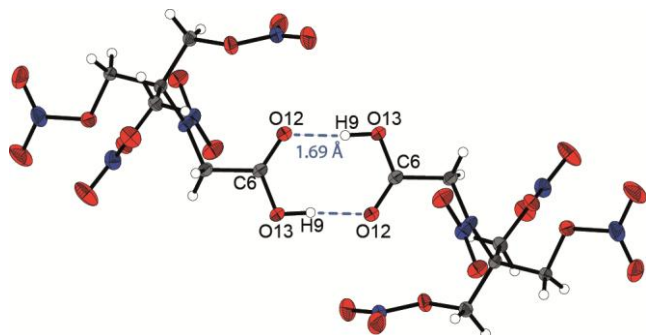


Figure 1.8: Dimers of **3** connected via hydrogen bonds of the carboxyl units.

Suitable single crystals of the nitratopropane **4** were obtained from an acetone–methanol mixture (1:1) after slow evaporation at room temperature. It crystallizes in the monoclinic space group *C*2/c with four formula units per unit cell (Figure 1.9).

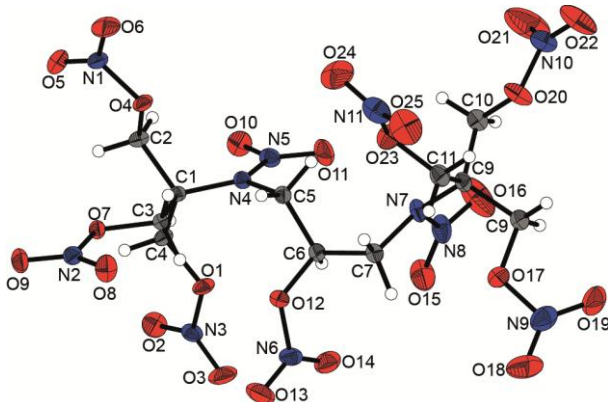


Figure 1.9: X-ray molecular structure of *N,N'*-(tris(nitratomethyl)methyl)-1,3-dinitramino-2-nitratopropane (**4**). Selected atom distances (Å) and angles (deg.): N4–N5 1.366(2), N5–O10 1.228(2), C6–O12 1.457(2), O12–N6 1.424(2), N6–O13 1.203(3), C5–C6–C7 111.8(2), C5–C6–O12 105.6(2), C7–C6–O12 106.4(2), C5–N4–N5–O11 –0.1(2), C5–N4–N5–O10 –179.5(2).

The crystal structure shows a remarkable high density (1.84 g cm^{-3} at 148 K) for organic nitrates. Presumably because of the absence of any classical proton donor, the structure itself does not exhibit substantial hydrogen bonding. The molecules arrange in layers with the tris(nitratomethyl)methyl moieties facing each other, which is visible along the crystallographic axis *b*.

Single crystals of the oxazolidone **5** were obtained from the crystallization in methanol. 5-Nitro-4,4-bis(nitratomethyl)-oxazolidone (**5**) crystallizes in the monoclinic space group *P2₁/c* with four formula units per unit cell and a density of 1.87 g cm^{-3} at 173 K (Figure 1.10).

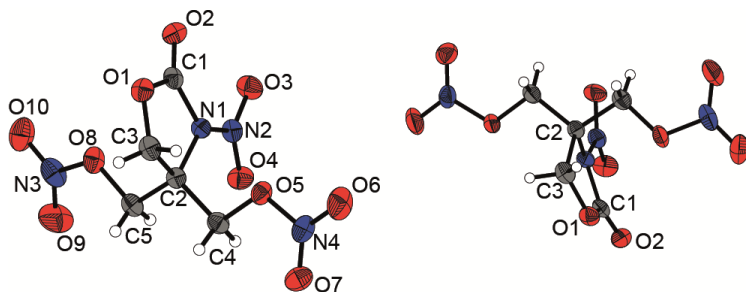


Figure 1.10: X-ray molecular structure of 5-nitro-4,4-bis(nitratomethyl)-oxazolidone (**5**) (left). Envelope-type structure of the heterocycle with orthogonal orientation of the ring to the two nitratomethyl units (right). Selected atom distances (Å) and angles (deg.): O1–C3 1.444(3), C1–O1 1.344(3), C1–O1 1.184(3), C1–N1–C2 112.2(2), N1–C2–C3 97.6(2), C2–C3–O1 106.3(2), C3–O1–C1 110.6(2), C3–O1–C1 110.6(2), O1–C1–N1 106.8(2), C5–C2–C4 108.4(2), C3–O1–C2–N1 0.9(3), C3–O1–C1–O2 180.0(3), O1–C2–C3–N1 23.6(2), C2–N1–N2–O3 178.1(2), C2–N1–N2–O4 –4.6(3), C2–C4–O5–N4 178.2(2), C4–O5–N4–O7 –1.0(3), C4–O5–N4–O6 178.3(2).

The two nitratomethyl branches are aligned in the exact opposing direction. Both units share the same plane, which is oriented orthogonal to the five-membered ring. The ring itself forms the expected envelope-type structure, with the atoms C3–O1–C2–N1 (0.9 °) and O2 on the same level and the quaternary carbon C2 out of plane (torsion angle O1–C2–C3–N1 23.6 °). Additionally, the nitro group attached to the ring is slightly twisted out of the ring plane by the same amount as the central carbon C2, creating very small torsion angles C2–N1–N2–O3 (−1.9 °) and C2–N1–N2–O4 (−4.6 °).

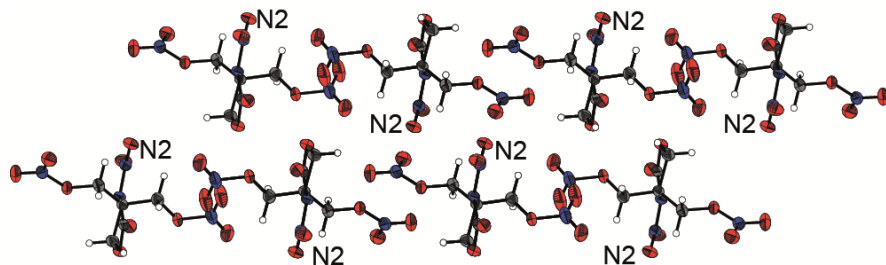


Figure 1.11: Layer structure of compound **5** with alternating orientation of the five-membered ring, visible along the crystallographic axis *b*.

Due to the lack of classical hydrogen bond donor groups, only a few weak non-classical hydrogen bonds are observed. The two methylene groups of the nitratomethyl arms act as proton donors and are connected to oxygen atoms of the nitrate and nitramino moieties of neighboring molecules, e.g. C4–H3–O7 (atom distance C–O 3.53 Å, bond angle C–H–O 154.6 °). The molecules align in layers, and the orientation of the molecules in one layer switches alternating, which is visible along the crystallographic axis *b* (Figure 1.11).

1.3.4 Thermal Stabilities and Energetic Properties

The physical and energetic properties of the nitrates **1–5** were determined and are summarized in Table 1.3. Physical properties include the thermal stability and sensitivities towards mechanical and electrostatic stimuli. Compounds **1–4** do not melt on heating and decompose directly between 104 °C (**2**) and 150 °C (**4**). The heterocyclic nitrate **5** melts at 120 °C and is thermally stable up to a temperature of 160 °C. The rather low thermal decomposition temperature of the nitrates **1–3** limits further practical application. One sample of compound **1** decomposed after several weeks, probably due to the release of nitric acid, induced by hydrolytic instability or incomplete purification. Compounds **2–5** did not show any form of decomposition for at least three months. The additional cyclic nitrocarbamate unit in **5** seems to stabilize this molecule.

1 Organic Nitrates Derived from TRIS

Friction and impact sensitivities were evaluated according to BAM standards, additionally the sensitivity towards electrostatic discharge was determined. Compounds **1**, **2** and **5** are regarded sensitive towards impact with values between 4 J and 10 J, while compounds **3** and **4** ($IS = 2$ J) are classified as very sensitive. All compounds are rated sensitive or less sensitive (**3**) in terms of friction sensitivity ($FS = 80\text{--}360$ N).

The structure and thereof the density of all compounds **1**–**5** were determined using single crystal X-ray diffraction and were recalculated to obtain the values at room temperature. The cyclic nitrate **5** shows the highest density with 1.84 g cm^{-3} , with the other nitrates ranging between $1.67\text{--}1.80\text{ g cm}^{-3}$. In combination with the calculated heat of formation (CBS-4M level), the energetic properties were estimated utilizing the EXPLO5 (Version 6.02) computer code. The nitrated malonamide **2** shows the lowest detonation velocity with $V_{\text{det}} = 7891\text{ m s}^{-1}$. The highest detonation velocity was found for compounds **4** and **5** with $V_{\text{det}} = 8550\text{ m s}^{-1}$ and $V_{\text{det}} = 8266\text{ m s}^{-1}$, respectively.

In comparison with PETN, compounds **4** and **5** are of particular interest. All three compounds have similar properties regarding decomposition temperature T_{dec} , density ρ , detonation velocity V_{det} and detonation pressure p_{CJ} (Table 1.2). While **4** shows a superior detonation velocity and is as sensitive towards friction and impact as PETN, the heterocyclic **5** is exceptional insensitive ($IS = 10$ J, $FS = 240$ N). Additionally, its melting point is about $20\text{ }^{\circ}\text{C}$ lower than the one of PETN, which makes it possibly suitable for melt castable explosives.

Table 1.2: Physical and sensitivity data of **4** and **5** in comparison with PETN.

	4	5	PETN
Formula	$\text{C}_{11}\text{H}_{17}\text{N}_{11}\text{O}_{25}$	$\text{C}_5\text{H}_6\text{N}_4\text{O}_{10}$	$\text{C}_5\text{H}_8\text{N}_4\text{O}_{12}$
T_{m} [$^{\circ}\text{C}$] ^[a]	–	120	141
T_{dec} [$^{\circ}\text{C}$] ^[a]	150	160	165
IS [J] ^[b]	2	10	3
FS [N] ^[b]	128	240	60
ρ [g cm^{-3}] ^[c]	1.80	1.84	1.78
V_{det} [m s^{-1}] ^[d]	8550	8266	8405
p_{CJ} [kbar] ^[d]	328	313	319

[a] Onset melting T_{m} and decomposition point T_{dec} from DSC measurements, heating rate $5\text{ }^{\circ}\text{C min}^{-1}$. [b] Sensitivity towards impact IS and friction FS . [c] Recalculated X-ray density at room temperature. [d] Predicted detonation velocity V_{det} and detonation pressure p_{CJ} .

The nitrates **2–5** exhibit a positive oxygen balance Ω_{CO} and their performance as oxidizers were determined (Table 1.3). Oxidizers are compounds which formally release oxygen when decomposed. The excess of oxygen enables the combustion of a fuel, which in return increases the burning temperature of a combustion system. The most important parameter for oxidizers in rocket propellant compositions is their specific impulse I_{sp} , which mainly depends on the burning temperature and the molar amount of gaseous products formed during combustion.³ The specific impulses for all energetic compounds were estimated for the neat substance, in compositions with 15 % aluminum and in compositions with 15 % aluminum combined with supplementary 14 % polymeric binder (6 % polybutadiene acrylic acid, 6 % polybutadiene acrylonitrile, 2 % bisphenol A ether).

Table 1.3: Physical and sensitivity data of **1–5** in comparison with AP.

	1	2	3	4	5	AP
Formula	$C_8H_{14}N_6O_{15}$	$C_{11}H_{16}N_8O_{20}$	$C_6H_9N_5O_{13}$	$C_{11}H_{17}N_{11}O_{25}$	$C_5H_6N_4O_{10}$	NH_4ClO_4
$FW [g\ mol^{-1}]$	434.23	580.29	359.16	703.31	282.12	117.49
$T_m [^{\circ}C]$ ^[a]	-	-	-	-	120	-
$T_{dec} [^{\circ}C]$ ^[a]	108	104	136	150	160	240
$IS [J]$ ^[b]	8	4	2	2	10	20
$FS [N]$ ^[b]	80	324	360	128	240	360
$ESD [J]$ ^[b]	0.7	0.6	0.6	0.4	0.5	-
$\rho [g\ cm^{-3}]$ ^[c]	1.69	1.67	1.73	1.80	1.84	1.95
$O [\%]$ ^[d]	55.3	55.1	57.9	56.9	56.7	54.5
$\Omega_{CO} [\%]$ ^[e]	0	+2.8	+11.1	+12.5	+11.3	+34.0
$\Omega_{CO_2} [\%]$ ^[e]	-29.5	-27.6	-15.6	-12.5	-17.0	+34.0
$\Delta_f H_m^{\circ}$ ^[f] [kJ mol ⁻¹]	-530.6	-1044.4	-614.8	-637.8	-752.4	-295.8
$V_{det} [m\ s^{-1}]$ ^[g]	8059	7891	8048	8550	8266	6368
$I_{sp} [s]$ ^[h]	259	244	257	261	245	157
$I_{sp} [s]$ ^[h] (15 % Al)	274	264	266	267	255	235
$I_{sp} [s]$ ^[h] (15 % Al, 14 % binder)	256	247	253	250	235	261

[a] Onset melting T_m and decomposition point T_{dec} from DSC measurements, heating rate 5 °C min⁻¹. [b] Sensitivity towards Impact IS , Friction FS and electrostatic discharge ESD . [c] Recalculated X-ray density at room temperature. [d] Oxygen content. [e] Oxygen balance assuming formation of CO and CO₂. [f] Energy of formation calculated by the CBS-4M method using Gaussian 09.¹² [g] Predicted detonation velocity. [h] Specific impulse I_{sp} of the neat compound and compositions with aluminum or aluminum and binder (6 % polybutadiene acrylic acid, 6 % polybutadiene acrylonitrile and 2 % bisphenol A ether) using the EXPLO5 (Version 6.02) program package (70 kbar, isobaric combustion, equilibrium expansion).¹³

1 Organic Nitrates Derived from TRIS

The standard oxidizer is ammonium perchlorate (AP), which boasts a specific impulse of $I_{sp} = 261$ s in an optimized binder/aluminum system (AP 76 %, Al 15 %, binder 14 %). If ammonium perchlorate is replaced with the new organic nitrates, the resulting compositions (**1–5** 76 %, Al 15 %, binder 14 %) provide specific impulses in the range of 235–256 s. Without the addition of a binder, the mixtures of oxidizer and aluminum (**1–5** 85 %, Al 15 %) yield values in the range of $I_{sp} = 244$ –274 s, which outnumbers the optimized composite of AP. The highest specific impulse for a neat compound was calculated for *N,N'*-(tris(nitratomethyl)-methyl)-1,3-dinitramino-2-nitratopropane (**4**) with $I_{sp} = 261$ s, hence equal with the ammonium perchlorate system.

1.4 Conclusion

Several new organic nitrates were synthesized and fully characterized in this study. The synthesis combines multiple advantages, such as economic and readily available starting materials, the facile nitration, the moderate-to-good yields and a fast work-up. The obtained products are already pure or readily purified with a simple crystallization. The molecular structure of all new compounds was determined using single crystal X-ray diffraction. Their energetic parameters were calculated and compared to the common secondary explosive PETN as well as the standard oxidizer ammonium perchlorate. The energetic performance data of 5-nitro-4,4-bis(nitratomethyl)oxazolidone (**5**) is comparable with the one from PETN, but the cyclic compound **5** is superior in terms of sensitivity towards impact and friction. Several formulations combining aluminum with the new nitrates **1–5** as oxidizers reach high values of specific impulses I_{sp} , which may even outnumber the optimized formulation of the ammonium perchlorate system AP/Al/binder.

1.5 Experimental Section

1.5.1 General Information

Solvents were dried and purified with standard methods. Tris(hydroxymethyl)-aminomethane (TRIS), bis(2-hydroxyethyl)amino-tris(hydroxymethyl)methane (BISTRIS) and *N*-(tris(hydroxymethyl)methyl)glycine (TRICINE) are commercially available and used without further purification. Raman spectra were recorded in glass tube with a Bruker MultiRAM FT-Raman spectrometer with a Klaastech DENICAFC LC-3/40 laser (Nd:YAG, 1064 nm, up to 1000 mW) in the range of 4000–400 cm^{-1} . Relative intensity is given in percent. IR spectra were recorded with a Perkin-Elmer Spectrum BX-FTIR spectrometer coupled with a Smiths ATR DuraSample IRII device. Measurements were recorded in the range of 4000–650 cm^{-1} . All Raman and IR

spectra were measured at ambient temperature. NMR spectra were recorded with JEOL Eclipse and Bruker TR 400 MHz spectrometers at 25 °C. Chemical shifts were determined in relation to external standards Me₄Si (¹H, 399.8 MHz); (¹³C, 100.5 MHz); MeNO₂ (¹⁴N, 28.9 MHz). Elemental analyses (CHN) were obtained with a Vario EL Elemental Analyzer.

The sensitivity data were acquired by measurements with a BAM drophammer and a BAM friction tester.³ Melting and decomposition points were determined by differential scanning calorimetry (DSC) using a Perkin-Elmer Pyris6 DSC at a heating rate of 5 °C min⁻¹. Measurements were performed in closed aluminum containers against empty containers up to 400 °C via nitrogen flows.

1.5.2 X-ray Crystallography

The crystal structure data were obtained using an Oxford Xcalibur CCD Diffraktometer with a KappaCCD detector at low temperature (173 K, 123 K). Mo-K_α radiation ($\lambda = 0.71073 \text{ \AA}$) was delivered by a Spellman generator (voltage 50 kV, current 40 mA). Data collection and reduction were performed using the CRYSTALIS CCD¹⁴ and CRYSTALIS RED¹⁵ software, respectively. The structures were solved by SIR92/SIR97¹⁶ (direct methods) and refined using the SHELX-97¹⁷ software, both implemented in the program package WinGX22.¹⁸ Finally, all structures were checked using the PLATON software.¹⁹ Structures displayed with ORTEP plots are drawn with thermal ellipsoids at 50 % probability level.

1.5.3 Computational Details

The theoretical calculations were achieved by using the Gaussian 09 program package¹² and were visualized by using GaussView 5.08.²⁰ Optimizations and frequency analyses were performed at the B3LYP level of theory (Becke's B3 three parameter hybrid functional by using the LYP correlation functional) with a cc-pVDZ basis set. After correcting the optimized structures with zero-point vibrational energies, the enthalpies and free energies were calculated on the CBS-4M (complete basis set) level of theory.²¹ The detonation parameters were obtained by using the EXPL05 (V6.02) program package.^{13, 22}

1.5.4 Synthesis

CAUTION! The nitrates **1–5** are energetic materials and show sensitivities in the range of secondary and primary explosives! They should be handled with caution during synthesis or manipulation and additional protective equipment (leather jacket, face shield, ear protection, Kevlar gloves) is strongly recommended.

1 Organic Nitrates Derived from TRIS

Bis(2-nitratoethyl)amino-tris(nitratomethyl)methane (1): BISTRIS (3.14 g, 15 mmol) was solved in 3 mL of glacial acetic acid and cooled with an ice bath. Simultaneously, more glacial acetic acid (14 mL), acetic anhydride (16 mL) and white fuming nitric acid (5.5 mL) were added with the temperature ranging between 9–13 °C. After 30 min at low temperature, the solution was poured on ice and a yellow oil precipitated, which was separated. The oil solidified after a short period of time and was recrystallized from boiling methanol to yield **1** (2.95 g, 45 %) as colorless crystalline blocks.

¹H NMR (acetone-D₆): δ = 4.9 (br, 6H, CH₂), 4.71 (t, 4H, ³J¹H,¹H) = 6 Hz, CH₂), (s, 4H, ³J¹H,¹H) = 6 Hz, CH₃); ¹³C{¹H} NMR (acetone-D₆): δ = 73.2 (CH₂CH₂N), 71.8 (CH₂C), 62.5 (C(CH₂)₃), 48.3 (CH₂CH₂N); ¹⁴N NMR (acetone-D₆): δ = -42 (ONO₂), -45 (ONO₂); Raman (800 mW): 3040 (31), 3010 (45), 2993 (76), 2967 (79), 2912 (29), 2897 (30), 2872 (28), 2859 (29), 1658 (17), 1646 (20), 1636 (29), 1622 (13), 1491 (16), 1472 (23), 1456 (26), 1442 (21), 1397 (12), 1374 (13), 1341 (11), 1323 (10), 1308 (18), 1296 (81), 1283 (64), 1273 (42), 1260 (17), 1244 (15), 1206 (9), 1184 (9), 1115 (21), 1061 (28), 1030 (10), 1006 (14), 974 (15), 962 (12), 949 (10), 892 (26), 865 (100), 852 (47), 836 (16), 771 (12), 755 (10), 736 (15), 712 (25), 691 (14), 670 (9) cm⁻¹. IR: 3567 (w), 2906 (w), 2362 (w), 1629 (vs), 1611 (s) 1487 (w), 1461 (w), 1439 (w), 1400 (w), 1931 (w), 1371 (w), 1341 (w), 1309 (w), 1271 (vs), 1183 (w), 1129 (w), 1115 (w), 1082 (w), 1006 (m), 989 (m), 964 (m), 946 (m), 893 (m), 859 (vs), 828 (vs), 770 (m), 753 (s), 732 (s), 710 (m), 689 (m) cm⁻¹. MS (EI) [m/z]: 434 [M⁺] <1 %, 358 [M⁺-CH₂ONO₂] 44 %, 46 [NO₂⁺] 100 %. C₈H₁₄N₆O₁₅ (434.23 g mol⁻¹): C 22.13, H 3.25, N 19.35; found C 22.15, H 3.51, N 19.22. Dec. point: 108 °C. Sensitivities (BAM): impact 8 J; friction 80 N; ESD 0.7 J (grain size 500–1000 µm).

N,N'-Bis(tris(nitratomethyl)methyl)malonamide (2): The starting material *N,N'*-bis(tris(hydroxymethyl)methyl)malonamide⁷ (620 mg, 2 mmol) was added drop-wise to ice-cold white fuming nitric acid (5 mL). After the solution was stirred at 0 °C for 1 hour, it was poured on ice to give a colorless precipitate. This solid was further purified by recrystallization from ethanol, yielding 640 mg (55%) of **2**.

¹H NMR (acetone-D₆): δ = 8.0 (br, 2H, NH), 5.04 (s, 12H, CH₂), 3.29 (s, 2H, CH₂); ¹³C{¹H} NMR (acetone-D₆): δ = 168.6 (CO), 70.1 (CH₂), 57.3 (C(CH₂)₃), 44.6 (COCH₂CO); ¹⁴N NMR (acetone-D₆): δ = -46 (NO₂); Raman (800 mW): 3027 (28), 3012 (35), 3000 (36), 2976 (85), 2908 (32), 1673 (41), 1651 (35), 1462 (40), 1390 (24), 1343 (21), 1299 (36), 1286 (100), 1263 (29), 1244 (28), 1183 (20), 1047 (48), 1026 (35), 921 (26), 905 (22), 875 (79), 856 (49), 733 (24), 684 (27), 626 (46), 599 (57), 562 (29), 532 (23), 480 (25), 449 (26), 425 (28), 381 (19), 373 (19), 308 (33), 294 (27), 269 (37), 253 (31), 229 (60) cm⁻¹. IR: 3293 (m), 3084 (w), 1736 (w), 1689 (w),

1640 (vs), 1570 (m), 1546 (m), 1463 (w), 1370 (m), 1320 (m), 1271 (vs), 1261 (vs), 1184 (m), 1035 (s), 1017 (s), 994 (m), 958 (w), 918 (w), 828 (vs), 748 (s), 732 (s), 702 (m), 650 (m), 634 (m) cm^{-1} . MS (EI) [m/z]: 582 [M^+] <1 %, 454 [$\text{M}^+ - 2(\text{ONO}_2)$] 100 %. $\text{C}_{11}\text{H}_{16}\text{N}_8\text{O}_{20}$ (580.29 g mol⁻¹): C 19.31, H 2.78, N 19.31; found C 23.07, H 2.94, N 19.01. Dec. point: 104 °C. Sensitivities (BAM): impact 4 J; friction 324 N; ESD 0.6 J (grain size <100 μm).

N-(Tris(nitratomethyl)methyl)nitramino glycine (3): TRICINE (358 mg, 2 mmol) was slowly added to ice-cold white fuming nitric acid (5 mL). After the solution was stirred at 0 °C for 2 hours, it was poured on ice to give a colorless precipitate. After recrystallization from ethanol, 433 mg (60 %) of compound **3** was obtained as a colorless solid.

¹H NMR (acetone-D₆): δ = 11.85 (s, 1H, CO_2H), 5.35 (s, 6H, CH_2), 4.84 (s, 2H, $\text{CH}_2\text{CO}_2\text{H}$); ¹³C{¹H} NMR (acetone-D₆): δ = 168.6 (CO), 70.4 (CH_2), 66.6 ($\text{C}(\text{CH}_2)_3$), 51.6 ($\text{CH}_2\text{CO}_2\text{H}$); ¹⁴N NMR (acetone-D₆): δ = -34 (NNO_2), -48 (ONO_2); Raman (800 mW): 3054 (22), 3037 (62), 2997 (71), 2986 (77), 2975 (65), 2956 (31), 2941 (17), 2934 (18), 1673 (27), 1658 (26), 1648 (18), 1634 (19), 1544 (18), 1489 (20), 1462 (37), 1451 (22), 1423 (23), 1403 (18), 1360 (16), 1331 (26), 1301 (100), 1287 (58), 1268 (36), 1254 (32), 1095 (45), 1075 (28), 957 (19), 941 (54), 908 (39), 889 (21), 863 (84), 846 (58), 822 (24), 734 (23), 698 (31), 653 (54), 638 (50), 582 (25), 559 (18), 539 (39), 480 (24), 450 (24), 419 (31), 394 (24), 358 (18) cm^{-1} . IR: 2922 (w), 1738 (m), 1649 (vs), 1623 (s), 1542 (s), 1461 (m), 1443 (m), 1419 (m), 1375 (w), 1351 (m), 1267 (vs), 1246 (vs), 1173 (w), 1121 (w), 1094 (w), 1075 (w), 1035 (w), 1022 (w), 959 (w), 940 (m), 982 (m), 833 (vs), 750 (m), 723 (m), 698 (m), 660 (s), 636 (m) cm^{-1} . MS (EI) [m/z]: 360 [M^+] <1 %, 283 [$\text{M}^+ - \text{CH}_2\text{ONO}_2$] 22 %, 46 [NO_2^+] 100 %. $\text{C}_6\text{H}_9\text{N}_5\text{O}_{13}$ (359.16 g mol⁻¹): C 20.06, H 2.53, N 19.50; found C 20.43, H 2.57, N 19.03. Dec. point: 136 °C. Sensitivities (BAM): impact 2 J; friction 360 N; ESD 0.6 J (grain size <100 μm).

N,N'-Bis(tris(nitratomethyl)methyl)-1,3-dinitramino-2-nitratopropane (4): *N,N'*-bis-(tris(hydroxymethyl)methyl)-1,3-diammonium-2-propanol dichloride⁸ (500 mg, 1.3 mmol) was dissolved in 3 mL glacial acetic acid and cooled with an ice bath. Simultaneously, more glacial acetic acid (14 mL), acetic anhydride (16 mL) and red fuming nitric (5.5 mL) were added with the temperature ranging between 9–13 °C. After 30 min at low temperature, the solution was poured on ice and a colorless solid precipitated. Compound **4** (576 mg) was obtained as NMR-pure substance in 63% yield.

¹H NMR (acetone-D₆): δ = 6.16 (m, 1H, CH), 5.145 (s, 6H, CHH), 5.142 (s, 6H, CHH), 4.57 (dd, 2H, $^1\text{J}(\text{H}, \text{H})$ = 16.6 Hz, $^3\text{J}(\text{H}, \text{H})$ = 3.2 Hz, CH_2), 4.33 (dd, 2H, $^1\text{J}(\text{H}, \text{H})$ = 16.7 Hz, $^3\text{J}(\text{H}, \text{H})$ = 8.6 Hz, CH_2); ¹³C{¹H} NMR (acetone-D₆): δ = 78.5 (CH), 70.2 (CH_2), 66.6 (CH_2), 51.2 ($\text{C}(\text{CH}_2)_3$);

1 Organic Nitrates Derived from TRIS

¹⁴N NMR (acetone-D₆): δ = -32 (NNO₂), -48 (ONO₂); Raman (400 mW): 3048 (12), 2990 (20), 2965 (13), 2505 (11), 2182 (14), 2119 (16), 1667 (45), 1652 (45), 1471 (53), 1435 (49), 1382 (52), 1297 (100), 1107 (44), 1057 (42), 1020 (43), 990 (44), 924 (42), 874 (55), 849 (55), 799 (45), 619 (68) cm⁻¹. IR: 2929 (w), 1752 (w), 1683 (m), 1659 (s), 1638 (vs), 1571 (m), 1539 (m), 1470 (m), 1434 (m), 1399 (w), 1372 (m), 1294 (s), 1273 (vs), 1162 (w), 1105 (m), 1069 (m), 1055 (m), 1015 (s), 998 (m), 950 (w), 925 (w), 843 (vs), 771 (m), 748 (s), 716 (m), 679 (m), 643 (w), 618 (w) cm⁻¹. MS (EI) [m/z]: 702 [M⁺] <1 %, 314 [M⁺ -C₅H₈N₄O₈] 100 %. C₁₁H₁₇N₁₁O₂₅. (703.31 g mol⁻¹): C 18.79, H 2.44, N 21.91; found C 19.43, H 2.66, N 20.79. Dec. point: 150 °C. Sensitivities (BAM): impact 2 J; friction 128 N; ESD 0.4 J (grain size <100 µm).

5-Nitro-4,4-bis(nitratomethyl)oxazolidone (5): 1.0 g (6.8 mmol) of 4,4-dimethylol-oxazolidone⁹ was added to precooled mixed acid (6 mL HNO₃/6 mL H₂SO₄) and the temperature was maintained at 5–10 °C during the addition. Afterwards the temperature was raised to 50 °C for 1 h. The reaction was poured on ice and the colorless precipitate was filtered off. Crystallization from methanol yielded 1.4 g (72 %) of pure 5-nitro-4,4-bis(nitratomethyl)oxazolidone (5) as colorless needles.

¹H NMR (acetone-D₆): δ = 5.40 (d, 2H, H_A, ²J¹H, ¹H) = 11.4 Hz, CH_AH_BONO₂), 5.20 (d, 2H, H_B, ²J¹H, ¹H) = 11.4 Hz, CH_AH_BONO₂), 4.79 (s, 2H, CH₂); ¹³C{¹H} NMR (acetone-D₆): δ = 147.1 (CO), 70.5 (CH₂), 66.4 (CH₂), 63.6 (C(CH₂)₃); ¹⁴N NMR (acetone-D₆): δ = -48 (NO₂), -52 (ONO₂); Raman (800 mW): 3034 (35), 2994 (66), 2949 (34), 1539 (18), 1471 (26), 1414 (23), 1404 (24), 1351 (29), 1306 (66), 1276 (40), 1045 (24), 971 (21), 942 (21), 857 (100), 829 (25), 643 (37), 495 (18), 252 (24) cm⁻¹. IR: 3031 (w), 2985 (w), 2913 (w), 1815 (m), 1647 (vs), 1632 (s), 1598 (m), 1466 (m), 1402 (w), 1391 (w), 1368 (w), 1279 (vs), 1260 (s), 1227 (m), 1170 (m), 1131 (m), 1092 (m), 1040 (m), 999 (s), 945 (w), 855 (s), 824 (s), 749 (s), 735 (s), 701 (s), 662 (w), 624 (m) cm⁻¹. MS (EI) [m/z]: 281 [M⁺] 1 %, 206 [M⁺ -CH₂ONO₂] 100 %. C₅H₆N₄O₁₀. (282.12 g mol⁻¹): C 21.29, H 2.14, N 19.86; found C 21.51, H 2.19, N 18.66. Mp.: 120 °C. Dec. point: 160 °C. Sensitivities (BAM): impact 10 J; friction 240 N; ESD 0.6 J (grain size 500 – 1000 µm).

1.6 References

- [1] a) J. Akhavan, *The Chemistry of Explosives*, Royal Society of Chemistry, **2011**; b) J. Köhler, R. Meyer, A. Homburg, *Explosives*, Wiley-VCH, Weinheim, **2007**.
- [2] J. P. Agrawal, *High Energy Materials*, Wiley-VCH, Weinheim, **2010**.
- [3] T. M. Klapötke, *Chemistry of High-Energy Materials*, De Gruyter, Berlin, **2015**.
- [4] D. E. Chavez, M. A. Hiskey, D. L. Naud, D. Parrish, *Angew. Chem. Int. Ed.* **2008**, *47*, 8307–8309.
- [5] T. M. Klapötke, B. Krumm, X. F. Steemann, K. Umland, *Z. Anorg. Allg. Chem.* **2010**, *636*, 2343–2346.
- [6] a) M. B. Frankel, US 3278578, **1966**; b) T. M. Klapötke, N. T. Mayr, *New Trends in Res. Energ. Mater., Proc. Semin.*, **10th**, **2007**, 773–782.
- [7] C. Fernandes, J. L. Wardell, J. M. S. Skakle, *Acta Crystallogr., Sect. C* **2002**, *58*, 499–502.
- [8] J. S. Pierce, J. H. Wotiz, US 2408096, **1946**.
- [9] A. T. Blomquist, F. T. Fiedorek, US 2485855, **1949**.
- [10] L. Stefaniak, G. A. Webb, M. Witanowski, *Annual Reports on NMR Spectroscopy*, Academic Press Inc, San Diego, **1993**, *25*, 63–64.
- [11] T. Steiner, *Angew. Chem. Int. Ed.* **2002**, *41*, 48–76.
- [12] M. J. Frisch, G. W. Trucks, H. B. Schlegel, G. E. Scuseria, M. A. Robb, J. R. Cheeseman, G. Scalmani, V. Barone, B. Mennucci, G. A. Petersson, H. Nakatsuji, M. Caricato, X. Li, H. P. Hratchian, A. F. Izmaylov, J. Bloino, G. Zheng, J. L. Sonnenberg, M. Hada, M. Ehara, K. Toyota, R. Fukuda, J. Hasegawa, M. Ishida, T. Nakajima, Y. Honda, O. Kitao, H. Nakai, T. Vreven, J. A. Montgomery Jr., J. E. Peralta, F. Ogliaro, M. J. Bearpark, J. Heyd, E. N. Brothers, K. N. Kudin, V. N. Staroverov, R. Kobayashi, J. Normand, K. Raghavachari, A. P. Rendell, J. C. Burant, S. S. Iyengar, J. Tomasi, M. Cossi, N. Rega, N. J. Millam, M. Klene, J. E. Knox, J. B. Cross, V. Bakken, C. Adamo, J. Jaramillo, R. Gomperts, R. E. Stratmann, O. Yazyev, A. J. Austin, R. Cammi, C. Pomelli, J. W. Ochterski, R. L. Martin, K. Morokuma, V. G. Zakrzewski, G. A. Voth, P. Salvador, J. J. Dannenberg, S. Dapprich, A. D. Daniels, Ö. Farkas, J. B. Foresman, J. V. Ortiz, J. Cioslowski, D. J. Fox, Gaussian, Inc., *Gaussian 09*, Wallingford, **2009**.
- [13] M. Suceska, *EXPLO5*, v.6.02, Zagreb, **2013**.
- [14] Oxford Diffraction Ltd., *CrysAlis CCD*, 1.171.35.11, Abingdon, Oxford (U.K.), **2011**.
- [15] Oxford Diffraction Ltd., *CrysAlis RED*, 1.171.35.11, Abingdon, Oxford (U.K.), **2011**.
- [16] A. Altomare, M. C. Burla, M. Camalli, G. L. Cascarano, C. Giacovazzo, A. Gualandi, A. G. G. Moliterni, G. Polidori, R. Spagna, *J. Appl. Crystallogr.* **1999**, *32*, 155–119.
- [17] a) G. M. Sheldrick, *Programs for Crystal Structure Determination*, University of Göttingen, Germany, **1997**; b) G. M. Sheldrick, *Acta Crystallogr.* **2008**, *64 A*, 112–122.
- [18] L. Farrugia, *J. Appl. Crystallogr.* **1999**, *32*, 837–838.
- [19] A. L. Spek, *Acta Crystallogr.* **2009**, *65 D*, 148–155.
- [20] R. D. Dennington, T. A. Keith, J. M. Millam, *GaussView*, v. 5.08, Semichem, Inc., Wallingford, **2009**.

1 Organic Nitrates Derived from TRIS

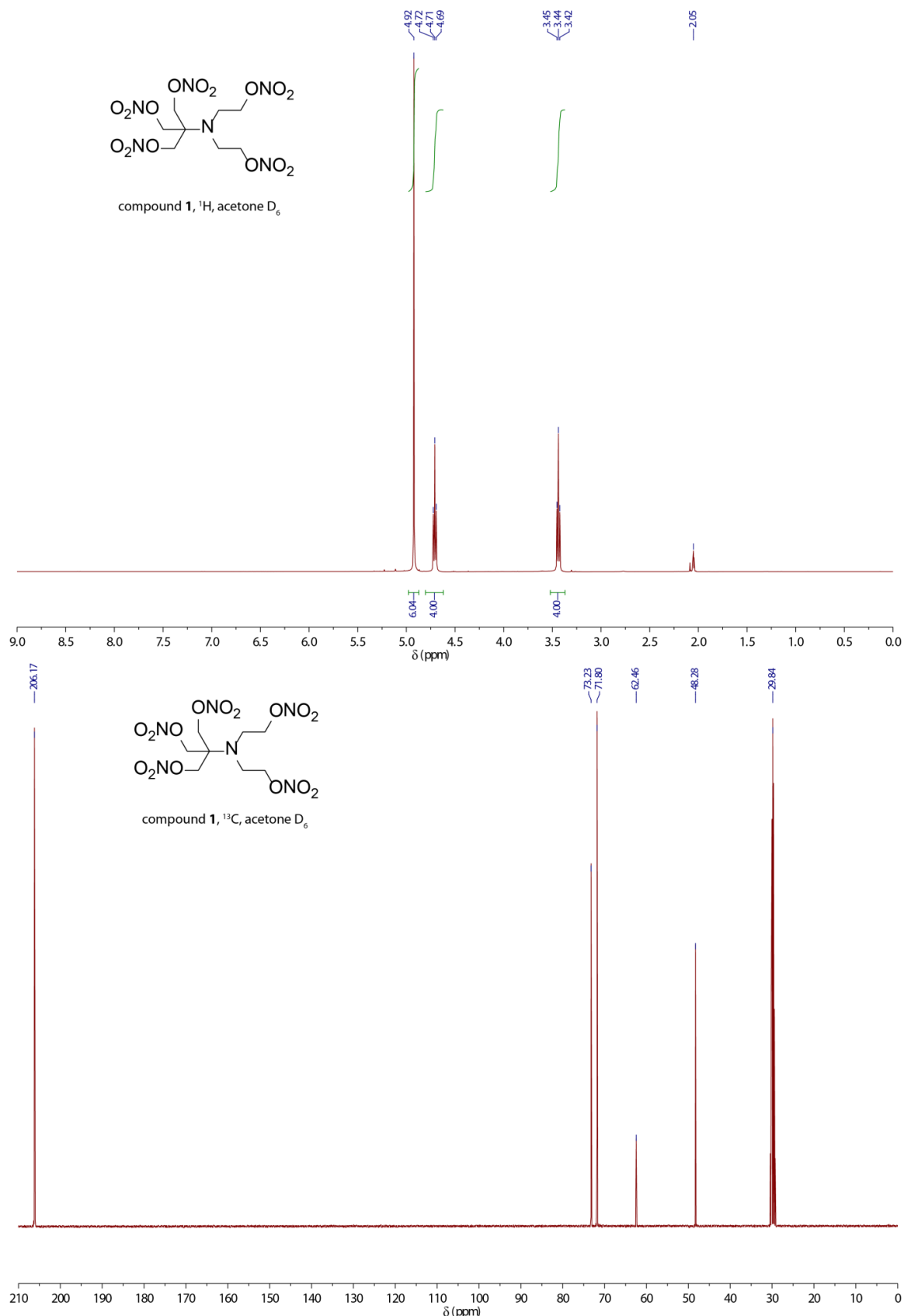
- [21] J. A. Montgomery, M. J. Frisch, J. W. Ochterski, G. A. Petersson, *J. Chem. Phys.* **2000**, *112*, 6532–6542.
- [22] M. Suceska, *Propellants Explos. Pyrotech.* **1991**, *16*, 197–202.

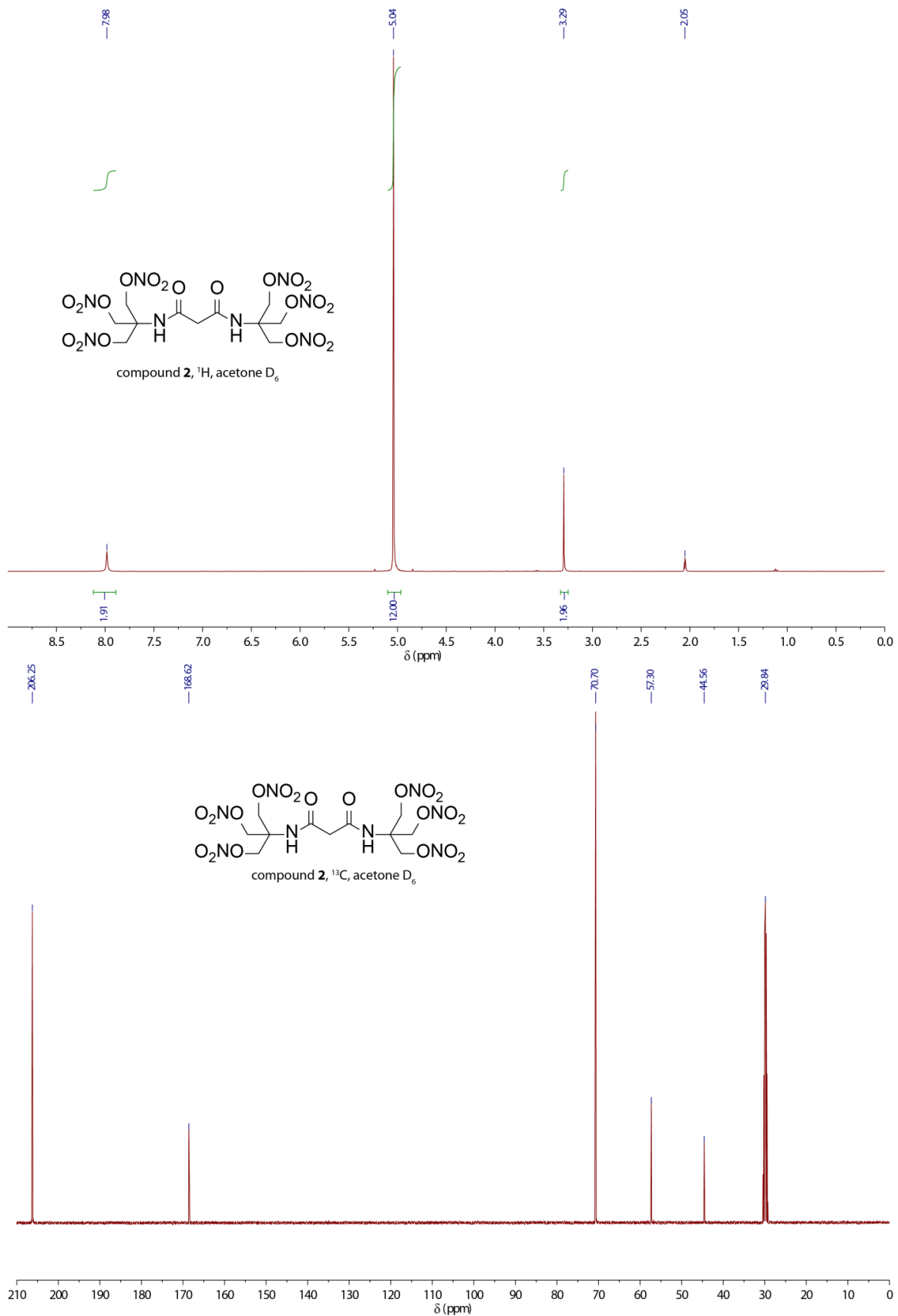
1.7 Supporting Information

- 1 ^1H and ^{13}C NMR data of nitrate **1**
- 2 ^1H and ^{13}C NMR data of nitrate **2**
- 3 ^1H and ^{13}C NMR data of nitrate **3**
- 4 ^1H and ^{13}C NMR data of nitrate **4**
- 5 ^1H and ^{13}C NMR data of nitrate **5**

1 Organic Nitrates Derived from TRIS

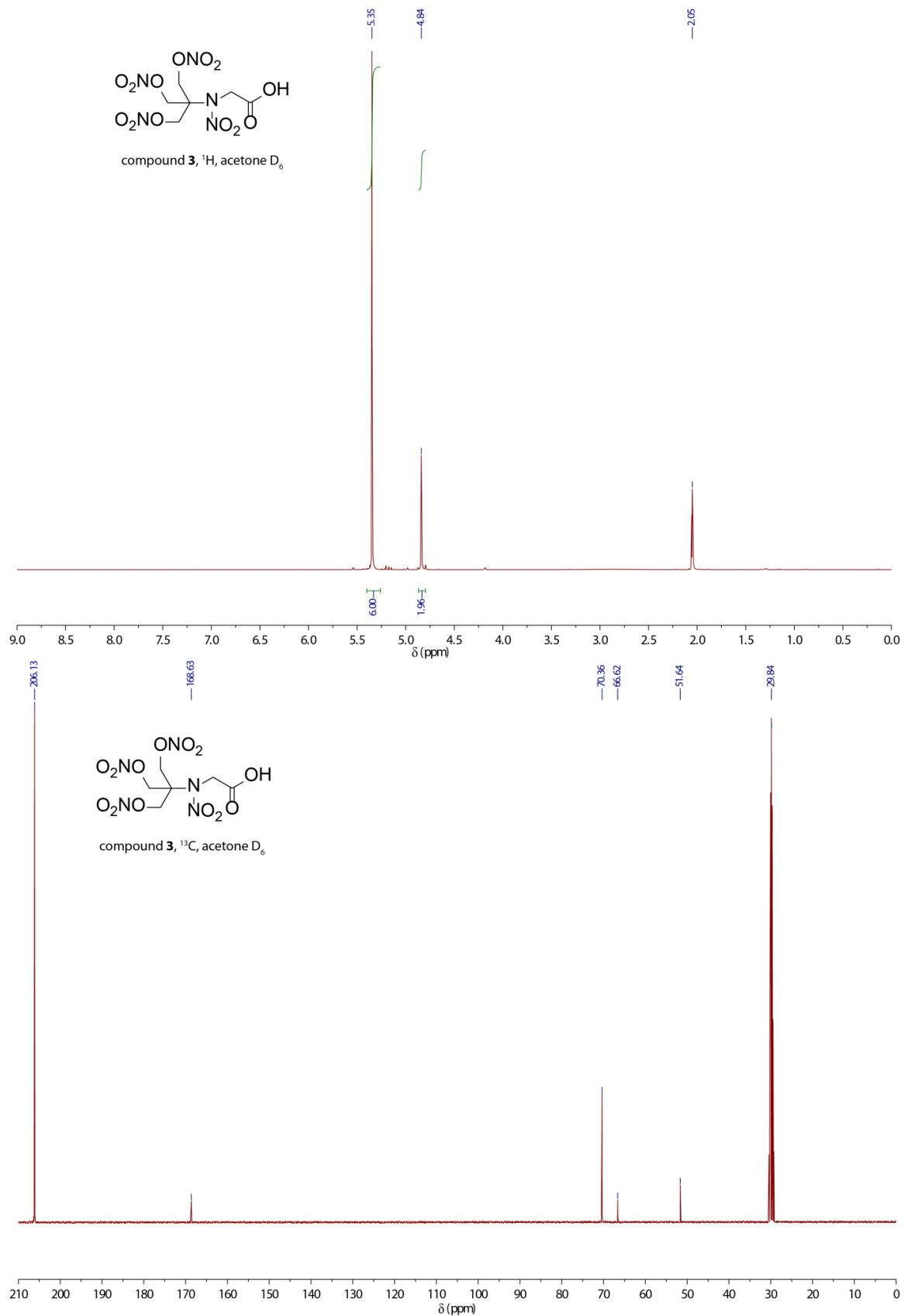
1 ^1H and ^{13}C NMR data of nitrate **1**

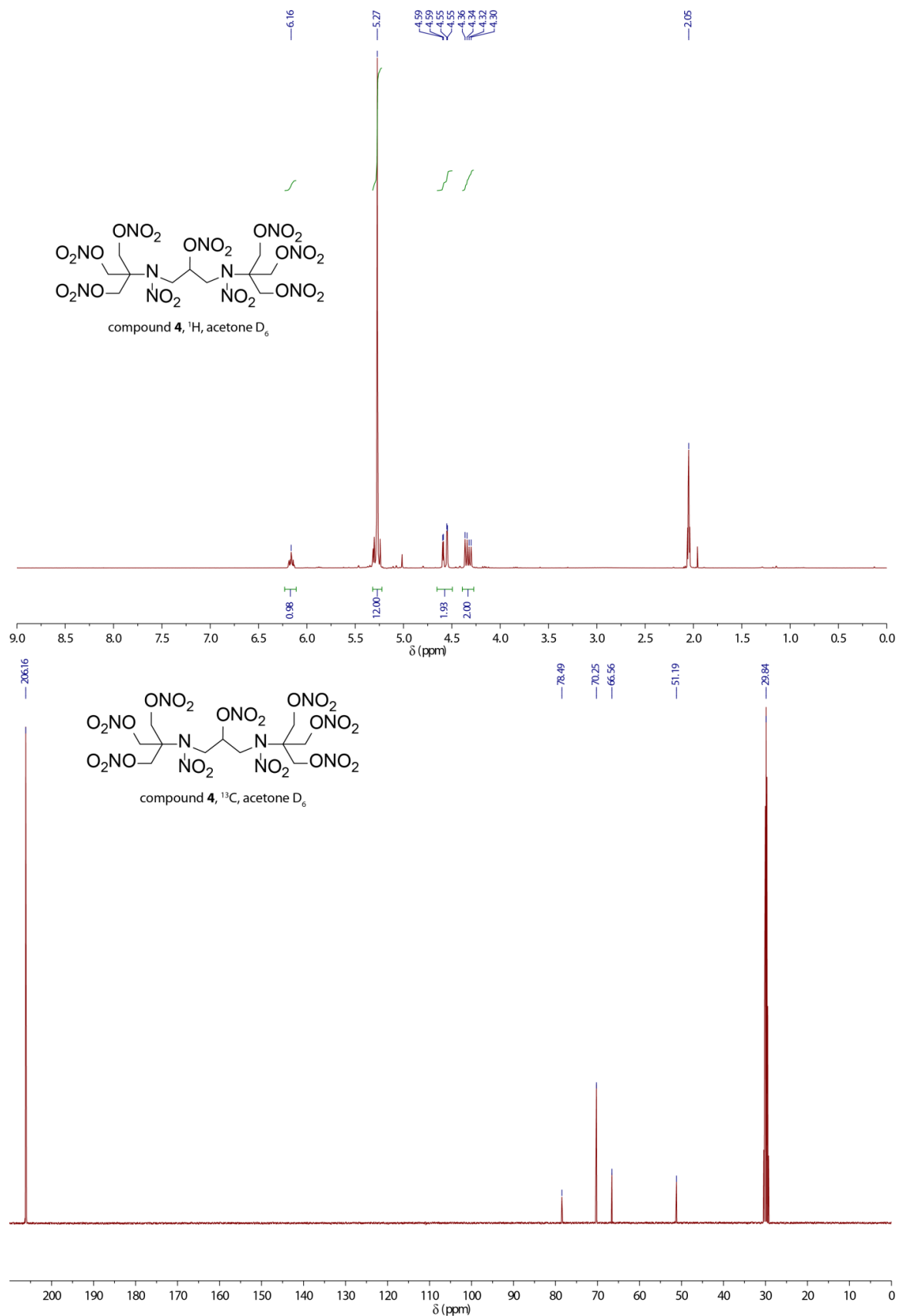


2 ^1H and ^{13}C NMR data of nitrate 2

1 Organic Nitrates Derived from TRIS

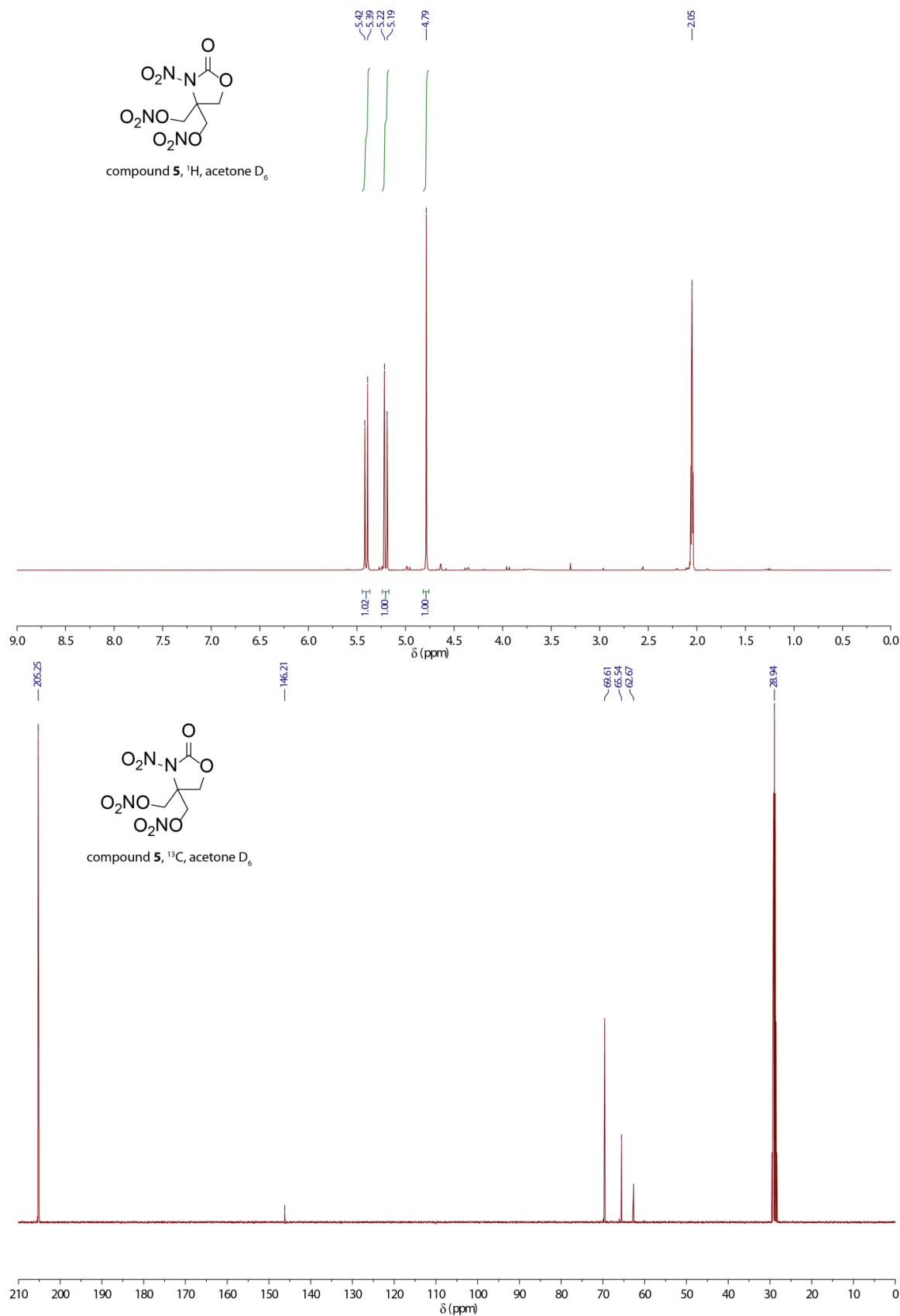
3 ^1H and ^{13}C NMR data of nitrate 3



4 ^1H and ^{13}C NMR data of nitrate **4**

1 Organic Nitrates Derived from TRIS

5 ^1H and ^{13}C NMR data of nitrate 5



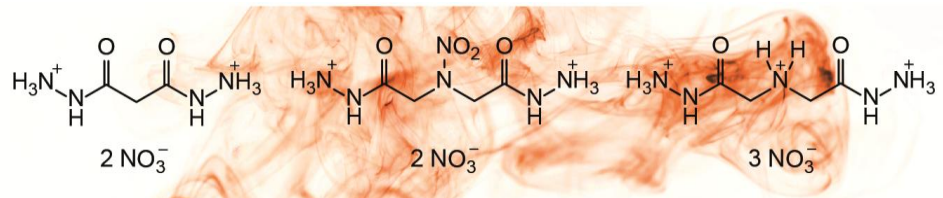
2 Ionic Nitrates Derived from Dihydrazides

DIHYDRAZINIUM NITRATES DERIVED FROM MALONIC AND IMINODIACETIC ACID

Thomas M. Klapötke, Burkhard Krumm, and Thomas Reith

as published in

Propellants, Explosives, Pyrotechnics **2018**, accepted



2.1 Abstract

Several hydrazinium nitrates were synthesized on the basis of malonic acid and iminodiacetic acid. The reaction of the corresponding ethyl esters with hydrazine hydrate yielded the dihydrazides in good-to-high yields and high purity. Subsequent protonation with diluted nitric acid or hydrochloric acid resulted in the corresponding nitrate and chloride salts. The neutral compounds and their salts were fully characterized, including multinuclear NMR spectroscopy, vibrational analysis, X-ray diffraction, differential thermal analysis and elemental analysis. The energies of formation were calculated with the GAUSSIAN program package and the detonation parameters were predicted using the EXPL05 computer code.

2.2 Introduction

The ongoing research for safe and environmentally benign energetic materials provides numerous approaches to find replacements for currently used explosives.¹ The development of various energetic salts has shown great potential in all fields of energetic materials, such as primary explosives (K_2DNABT)², secondary explosives (TKX-50)³ and high energy dense oxidizers (ADN)⁴ (Figure 2.1).

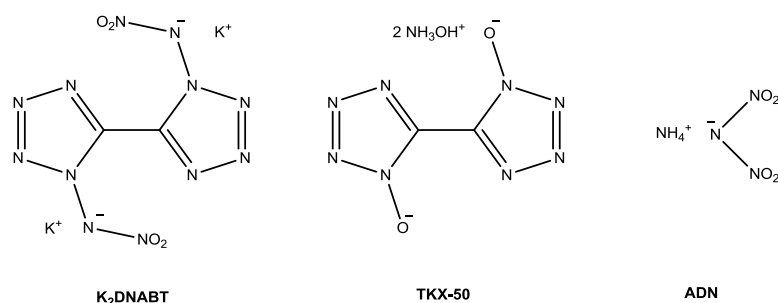


Figure 2.1: Potassium 1,1'-dinitramino-5,5'-bistetrazole (K_2DNABT), dihydroxylammonium 5,5'-bistetrazole-1,1'-diolate (TKX-50) and ammonium dinitramide (ADN).

The recent synthesis and characterization of the nitrate and dinitrate salts of diaminourea⁵ and oxalyldihydrazide⁶ (Figure 2.2) prompted us for further studies on organic hydrazinium nitrates, also because of their scalable and cost-efficient synthesis in combination with good performance and toxicity values.

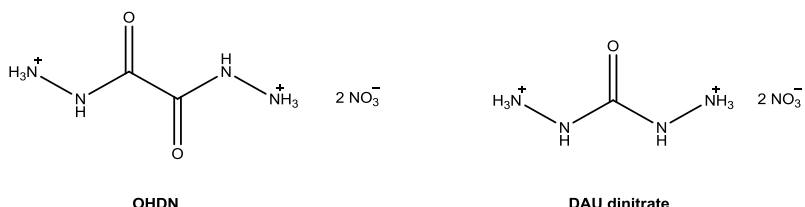


Figure 2.2: Oxalyldihydrazinium dinitrate (OHDN) and diaminourea (DAU) dinitrate.

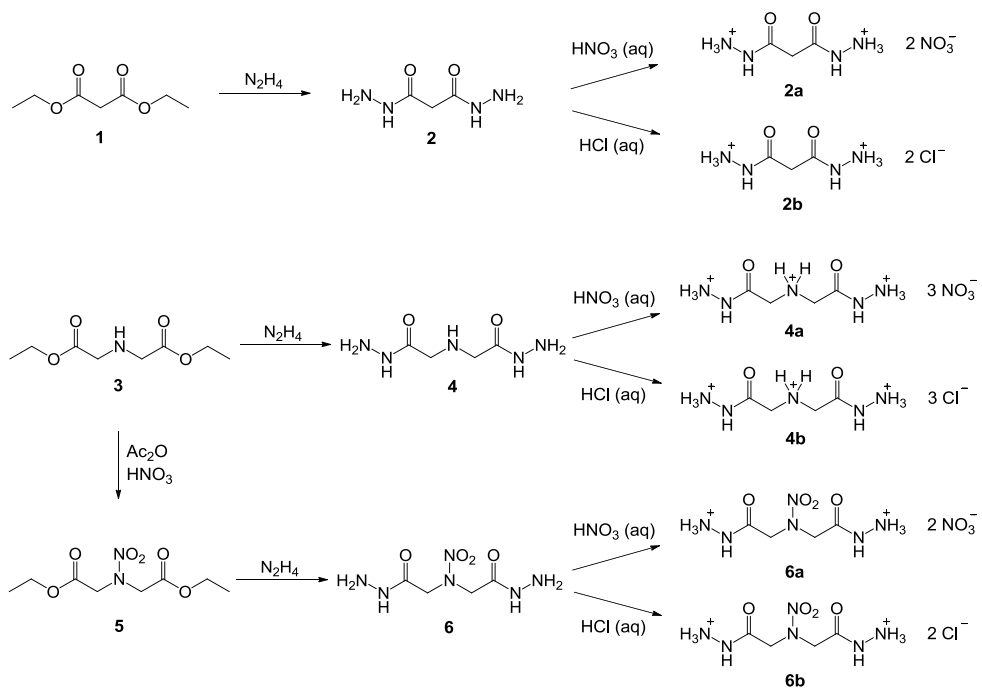
The mononitrates of diaminourea and oxalyldihydrazide are much more stable in terms of thermal decomposition and external stimuli like impact and friction in comparison to the corresponding dinitrates. Therefore, the mononitrates are competitors in the field of insensitive munitions, whereas the positive oxygen balance of the dinitrates distinguishes them as possible high energy dense oxidizers (HEDOs) to replace ammonium perchlorate.⁵⁻⁶

In order to synthesize thermally stable dinitrates, spacers were introduced to separate the hydrazide groups. An introduction of oxygen would lead to acid anhydride type compounds, which are highly sensitive to hydrolysis.⁷ Furthermore, the incorporation of nitrogen as spacer results in iminodicarbonyl dihydrazide and hydrazinedicarbonyl dihydrazide.⁸ The hydrazides of both molecules are known, but undergo a fast acid-catalyzed cyclization to urazole and urazine, respectively, which prevents the formation of nitrate salts.^{8b} As a consequence, carbon based spacers are introduced between the hydrazide units leading to malonic acid derivatives. Additionally, 2-azapropylene units as a combination of the latter forming iminodiacetic acid derivatives, were investigated.

2.3 Results and Discussion

2.3.1 Synthesis

The diethylesters **1** and **3** were either commercially available or synthesized from the corresponding acid according to literature procedures.⁹ The dihydrazides **2** and **4** can easily be obtained by the conversion of the diethylesters (**1**, **3**) with hydrazine hydrate described in literature.^{10, 11} The nitramino compound **5** was obtained from a nitration of **3** in a mixture of acetic anhydride and anhydrous nitric acid. The reaction with hydrazine hydrate at low temperatures yielded the dihydrazide **6** in good yields. The three dihydrazides were converted into their corresponding nitrate (**4a**, **6a**) and chloride salts (**4b**, **6b**) by protonation with diluted nitric acid or hydrochloric acid using different ratios and purification methods (Scheme 2.1).



Scheme 2.1: Synthesis of the nitrate salts **2a**, **4a** and **6a** from malonic acid diethylester (**1**) and aminodiacetic acid diethylester (**3**).

All compounds are colorless, crystalline solids. The hydrazides were obtained in good yields and high purity and were used without further purification. The chloride salts are easily obtainable, as some can be precipitated from the aqueous phase. Purification of the nitrates is more challenging due to their high hygroscopicity, especially regarding the trinitrate **4a**.

2.3.2 NMR Spectroscopy

All compounds were characterized by ^1H and ^{13}C NMR spectroscopy, additionally the ^{14}N NMR spectra for the nitramino containing compounds **5**, **6**, **6a** and **6b** and the nitrates **2a** and **4a** were recorded.

The NMR spectra of nitraminodiacetic acid diethylester (**5**) were recorded in acetone- D_6 . In the ^1H NMR spectrum the ethyl moieties are observed as quartet at 4.21 ppm and triplet at 1.25 ppm ($^3J = 7.1$ Hz). The methylene units next to the nitramine group are observed as singlet at 4.69 ppm. In the ^{13}C NMR spectrum the two non-equivalent methylene groups are observed at 62.2 and 54.0 ppm and the methyl group at 14.4 ppm. The carbonyl carbon atoms are observed in the low field at 167.6 ppm. In the ^{14}N NMR spectrum, a single signal for the nitro nitrogen is detected at -30 ppm.

The NMR spectra of the hydrazides and derived salts were recorded in DMSO-D_6 except **6**, which decomposes in DMSO and therefore was recorded in D_2O .

Regarding the ^1H NMR spectra of the hydrazides **2** and **4**, the signal for the methylene groups can be observed between 3.06 and 2.90 ppm, while the NH resonance is found as a broad signal around 4.2 ppm and the NH_2 resonances are more low field shifted at 9.0 ppm. For the hydrazide **6** the methylene signal is observed at 4.56 ppm, whereas the resonances of the hydrazide groups are not detectable in D_2O . In the ^{13}C NMR spectra all dihydrazides show the corresponding resonances for the carbonyl groups (**2**: 166.0 ppm, **4**: 169.9 ppm, **6**: 167.8 ppm) and the methylene groups (**2**: 40.0 ppm, **4**: 51.0 ppm, **6**: 54.1 ppm). The resonance of the nitro group of **6** is visible at -30 ppm in the ^{14}N NMR spectrum, whereas all hydrazine and amino nitrogen resonances are typically not detected.

Concerning the nitrates **2a**, **4a** and **6a**, their ^1H NMR spectra show the signals for the methylene groups as sharp signal between 4.68–3.35 ppm. The NH , NH_2 and NH_3^+ resonances are broadened due to the quadrupole influence of the neighboring nitrogen atoms. For the malonyl salt **2a**, the NH signal is observed at 11.2 ppm and the NH_2 signal is observed at 9.7 ppm. In the ^1H NMR spectra of the triple protonated salt **4a**, the signals for the NH , NH_2^+ and NH_3^+ groups are very broad and overlap between 12 ppm and 8 ppm. The NH signal for the salt **6a** is found at 11.2 ppm and the NH_3^+ signal is broadened in the area between 11 ppm and 8.5 ppm. In the ^{13}C NMR spectra, the methylene groups are observed at 39.1 (**2a**), 46.0 (**4a**) and 53.4 (**6a**) ppm, and the carbonyl carbon atoms are found between 164.6–165.6 ppm. For the ^{14}N NMR spectra, all compounds show the resonance of the nitrate anion at -4 ppm to -5 ppm, and **6a** shows an additional signal for the nitramine unit at -30 ppm.

In the ^1H NMR spectra of the chloride salts **2b**, **4b** and **6b** the methylene groups are observed at 3.42 ppm (**2b**), 3.98 ppm (**4b**) and 4.71 ppm (**6b**). The NH , NH_2 and NH_3 resonances are broadened and shown between 13 ppm and 9 ppm. In the ^{13}C NMR spectra the compounds show the corresponding signals for the carbonyl (165.5–164.4 ppm) and methylene (53.4–39.0 ppm) carbon groups. In the ^{14}N NMR spectrum of the chloride salt **6b** the nitrogen of the nitramine moiety is observed at -29 ppm.

2.3.3 Single Crystal Structure Analysis

Single crystals suitable for structure determination were obtained for the ethyl ester **5**, the dihydrazide **6** and the nitrate salt **6a** recorded at 143 K (Table 2.1).

Table 2.1: Crystal data, details of the structure determinations and refinement of **5**, **6** and **6a**.

	5	6	6a
formula	$\text{C}_8\text{H}_{14}\text{N}_2\text{O}_6$	$\text{C}_4\text{H}_{10}\text{N}_6\text{O}_4$	$\text{C}_4\text{H}_{12}\text{N}_8\text{O}_{10}$ * $2(\text{CH}_3)_2\text{SO}$
$FW [\text{g mol}^{-1}]$	234.21	206.16	488.47
$T [\text{K}]$	143	143	143
$\lambda [\text{\AA}]$	0.71073	0.71073	0.71073
crystal system	orthorhombic	monoclinic	monoclinic
space group	$Pca2_1$	$P2_1/c$	Pn
crystal size [mm]	0.4 x 0.21 x 0.21	0.31 x 0.27 x 0.04	0.23 x 0.21 x 0.02
crystal habit	colorless needle	colorless platelet	colorless platelet
$a [\text{\AA}]$	17.385 (10)	14.672 (6)	8.096 (6)
$b [\text{\AA}]$	5.849 (3)	6.723 (3)	5.652 (4)
$c [\text{\AA}]$	11.049 (7)	8.077 (3)	22.529 (2)
$\alpha [\text{deg}]$	90	90	90
$\beta [\text{deg}]$	90	96.46 (4)	90.41 (8)
$\gamma [\text{deg}]$	90	90	90
$V [\text{\AA}^3]$	1123.5 (11)	791.6 (6)	1030.9 (2)
Z	4	4	2
$\rho_{\text{calc.}} [\text{g cm}^{-3}]$	1.38	1.73	1.57
μ	0.119	0.152	0.333
$F(000)$	496	432	512
2Θ range [deg]	4.96 – 30.62	5.00 – 31.49	4.48 – 29.48
index ranges	$-23 \leq h \leq 22$ $-7 \leq k \leq 7$ $-14 \leq l \leq 14$	$-18 \leq h \leq 15$ $-8 \leq k \leq 8$ $-9 \leq l \leq 10$	$-10 \leq h \leq 10$ $-5 \leq k \leq 7$ $-29 \leq l \leq 30$
reflections collected	9423	5663	8916
reflections unique	2719	1610	4661
parameters	145	151	275
GooF	1.041	1.058	1.010
$R_1 / wR_2 [I > 2\sigma(I)]$	0.0363 / 0.0857	0.0311 / 0.0722	0.0469 / 0.0773
R_1 / wR_2 (all data)	0.0455 / 0.0920	0.0378 / 0.0764	0.0657 / 0.0841
max / min residual electron density [\AA^{-3}]	-0.259 / 0.224	-0.241 / 0.294	-0.272 / 0.362
CCDC	1821952	1821953	1821954

Single crystals from the nitramine **5** were obtained from ethyl acetate by slow evaporation at room temperature. The nitraminodiacetic acid diethylester (**5**) crystallizes in the orthorhombic space group *Pca*2₁ with four molecules of **5** in the unit cell and a density of 1.38 g cm⁻³ at 143 K (Figure 2.3).

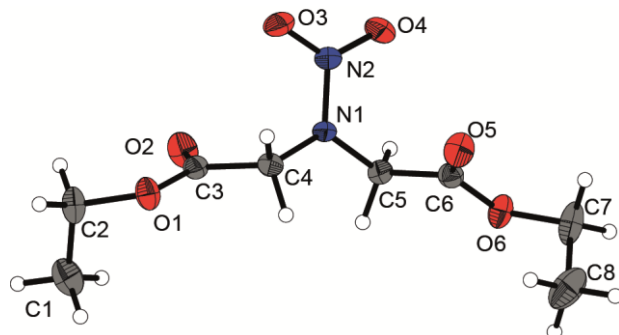


Figure 2.3: X-ray molecular structure of nitraminodiacetic acid diethylester (**5**). Selected atom distances (Å) and angles (deg.): N1–N2 1.342 (2), N1–C4 1.443 (2), N1–C5 1.447 (2), C3–O2 1.193 (2), C3–O1 1.332 (2), C4–N1–C5 123.9 (1), C4–N1–N2 118.1 (1), C4–C3–O2 125.3 (2), O1–C3–O2 125.9 (1); C4–N1–N2–O3 -9.4 (2), C4–N1–N2–O4 170.7 (1), C5–N1–N2–O3 177.5 (1), C5–N1–N2–O4 -2.4 (2).

In the crystalline state compound **5** shows the expected high planarity along the carbonyl units (e.g. torsion angle C4–C3–O1–O2 = 178.2 °). Rather unusual, the nitramino moiety is in planar alignment C4–C5 without avoiding any steric hindrance (e.g. torsion angle O4–N2–N1–C5 = -2.4 °). Regarding the intermolecular structure, the molecules are stacked with the nitramino groups pointing at the amino nitrogen of the neighboring molecule. Weak non-classical hydrogen bonding may explain this molecular grouping. Examples are observed between the nitro oxygens O3 and O4 and the methylene hydrogens C4–H7 and C5–H8 (e.g. DHA C4–H7···O3, bond angle DHA = 149.6 °, d(D–A) = 3.25 Å, d(A–H) = 2.26 Å).¹²

Single crystals from the dihydrazide **6** were obtained from the aqueous work-up by slow evaporation at room temperature. The nitraminodiacetyl dihydrazide (**6**) crystallizes in the monoclinic space group *P*2₁/c with four molecules of **6** in the unit cell and a density of 1.73 g cm⁻³ at 143 K (Figure 2.4). The crystal structure of nitraminodiacetyl dihydrazide (**6**) is much more twisted in comparison to the diethylester precursor **5**. This can be explained with the strong intramolecular hydrogen bonding between the two hydrazide branches (DHA N5–H8···O1, bond angle DHA = 170.5 °, d(D–A) = 2.84 Å, d(H–A) = 2.02 Å). As a consequence, the proton donating branch is less planar than the proton accepting one (e.g. torsion angles C2–C1–N2–H3 -2.0 ° and C3–C4–N5–H8 -8.0 °).

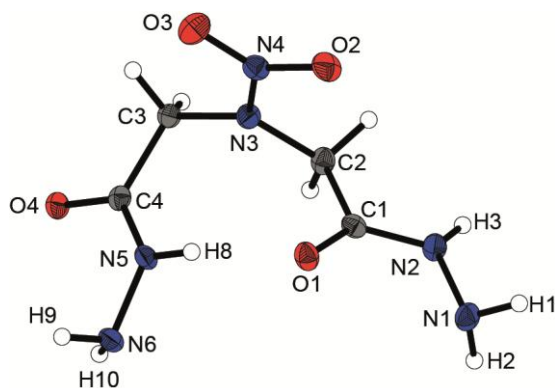


Figure 2.4: X-ray molecular structure of nitraminodiacyl dihydrazide (**6**). Selected atom distances (Å) and angles (deg.): N3–N4 1.352 (2), N4–O3 1.229 (2), C1–O1 1.233 (2), C1–N2 1.330 (2), N1–N2 1.418 (2), N1–H1 0.89 (2), N1–H2 0.91 (2), N2–H3 (2); C2–N3–N4 117.5 (1), C3–N3–N4 119.3 (1), C2–C1–O1 121.9 (1), C2–C1–N2 113.1 (1), N2–C1–O1 124.9 (1); C3–N3–N4–O3 5.0 (2), C3–N3–N4–O2 –176.0 (1), C2–N3–N4–O3 179.7 (1), C2–N3–N4–O2 –1.3 (2), C2–C1–O1–N2 178.2 (2), C2–C1–N2–N1 –169.9 (1), O1–C1–N2–N1 8.4 (2), C2–C1–N2–H3 –2.0 (14), O1–C1–N2–H3 176.4 (14), C3–C4–N5–H8 –8.0 (13), O4–C4–N5–H8 172.9 (13).

Similar to ester **5**, the dihydrazide **6** also shows the high planarity around the nitramino center (torsion angle C2–N3–N4–O2 = –1.2 °). In combination with the twisted structure, multiple intermolecular hydrogen bonds between the free carbonyl oxygen O4 and neighboring hydrazide groups lead to a significant higher density of compound **6** in comparison with the precursor **5** (**5** = 1.38 g cm^{–3}, **6** = 1.73 g cm^{–3}, at 148 K).

Single crystals from the nitrate salt **6a** were obtained from dimethyl sulfoxide by slow evaporation at room temperature. The nitraminodiacyl dihydrazinium dinitrate (**6a**) crystallizes in the monoclinic space group *Pn* with two molecules of **6a** and four solvent molecules DMSO in the unit cell and a density of 1.57 g cm^{–3} at 143 K (Figure 2.5). The crystal structure of the solvent containing nitrate salt **6a** shows many characteristics of the neutral precursor **6**. The structure is twisted again due to intramolecular hydrogen bonding between the two hydrazinium branches. This time, the proton donating dihydrazinium unit is more planar than the proton accepting one (e.g. torsion angles C2–C1–N2–H4 –17.8 ° and C3–C4–N5–H9 –1.0 °). In line with compounds **5** and **6** the nitramino moiety of **6a** shows a high planarity with the carbon atoms C2 and C3.

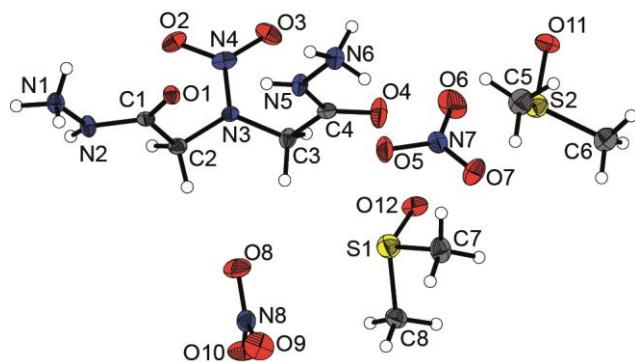


Figure 2.5: X-ray molecular structure of nitraminodiacetyl dihydrazinium dinitrate (**6a**). Selected atom distances (Å) and angles (deg.): N3–N4 1.343 (3), C1–O1 1.221 (4), C1–N2 1.340 (4), N1–N2 1.419 (3); C2–C1–O1 122.3 (3), N2–C1–O1 124.1 (3), C1–N2–N1 117.0 (2); C2–N3–N4–O2 4.8 (4), C2–N3–N4–O3 –177.2 (2), C3–N3–N4–O2 174.0 (2), C3–N3–N4–O3 –7.9 (4), C2–C1–N2–N1 178.9 (2), O1–C1–N2–N1 1.9 (4), C2–C1–N2–H4 –17.8 (4), O1–C1–N2–H4 165.2 (3), C3–C4–N5–H9 –1.0 (4), O4–C4–N5–H9 179.9 (3).

The intermolecular structure is dominated by several strong hydrogen bonds between the hydrazinium moieties and the nitrate anions as well as the DMSO molecules (Figure 2.6, e.g. DHA N1–H1···O10, bond angle DHA = 155.4 °, d(D–A) = 2.80 Å, d(H–A) = 1.95 Å).

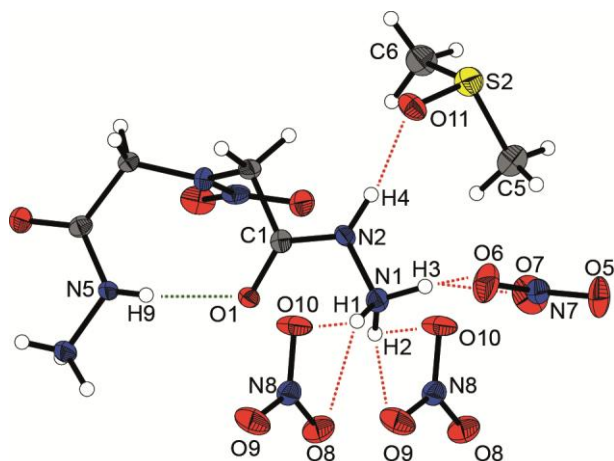


Figure 2.6: Classical intramolecular and intermolecular hydrogen bonds in the crystal structure of **6a**.

2.3.4 Thermal Stabilities and Energetic Properties

The thermal stabilities of all compounds were determined by Differential Thermal Analysis (DTA) measurements. The temperature range of 15–400 °C was recorded with a heating rate of 5 °C min^{–1}. The nitrate salt of malonyldihydrazide (**2a**) has a decomposition temperature of 266 °C. The trinitrate **4a** decomposes at 160 °C and the nitramine containing salt **6a** decomposes at 131 °C. The chloride salts have a decomposition temperature of 195 °C (**2b**),

2 Ionic Nitrates Derived from Dihydrazides

201 °C (**4b**) and 168 °C (**6b**). The neutral hydrazide compounds **2**, **4** and **6** melt at 182 °C (**2**) and 124 °C (**4**) and the hydrazides decompose at 195 °C (**2**), 216 °C (**4**) and 130 °C (**6**).

Friction and impact sensitivities were evaluated according to BAM standards, additionally the sensitivity towards electrostatic discharge was determined. The nitrates **2a**, **4a** and **6a** are rated sensitive towards impact, with values between 10 J (**4a**, **6a**) and 20 J (**2a**). The chlorides (**2b**, **4b**) and the neutral hydrazides (**2**, **4**) of malonic acid and aminodiacetic acid are insensitive towards impact. Nitramine containing compounds **5** (15 J) and **6** (10 J) are sensitive towards impact. Regarding friction sensitivities, the nitrates **2a** (324 N), **4a** (80 N) and **6a** (192 N) are rated sensitive. The chlorides (**2b**, **4b**, **6b**) and the neutral hydrazides (**2**, **4**, **6**) are not considered sensitive towards friction. The physical properties of the nitrate salts **2a** and **6a** were determined and are summarized in Table 2.2.

Table 2.2: Physical and sensitivity data of **2a** and **6a** in comparison with AP

	2a	6a	AP
Formula	C ₃ H ₁₀ N ₆ O ₈	C ₄ H ₁₂ N ₈ O ₁₀	NH ₄ ClO ₄
FW [g mol ⁻¹]	258.15	332.19	117.49
T _{dec} [°C] ^[a]	266	131	240
IS [J] ^[b]	20	10	20
FS [N] ^[b]	324	192	360
ESD [J] ^[b]	1.5	0.4	-
ρ [g cm ⁻³] ^[c]	1.65	1.65	1.95
O [%] ^[d]	49.6	48.2	54.5
Ω _{CO} [%] ^[e]	0	0	+34.0
Ω _{CO₂} [%] ^[e]	-18.6	-19.2	+34.0
Δ _f H _m ° [kJ mol ⁻¹] ^[f]	-785.0	-708.9	-295.8
V _{det} [m s ⁻¹] ^[g]	7830	7998	6368
I _{sp} [s] ^[h]	214	231	157
I _{sp} [s] (15 % Al) ^[h]	245	254	235
I _{sp} [s] (15 % Al 14 % binder) ^[h]	225	227	261

[a] Onset decomposition point T_{dec} from DTA measurements, heating rate 5 °C min⁻¹. [b] Sensitivity towards impact IS, friction FS and electrostatic discharge ESD. [c] Estimated density at room temperature. [d] Oxygen content. [e] Oxygen balance assuming formation of CO and CO₂. [f] Energy of formation calculated by the CBS-4M method using Gaussian 09.¹⁵ [g] Predicted detonation velocity. [h] Specific impulse I_{sp} of the neat compound and compositions with aluminium or aluminium and binder (6 % polybutadiene acrylic acid, 6 % polybutadiene acrylonitrile and 2 % bisphenol A ether) using the EXPL05 (Version 6.03) program package (70 kbar, isobaric combustion, equilibrium to throat and frozen to exit).^{23a}

The densities and cell volumes of malonyl dihydrazinium dinitrate (**2a**) and nitraminodiacetyl dihydrazinium dinitrate (**6a**) were estimated by comparison with the crystal structures of the neutral hydrazides **2**¹³ and **6** and the solvent containing crystal structure of compound **6a**.

Both dinitrates **2a** and **6a** develop a detonation velocity of around 8000 m s^{-1} obtained from theoretical calculations. The values range between the secondary explosives TNT and PETN and are inferior to the diaminourea and oxalyldihydrazide dinitrate salts.⁵⁻⁶ The estimated density of both nitrate salts (**2a**, **6a**) is crucially lower than the density of the compared compounds, hence this result is to be expected. The specific impulse of the neat compound as well as in combination with 15 % aluminum yields superior specific impulses I_{sp} compared to ammonium perchlorate (AP). By the addition of polymeric binders the composite with ammonium perchlorate clearly shows the highest specific impulse. The oxygen balance of compounds **2a** and **6a** is not sufficient for a complete oxidation, therefore the specific impulse drops by the addition of the carbon based binder system.

2.4 Conclusion

Three new polynitrate and –chloride hydrazides as well as two new neutral nitramines were synthesized and fully characterized in this study. The investigated syntheses are feasible and cost-efficient through economic starting materials and high yields. Little to none purification is necessary to obtain the final compounds in high purity. Unfortunately the nitrate salts **2a**, **4a** and **6a** are hygroscopic which limits their application. The nitrates show some interesting physical properties, e.g. their low sensitivity towards impact and friction and the high thermal stability of malonyl dihydrazide dinitrate (**2a**). Their specific impulse in combination with aluminum exceeds the performance of AP. The addition of high amounts of binder reduces the I_{sp} significantly. The chloride salts in general, are interesting precursors, e.g. in metathesis reactions to form the perchlorate and dinitramide salts.

2.5 Experimental Section

2.5.1 General Information

Solvents were dried and purified with standard methods. Diethylmalonate and iminodiacetic (i.e. aminodiacetic) acid are commercially available and used without further purification. Raman spectra were recorded in glass tubes with a Bruker MultiRAM FT-Raman spectrometer with a Klaastech DENICAFC LC-3/40 laser (Nd:YAG, 1064 nm, up to 1000 mW) in the range of 4000-400 cm^{-1} . Relative intensity is given in percent. IR spectra were recorded with a Perkin-

2 Ionic Nitrates Derived from Dihydrazides

Elmer Spectrum BX-FTIR spectrometer coupled with a Smiths ATR DuraSample IRII device. Measurements were recorded in the range of 4000-650 cm⁻¹. All Raman and IR spectra were measured at ambient temperature. NMR spectra were recorded with JEOL Eclipse and Bruker TR 400 MHz spectrometers at 25 °C. Chemical shifts were determined in relation to external standards Me₄Si (¹H, 399.8 MHz); (¹³C, 100.5 MHz); MeNO₂ (¹⁴N, 28.9 MHz). Elemental analyses (CHN) were obtained with a Vario EL Elemental Analyzer.

The sensitivity data were acquired by measurements with a BAM drophammer and a BAM friction tester.¹ Melting and decomposition points were determined by differential thermal calorimetry (DTA) using a OZM Research DTA 552-Ex instrument at a heating rate of 5 °C min⁻¹. Measurements were performed in open glass vessels against a reference material up to 400 °C.

2.5.2 X-ray Crystallography

The crystal structure data were obtained using an Oxford Xcalibur CCD Diffraktometer with a KappaCCD detector at low temperature (143 K). Mo-K_α radiation ($\lambda = 0.71073 \text{ \AA}$) was delivered by a Spellman generator (voltage 50 kV, current 40 mA). Data collection and reduction were performed using the CRYSTALIS CCD¹⁴ and CRYSTALIS RED¹⁵ software, respectively. The structures were solved by SIR92/SIR97¹⁶ (direct methods) and refined using the SHELX-97¹⁷ software, both implemented in the program package WinGX22.¹⁸ Finally, all structures were checked using the PLATON software.¹⁹ Structures displayed with ORTEP plots are drawn with thermal ellipsoids at 50 % probability level.

2.5.3 Computational Details

The theoretical calculations were achieved by using the Gaussian 09 program package²⁰ and were visualized by using GaussView 5.08.²¹ Optimizations and frequency analyses were performed at the B3LYP level of theory (Becke's B3 three parameter hybrid functional by using the LYP correlation functional) with a cc-pVDZ basis set. After correcting the optimized structures with zero-point vibrational energies, the enthalpies and free energies were calculated on the CBS-4M (complete basis set) level of theory.²² The detonation parameters were obtained by using the EXPLO5 (V6.03) program package.²³

2.5.4 Synthesis

CAUTION! The nitrate salts **2a**, **4a** and **6a**, and the nitramines **5** and **6** are energetic materials and show sensitivities in the range of primary and secondary explosives! They should be handled with caution during synthesis or manipulation and additional protective equipment (leather jacket, face shield, ear protection, Kevlar gloves) is strongly recommended.

Malonyl dihydrazide (2): The dihydrazide was synthesized according to literature¹⁰: Diethylmalonate (**1**, 24.0 g, 150 mmol) was dissolved in ethanol (220 mL) and hydrazine monohydrate (18.0 mL, 371 mmol) was added. The solution was refluxed at 90 °C for 4 h. On cooling a white crystalline solid precipitated. After filtration and washings with ethanol malonyl dihydrazide (13.6 g, 69 %) was obtained as pure product.

¹H NMR (DMSO-D₆): δ = 9.1 (br, 2H, NH), 4.2 (br, 4H, NH₂), 2.89 (s, 2H, CH₂); ¹³C{¹H} NMR (DMSO-D₆): δ = 166.0 (CO), 40.1 (CH₂).

Malonyl dihydrazinium dinitrate (2a): 2M nitric acid (10 mL, 20.0 mmol) was added to a suspension of malonyl dihydrazide (**2**, 1.3 g, 10.0 mmol) in water (5 mL) at room temperature. After 10 minutes the remaining solvent was removed at reduced pressure and the resulting colorless product was dried under high vacuum. Malonyl dihydrazinium dinitrate (**2a**, 1.3 g, 99 %) was obtained quantitatively in high purity.

¹H NMR (DMSO-D₆): δ = 11.2 (br, 2H, NH), 9.7 (br, 6H, NH₃⁺), 3.35 (s, 2H, CH₂); ¹³C{¹H} NMR (DMSO-D₆): δ = 165.0 (CO), 39.1 (CH₂); ¹⁴N NMR (DMSO-D₆): δ = -4 (NO₃⁻). Raman (800 mW): 3005 (8), 2964 (11), 1858 (2), 1693 (15), 1592 (8), 1445 (5), 1317 (8), 1194 (8), 1104 (10), 1048 (100), 958 (16), 910 (6), 848 (3), 719 (9), 582 (7), 448 (4), 390 (6) cm⁻¹. IR: 3178 (m), 2999.0 (m), 2686 (m), 1684 (m), 1582 (s), 1532 (m), 1296 (vs), 1185 (s), 1040 (m), 958 (m), 848 (w), 821 (m), 664 (w), 616 (w), 569 (m), 481 (w), 449 (w) cm⁻¹. C₃H₁₀N₆O₈ (258.15 g mol⁻¹): C 13.96, H 3.90, N 32.56; found C 13.68, H 4.17, N 31.08. Dec. point: 266 °C. Sensitivities (BAM): impact 20 J; friction 324 N; ESD >1.5 J (grain size <100 µm).

Malonyl dihydrazinium dichloride (2b): Malonyl dihydrazide (**2**, 3.0 g, 22.7 mmol) was dissolved in ethanol (5 mL) and heated to the reflux point. Water was added until the starting material dissolved. Concentrated hydrochloric acid was added dropwise to the hot solution in excess and the dichloride **2b** (4.6 g, 99 %) was obtained as a colorless crystalline solid in quantitative yield and high purity after filtration.

¹H NMR (DMSO-D₆): δ = 11.4 (br, 2H, NH), 10.6 (br, 6H, NH₃⁺), 3.42 (s, 2H, CH₂); ¹³C{¹H} NMR (DMSO-D₆): δ = 164.8 (CO), 39.0 (CH₂); Raman (800 mW): 3010 (3), 3088 (5), 3065 (3), 3047

2 Ionic Nitrates Derived from Dihydrazides

(6), 3008 (4), 2978 (35), 2922 (100), 2895 (3), 2882 (3), 2852 (3), 2846 (15), 2830 (3), 2766 (3), 2673 (28), 2609 (2), 2599 (2), 2569 (4), 2569 (3), 1959 (8), 1695 (81), 1670 (6), 1589 (3), 1573 (8), 1523 (16), 1494 (12), 1286 (8), 1228 (48), 1152 (58), 1088 (28), 1076 (8), 953 (92) 927 (7), 694 (34), 586 (10), 492 (3), 481 (3), 462 (3), 447 (2), 415 (21), 386 (13), 333 (2), 292 (6), 275 (13), 230 (25) cm^{-1} . IR: 3265 (w), 2843 (s), 2660 (vs), 1954 (w), 1566 (m), 1696 (vs), 1666 (m), 1582 (m), 1519 (vs), 1491 (s), 1425 (w), 1376 (s), 1284 (w), 1219 (m), 1148 (m), 1074 (m), 953 (w), 925 (w), 803 (w) cm^{-1} . $\text{C}_3\text{H}_{10}\text{Cl}_2\text{N}_4\text{O}_2$ (205.04 g mol⁻¹): C 17.57, H 4.92, N 27.32; found C 17.5, H 4.76, N 27.34. T_{melt} : 182 °C, Dec. point: 195 °C

Aminodiacetic acid diethylester (3): The ester was synthesized according to literature⁹: Concentrated sulfuric acid (20 mL) was added dropwise to a solution of iminodiacetic acid (aminodiacetic acid, 26.6 g, 200 mmol) in dry ethanol (300 mL). The solution was refluxed at 90 °C for 24 h. After cooling, ethanol was removed under reduced pressure and the remaining aqueous phase was diluted with water (100 mL) and neutralized with sodium bicarbonate. The solution was extracted three times with diethyl ether (50 mL) and the combined organic phases were washed with water (100 mL) and a saturated sodium chloride solution (100 mL). The organic solvent was removed under reduced pressure and aminodiacetic acid diethylester (6.7 g, 18 %) was obtained as a colorless oil.

¹H NMR (Acetone-D₆): δ = 4.13 (q, 4H, ³ J ¹H, ¹H) = 7.2 Hz, CH_2CH_3), 3.41 (s, 4H, CH_2), 1.22 (t, 6H, ³ J ¹H, ¹H) = 7.2 Hz, CH_3); ¹³C{¹H} NMR (Acetone-D₆): δ = 172.4 (CO), 60.9 (CH_2), 50.4 (CH_2), 14.5 (CH_3).

Aminodiacetyl dihydrazide (4):¹¹ Hydrazine monohydrate (3.0 g, 60 mmol) was dissolved in a solvent mixture of methanol (7 mL) and diethyl ether (7 mL). Aminodiacetic acid diethylester (3, 3.74 g, 19.8 mmol) was added dropwise at -10 °C. The reaction mixture was stirred at -10 °C for 2h and a colorless crystalline precipitate was formed. After filtration the product was washed with diethyl ether and aminodiacetyl dihydrazide (2.0 g, 63 %) was obtained as a pure compound.

¹H NMR (DMSO-D₆): δ = 9.06 (s, 2H, NH), 4.2 (br, 4H, NH_2), 3.06 (s, 4H, CH_2); ¹³C{¹H} NMR (DMSO-D₆): δ = 168.9 (CO), 51.0 (CH_2). Raman (800 mW): 3341 (10), 3310 (18), 3277 (17), 3264 (15), 3230 (13), 3121 (24), 2947 (23), 2919 (36), 2893 (35), 2867 (16), 2839 (25), 1670 (16), 1634 (33), 1438 (22), 1427 (45), 1377 (27), 1342 (18), 1318 (17), 1305 (15), 1280 (40), 1252 (100), 1215 (21), 1172 (43), 1135 (16), 1092 (13), 1014 (16), 951 (30), 933 (28), 915 (48), 694 (20), 607 (12), 580 (26), 534 (12), 487 (24), 448 (23), 385 (30), 363 (15), 326 (16), 295 (17), 252 (18) cm^{-1} . IR: 3340 (w), 3311 (m), 3275 (m), 3252 (m), 3116 (m), 3004 (w), 2840 (m),

2199 (w), 2128 (w), 1670 (s), 1629 (s), 1586 (vs), 1508 (m), 1481 (m), 1439 (m), 1426 (m), 1378 (w), 1341 (w), 1303 (m), 1283 (m), 1251 (m), 1214 (w), 1180 (w), 1009 (s), 968 (m), 944 (s), 932 (s), 911 (m), 824 (s), 760 (s), 723 (s), 694 (m) cm^{-1} . $\text{C}_4\text{H}_{11}\text{N}_5\text{O}_2$ (161.16 g mol $^{-1}$): C 29.81, H 6.88, N 43.46; found C 29.89, H 6.61, N 43.44. T_{melt} : 124 °C, Dec. point: 216 °C. Sensitivities (BAM): impact >40 J; friction >360 N; ESD >1.5 J (grain size <100 μm).

Ammoniumdiacetyl dihydrazinium trinitrate monohydrate (4a): Aminodiacyl dihydrazide (**4**, 1.0 g, 6.2 mmol) was dissolved in a small amount of water (2 mL) and diluted nitric acid (60 %, 0.63 mL, 20.5 mmol) was added dropwise at -10 °C. After 30 minutes, the solvent was removed under reduced pressure as cold as possible. The crude product was washed with methanol and dried again under reduced pressure. This procedure may be repeated until the pure product is obtained. Ammoniumdiacetyl dihydrazinium trinitrate (0.6 g, 42 %) was isolated as colorless crystalline compound.

^1H NMR (DMSO-D₆): δ = 12–9 (br, 10H, NH, NH₂, NH₃), 3.99 (s, 4H, CH₂); $^{13}\text{C}\{^1\text{H}\}$ NMR (DMSO-D₆): δ = 164.6 (CO), 46.0 (CH₂); ^{14}N NMR (DMSO-D₆): δ = -4 (NO₃⁻). Raman (800 mW): 2967 (17), 1716 (9), 1587 (7), 1437 (8), 1202 (6), 1103 (9), 1047 (100), 950 (8), 724 (11), 442 (5) cm^{-1} . IR: 2972 (m), 2686 (m), 2126 (w), 1951 (w), 1709 (m), 1539 (m), 1278 (s), 1101 (m), 1033 (s), 926 (m), 852 (m), 819 (s), 729 (m) cm^{-1} . $\text{C}_4\text{H}_{14}\text{N}_8\text{O}_{11} \cdot \text{H}_2\text{O}$ (368.22 g mol $^{-1}$): C 13.05, H 4.38, N 30.43; found C 13.06, H 4.17, N 29.21. Dec. point: 160 °C. Sensitivities (BAM): impact 10 J; friction 80 N; ESD 0.4 J (grain size <100 μm).

Ammoniumdiacetyl dihydrazinium trichloride (4b):¹¹ Aminodiacyl dihydrazide (**4**, 1.0 g, 6.2 mmol) was dissolved in a small amount of water (2 mL) and concentrated hydrochloric acid (0.63 mL, 20.5 mmol) was added dropwise at -10 °C. After 30 minutes, the solvent was removed under reduced pressure as cold as possible. The crude product was washed with methanol and dried again under reduced pressure. This procedure may be repeated until the pure product is obtained. Ammoniumdiacetyl dihydrazinium trichloride (1.4 g, 96 %) was isolated as colorless crystalline compound.

^1H NMR (DMSO-D₆): δ = 13–9 (br, 10H, NH, NH₂, NH₃), 3.98 (s, 4H, CH₂); $^{13}\text{C}\{^1\text{H}\}$ NMR (DMSO-D₆): δ = 164.4 (CO), 45.9 (CH₂). Raman (800 mW): 2949 (100), 1858 (18), 1709 (47), 1520 (25), 1432 (34), 1192 (32), 1170 (26), 1099 (34), 947 (38), 552 (17), 489 (28), 437 (28) cm^{-1} . IR: 4070 (w), 2847 (s), 2642 (s), 2366 (m), 2342 (m), 2184 (m), 1974 (w), 1698 (vs), 1507 (s), 1496 (s), 1434 (s), 1418 (s), 1378 (m), 1348 (s), 1285 (m), 1202 (s), 1102 (m), 1022 (m), 925 (m), 830 (m) cm^{-1} . $\text{C}_4\text{H}_{14}\text{Cl}_3\text{N}_5\text{O}_2$ (270.54 g mol $^{-1}$): C 17.76, H 5.22, N 25.89; found C

17.55, H 5.63, N 25.01. T_{melt} : 139 °C, Dec. point: 201 °C. Sensitivities (BAM): impact >40 J; friction >360 N; ESD 0.6 J (grain size <100 µm).

Nitraminodiacetic acid diethylester (5): To a solution of aminodiacetic acid diethylester (3, 2.1 g, 11.3 mmol) in acetic anhydride (10 mL), concentrated nitric acid (7.5 mL) was added dropwise at –10 °C. The solution was stirred for 2 h at –10 °C and another 2 h at room temperature. The reaction mixture was poured on ice (150 mL) and the formed precipitate was filtered and washed with cold water. The yellowish powder turned colorless upon drying on air and nitraminodiacetic acid diethylester (2.5 g, 96 %) was obtained.

^1H NMR (Acetone-D₆): δ = 4.69 (s, 4H, CH₂), 4.21 (q, 4H, $^3J^{1\text{H}}{^1\text{H}} = 7.1$ Hz, CH₂CH₃), 1.25 (t, 6H, $^3J^{1\text{H}}{^1\text{H}} = 7.1$ Hz, CH₃); $^{13}\text{C}\{{^1\text{H}}\}$ NMR (Acetone-D₆): δ = 167.6 (CO), 62.1 (CH₂), 54.0 (CH₂), 14.4 (CH₃); ^{14}N NMR (Acetone-D₆): δ = –30 (NO₂). Raman (800 mW): 3228 (3), 3055 (5), 2991 (52), 2977 (48), 2967 (56), 2939 (56), 2875 (14), 2754 (4), 2724 (4), 2544 (9), 1859 (5), 1757 (7), 1744 (19), 1528 (6), 1457 (21), 1445 (17), 1397 (7), 1378 (14), 1364 (9), 1330 (8), 1306 (18), 1295 (30), 1171 (5), 1125 (16), 1094 (15), 1018 (7), 967 (7), 925 (7), 893 (100), 868 (8), 841 (9), 805 (7), 700 (6), 668 (8), 472 (6), 444 (10), 426 (17), 400 (6), 355 (7), 334 (8), 266 (5) cm^{–1}. IR: 4060 (w), 2987 (w), 2940 (w), 2904 (w), 2838 (w), 2346 (w), 2208 (w), 2173 (w), 2122 (w), 2096 (w), 2053 (w), 1990 (w), 1928 (w), 1838 (w), 1744 (s), 1705 (w), 1521 (m), 1465 (w), 1453 (m), 1405 (m), 1377 (m), 1328 (m), 1297 (m), 1225 (m), 1203 (vs), 1168 (m), 1123 (w), 1094 (m), 1014 (s), 966 (m), 958 (m), 915 (w), 866 (w), 804 (w), 764 (w), 725 (m), 700 (w), 657 (m) cm^{–1}. C₈H₁₄N₂O₆ (234.21 g mol^{–1}): C 41.03, H 6.03, N 11.96; found C 41.16, H 5.94, N 11.99. T_{melt} : 58 °C, Dec. point: 233 °C. Sensitivities (BAM): impact >40 J; friction >360 N; ESD >1.5 J (grain size <100 µm).

Nitraminodiacetyl dihydrazide (6): Hydrazine monohydrate (5.0 g, 100 mmol) was dissolved in a solvent mixture of methanol (15 mL) and diethyl ether (15 mL). Nitraminodiacetic acid diethylester (5, 5.8 g, 25 mmol) was added dropwise at –10 °C. The reaction mixture was stirred at –10 °C for 2h and a colorless crystalline precipitate was formed. After filtration the product was washed with diethyl ether and nitraminodiacetyl dihydrazide (3.9 g, 75 %) was obtained as a colorless solid.

^1H NMR (D₂O): δ = 4.56 (s, 4H, CH₂); $^{13}\text{C}\{{^1\text{H}}\}$ NMR (D₂O): δ = 167.8 (CO), 54.1 (CH₂); ^{14}N NMR (D₂O): δ = –30 (NO₂). Raman (800 mW): 3353 (10), 3282 (14), 3239 (8), 3200 (16), 3005 (15), 2986 (18), 2949 (35), 1672 (12), 1644 (19), 1553 (13), 1512 (13), 1441 (15), 1413 (20), 1379 (15), 1337 (50), 1318 (39), 1288 (51), 1256 (25), 1207 (11), 1152 (22), 1127 (40), 1110 (39), 1006 (28), 955 (58), 933 (28), 873 (100), 743 (11), 699 (10), 670 (19), 649 (33), 569 (17), 454

(27), 408 (51), 387 (32), 340 (33), 274 (21), 241 (22) cm^{-1} . IR: 3352 (w), 3215 (m), 3004 (m), 1680 (s), 1611 (m), 1550 (s), 1510 (s), 1440 (s), 1408 (m), 1377 (s), 1338 (s), 1285 (s), 1251 (vs), 1100 (s), 994 (s), 952 (vs), 903 (s), 786 (s), 740 (vs), 699 (s) cm^{-1} . $\text{C}_4\text{H}_{10}\text{N}_6\text{O}_4$ (206.16 g mol⁻¹): C 23.30, H 4.89, N 40.76; found C 23.27, H 5.02, N 40.72. Dec. point: 130 °C. Sensitivities (BAM): impact 15 J; friction >360 N; ESD 1.0 J (grain size <100 μm).

Nitraminodiacetyl dihydrazinium dinitrate (6a): Nitraminodiacetyl dihydrazide (**6**, 1.0 g, 3.88 mmol) was dissolved in a small amount of water (2 mL) and diluted nitric acid (60 %, 0.6 mL, 7.7 mmol) was added dropwise at -10 °C. After 30 minutes, the solvent was removed under reduced pressure as cold as possible. The crude product was washed with methanol and dried again under reduced pressure. This procedure may be repeated until the pure product is obtained. Nitraminodiacetyl dihydrazinium dinitrate (0.7 g, 85 %) was isolated as colorless compound.

¹H NMR (DMSO-D₆): δ = 11.2 (br, 2H, NH), 11–8.5 (br, 6H, NH₃), 4.68 (s, 4H, CH₂); ¹³C{¹H} NMR (DMSO-D₆): δ = 165.6 (CO), 53.4 (CH₂); ¹⁴N NMR (DMSO-D₆): δ = -5 (NO₃⁻), -29 (NO₂). Raman (800 mW): 3000 (14), 2963 (21), 1700 (17), 1601 (9), 1541 (10), 1443 (9), 1409 (10); 1334 (12), 1289 (19), 1203 (10), 1120 (11), 1087 (12), 1048 (100), 958 (12), 935 (20), 880 (30), 728 (14), 668 (8), 446 (13), 364 (12) cm^{-1} . IR: 4337 (w), 3614 (w), 2996 (m), 2706 (w), 2359 (w), 1961 (w), 1698 (m), 1521 (m), 1285 (s), 1183 (s), 1039 (m), 952 (m), 877 (m), 822 (m), 764 (m), 720 (m) cm^{-1} . $\text{C}_4\text{H}_{12}\text{N}_8\text{O}_{10}$ (332.18 g mol⁻¹): C 14.46, H 3.64, N 33.73; found C 14.74, H 3.90, N 33.58. Dec. point: 131 °C. Sensitivities (BAM): impact 10 J; friction 192 N; ESD 0.4 J (grain size <100 μm).

Nitraminodiacetyl dihydrazinium dichloride (6b): Nitraminodiacetyl dihydrazide (**6**, 1.0 g, 4.85 mmol) was dissolved in a small amount of water (2 mL) and concentrated hydrochloric acid (0.87 mL, 10.2 mmol) was added dropwise at -10 °C. After 30 minutes, the solvent was removed under reduced pressure as cold as possible. The crude product was washed with methanol and dried again under reduced pressure. This procedure may be repeated until the pure product is obtained. Nitraminodiacetyl dihydrazinium dichloride (1.1 g, 73 %) was isolated as colorless crystalline compound.

¹H NMR (DMSO-D₆): δ = 11.6 (br, 2H, NH), 11.5–10 (br, 6H, NH₃), 4.71 (s, 4H, CH₂); ¹³C{¹H} NMR (DMSO-D₆): δ = 165.5 (CO), 53.5 (CH₂); ¹⁴N NMR (DMSO-D₆): δ = -29 (NO₂). Raman (800 mW): 2989 (64), 2949 (70), 2904 (45), 2630 (16), 1786 (11), 1720 (82), 1559 (21), 1530 (23), 1481 (25), 1460 (25), 1408 (20), 1390 (41), 1329 (18), 1308 (25), 1288 (36), 1230 (31), 1178 (42), 1168 (37), 1141 (23), 1101 (12), 1085 (26), 959 (31), 935 (53), 887 (100), 669 (27),

2 Ionic Nitrates Derived from Dihydrazides

574 (11), 492 (16), 483 (14), 433 (20), 416 (20), 402 (21), 308 (30) cm^{-1} . IR: 4077 (w), 3168 (m), 2988 (m), 2834 (m), 2729 (m), 2641 (m), 2348 (w), 2200 (w), 2116 (w), 2084 (w), 2060 (w), 1997 (w), 1928 (w), 1813 (w), 1719 (s), 1710 (s), 1594 (m), 1557 (s), 1542 (s), 1485 (s), 1456 (s), 1408 (w), 1396 (m), 1330 (w), 1307 (s), 1288 (s), 1227 (s), 1167 (vs), 1139 (s), 1079 (m), 952 (m), 934 (m), 886 (w), 828 (w); 769 (w), 668 (m) cm^{-1} . $\text{C}_4\text{H}_{12}\text{Cl}_2\text{N}_6\text{O}_4$ (279.08 g mol⁻¹): C 17.21, H 4.33, N 30.11; found C 17.41, H 4.40, N 30.02. Dec. point: 168 °C. Sensitivities (BAM): impact 10 J; friction >360 N; ESD 1.0 J (grain size <100 μm).

2.6 References

- [1] T. M. Klapötke, *Chemistry of High-Energy Materials*, 4th ed., De Gruyter, Berlin, 2015.
- [2] D. Fischer, T. M. Klapötke, J. Stierstorfer, *Angew. Chem.* **2014**, *126*, 8311–8314; *Angew. Chem. Int. Ed.* **2014**, *53*, 8172–8175.
- [3] N. Fischer, D. Fischer, T. M. Klapötke, D. G. Piercy, J. Stierstorfer, *J. Mater. Chem.* **2012**, *22*, 20418–20422.
- [4] a) K. O. Christe, W. W. Wilson, M. A. Petrie, H. H. Michels, J. C. Bottaro, R. Gilardi, *Inorg. Chem.* **1996**, *35*, 5068–5071. b) J. C. Bottaro, P. E. Penwell, R. J. Schmitt, *J. Am. Chem. Soc.* **1997**, *119*, 9405–9410.
- [5] N. Fischer, T. M. Klapötke, J. Stierstorfer, *Propellants, Explos., Pyrotech.* **2011**, *36*, 225–232.
- [6] D. Fischer, T. M. Klapötke, J. Stierstorfer, *J. Mater. Chem.* **2014**, *32*, 37–49.
- [7] K. S. Khariton, M. E. Soshkevich, L. V. Kurtev, A. A. Shamshurin, *Suom. Kemistil. B* **1968**, *41*, 372–374.
- [8] a) Y.-H. Joo, B. Twamley, S. Garg, J. M. Shreeve, *Angew. Chem.* **2008**, *120*, 6332–6335; *Angew. Chem. Int. Ed.* **2008**, *47*, 6236–6239 b) O. Diels, *Ber. Dtsch. Chem. Ges.* **1903**, *36*, 736–748.
- [9] H. S. Park, Q. Lin, A. D. Hamilton, *J. Am. Chem. Soc.* **1999**, *121*, 8–13.
- [10] A. Alborzi, S. Zahmatkesh, A. Yazdanpanah, *Polym. Bull.* **2013**, *70*, 3359–3372.
- [11] T. Curtius, O. Hofmann, *J. Prakt. Chem.* **1917**, *96*, 202–235.
- [12] T. Steiner, *Angew. Chem.* **2002**, *114*, 50–80; *Angew. Chem. Int. Ed.* **2002**, *41*, 48–76.
- [13] C. Miravitlles, J. L. Briano, F. Plana, M. Font-Altaba, *Cryst. Struct. Commun.* **1975**, 81–84.
- [14] Oxford Diffraction Ltd., *CrysAlis CCD*, 1.171.35.11, Abingdon, Oxford (U.K.), 2011.
- [15] Oxford Diffraction Ltd., *CrysAlis RED*, 1.171.35.11, Abingdon, Oxford (U.K.), 2011.
- [16] A. Altomare, M. C. Burla, M. Camalli, G. L. Cascarano, C. Giacovazzo, A. Gualandi, A. G. G. Moliterni, G. Polidori, R. Spagna, *J. Appl. Crystallogr.* **1999**, *32*, 155–119.
- [17] a) G. M. Sheldrick, *Programs for Crystal Structure Determination*, University of Göttingen, Germany, 1997; b) G. M. Sheldrick, *Acta Crystallogr.* **2008**, *64 A*, 112–122.
- [18] L. Farrugia, *J. Appl. Crystallogr.* **1999**, *32*, 837–838.
- [19] A. L. Spek, *Acta Crystallogr.* **2009**, *65 D*, 148–155.
- [20] M. J. Frisch, G. W. Trucks, H. B. Schlegel, G. E. Scuseria, M. A. Robb, J. R. Cheeseman, G. Scalmani, V. Barone, B. Mennucci, G. A. Petersson, H. Nakatsuji, M. Caricato, X. Li, H. P. Hratchian, A. F. Izmaylov, J. Bloino, G. Zheng, J. L. Sonnenberg, M. Hada, M. Ehara, K. Toyota, R. Fukuda, J. Hasegawa, M. Ishida, T. Nakajima, Y. Honda, O. Kitao, H. Nakai, T. Vreven, J. A. Montgomery Jr., J. E. Peralta, F. Ogliaro, M. J. Bearpark, J. Heyd, E. N. Brothers, K. N. Kudin, V. N. Staroverov, R. Kobayashi, J. Normand, K. Raghavachari, A. P. Rendell, J. C. Burant, S. S. Iyengar, J. Tomasi, M. Cossi, N. Rega, N. J. Millam, M. Klene, J. E. Knox, J. B. Cross, V. Bakken, C. Adamo, J. Jaramillo, R. Gomperts, R. E. Stratmann, O. Yazyev, A. J. Austin, R. Cammi, C. Pomelli, J. W. Ochterski, R. L. Martin, K. Morokuma, V. G. Zakrzewski, G. A. Voth, P. Salvador, J. J.

2 Ionic Nitrates Derived from Dihydrazides

Dannenberg, S. Dapprich, A. D. Daniels, Ö. Farkas, J. B. Foresman, J. V. Ortiz, J. Cioslowski, D. J. Fox, Gaussian, Inc., *Gaussian 09*, Wallingford, **2009**.

[21] R. D. Dennington, T. A. Keith, J. M. Millam, *GaussView*, v. 5.08, Semichem, Inc., Wallingford, **2009**.

[22] J. A. Montgomery, M. J. Frisch, J. W. Ochterski, G. A. Petersson, *J. Chem. Phys.* **2000**, *112*, 6532–6542.

[23] a) M. Suceska, *EXPLO5*, v. 6.03, Zagreb, **2015**; b) M. Suceska, *Propellants, Explos., Pyrotech.* **1991**, *16*, 197–202.

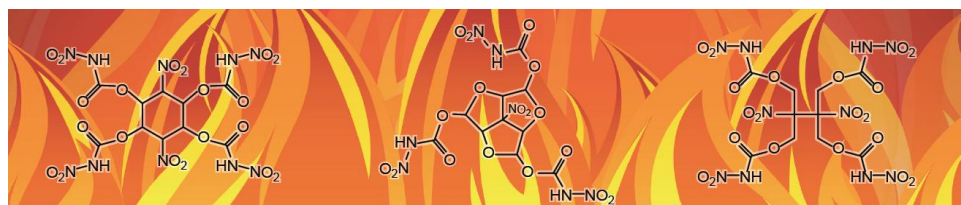
3 Polynitrocaramates Derived from Nitromethane

POLYNITROCARBAMATES DERIVED FROM NITROMETHANE

Thomas M. Klapötke, Burkhard Krumm, and Thomas Reith

as published in

Zeitschrift für Anorganische und Allgemeine Chemie **2017**, 643, 1474–1481

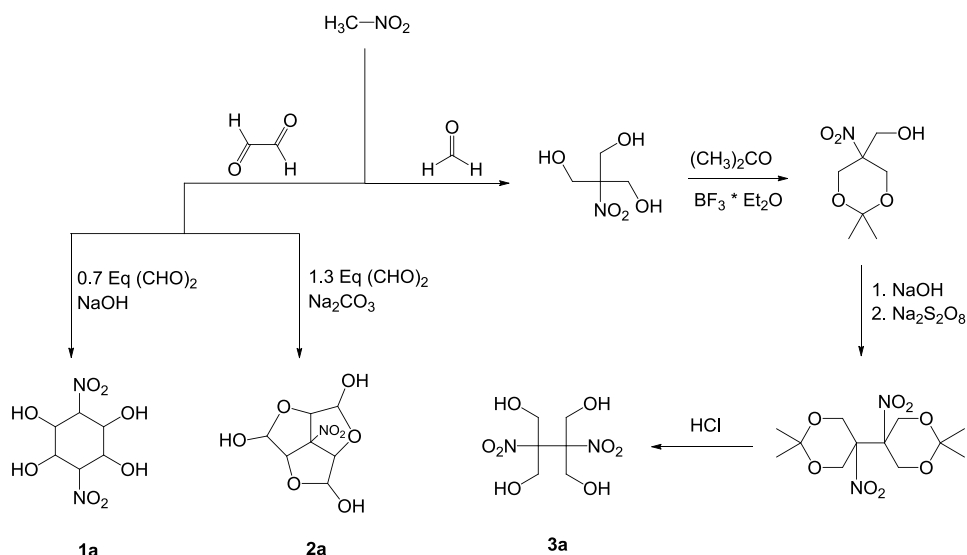


3.1 Abstract

A variety of energetic compounds combining nitro with nitrocarbamate groups were synthesized. The precursors, polynitro alcohols, were obtained by the condensation of the readily available starting material nitromethane with the small aliphatic aldehydes formaldehyde and glyoxal. The conversion into carbamates was achieved with the reactive chlorosulfonyl isocyanate (CSI) and a final nitration yielded the polynitrocaramates. The new compounds were fully characterized, including multinuclear NMR spectroscopy, vibrational analysis, mass spectrometry, differential scanning calorimetry and elemental analysis. The energies of formation were calculated with the GAUSSIAN program package and the detonation parameters were predicted using the EXPL05 computer code. Due to the positive oxygen balance (Ω_{CO}) of the presented compounds, their performance data as oxidizers were determined and compared to the common oxidizer ammonium perchlorate.

3.2 Introduction

The search for high energy dense oxidizers (HEDOs) is one of the priorities in the development of new energetic materials.¹ Environmentally friendly and insensitive alternatives are under investigation to replace ammonium perchlorate as oxidizer in composite rocket propellants, e.g. dinitramide salts and compounds utilizing the trinitromethyl moiety.^{1a, 2} In the recent years, the research of primary nitrocarbamates was initiated, and several promising substances were synthesized and characterized.^{1b, 3} Trinitroethyl nitrocarbamate (TNE-NC) for example combines a high oxygen balance with moderate sensitivities and develops high specific impulses on aluminum based propulsion systems.^{1b, 1d} The synthesis of primary nitrocarbamates usually starts from the corresponding alcohols, which are transferred into the carbamates by the facile reaction with chlorosulfonyl isocyanate (CSI). The nitration in pure nitric acid or mixed acids produces the nitrocarbamates in high yields and purity.^{1b, 3} In general, the nitrocarbamates are thermally and mechanically (impact, friction) less sensitive in comparison with their corresponding nitrates, in addition they are more stable towards decomposition by alkaline hydrolysis or nucleophilic attacks.³ The condensation of nitromethane with formaldehyde and glyoxal yields a variety of nitro- and polynitro alcohols by one-pot procedures.⁴ Both aliphatic aldehydes, nitromethane and sodium hydroxide are economic and commercially available starting materials and the reactions are facile with moderate-to-high yields.



Scheme 3.1: Syntheses of nitro- and polynitro alcohols (**1a**–**3a**).

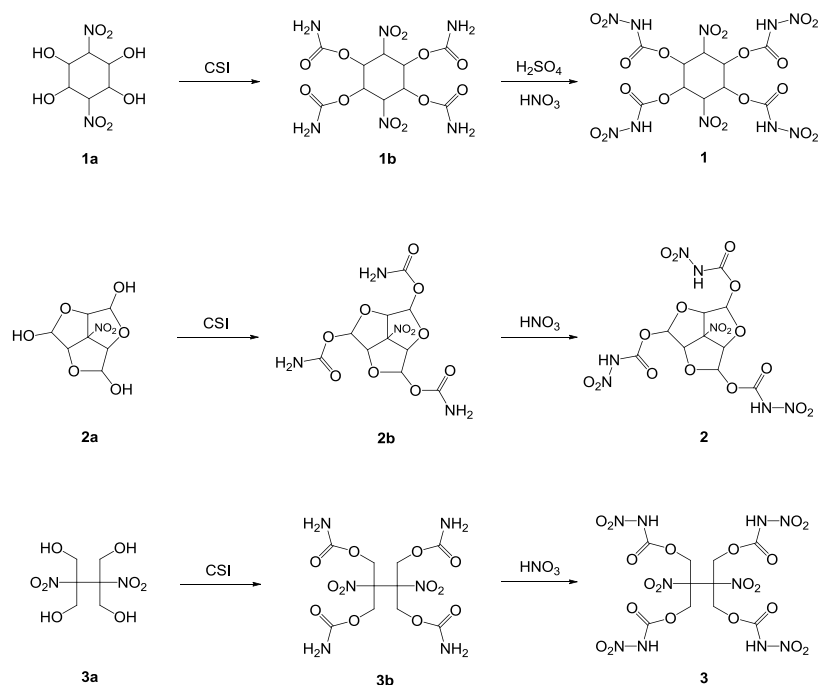
Another interesting polynitro alcohol, 2,3-bis(hydroxymethyl)-2,3-dinitrobutane-1,4-diol, was investigated in 2008 and prepared by a five-step synthesis, starting repeatedly from nitromethane and formaldehyde. The obtained tris(hydroxymethyl)nitromethane is transferred into a dioxane derivative, homocoupled and deprotected to finally yield a tetravalent alcohol.⁵ In conclusion, the resulting alcohols are desirable precursors for the synthesis of primary nitrocarbamates (Scheme 3.1).

3.3 Results and Discussion

3.3.1 Synthesis

The alcohol precursors **1a** and **2a** were synthesized from nitromethane and glyoxal according to literature.^{4b, 4c} 2,3-Bis(hydroxymethyl)-2,3-dinitrobutane-1,4-diol (**3a**) was synthesized in a multi-step synthesis from tris(hydroxymethyl)nitromethane following literature procedures.⁵ The carbamates **1b**, **2b** and **3b** were obtained in high yields and purity from the reaction of the corresponding alcohols with CSI followed by an aqueous work-up. The primary nitrocarbamates **1**, **2** and **3** are obtained by the final nitration in mixed acid (**1**) or pure HNO_3 (**2**, **3**) (Scheme 3.2).

3 Polynitrocarbamates Derived from Nitromethane



Scheme 3.2: Synthesis of carbamates (**1b–3b**) and nitrocarbamates (**1–3**) from simple nitro- and polynitro alcohols (**1a–3a**).

All compounds with the exception of **3a** and **3b** (yellowish) are colorless solids. The alcohol precursors (**1a–3a**) and were used as obtained from the literature reactions without further purification. The carbamates (**1b–3b**) precipitated directly from the aqueous work-up as elemental analysis pure compounds. The nitrocarbamates **1** and **3** precipitated immediately after the addition on crushed ice as pure colorless solids. Compound **2** was extracted with ethyl acetate from the aqueous phase. The new syntheses combine high yields over 80 % with short reaction times and facile work-ups.

3.3.2 NMR Spectroscopy

All compounds except **1b** were characterized by ¹H and ¹³C NMR spectroscopy, additionally the ¹⁴N NMR spectra of the nitrocarbamates **1–3** were recorded. The carbamates were dissolved in DMSO-D₆ and the nitrocarbamates were dissolved in acetone-D₆, while compound **1b** decomposed in all available deuterated solvents.

Regarding the ¹H NMR spectrum of the cyclohexane derivative **1**, the ten hydrogen atoms are detected as four resonances due to the high symmetry. The four acidic NH protons are observed in the expected range at 13.9 ppm as one broadened signal. The two identical hydrogen atoms connected to the nitrated carbons HCNO₂ are observed as a triplet at 6.45 ppm, ³J(¹H, ¹H) = 3.0 Hz. The four nitrocarbamate branches are split into two groups, with two branches in equatorial and two branches in axial conformation. As a consequence, the

four remaining hydrogen atoms are observed as two resonances at 6.03 ppm and 5.77 ppm, both coupling with each other and the proton of $HCNO_2$, resulting in a doublet of doublets. In the $^{13}C\{^1H\}$ NMR the carbonyl groups of the nitrocarbamate branches are also split up and are observed at 147.6 ppm and 147.4 ppm, respectively. The nitrated carbon atoms are shown at 80.7 ppm, while the remaining four carbon atoms of the cyclohexane structure are found at 70.7 ppm and 69.3 ppm. In the ^{14}N NMR spectrum of **1** the aliphatic nitro groups are found at -10 ppm and the nitramine groups are observed at -48 ppm.

Due to the high symmetry of compounds **2b** and **2** only three signals appear in the 1H NMR spectra. The carbamate protons NH_2 in **2b** are observed as two broad resonances at 6.93 ppm and 6.88 ppm due to the restricted rotation along the $C-NH_2$ bond.^{1d} The three protons bound to carbon atoms with two neighboring oxygen atoms ($HC(O)O$) show their resonance at 6.09 ppm. The remaining three protons, which are bound to the carbon next to the CNO_2 center, show their respective resonance as a singlet at 5.30 ppm. In the $^{13}C\{^1H\}$ NMR of compound **2b** the expected four resonances are observable at 154.1 ppm for the carbonyl group, at 104.9 ppm for the CNO_2 center carbon and at 101.0/91.2 ppm for the six remaining carbon atoms in the ring system.

The acidic nitrocarbamate NH protons of compound **2** can be observed as broad resonances at 13.7 ppm in the 1H NMR spectrum. The three $HC(O)O$ protons are shifted to 6.47 ppm and the three $HC(O)C$ protons appear at 5.62 ppm. In the $^{13}C\{^1H\}$ NMR of compound **2** the corresponding four resonances are observed at 147.2 ppm for the carbonyl group, at 105.1 ppm for the CNO_2 center carbon and at 103.1/92.8 ppm for the six remaining carbon atoms of the polycycle. The ^{14}N NMR spectrum of **2** shows two resonances at -10 ppm and -46 ppm, which can be assigned to the nitrogen atoms of the single nitro group in the molecule center and those of the three nitramine groups, respectively.

The carbamate **3b** shows two resonances in the 1H NMR spectrum. The carbamate NH_2 protons are located at 6.8 ppm and the four identical methylene groups are observed as singlet at 4.65 ppm. In the $^{13}C\{^1H\}$ NMR, the carbonyl groups are shifted to 154.7 ppm, the nitrated carbons show their resonance at 92.0 ppm and the methylene carbon resonances are observed at 60.9 ppm.

The 1H NMR spectrum of nitrocarbamate **3** differs from the precursor **3b**. The resonances of the acidic NH protons are observed in the expected range at 13.9 ppm as a very broad signal. In contrast to the carbamate precursor, the resonance signal of the four methylene groups is split up. The resonances of the *AB* system are observed as two doublets at 5.15 ppm and

3 Polynitrocarbamates Derived from Nitromethane

5.08 ppm with a geminal coupling constant of ${}^2J({}^1\text{H}, {}^1\text{H}) = 12.3$ Hz. In the ${}^{13}\text{C}\{{}^1\text{H}\}$ NMR the three signals are observed at 147.6 ppm for the carbonyl carbons, at 92.2 ppm for the nitrated carbons and at 62.7 ppm for the methylene carbons. In the ${}^{14}\text{N}$ NMR spectrum of **3** the aliphatic nitro group is found at -10 ppm and those of the nitramine groups are observed at -47 ppm.

In the vibrational spectra (IR and Raman) of compounds **1–3**, the N–H stretching vibrations of the nitramine groups are found at $3300\text{--}2980\text{ cm}^{-1}$. The carbonyl C=O stretching vibrations of the nitrocarbamates are detected at $1790\text{--}1770\text{ cm}^{-1}$. In comparison, the corresponding carbamates show these carbonyl resonances at $1740\text{--}1690\text{ cm}^{-1}$. The aliphatic nitro groups and the nitramine groups show the asymmetric stretching vibrations of the NO_2 group at $1620\text{--}1550\text{ cm}^{-1}$, whereas the symmetric stretching vibrations are observed in the range of $1420\text{--}1350\text{ cm}^{-1}$.⁶

3.3.3 Single Crystal Structure Analysis

Solvent containing single crystals suitable for structure determination were obtained for the carbamate **3b** and the nitrocarbamates **2** and **3**, and the measurements were recorded at 100 K and 143 K (Table 3.1).

Table 3.1: Crystal data, details of the structure determinations and refinement of **2**, **3b** and **3**.

	2	3b	3
formula	$\text{C}_{10}\text{H}_9\text{N}_7\text{O}_{17} \cdot 2\text{H}_2\text{O}$	$\text{C}_{10}\text{H}_{16}\text{N}_6\text{O}_{12} \cdot 2\text{CH}_3\text{CN}$	$\text{C}_{10}\text{H}_{12}\text{N}_{10}\text{O}_{20} \cdot 4\text{H}_2\text{O}$
<i>FW</i> [g mol ⁻¹]	535.25	494.37	664.32
<i>T</i> [K]	100	143	143
<i>λ</i> [Å]	0.71073	0.71073	0.71073
crystal system	monoclinic	monoclinic	monoclinic
space group	<i>P</i> 2 ₁	<i>C</i> 2/c	<i>C</i> 2/c
crystal size [mm]	0.10 x 0.08 x 0.01	0.21 x 0.08 x 0.08	0.21 x 0.18 x 0.15
crystal habit	colorless plate	colorless block	colorless block
<i>a</i> [Å]	7.97 (1)	21.26 (2)	15.64 (8)
<i>b</i> [Å]	7.74 (1)	6.76 (3)	11.80 (5)
<i>c</i> [Å]	16.58 (3)	18.36 (2)	13.48 (7)
<i>α</i> [deg]	90	90	90
<i>β</i> [deg]	103.3 (5)	123.9 (1)	95.5 (5)
<i>γ</i> [deg]	90	90	90
<i>V</i> [Å ³]	995.6 (5)	2190.8 (3)	1476.1 (2)
<i>Z</i>	2	4	4
<i>ρ</i> _{calc.} [g cm ⁻³]	1.76	1.50	1.78
<i>μ</i>	0.175	0.132	0.178
<i>F</i> (000)	534	1032	1368
2Θ range [deg]	2.52 – 25.34	4.59 – 31.94	4.67 – 31.74
index ranges	$-9 \leq h \leq 9$ $-9 \leq k \leq 9$ $-19 \leq l \leq 19$	$-28 \leq h \leq 30$ $-9 \leq k \leq 9$ $-26 \leq l \leq 16$	$-22 \leq h \leq 22$ $-16 \leq k \leq 16$ $-19 \leq l \leq 18$
reflections collected	11634	11486	12596
reflections unique	3608	3332	3758
parameters	325	155	199
GoOF	1.346	1.041	1.049
<i>R</i> ₁ / <i>wR</i> ₂ [<i>I</i> > 2σ(<i>I</i>)]	0.1251 / 0.3283	0.0412 / 0.1011	0.0469 / 0.1219
<i>R</i> ₁ / <i>wR</i> ₂ (all data)	0.1455 / 0.3238	0.0530 / 0.1092	0.0688 / 0.1363
max / min residual electron density [Å ⁻³]	-0.656 / 0.759	-0.226 / 0.442	-0.299 / 0.476
CCDC	1562166	1562167	1562168

Single crystals of the carbamate **3b** were obtained from a mixture of acetonitrile and water by slow evaporation at room temperature. The 2,3-bis(hydroxymethyl)-2,3-dinitro-1,4-butanediol tetracarbamate (**3b**) crystallizes in the monoclinic space group *C*2/c with four molecules of **3b** and eight molecules acetonitrile in the unit cell and a density of 1.50 g cm⁻³ at 143 K (Figure 3.1).

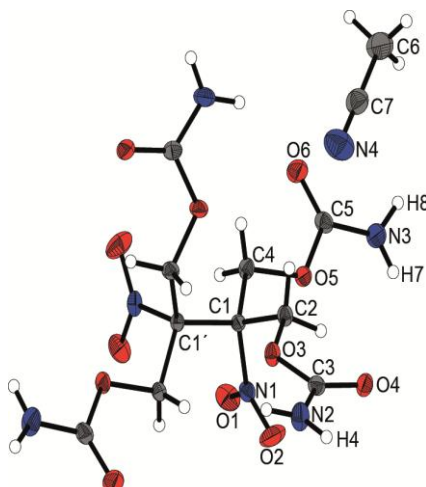


Figure 3.1: X-ray molecular structure of 2,3-bis(hydroxymethyl)-2,3-dinitro-1,4-butanediol tetracarbamate (**3b**). Selected atom distances (Å) and angles (deg.): C1–C1' 1.569 (2), C1–N1 1.548 (1), C3–O4 1.220 (2), C3–N2 1.328 (2), N2–H3 0.869 (1), N2–H4 0.869 (1); C4–C1–C2 108.6 (1), C4–C1–N1 106.0 (1), C4–C1–C1' 112.9 (1), C2–O3–C3 116.6 (1), N4–C7–C6 179.3 (2); N1–C1–C1'–N1' –81.4 (1), C2–O3–C3–O4 –4.3 (2), O3–C3–N2–H3 –9.8 (2), O3–C3–N2–H3 –178.2 (1).

In the crystalline state of compound **3b**, the two nitro groups develop a gauche conformation with a torsion angle N1–C1–C1'–N1' of 81.4 °. The four carbamate branches show a high planarity originating from the delocalized nitrogen lone pair (N2 and N3). All torsion angles along the carbamate moieties are below 5 ° with the exception of O3–C3–N2–H3 (–9.8 °) and the respective O5–C5–N3–H8 (10.5 °). Probably, the two hydrogen atoms H3 and H8 are out of their planes due to strong hydrogen bond interactions. The angle N2–H3···N4 measures 165.1 ° with a proton–acceptor distance H3···N4 of 2.528 Å, indicating a strong N–H···N interaction between the carbamate proton donor system N2–H3 and the acetonitrile molecule. In contrast, the hydrogen atom H8 is part of strong N–H···O hydrogen bonds in which a neighboring carbonyl oxygen atom O4 works as proton acceptor.

Single crystals of the nitrocarbamate **3** were obtained from a mixture of acetone and water by slow evaporation at room temperature. The 2,3-bis(hydroxymethyl)-2,3-dinitro-1,4-butanediol tetrancarbamate (**3**) crystallizes in the monoclinic space group *C*2/c with four molecules of

3 and sixteen molecules water in the unit cell and a density of 1.78 g cm^{-3} at 143 K (Figure 3.2).

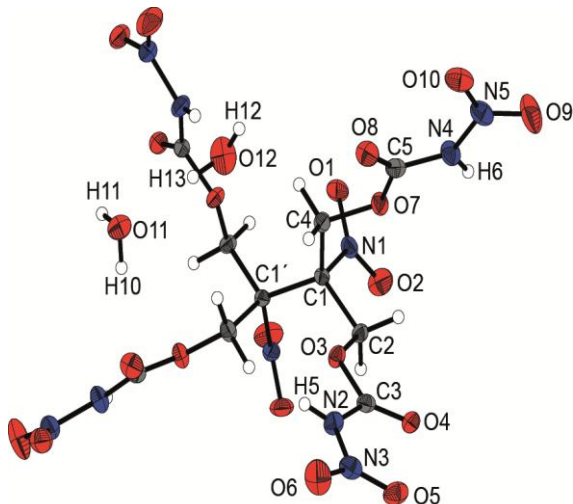


Figure 3.2: X-ray molecular structure of 2,3-bis(hydroxymethyl)-2,3-dinitro-1,4-butanediol tetranitrocaramate (**3**). Selected atom distances (Å) and angles (deg.): C1–C1' 1.579 (2), C1–N1 1.545 (2), C3–O4 1.195 (2), C3–N2 1.382 (2), N2–N3 1.368 (2), N2–H5 0.832 (1); C4–C1–C2 109.7 (1), C4–C1–N1 106.0 (1), C4–C1–C1' 113.9 (1), C2–O3–C3 115.3 (1); N1–C1–C1'–N1' 62.7 (1), C2–O3–C3–O4 6.7 (2), O3–C3–N2–N3 –175.7 (1), C3–N2–N3–O5 –2.8 (3), C3–N2–N3–O6 176.4 (2).

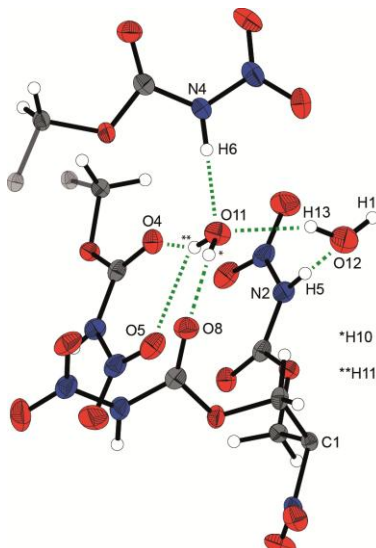


Figure 3.3: Hydrogen bonding in compound **3**. Strong hydrogen bonds occur between the nitrocaramate branches and the water solvent molecules. Only parts of the whole molecules are shown for clarity.

Classical hydrogen bonds are observed between **3** (nitramine hydrogen, e.g. DHA N4–H6–O11, bond angle DHA = 179.2° , $d(\text{D–H}) = 0.90 \text{ \AA}$, $d(\text{A–H}) = 1.85 \text{ \AA}$) and the crystal water as well as between the water molecules themselves (Figure 3.3). In addition, the water hydrogen atoms

form hydrogen bonds to the carbonyl oxygen atoms of the nitrocarbamate unit (e.g. O11–H11–O4, bond angle DHA = 152.6 °, d(D–H) = 0.83 Å, d(A–H) = 2.08 Å).

The nitrocarbamate **3** and the carbamate **3b** crystallize in the same space group *C*2/c, while both structures contain polar solvent molecules. In accordance with the carbamate structure of **3b**, the two aliphatic nitro groups of the nitrocarbamate **3** are in gauche conformation. In comparison, the torsion angle N1–C1–C1’–N1’ is shortened (**3b** 81.4 °, **3** 62.7 °), probably because the nitrocarbamate branches have a stronger repulsion with each other, forcing a more staggered conformation. The nitrocarbamate branches are planar structures with torsion angles up to 6.7 ° (C2–O3–C3–O4).

Single crystals of the nitrocarbamate **2** were obtained from a mixture of acetone and water by slow evaporation at room temperature. Compound **2** crystallizes in the monoclinic space group *P*2₁ with two molecules of **2** and four molecules water in the unit cell and a density of 1.76 g cm^{–3} at 100 K (Figure 3.4).

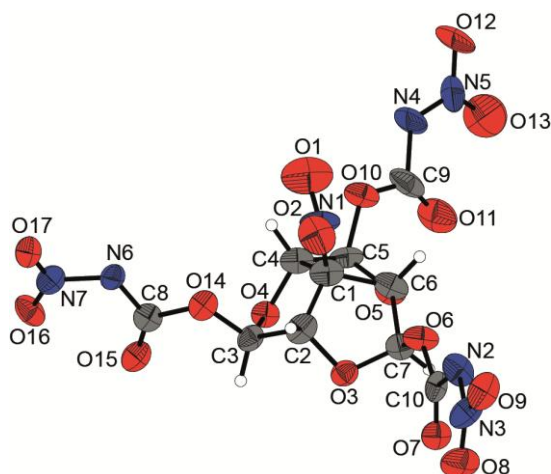


Figure 3.4: X-ray molecular structure of 6b-Nitrohexahydro-2H-1,3,5-trioxacyclopenta[cd]pentalene-2,4,6-triol trinitrocarbamate (**2**). The crystallographic data was only obtained for a highly disordered single crystal. Splitting the atom positions did not yield a more reliable structure refinement. The two crystal water moieties are not shown for clarity. Thermal ellipsoids represent the 50 % probability level.

The obtained structure was shown to be heavily disordered. The central nitro group, one of the nitrocarbamate branches, and the solvent molecules were very difficult to refine. Splitting their positions as well as additional restrictions did not yield in a better structure refinement. In the crystalline state, the fused ring system forms a hemisphere like conformation. The nitro group is located on top of the hemisphere and the nitrocarbamate branches are facing towards it (Figure 3.5).

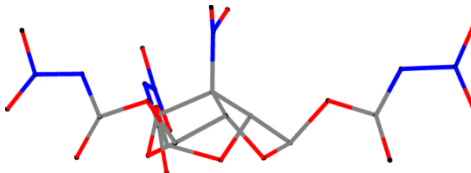


Figure 3.5: Side view of compound **2**. The three five-membered rings form a hemisphere-type conformation. For clarity, the wire model and no solvent molecules or hydrogen atoms are displayed.

The central aliphatic nitro group (N1, O1, O2) seems to prevent a threefold axis in molecule center (Figure 3.6).

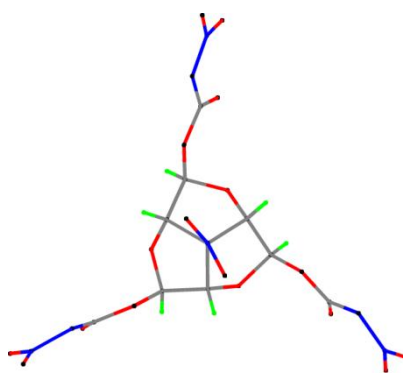


Figure 3.6: Top view of compound **2**. The molecule shows a high symmetry interrupted by the central aliphatic nitro moiety.

3.3.4 Thermal Stabilities and Energetic Properties

The physical properties of the nitrocaramates **1–3** were determined and are summarized in Table 3.2. The thermal stability of compounds **1–3** as well as of the carbamate precursors **1b–3b** were determined by Differential Scanning Calorimetry (DSC) measurements. The temperature range of 15–400 °C was recorded with a heating rate of 5 °C min^{−1}. The nitrocaramates **1–3** decompose at 160 °C (**1**) and 172 °C (**2, 3**) and do not melt before decomposition. The carbamate precursors have a decomposition point of at least 212 °C with the exception of **1b**, which is decomposed already at 122 °C.

Friction and impact sensitivities were evaluated according to BAM standards, additionally the sensitivity towards electrostatic discharge was determined. All compounds **1–3** are rated sensitive towards impact, with the nitrocaramate **1** having the highest (4 J) and compound **3**

3 Polynitrocarbamates Derived from Nitromethane

showing the lowest (25 J) impact sensitivity. The carbamates **1b–3b** showed no sensitivity to impact (>40 J). All compounds are rated insensitive in terms of friction sensitivity (FS > 360 N).

The densities of all nitrocarbamates were determined via pycnometer measurements. Compound **3** shows the highest density of almost 1.9 g cm⁻³ at room temperature and all compounds **1–3** have a density over 1.7 g cm⁻³. All synthesized nitrocarbamates have a positive oxygen balance Ω_{CO} and were evaluated as oxidizers.

Table 3.2. Physical and sensitivity data of **1–3** in comparison with AP.

	1	2	3	AP
Formula	C ₁₀ H ₁₀ N ₁₀ O ₂₀	C ₁₀ H ₉ N ₇ O ₁₇	C ₁₀ H ₁₂ N ₁₀ O ₂₀	NH ₄ ClO ₄
FW [g mol ⁻¹]	590.24	499.22	592.26	117.49
T _m [°C] ^[a]	-	-	-	-
T _{dec} [°C] ^[a]	160	172	172	240
IS [J] ^[b]	4	10	25	20
FS [N] ^[b]	360	360	360	360
ESD [J] ^[b]	1.0	1.0	0.9	-
ρ [g cm ⁻³] ^[c]	1.71	1.78	1.89	1.95
O [%] ^[d]	54.2	54.5	54.0	54.5
Ω _{CO} [%] ^[e]	13.6	8.0	10.8	+34.0
Ω _{CO₂} [%] ^[e]	-13.6	-24.0	-16.2	+34.0
Δ _f H _m ^{o[fl]} [kJ mol ⁻¹]	-1275.0	-1309.2	-1441.5	-295.8
V _{det} [m s ⁻¹] ^[g]	7702	7681	8298	6368
I _{sp} [s] ^[h]	233	215	228	157
I _{sp} [s] (15% Al) ^[h]	246	240	245	235
I _{sp} [s] (15% Al) _{14% binder} ^[h]	227	224	228	261

[a] Onset melting T_m and decomposition point T_{dec} from DSC measurements, heating rate 5 °C min⁻¹. [b] Sensitivity towards impact IS, friction FS and electrostatic discharge ESD. [c] Recalculated X-ray density at room temperature. [d] Oxygen content. [e] Oxygen balance assuming formation of CO and CO₂. [f] Energy of formation calculated by the CBS-4M method using Gaussian 09.⁷ [g] Predicted detonation velocity. [h] Specific impulse I_{sp} of the neat compound and compositions with aluminum or aluminum and binder (6 % polybutadiene acrylic acid, 6 % polybutadiene acrylonitrile and 2 % bisphenol A ether) using the EXPLO5 (Version 6.02) program package (70 kbar, isobaric combustion, equilibrium expansion).⁸

The heat of formation was calculated with the GAUSSIAN program package, and in combination with the experimental density the energetic properties were estimated utilizing the EXPLO5 computer code. All nitrocarbamates **1–3** have a detonation velocity of at least 7700 m s⁻¹. The

non-cyclic nitrocarbamate **3** shows the highest detonation velocity at almost 8300 m s^{-1} , which might originate from its high density. In comparison to the common oxidizer ammonium perchlorate (AP), the neat compounds as well as the compositions with 15 % aluminum as fuel show a higher specific impulse. The highest value is given for compound **1** and 15 % aluminum with a specific impulse of $I_{\text{sp}} = 246\text{ s}$. The oxygen balance of **1-3** seams not to be sufficient for compositions with additionally 14 % binder. In composition with only 71 % oxidizer (15 % Al, 14 % binder), the specific impulses for compounds **1-3** drop significantly. In contrast, the nitrocarbamates **1-3** are not salts like AP and a lower percentage of binder might be satisfactory for an optimal combustion behavior.

3.4 Conclusion

Three new energetic nitrocarbamates, cyclic (**1**), polycyclic (**2**) and acyclic (**3**), were synthesized and fully characterized in this study. All syntheses have their origin in the easily available nitromethane. The syntheses combine several advantages, such as economic and readily available starting materials, the facile nitrations, the high yields and a fast work-up. The obtained nitrocarbamates are already pure after synthesis and only need to be dried (**3**). Their energetic parameters were calculated and compared to the common oxidizer ammonium perchlorate. All nitrocarbamates **1-3** have a detonation velocity of at least 7700 m s^{-1} and the compositions with aluminum exceed the specific impulse of the AP variant. The addition of high amounts of binder reduces the I_{sp} significantly.

3.5 Experimental Section

3.5.1 General Information

Solvents were dried and purified with standard methods. Nitromethane and tris(hydroxymethyl) nitromethane are commercially available and used without further purification. Raman spectra were recorded in glass tube with a Bruker MultiRAM FT-Raman spectrometer with a Klaastech DENICAFC LC-3/40 laser (Nd:YAG, 1064 nm, up to 1000 mW) in the range of 4000-400 cm^{-1} . Relative intensity is given in percent. IR spectra were recorded with a Perkin-Elmer Spectrum BX-FTIR spectrometer coupled with a Smiths ATR DuraSample IRII device. Measurements were recorded in the range of 4000-650 cm^{-1} . All Raman and IR spectra were measured at ambient temperature. NMR spectra were recorded with JEOL Eclipse and Bruker TR 400 MHz spectrometers at 25 °C. Chemical shifts were determined in relation to external standards Me_4Si (^1H , 399.8 MHz); (^{13}C , 100.5 MHz); MeNO_2 (^{14}N , 28.9 MHz). Elemental analyses (CHN) were obtained with a Vario EL Elemental Analyzer.

3 Polynitrocaramates Derived from Nitromethane

The sensitivity data were acquired by measurements with a BAM dropammer and a BAM friction tester.^{1a} Melting and decomposition points were determined by differential scanning calorimetry (DSC) using a Perkin-Elmer Pyris6 DSC at a heating rate of 5 °C min⁻¹. Measurements were performed in closed aluminum containers against empty containers up to 400 °C via nitrogen flows.

3.5.2 X-ray Crystallography

The crystal structure data were obtained using an Oxford Xcalibur CCD Diffraktometer with a KappaCCD detector at low temperature (173 K, 123 K). Mo-K_α radiation ($\lambda = 0.71073 \text{ \AA}$) was delivered by a Spellman generator (voltage 50 kV, current 40 mA). Data collection and reduction were performed using the CRYSTALIS CCD⁹ and CRYSTALIS RED¹⁰ software, respectively. The structures were solved by SIR92/SIR97¹¹ (direct methods) and refined using the SHELX-97¹² software, both implemented in the program package WinGX22.¹³ Finally, all structures were checked using the PLATON software.¹⁴ Structures displayed with ORTEP plots are drawn with thermal ellipsoids at 50 % probability level.

3.5.3 Computational Details

The theoretical calculations were achieved by using the Gaussian 09 program package⁷ and were visualized by using GaussView 5.08.¹⁵ Optimizations and frequency analyses were performed at the B3LYP level of theory (Becke's B3 three parameter hybrid functional by using the LYP correlation functional) with a cc-pVDZ basis set. After correcting the optimized structures with zero-point vibrational energies, the enthalpies and free energies were calculated on the CBS-4M (complete basis set) level of theory.¹⁶ The detonation parameters were obtained by using the EXPL05 (V6.02) program package.^{8, 17}

3.5.4 Synthesis

CAUTION! The nitrocaramates **1–3** are energetic materials and show sensitivities in the range of secondary explosives! They should be handled with caution during synthesis or manipulation and additional protective equipment (leather jacket, face shield, ear protection, Kevlar gloves) is strongly recommended.

1,4-Dideoxy-1,4-dinitro-neo-inositol tetracarbamate (1b): The alcohol precursor 1,4-dideoxy-1,4-dinitro-neo-inositol (**1a**, 1.50 g, 6.3 mmol) was added slowly to a ice-cooled solution of chlorosulfonyl isocyanate (CSI, 3.92 g, 27.7 mmol) in dry acetonitrile (30 mL). The ice bath was removed after the complete addition and stirring at room temperature was continued for

one hour. The solution was cooled again with an ice bath and cold water (20 mL) was added slowly. After 10 minutes, the acetonitrile was removed under reduced pressure and the precipitated solid was collected by filtration and washed with cold water to obtain the pure carbamate **1b** (2.46 g, 95 %).

Raman (800 mW): 3391 (5), 3109 (5), 3094 (5), 3020 (17), 2993 (51), 2963 (51), 2962 (27), 2261 (5), 1718 (14), 1590 (10), 1554 (15), 1395 (12), 1366 (45), 1345 (19), 1295 (15), 1259 (16), 1218 (14), 1159 (9), 1115 (19), 1095 (11), 1058 (100), 1025 (18), 942 (39), 907 (12), 878 (13), 821 (5), 767 (18), 745 (12), 683 (14), 651 (13), 589 (9), 556 (23), 537 (27), 460 (9), 353 (25), 296 (33), 251 (54) cm^{-1} . IR: 3478 (w), 3386 (w), 1705 (vs), 1551.24 (s), 1407 (m), 1355 (s), 1305 (s), 1225 (w), 1123 (s), 1097 (s), 989 (w), 943 (w), 916 (w), 889 (w), 860 (w), 822 (w), 772 (m), 646 (m), 613 (w), 510 (m) cm^{-1} . $\text{C}_{10}\text{H}_{14}\text{N}_6\text{O}_{12}$ (364.22 g mol $^{-1}$): C 29.28, H 3.44, N 20.49; found C 29.26, H 3.58, N 18.72. Dec. point: 122 °C. Sensitivities (BAM): impact 40 J; friction 360 N (grain size <100 μm).

1,4-Dideoxy-1,4-dinitro-neo-inositol tetranitrocarbamate (1): 5 ml of fuming nitric acid were dropped into 5 ml of concentrated sulfuric at 0 °C. The nitration mixture was cooled with an ice bath and 1,4-dideoxy-1,4-dinitro-neo-inositol tetracarbamate (**1b**, 1.00 g, 2.4 mmol) were added in small portions below 5 °C. The solution was stirred at this temperature for one hour and then poured into ice water (100 mL). The precipitate was filtered and washed with cold water to obtain the pure nitrocarbamate **1** (1.21 g, 84 %) as a colorless solid.

^1H NMR (acetone- D_6): δ = 13.9 (br, 4H, NH), 6.35 (t, 2H, $^3J(^1\text{H}, ^1\text{H})$ = 3.0 Hz, HCNO_2), 6.03/5.77 (m, 4H, HCO); $^{13}\text{C}\{^1\text{H}\}$ NMR (acetone- D_6): δ = 147.6 (CO), 147.4 (CO), 80.7 (CH), 70.7 (CH), 69.3 (CH); ^{14}N NMR (acetone- D_6): δ = -10 (CNO $_2$), -48 (NHNO $_2$). Raman (800 mW): 2981 (39), 1789 (52), 1616 (41), 1568 (39), 1440 (41), 1373 (62), 1357 (83), 1346 (80), 1315 (100), 1282 (48), 1264 (40), 1243 (42), 1185 (47), 1031 (50), 993 (66), 920 (57), 833 (37), 728 (37), 571 (42), 546 (44), 520 (37), 478 (44), 459 (80), 405 (56), 345 (56), 295 (49), 263 (78), 251 (68), 213 (54) cm^{-1} . IR: 3214 (w), 2987 (w), 1788 (s), 1690 (w), 1638 (m), 1617 (m), 1569 (s), 1442 (s), 1400 (w), 1354 (w), 1323 (m), 1354 (w), 1155 (vs), 1101 (vs), 1036 (m), 990 (s), 966 (m), 910 (m), 849 (m), 831 (w), 813 (w), 745 (m), 731 (w), 712 (w), 620 (m), 565 (m), 519 (m) cm^{-1} . $\text{C}_{10}\text{H}_{10}\text{N}_{10}\text{O}_{20}$ (590.24 g mol $^{-1}$): C 20.35, H 1.71, N 23.73; found C 20.26, H 2.05, N 21.57. Dec. point: 160 °C. Sensitivities (BAM): impact 4 J; friction 360 N (grain size <100 μm).

6b-Nitrohexahydro-2H-1,3,5-trioxacyclopenta[cd]-pentalene-2,4-6-triol tricarbamate (2b): The alcohol precursor 6b-nitrohexahydro-2H-1,3,5-trioxacyclopenta[cd]-pentalene-2,4-6-triol (**2a**, 1.40 g, 6.0 mmol) was added slowly to a ice-cooled solution of chlorosulfonyl isocyanate

3 Polynitrocarbamates Derived from Nitromethane

(CSI, 2.85 g, 20.0 mmol) in dry acetonitrile (25 mL). The ice bath was removed after the complete addition and stirring at room temperature was continued for one hour. The solution was cooled again with an ice bath and cold water (10 mL) was added slowly. After 10 minutes, the acetonitrile was removed under reduced pressure and the precipitated solid was collected by filtration and washed with cold water to obtain the pure carbamate **2b** (1.74 g, 80 %).

¹H NMR (DMSO-D₆): δ = 6.9 (br, 6H, NH₂), 6.09 (s, 3H, HC(O)O), 5.30 (s, 3H, HC(O)C); ¹³C{¹H} NMR (DMSO-D₆): δ = 154.1 (C(O)N), 104.9 (CNO₂), 101.0 (C(O)O), 91.2 (C(O)C). Raman (800 mW): 3284 (11), 3029 (59), 3020 (75), 3009 (100), 2988 (62), 2980 (62), 2938 (17), 2255 (10), 1741 (29), 1703 (33), 1599 (22), 1557 (34), 1389 (35), 1370 (32), 1352 (56), 1311 (40), 1285 (37), 1267 (22), 1131 (56), 1106 (52), 1106 (52), 1050 (42), 1019 (65), 1008 (87), 978 (45), 921 (35), 902 (30), 869 (65), 836 (14), 807 (89), 732 (18), 635 (20), 587 (39), 471 (80), 454 (32), 406 (91), 298 (51), 268 (62) cm⁻¹. IR: 3502 (w), 3409 (w), 3336 (w), 3282 (w), 3198 (w), 1732 (s), 1705 (s), 1598 (m), 1557 (s), 1393 (m), 1347 (s), 1333 (s), 1279 (m), 1163 (w), 1134 (m), 1102 (m), 1053 (m), 1017 (vs), 964 (vs), 912 (m), 832 (m), 803 (m), 772 (m), 633 (m), 583 (m) cm⁻¹. C₁₀H₁₂N₄O₁₁ (364.22 g mol⁻¹): C 32.98, H 3.32, N 15.38; found C 32.31, H 3.49, N 14.84. Dec. point: 212 °C. Sensitivities (BAM): impact 40 J; friction 360 N (grain size <100 µm).

6b-Nitrohexahydro-2H-1,3,5-trioxacyclopenta[cd]-pentalene-2,4-6-triol trinitrocarbamate (2): 5 ml of fuming nitric acid were cooled with an ice bath 6b-nitrohexahydro-2H-1,3,5-trioxacyclopenta[cd]-pentalene-2,4-6-triol tricarbamate (**2b**, 1.85 g, 5.1 mmol) was added in small portions below 5 °C. The solution was stirred at this temperature for one hour and then poured into ice water (100 mL). The precipitate was filtered and washed with cold water to obtain the pure nitrocarbamate **2** (2.10 g, 83 %) as a colorless solid.

¹H NMR (acetone-D₆): δ = 13.7 (br, 3H, NH), 6.47 (s, 3H, HC(O)O), 5.62 (s, 3H, HC(O)C); ¹³C{¹H} NMR (acetone-D₆): δ = 147.2 (C(O)N), 105.1 (CNO₂), 103.1 (C(O)O), 92.8 (C(O)C); ¹⁴N NMR (acetone-D₆): δ = -10 (CNO₂), -46 (NHNO₂). Raman (800 mW): 3015 (43), 1780 (19), 1618 (13), 1561 (14), 1448 (13), 1371 (18), 1355 (26), 1328 (55), 1328 (55), 1294 (17), 1111 (11), 1049 (41), 1031 (100), 995 (20), 975 (15), 873 (24), 805 (31), 589 (11), 472 (40), 424 (11), 391 (27), 294 (15), 260 (26), 216 (27) cm⁻¹. IR: 3787 (w), 3199 (w), 3028 (w), 1775 (m), 1608 (m), 1560 (m), 1445 (m), 1374 (w), 1325 (m), 1293 (w), 1160 (s), 1135 (s), 1108 (m), 1972 (s), 969 (m), 921 (vs), 853 (m), 804 (m), 787 (m), 744 (m), 636 (m), 599 (m), 587 (m) cm⁻¹. C₁₀H₉N₇O₁₇ (499.22 g mol⁻¹): C 24.06, H 1.82, N 19.64; found C 23.13, H 2.13, N 16.95. Dec. point: 172 °C. Sensitivities (BAM): impact 10 J; friction 360 N; (grain size <100 µm).

2,3-Bis(hydroxymethyl)-2,3-dinitro-1,4-butanediol tetracarbamate (3b): The alcohol precursor 2,3-bis(hydroxymethyl)-2,3-dinitro-1,4-butanediol (**3a**, 1.56 g, 6.5 mmol) was added slowly to a ice-cooled solution of chlorosulfonyl isocyanate (CSI, 4.21 g, 29.7 mmol) in dry acetonitrile (25 mL). The ice bath was removed after the complete addition and stirring at room temperature was continued for one hour. The solution was cooled again with an ice bath and cold water (15 mL) was added slowly. After 10 minutes, the acetonitrile was removed under reduced pressure and the precipitated solid was collected by filtration and washed with cold water to obtain the pure carbamate **3b** (2.37 g, 88 %).

¹H NMR (DMSO-D₆): δ = 6.8 (br, 8H, NH₂), 4.65 (s, 8H, CH₂); ¹³C{¹H} NMR (DMSO-D₆): δ = 154.7 (CO), 92.0 (CNO₂), 60.9 (CH₂). Raman (800 mW): 3056 (6), 3031 (8), 3004 (6), 2991 (52), 1702 (37), 1622 (9), 1568 (32), 1461 (7), 1449 (19), 1367 (28), 1335 (9), 1293 (23), 1285 (6), 1215 (5), 1133 (5), 1104 (27), 1042 (6), 964 (52), 923 (24), 890 (33), 861 (41), 805 (16), 764 (7), 687 (15), 633 (10), 512 (15), 384 (24), 312 (11), 291 (41), 221 (13) cm⁻¹. IR: 3477 (m), 3312 (m), 3197 (w), 1706 (vs), 1606 (m), 1593 (m), 1559 (s), 1470 (m), 1414 (s), 1327 (vs), 1279 (m), 1125 (m), 1102 (s), 1063 (vs), 961 (m), 931 (m), 888 (m), 860 (m), 804 (w), 771 (m), 762 (m), 631 (m), 529 (m) cm⁻¹. C₁₀H₁₆N₆O₁₂ (412.27 g mol⁻¹): C 29.13, H 3.91, N 20.38; found C 29.23, H 3.87, N 20.21. T_{melt}: 207. Dec. point: 214 °C. Sensitivities (BAM): impact 40 J; friction 360 N (grain size <100 µm).

2,3-Bis(hydroxymethyl)-2,3-dinitro-1,4-butanediol tetranitrocaramate (3): 5 ml of fuming nitric acid were cooled with an ice bath and 2,3-bis(hydroxymethyl)-2,3-dinitro-1,4-butanediol tetracarbamate (**3b**, 0.83 g, 2 mmol) was added in small portions below 5 °C. The solution was stirred at this temperature for one hour and then poured into ice water (100 mL). The precipitate was filtered and washed with cold water to obtain the nitrocaramate **3** (1.12 g, 95 %) as a colorless solid. The compound was dried at 50 °C under reduced pressure to remove traces of water.

¹H NMR (acetone-D₆): δ = 13.9 (br, 4H, NH), 5.15/5.08 (8H, ²J¹H,¹H) = 12.3 Hz, CH_AH_B); ¹³C{¹H} NMR (acetone-D₆): δ = 147.6 (CO), 92.2 (CNO₂), 62.7 (CH₂); ¹⁴N NMR (acetone-D₆): δ = -10 (CNO₂), -47 (NHNO₂). Raman (800 mW): 3059 (37), 2997 (46), 2985 (45), 1776 (43), 1578 (43), 1474 (22), 1449 (44), 1406 (22), 1327 (100), 1274 (37), 1191 (23), 1143 (24), 1129 (23), 1061 (41), 986 (24), 867 (35), 551 (19), 465 (71), 452 (31), 369 (48), 345 (28), 334 (24), 302 (22), 292 (24), 284 (25), 272 (29), 238 (48) cm⁻¹. IR: 3634 (w), 3566 (w), 3489 (w), 2981 (w), 2771 (w), 1778 (m), 1595 (m), 1565 (s), 1470 (m), 1446 (m), 1331 (m), 1176 (vs), 1124 (m), 1104 (m), 988 (m), 966 (m), 928 (w), 861 (m), 807 (m), 786 (m), 740 (s), 730 (s), 699 (m), 636 (w), 575 (m), 547 (m), 519 (m) cm⁻¹. C₁₀H₁₂N₁₀O₂₀ (592.26 g mol⁻¹): C 20.28, H 2.04, N 23.65;

3 Polynitrocaramates Derived from Nitromethane

found C 21.78, H 2.62, N 19.17. Dec. point: 172 °C. Sensitivities (BAM): impact 25 J; friction 360 N; (grain size <100 µm).

3.6 References

- [1] a) T. M. Klapötke, *Chemistry of High-Energy Materials*, De Gruyter, Berlin, **2015**; b) Q. J. Axthammer, B. Krumm, T. M. Klapötke, *J. Org. Chem.* **2015**, 6329–6335; c) T. M. Klapötke, B. Krumm, R. Moll, *Chem. Eur. J.* **2013**, 19, 12113–12123. d) Q. J. Axthammer, T. M. Klapötke, B. Krumm, R. Moll, S. F. Rest, *Z. Anorg. Allg. Chem.* **2014**, 640, 76–83;
- [2] J. P. Agrawal, *High Energy Materials*, Wiley-VCH, Weinheim, **2010**.
- [3] a) Q. J. Axthammer, B. Krumm, T. M. Klapötke, *Eur. J. Org. Chem.* **2015**, 723–729; b) Q. J. Axthammer, T. M. Klapötke, B. Krumm, *Z. Anorg. Allg. Chem.* **2016**, 642, 211–218; c) Q. J. Axthammer, T. M. Klapötke, B. Krumm, T. Reith, *Inorg. Chem.* **2016**, 55, 4683–4692.
- [4] a) R. A. Aitken, K. M. Aitken, *Science of Synthesis* **2010**, 41, 9–258; b) F. W. Lichtenhaler, H. O. L. Fischer, *J. Am. Chem. Soc.* **1961**, 83, 2005–12; c) S. Cudziło, M. Nita, A. Chołuj, M. Szala, W. Danikiewicz, G. Spólnik, S. Krompiec, S. Michalik, M. Krompiec, A. Świtlicka, *Propellants Explos. Pyrotech.* **2012**, 37, 261–266.
- [5] D. E. Chavez, M. A. Hiskey, D. L. Naud, D. Parrish, *Angew. Chem. Int. Ed.* **2008**, 47, 8307–8309.
- [6] G. Socrates, *Infrared and Raman Characteristic Group Frequencies*, John Wiley & Sons Ltd., Chichester, **2001**.
- [7] M. J. Frisch, G. W. Trucks, H. B. Schlegel, G. E. Scuseria, M. A. Robb, J. R. Cheeseman, G. Scalmani, V. Barone, B. Mennucci, G. A. Petersson, H. Nakatsuji, M. Caricato, X. Li, H. P. Hratchian, A. F. Izmaylov, J. Bloino, G. Zheng, J. L. Sonnenberg, M. Hada, M. Ehara, K. Toyota, R. Fukuda, J. Hasegawa, M. Ishida, T. Nakajima, Y. Honda, O. Kitao, H. Nakai, T. Vreven, J. A. Montgomery Jr., J. E. Peralta, F. Ogliaro, M. J. Bearpark, J. Heyd, E. N. Brothers, K. N. Kudin, V. N. Staroverov, R. Kobayashi, J. Normand, K. Raghavachari, A. P. Rendell, J. C. Burant, S. S. Iyengar, J. Tomasi, M. Cossi, N. Rega, N. J. Millam, M. Klene, J. E. Knox, J. B. Cross, V. Bakken, C. Adamo, J. Jaramillo, R. Gomperts, R. E. Stratmann, O. Yazyev, A. J. Austin, R. Cammi, C. Pomelli, J. W. Ochterski, R. L. Martin, K. Morokuma, V. G. Zakrzewski, G. A. Voth, P. Salvador, J. J. Dannenberg, S. Dapprich, A. D. Daniels, Ö. Farkas, J. B. Foresman, J. V. Ortiz, J. Cioslowski, D. J. Fox, Gaussian, Inc., *Gaussian 09*, Wallingford, **2009**.
- [8] M. Suceska, *EXPLO5*, v. 6.02, Zagreb, **2013**.
- [9] Oxford Diffraction Ltd., *CrysAlis CCD*, 1.171.35.11, Abingdon, Oxford (U.K.), **2011**.
- [10] Oxford Diffraction Ltd., *CrysAlis RED*, 1.171.35.11, Abingdon, Oxford (U.K.), **2011**.
- [11] A. Altomare, M. C. Burla, M. Camalli, G. L. Cascarano, C. Giacovazzo, A. Gualandi, A. G. G. Moliterni, G. Polidori, R. Spagna, *J. Appl. Crystallogr.* **1999**, 32, 155–119.
- [12] a) G. M. Sheldrick, *Programs for Crystal Structure Determination*, University of Göttingen, Germany, **1997**; b) G. M. Sheldrick, *Acta Crystallogr.* **2008**, 64 A, 112–122.
- [13] L. Farrugia, *J. Appl. Crystallogr.* **1999**, 32, 837–838.
- [14] A. L. Spek, *Acta Crystallogr.* **2009**, 65 D, 148–155.
- [15] R. D. Dennington, T. A. Keith, J. M. Millam, *GaussView*, v. 5.08, Semichem, Inc., Wallingford, **2009**.

3 Polynitrocaramates Derived from Nitromethane

- [16] J. A. Montgomery, M. J. Frisch, J. W. Ochterski, G. A. Petersson, *J. Chem. Phys.* **2000**, *112*, 6532–6542.
- [17] M. Suceska, *Propellants Explos. Pyrotech.* **1991**, *16*, 197–202.

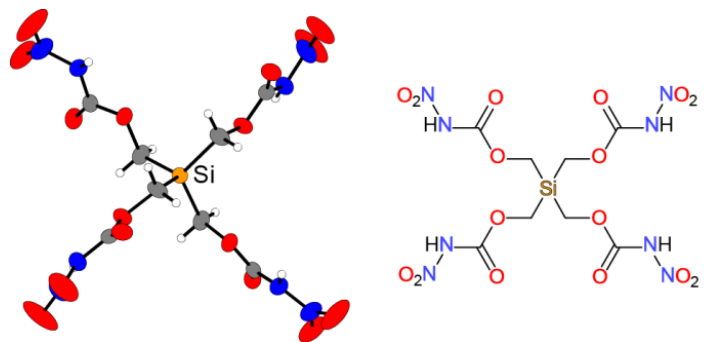
4 Silicon Analogues of Neo-Pentane Derivatives

ENERGETIC SILA-NITROCARBAMATES: SILICON ANALOGUES OF NEO-PENTANE DERIVATIVES

Quirin J. Axthammer, Thomas M. Klapötke, Burkhard Krumm, and Thomas Reith

as published in

Inorganic Chemistry **2016**, *55*, 4683–4692

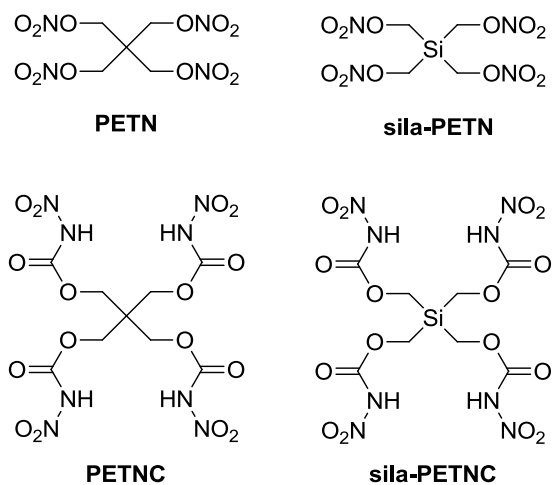


4.1 Abstract

Four silanes based on the neo-pentane skeleton $\text{Me}_{4-x}\text{Si}(\text{CH}_2\text{R})_x$ containing carbamate groups ($x = 1-4$, $\text{R} = \text{OC(O)NH}_2$) have been prepared via the corresponding alcohols $\text{Me}_{4-x}\text{Si}(\text{CH}_2\text{OH})_x$, starting from the chlorosilanes $\text{Me}_{4-x}\text{SiCl}_x$. Subsequent nitration leads to the corresponding primary nitrocarbamates ($\text{R} = \text{OC(O)NHNO}_2$), examined for the purpose as potential energetic materials, including the silicon analogue of pentaerythritol tetranitrocarbamate (sila-PETNC) and a siloxane based nitrocarbamate side-product. All compounds were thoroughly characterized by spectroscopic methods including X-ray diffraction. Thermal stabilities and sensitivities towards impact and friction were examined, as well as detonation values by calculating energies of formation using the EXPLO5 V6.02 software.

4.2 Introduction

Recently, the class of primary nitrocarbamate compounds was examined as potential energetic materials and as well as ligands for metal complexes.¹ Among them, the neo-pentane derivative pentaerythritol tetranitrocarbamate (PETNC, Scheme 4.1) was synthesized by a two-step synthesis starting from pentaerythritol.^{1b} The reaction with the useful reagent chlorosulfonyl isocyanate (CSI) allowed an easy access to the tetracarbamate of pentaerythritol, which upon further nitration forms PETNC. In comparison with the well known and widely used explosive pentaerythritol tetranitrate (PETN), the nitrocarbamate PETNC shows an increased thermal stability as well as lower sensitivities against friction and impact.^{1b, 2}



Scheme 4.1: Structures of PETN, PETNC and their silicon analogues.

The compound tetrakis(nitratomethyl)silane (sila-PETN), the silicon derivative of PETN, was investigated in 2007.³ This highly sensitive material was shown to exhibit a higher heat of explosion, based on the highly exothermic reaction forming silicon dioxide.⁴ Unfortunately, the extraordinarily high sensitivity of sila-PETN inhibits full characterization and further applications.³ In accordance, the synthesis and study of minor substituted silicon based neo-pentane nitrates feature much higher sensitivities than their corresponding carbon analogues, and as a consequence, exhibit better handling compared to sila-PETN.⁵ Furthermore, the first structural studies of silicon containing nitrate esters were established.

One of the points of interest for us in this study is, if a hereto unknown sila-PETNC compound would outperform the carbon derivative PETNC, and furthermore, would be less sensitive than the sila-PETN. Apart from this, the stabilization with nitrocarbamates compared to nitrate esters of silicon compounds should be examined and discussed. Therefore, in addition to sila-PETNC, the minor substituted sila-neo-pentane derivatives containing nitrocarbamate moieties as shown in Scheme 4.2, were synthesized and examined, including their stability and sensitivities regarding friction and impact.

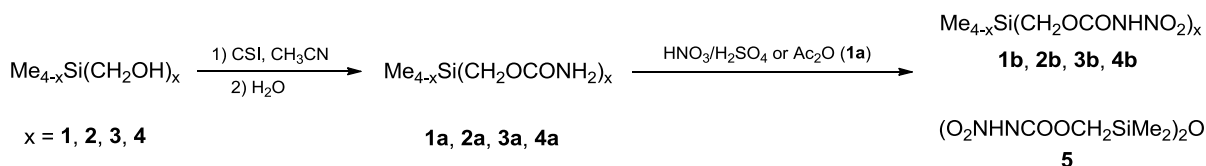
4.3 Results and Discussion

4.3.1 Synthesis

The alcohol precursor compounds $\text{Me}_{4-x}\text{Si}(\text{CH}_2\text{OH})_x$ were synthesized from the corresponding chlorosilanes $\text{Me}_{4-x}\text{SiCl}_x$ according to literature procedures.⁵⁻⁶ The first step is the conversion into the chloromethylsilanes $\text{Me}_{4-x}\text{Si}(\text{CH}_2\text{Cl})_x$ by treatment with *n*-butyl lithium and bromochloromethane at -78°C in THF/hexanes. During these studies a modified and simplified synthesis procedure is developed for the important precursor tetrakis(chloromethyl)silane, $\text{Si}(\text{CH}_2\text{Cl})_4$, avoiding the use of time-consuming column chromatography (described in detail in the Exp. Section). The chloromethylsilanes were converted into the acetoxyethylsilanes $\text{Me}_{4-x}\text{Si}(\text{CH}_2\text{OCOCH}_3)_x$ with sodium acetate in refluxing dimethylformamide. With an acid catalyzed methanolysis using acetyl chloride, the final conversion into the alcohols $\text{Me}_{4-x}\text{Si}(\text{CH}_2\text{OH})_x$ was achieved.

The reaction of the alcohols with equivalent amounts of the reagent chlorosulfonyl isocyanate (CSI) and subsequent hydrolysis yielded the corresponding carbamates $\text{Me}_{4-x}\text{Si}(\text{CH}_2\text{OCONH}_2)_x$ **1a** ($x = 1$ (**1a**), 2 (**2a**), 3 (**3a**), and 4 (**4a**)). In comparison to other carbamate functionalizing routes, the usage of CSI has several advantages in the synthesis towards primary carbamates, for instance fast reaction times, high yields and prevention of multi-addition.^{1b} The carbamates

1a and **2a** were previously synthesized via the chloroformate–ammonia route, a multi-step strategy with lower yields, but characterized only by melting points and elemental analyses.⁷ The nitrocarbamates **2b**, **3b** and **4b** were obtained by treatment of the carbamates (**2a–4a**) with anhydrous nitric acid and concentrated sulfuric acid, followed by an aqueous work up (Scheme 4.2).



Scheme 4.2: Syntheses of silicon containing carbamates (1a–4a) and nitrocarbamates (1b–4b and 5).

The synthesis of the trimethylsilylmethyl nitrocarbamate **1b** was successful by a slightly modified protocol via the nitration of **1a** using a less oxidizing mixture, anhydrous nitric acid and acetic anhydride. Applying mixed acid as above with **1a**, the reaction follows a different pathway by oxidative abstraction of a methyl group, and the formation of the disiloxane **5** was observed and also could be isolated (Scheme 4.2). All carbamates and nitrocarbamates are colorless solids, which are purified by recrystallization or precipitation. In the case of tetrakis(carbamoylmethyl)silane (**4a**) and tetrakis(nitrocarbamoylmethyl)silane (**4b**), pure products precipitate in good yields from the standard reaction work-up. The yields of the other nitrocarbamates are rather low, possibly due to the harsh nitration conditions, resulting partially in cleavage of the carbamate molecules.

4.3.2 NMR and Vibrational Spectroscopy

In the ^1H NMR spectra of the carbamates **1a–4a** and nitrocarbamates **1b–4b**, with increasing number of carbamate/nitrocarbamate moieties per silicon atom a slight low field shift of the NH_2/NH , CH_2 and CH_3 signals is observed. The ^1H NMR resonances of the nitrated compounds **1b–4b** are in general shifted towards lower field in comparison with the corresponding carbamates, most significantly observed with the NH_2/NH resonance. The nitration of the carbamate nitrogen NH_2 causes a strong acidification and deshielding of the nitramino NH proton from 6.34–6.45 ppm to 13.2–13.4 ppm with additional broadening of the resonance.

In the $^{13}\text{C}\{^1\text{H}\}$ NMR spectra, both the CH_2 and CH_3 signals are shifted to lower field for every additional carbamate/nitrocarbamate unit connected to the silicon center and are rather unaffected upon nitration. The opposite occurs for the carbonyl resonance, which is almost independent from the substitution pattern, but is strongly influenced by nitration. The carbonyl

resonance observed in the region of 157.7–158.1 ppm for the carbamates **1a–4a** shifts to high field around 150.4–150.7 ppm for the nitrocarbamates **1b–4b**. The ^{13}C NMR resonances of sila-PETNC (**4b**) [150.7 (CO) and 55.6 (CH₂), acetone-D₆], when compared to those of the carbon analogue PETNC [148.9 (CO) and 64.3 (CH₂), DMSO-D₆],^{1b} show a significant difference for the CH₂ resonance, because of the adjacent silicon or carbon, resulting in a highfield shift in the case of silicon. The ^{15}N NMR resonances of sila-PETNC (**4b**) with -45.3 (NO₂) and -190.4 (NH, br) are in the similar region as detected for the carbon analogue PETNC. Also, similar as found for PETNC,^{1b} coupling of the nitramine nitrogen with the acidic hydrogen is not observed, due to rapid exchange with the solvent deuterium. The ^{29}Si NMR resonance is strongly dependent on the number of carbamate moieties, respectively nitrocarbamate units. Each additional unit attached to the sila-neo-pentane skeleton leads to a high field shift of the ^{29}Si NMR resonance, ranging from -0.4 to -15.5 ppm for the carbamates **1a–4a** and 0.4 to -9.8 ppm for the nitrocarbamates **1b–4b** (Figure 4.1).

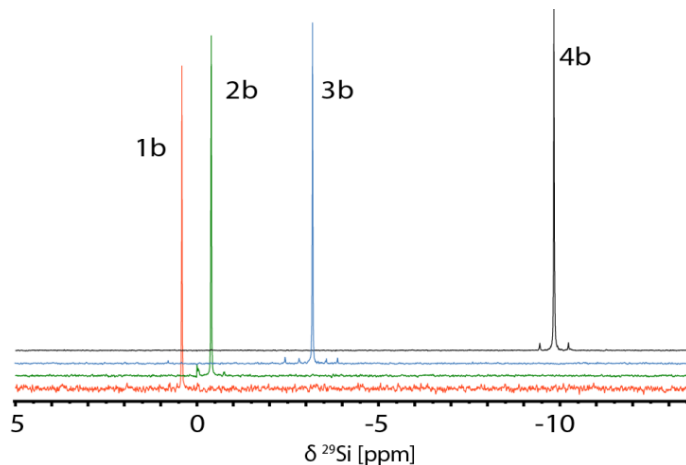


Figure 4.1: Influence of the substitution pattern to the ^{29}Si NMR resonance for the nitrocarbamates **1b**, **2b**, **3b** and **4b** (in acetone-D₆).

The $^1\text{H}/^{13}\text{C}/^{15}\text{N}$ NMR spectra of the nitrocarbamate containing a siloxane unit **5** are obviously very similar to those of the nitrocarbamate **1b**, except the integral ratios in the ^1H NMR spectra. However, a major difference is detected in the ^{29}Si NMR resonances, due to the presence of an oxygen atom bound to silicon. Therefore, due to the deshielding effect of the electron withdrawing oxygen, the resonance of **5** is low-field shifted to 3.5 ppm, compared to that of **1b** at 0.6 ppm.

In the vibrational spectra (IR and Raman) the N–H stretching vibrations for the carbamates **1a–4a** and nitrocarbamates **1b–4b** and **5** are found at 3450–3200 cm^{-1} . The carbonyl C=O stretching vibration of the carbamates **1a–4a** is detected in the region of 1703–1665 cm^{-1} .

Upon nitration, this vibration is shifted to higher wavenumbers at 1773–1735 cm^{–1} for the nitrocarbamates **1b–4b** and **5**. Additionally, the nitrocarbamates show the symmetrical and asymmetrical stretching vibrations of the nitro group, typically located at 1623–1604 cm^{–1} and 1336–1291 cm^{–1}. The disiloxane unit in **5** shows a strong signal at 1076 cm^{–1} typical for the Si–O stretching vibration.⁸

4.3.3 Single Crystal Structure Analysis

Carbamate Structures

Single crystals suitable for X-ray diffraction measurements of compounds **2a**, **3a** and **4a** were obtained at ambient temperature from toluene, dioxane and water, respectively. The carbamates **2a** (Figure 4.2), **3a** (Figure 4.3) and **4a** (Figure 4.4a) show similar features regarding the symmetry around silicon.

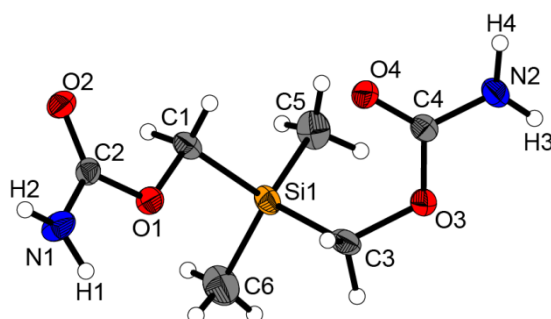


Figure 4.2: X-ray molecular structure of bis(carbamoylmethyl) dimethylsilane (**2a**). Selected atom distances [Å] and bond angles [deg]: Si1–C6 1.862(4), Si1–C5 1.867(4), Si1–C1 1.879(3), Si1–C3 1.893(3), O2–C2 1.225(3), O1–C2 1.347(3), O1–C1 1.467(4), N1–C2 1.346(4), N1–H2 0.94(4), N1–H1 0.89(3); C1–O1–C2–O2 2.3(4), C1–O1–C2–N1 –179.6(2), C2–O1–C1–Si1 –176.9(2).

The silicon atom in the center of compounds **2a–4a** is surrounded by the methyl and methylene carbon units in an almost perfect tetrahedral sphere. The atom distances Si–C are in the range of 1.854–1.893 Å, the C–Si–C bond angles with 102.70–115.68 ° differ only slightly from the ideal tetrahedral angle of 109.47 °.

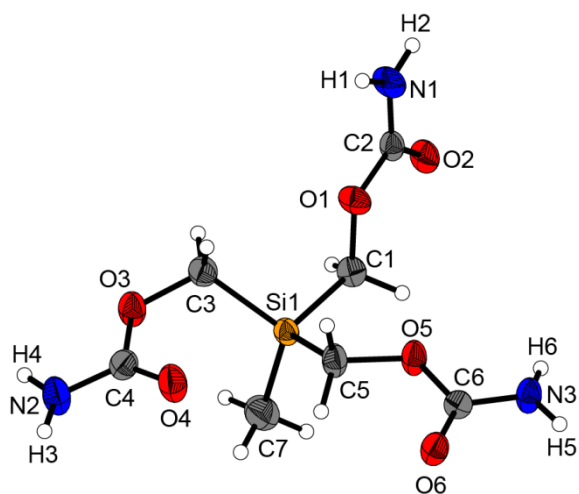


Figure 4.3: X-ray molecular structure of tris(carbamoylmethyl) methylsilane (**3a**) (dioxane solvate omitted). Selected atom distances [Å] and bond angles [deg]: Si–C7 1.854(2), Si–C1 1.879(2), Si–C5 1.883(2), Si–C3 1.884(2), O1–C2 1.351(2), O1–C1 1.450(2), O2–C2 1.221(2), N1–C2 1.324(3), N1–H2 0.83(2), N1–H1 0.86(2); C1–O1–C2–O2 –3.6(3), C1–O1–C2–N1 177.58(17).

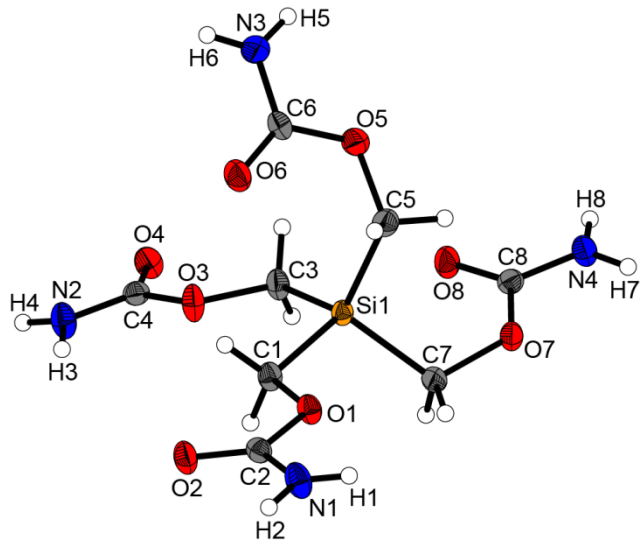


Figure 4.4a: X-ray molecular structure of tetrakis(carbamoylmethyl)silane (**4a**). Selected atom distances [Å] and bond angles [deg]: Si1–C1 1.890(2), O1–C2 1.357(2), O1–C1 1.456 (2), O2–C2 1.225(2), N1–C2 1.324(2), N1–H1 0.84 (2), N1–H2 0.92(2); C2–O1–C1–Si1 175.0(1), C3–Si1–C1–O1 176.7(1), C1–O1–C2–O2 –1.5(2), C1–O1–C2–N1 178.4(1), C4–O3–C3–Si1 –175.4(1), C1–Si1–C3–O3 14.2(1), C1–Si1–C7–O7 –151.9(1), C3–Si1–C7–O7 94.6(1), C1–Si1–C5–O5 –108.0(1), C3–Si1–C5–O5 8.9(1), C3–O3–C4–O4 –7.5(2), C3–O3–C4–N2 173.8(1).

The carbamate units show a quite good planarity in all three compounds (**2a–4a**). The strongest misalignment is represented by the torsion angles C–O–C–N and C–O–C–O and

amounts always less than 10 °. The planarity can be interpreted as a delocalized π -system, which was confirmed regarding the quiet short atom distances.^{1b} In all three compounds (**2a–4a**), the atom distance of the bridging oxygen atom and the carbonyl carbon is shortened to a distance between 1.347 to 1.357 Å. This implicates a substantial double bond character in between a C–O double bond (1.20 Å) and a single bond (1.43 Å). In accordance, the carbonyl C=O double bond is slightly enlarged to 1.225–1.221 Å. More so, the distance of the C–N bond values at 1.324 to 1.346 Å. Considering a standard C–N single bond with 1.47 Å, this indicates a strong double bond character. The free electron pair of the amino nitrogen seems to be delocalized all over the carbamate system, thus stabilizing it and favoring a planar conformation.

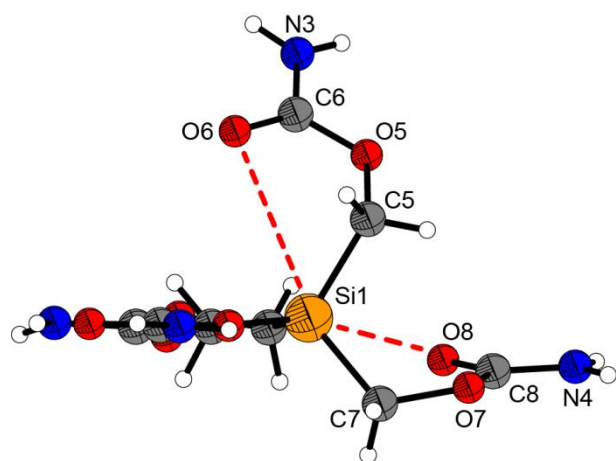


Figure 4.4b: X-ray molecular structure of tetrakis(carbamoylmethyl)silane (**4a**). Red dotted lines represent attractive interactions between Si1…O6 (3.24 Å) and Si1…O8 (2.86 Å).

Surprisingly, all carbamate structures **2a–4a** show a noticeable short distance between the silicon atom in the center of the molecule and at least one carbonyl oxygen atom of the carbamate moieties.⁹ The compound tetrakis(carbamoylmethyl)silane (**4a**) shares this feature with two carbamate arms, ending up with a pseudo hexavalent coordination shown in Figure 4.4b. This conformation enforces an elongation of the Si–C–O bond angle (Table 4.1). Furthermore, the torsion angles Si–C–O–C of those two substitutes differ significantly, in sharp contrast with the two remaining carbamate arms developing one plane with the silicon center.

The carbamate moieties also define the majority of intra- and intermolecular interactions in compounds **2a–4a**. Especially the hydrogen bonds between the amino hydrogens and neighboring carbonyl oxygens are very strong. Consequently, the carbamate moieties attract each other and develop a layered structure of the molecules at the macromolecular view level.

Table 4.1: Selected bond angles [°], torsion angles [°] and atom distances [Å] of tetrakis(carbamoylmethyl)silane (**4a**).

	Si1-C1-O1-C2	Si1-C3-O3-C4	Si-C5-O5-C6	Si1-C7-O7-C8
bond angle Si-C-O	111.8	107.1	116.8	115.7
torsion angle Si-C-O-C	-5.0	4.6	74.0	-58.2
d (Si…O)	O2: 4.52	O4: 4.58	O6: 3.24	O8: 2.86

Nitrocarbamate Structures

The crystal structures of nitrocarbamoylmethyltrimethylsilane (**1b**) and bis(nitrocarbamoylmethyl) dimethylsilane (**2b**) (Figures 4.5a, 4.5b and 4.6) display similar features as their previously discussed carbamate analogues **2a** and **3a** in regards to the almost identical Si–C atom distances and C–Si–C bond angles.

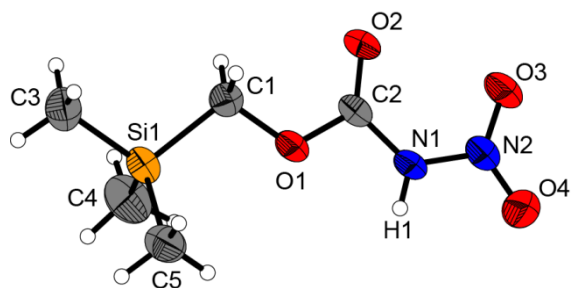


Figure 4.5a: X-ray molecular structure of nitrocarbamoylmethyltrimethylsilane (**1b**). Selected atom distances [Å] and bond angles [deg]: Si–C3 1.849(3), Si–C5 1.852(3), Si–C4 1.859(3), Si–C1 1.887(3), O1–C2 1.327(3), O1–C1 1.465(3), O2–C2 1.193(2), O4–N2 1.206(3), N2–O3 1.210(2), N2–N1 1.361(3), C2–N1 1.376(3), N1–H1 0.80(2), C3–Si–C5 111.37(13), C3–Si–C4 112.02(14), C5–Si–C4 111.49(14), C3–Si–C1 106.28(12), C5–Si–C1 108.36(13), C4–Si–C1 107.01(14); C1–O1–C2–O2 -6.3(4), C1–O1–C2–N1 173.1(2), O4–N2–N1–C2 -177.0(3), O3–N2–N1–C2 3.0(4), O2–C2–N1–N2 -6.6(4), O1–C2–N1–N2 174.0(2), O4–N2–N1–H1 -5.5(20), O3–N2–N1–H1 174.4(20).

The planarity of the nitrocarbamate moiety in compound **1b** is comparable to the planar carbamate structures in **2a**–**4a**. The *N*-hydrogen atom is part of strong classical hydrogen bonds to neighbored carbonyl and nitro functions. Additionally, multiple improper hydrogen bonds with carbon as hydrogen donor can be observed as shown in Figure 4.5b. Overall, the nitrocarbamate functions align to each other and develop a layer-like structure.

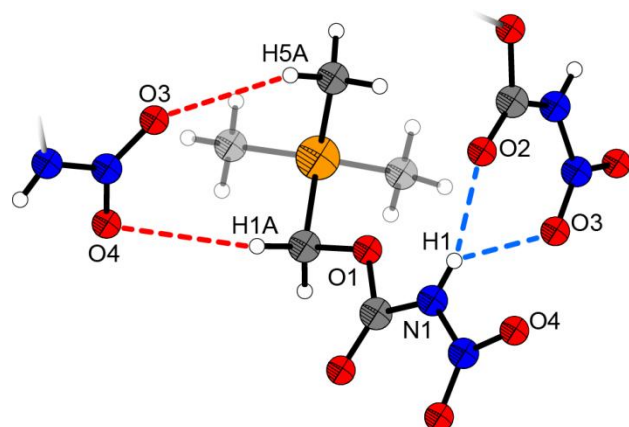


Figure 4.5b. Classical (blue dotted lines) and improper (red dotted lines) hydrogen bonds in **1b**.

The planarity of the nitrocarbamate moiety in compound **1b** is comparable to the planar carbamate structures in **2a–4a**. The *N*-hydrogen atom is part of strong classical hydrogen bonds to neighbored carbonyl and nitro functions. Additionally, multiple improper hydrogen bonds with carbon as hydrogen donor can be observed as shown in Figure 4.5b. Overall, the nitrocarbamate functions align to each other and develop a layer-like structure.

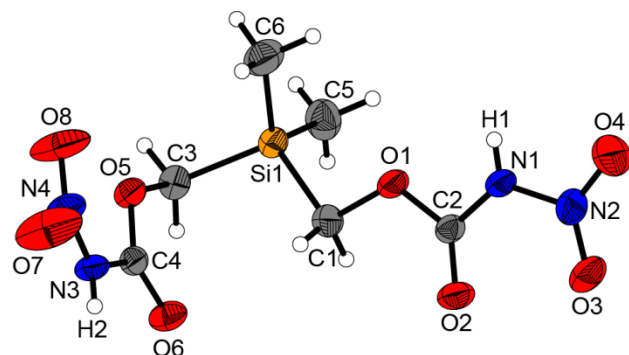


Figure 4.6: X-ray molecular structure of bis(nitrocarbamoylmethyl) dimethylsilane (**2b**). Selected atom distances [Å] and bond angles [deg]: Si–C5 1.851(2), Si–C1 1.883(2), O1–C2 1.318(2), O1–C1 1.462(2), O2–C2 1.188(2), O3–N2 1.205(2), N1–N2 1.371(2), N1–C2 1.383(2), N1–H1 0.77(2), O4–N2 1.211(2); C2–N1–N2–O3 –12.1(3), C2–N1–N2–O4 167.0(2), C1–O1–C2–O2 4.9(3), C1–O1–C2–N1 –174.2(2), N2–N1–C2–O2 7.5(3), N2–N1–C2–O1 –173.4 (2).

The nitro groups of the bisnitrocarbamate **2b** are substantially out of plane, resulting in torsion angles C–N–N–O of 12.1 °, 18.3 ° and 20.5 °. In comparison with the corresponding carbamate **2a**, the atom distances O–C and C=O are shortened upon nitration (from average 1.23 Å in the carbamate to 1.19 Å in the nitrocarbamate), while the distance C–N is enlarged (from 1.35 Å in

2a to 1.38 Å in **2b**). The nitro groups in both structures (**1b** and **2b**) are located in *cis*-position with respect to the carbonyl group.

The sila-PETNC (**4b**) (Figure 4.7) crystallizes in the same tetragonal space group $P-42_1c$ as the carbon analogue PETNC.^{1b} The unit cell contains two molecules, while the asymmetric unit is only represented by one fourth of the molecule, induced by the four-fold rotoinversion axis and two glide planes through the central silicon atom. The four nitrocarbamate units are involved in several strong classical hydrogen bonds, with the N–H linking to oxygen of a neighboring carbonyl and nitro functions. The strong intermolecular forces of sila-PETNC lead to a layer-like structure, comparable to the nitrocarbamates **1b** and **2b** and identical to the structure of PETNC.^{1b} The density of sila-PETNC (1.70 g cm⁻³) is lower than that of PETNC (1.77 g cm⁻³), which can be explained on an intramolecular reasons. The major difference in both structures is the atom distance between the center atoms and their surrounding methylene groups. In PETNC, the atom distance of the centering carbon to its closest neighbor amounts to 1.533 Å, whereas the atom distance in sila-PETNC with Si1–C1 = 1.868 Å is much larger.^{1b}

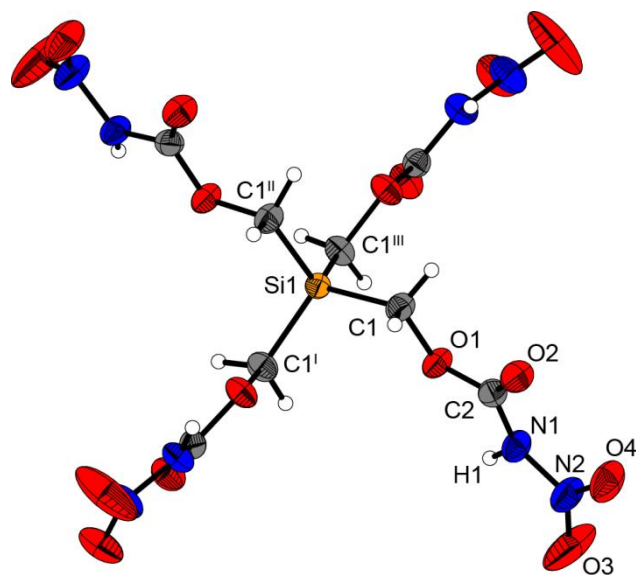


Figure 4.7: X-ray molecular structure of sila-PETNC (**4b**). Selected atom distances [Å] and bond angles [deg]: Si–C1 1.868(2), O1–C2 1.337(3), O1–C1 1.461(3), O2–C2 1.191(3), O3–N2 1.204(4), O4–N2 1.198(3), N1–N2 1.368(3), N1–C2 1.387(3), N1–H3 0.84(3); C1–O1–C2–O2 4.6(3), C1–O1–C2–N1 –176.6(2), N2–N1–C2–O2 –9.4(4), N2–N1–C2–O1 171.8(2), C2–N1–N2–O4 21.4(4), C2–N1–N2–O3 –162.0(2), C2–O1–C1–Si1 170.7(1).

The structure of the siloxane **5** consist of one and a half asymmetric units, the structure shown in Figure 4.8 represents the symmetrical unit created with inversion center. The inversion

center is located in between both silicon atoms Si1 and Si1^I, therefore the bridging oxygen position gets split into O1 and O1^I and is occupied half each. The atom distances Si1–O1 and Si1–O1^I differ with 1.61 Å and 1.70 Å, respectively, and lie in between a Si–O single (1.77 Å) and double (1.54 Å) bond. Another characteristic is the obtuse angle Si1–O1–Si1^I = 147.6 °, which is in the range of other disiloxane structures of disilylether (144.1 °), hexafluorodisiloxane (156 °) and hexakis(chloromethyl) disiloxane (161.9 °).¹⁰

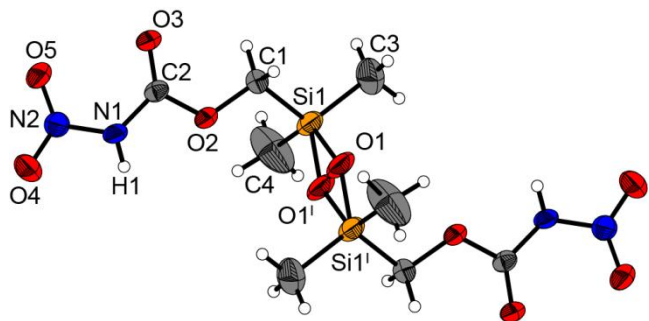


Figure 4.8: X-ray molecular structure of 1,3-bis(nitrocaramoylmethyl)-1,1,3,3-tetramethyldisiloxane (**5**). Selected atom distances [Å] and bond angles [deg]: C1–O2 1.466(3), C1–Si1 1.867(3), C2–O3 1.190(2), C2–O2 1.318(2), C2–N1 1.388(3), C4–Si1 1.827(4), C3–Si1 1.837(3), N1–N2 1.377(3), N1–H3 0.81(2), N2–O4 1.213(2), N2–O5 1.216(2), O1–Si1^I 1.613(4), O1–Si1 1.694(4); Si1^I–O1–Si1 147.6(2); O3–C2–N1–N2 –14.9(4), O2–C2–N1–N2 165.5(2), C2–N1–N2–O4 –169.5(2), C2–N1–N2–O5 11.8(3), N1–C2–O2–C1 178.46(18), Si1–C1–O2–C2 151.27(16).

Compared with the monosubstituted nitrocarbamate **1b**, the nitrocarbamate units of the disiloxane **5** deviate significantly from planarity, as is the case for the bisnitrocarbamate **2b**. Both nitrocarbamate units are located in antiperiplanar fashion to each other to avoid sterical hindrance.

4.3.4 Thermal Stabilities and Energetic Properties

The physical and energetic properties of the nitrocarbamates **1b–4b** and **5** were determined and are summarized in Table 4.2. Their thermal stabilities were measured with a differential scanning calorimetry (DSC) at a heating rate of $5\text{ }^{\circ}\text{C min}^{-1}$. The melting points increase with the number of nitrocarbamate groups from **1b** to **3b**, whereas sila-PETNC (**4b**) decomposes without melting. All nitrocarbamates are at least thermally stable up to $142\text{ }^{\circ}\text{C}$ (onset temperature) with sila-PETNC having the highest decomposition point of $170\text{ }^{\circ}\text{C}$. The sensitivities against friction and impact were evaluated according to BAM standards.¹¹ Both molecules with a single nitrocarbamate moiety per silicon atom, **1b** and **5**, can be classified as less sensitive against both, friction and impact ($\text{FS} = 360\text{ N}$ and $\text{IS} = 35\text{ J}$). One more

nitrocarbamate attached to the silicon center in **2b** with an IS of 3 J can already be considered very sensitive towards impact, while being sensitive towards friction (192 N), but here always large-sized crystals (compared to the other nitrocarbamates) could be considered for measurements. Further nitrocarbamate groups in **3b** (FS = 240 N and IS = 5 J) and **4b** (FS = 240 N and IS = 3 J) somewhat surprisingly do not further enhance the sensitivity.

A very important property for energetic materials is their density, as it directly affects multiple performance parameters, such as detonation velocity and detonation pressure.¹¹ The density of the compounds **1b**, **2b** and **4b** increases with the number of nitrocarbamate moieties attached to the silicon center up to 1.67 g cm⁻³. As expected, sila-PETNC (**4b**) shows the highest detonation velocity and the highest detonation pressure.

Table 4.2: Physical and energetic properties of nitrocarbamates **1b**–**4b** and **5**.

	1b	2b	3b	4b	5
Formula	SiC ₅ H ₁₂ N ₂ O ₄	SiC ₆ H ₁₂ N ₄ O ₈	SiC ₇ H ₁₂ N ₆ O ₁₂	SiC ₈ H ₁₂ N ₈ O ₁₆	Si ₂ C ₈ H ₁₈ N ₄ O ₉
FW / g mol ⁻¹	192.25	296.27	400.29	504.31	370.42
IS / J ^[a]	35	3	5	3	35
FS / N ^[b]	360	192	240	240	360
N / %	14.57	18.91	20.99	22.22	15.13
Q _{CO2} / % ^[c]	-116.5	-64.8	-40.0	-25.4	-86.6
Q _{CO} / % ^[c]	-74.9	-32.4	-12.0	0	-51.8
T _{melt} / °C	50	100	133	–	68
T _{dec.} / °C	155	142	138	170	150
ρ / g cm ⁻³ (RT)	1.191	1.494	1.55 ^[f]	1.669	1.370
Δ _f H _m ° / kJ mol ⁻¹ ^[d]	-655.4	-900.5	-1134.7	-1364.0	-1585.8
Δ _f U° / kJ kg ⁻¹ ^[d]	-3286.7	-2934.8	-2738.6	-2613.7	-4170.6
Δ _{Ex} Q° / kJ kg ⁻¹ ^[e]	-4359	-4729	-4654	-4671	-3628
p _{CJ} / kbar ^[e]	81	142	170	207	92
V _{det.} / m s ⁻¹ ^[e]	5393	6302	6698	7147	5438
V ₀ / L kg ⁻¹ ^[e]	707	691	702	669	631

[a] Impact sensitivity. [b] Friction sensitivity. [c] Oxygen balance assuming formation of CO and CO₂. [d] Energy and enthalpy of formation calculated by the CBS-4M method using Gaussian 09.¹² [e] Predicted heat of explosion, detonation pressure, detonation velocity and volume of gaseous products calculated by using the EXPLO5 (Version 6.02) program package.¹³ [f] Predicted density.

Again, somewhat unexpected, the dinitrocarbamate **2b** has the highest heat of explosion of all in this study measured nitrocarbamates. The high amounts of gaseous product per mass of

compounds **1b** and **2b** are based on the incomplete detonation reaction forced by the large negative oxygen balance of those compounds.

The physical and energetic properties of sila-PETNC (**4b**) were compared to the related materials (Scheme 4.1 and Table 4.3) as indicated in the introduction. Concerning the sensitivities, sila-PETNC exhibits an impact sensitivity of 3 J and a friction sensitivity of 240 N, and therefore is expectedly much less sensitive compared to the nitrate ester sila-PETN (IS < 1 J, FS < 10 N). As expected from the empirical knowledge given from PETN and sila-PETN, the values for sila-PETNC are lower in regard to its carbon analogue PETNC and match roughly with the nitrate ester PETN. Considering the thermal stability, the carbon nitrocarbamate PETNC is more stable than sila-PETNC, which is again in the range of PETN (196 °C, 170 °C and 165 °C respectively).^{1b, 2}

The heat of explosion of sila-PETNC is considerably higher compared to PETNC, which is explained with the very high molar heat of formation of silicon dioxide.¹⁴ Nevertheless, in regards of energetic parameters such as detonation velocity, detonation pressure and produced amount of gas per mass, PETNC excels its silicon analogue.

Table 4.3: Physical and energetic properties (conditions/parameters as Table 4.2) of PETN, PETNC, sila-PETN and sila-PETNC (**4b**).^{1b, 2-3}

	PETN	PETNC	sila-PETN	sila-PETNC
Formula	C ₅ H ₈ N ₄ O ₁₂	C ₉ H ₁₂ N ₈ O ₁₆	C ₄ H ₈ N ₄ O ₁₂ Si	C ₈ H ₁₂ N ₈ O ₁₆ Si
IS / J	3 – 4	8	–	3
FS / N	60 – 80	360	–	240
N / %	17.7	23.0	16.9	22.2
Q _{CO2} / %	+15.2	+3.3	+9.6	0
Q _{CO} / %	-10.1	-26.2	-9.6	-25.4
T _{dec.} / °C	165	196	–	170
T _{melt} / °C	143	–	–	–
ρ / g cm ⁻³ (RT)	1.78	1.76	–	1.64
Δ _f H _m ° / kJ mol ⁻¹	-561	-1311	-1568	-2240
Δ _{Ex} U° / kJ kg ⁻¹	-5980	-4034	–	-4671
p _{CJ} / kbar	319	248	–	207
V _{det.} / m s ⁻¹	8405	7742	–	7147
V ₀ / L kg ⁻¹	743	727	–	695

The density of PETNC is remarkably higher than the density of sila-PETNC, which might be the main reason for this. Since both compounds crystallize in the identical tetragonal space group $P-42_1c$, the difference is found intra-molecular as explained in the structure discussion. Apart from the density, the formation of silicon dioxide leads to a lower amount of gaseous products per mass. Silicon dioxide is a solid compound and the molar mass of sila-PETNC exceeds the one of PETNC, resulting in lower molar equivalents per mass. Furthermore, the formation of SiO_2 , in contrast to CO_2 , does not show a similar equilibrium with a gaseous mono-oxide (i.e. CO), but is converted quantitatively, which affects the oxygen balance Ω_{CO} negatively.¹¹

As an extension for the numbering system of Scheme 4.2, the compound with $x = 0$, i.e. tetramethylsilane, was considered also in this study in comparison to the carbon analogue neopentane. Using the well known data from the literature for the enthalpies of formation for tetramethylsilane, SiMe_4 , $\Delta H^\circ_f(\text{SiMe}_4(\text{liq})) = -313.6 \text{ kJ mol}^{-1}$ and neopentane, CMe_4 , $\Delta H^\circ_f(\text{CMe}_4(\text{liq})) = -190.3 \text{ kJ mol}^{-1}$ ¹⁵ and the approximate densities for the liquid states of 0.65 g cm^{-3} (SiMe_4) and 0.6 g cm^{-3} (CMe_4), the enthalpies of combustion for both compounds using liquid oxygen as the oxidizer and an oxygen balance of $\Omega = 0 \%$ were calculated,¹³ under the following conditions: chamber pressure = 70 bar, atmospheric pressure = 1 bar, isobaric combustion, and equilibrium expansion. As to be expected, the heat of combustion for SiMe_4 ($\Delta H^\circ_{\text{comb}} = -5469 \text{ kJ kg}^{-1}$, F:O ratio = 0.255 : 0.745) is slightly lower than that of neopentane ($\Delta H^\circ_{\text{comb}} = -5899 \text{ kJ kg}^{-1}$, F:O ratio = 0.22 : 0.78), due the higher atomic mass of silicon compared to carbon. On the other hand, for the heats of explosion of sila-PETNC and PETNC, the value of the silicon compound is more exothermic due to the higher enthalpy of formation in the absence of additional oxygen in the detonation process.

4.4 Conclusion

Several new silicon-centered carbamates and nitrocarbamates of the types $\text{Me}_{4-x}\text{Si}(\text{CH}_2\text{OCONH}_2)_x$ and $\text{Me}_{4-x}\text{Si}(\text{CH}_2\text{OC(O)NHNO}_2)_x$ ($x = 1-4$) and a siloxane based nitrocarbamate were synthesized and characterized in this study. The multi-step synthesis starts from commercially available methyl chlorosilanes and silicon tetrachloride via the corresponding chloromethyl silanes, acetates and sila-alcohols. Treatment with chlorosulfonyl isocyanate resulted in the formation of the sila-carbamates, which were nitrated to give the corresponding sila-nitrocarbamates. The new product class was examined in several aspects such as spectroscopic data, sensitivity and structural behavior. Energetic materials combining silicon with the nitrocarbamate unit are substantially less sensitive compared to silicon nitrates or azides and stand out with high heats of explosion. With the synthesis of sila-PETNC a

manageable silicon-based energetic material was designed, which was compared to the related sila-PETN, PETN and PETNC. It shows an extraordinary higher stability against outer stimuli compared to sila-PETN, and at the same time is superior to PETNC in terms of heat of explosion. Nevertheless, sila-PETNC is inferior to its carbon analogue PETNC and especially PETN in regards of detonation pressure, detonation velocity and amounts of gaseous products.

4.5 Experimental Section

4.5.1 General Information

Solvents were dried and purified with standard methods. Trimethylsilyl methanol, bis(chloromethyl) dimethylsilane, trichloromethylsilane, silicon tetrachloride and chlorosulfonyl isocyanate were commercially available and used without further purification. Raman spectra were recorded in glass tube with a Bruker MultiRAM FT-Raman spectrometer with a Klaastech DENICAFC LC-3/40 laser (Nd:YAG, 1064 nm, up to 1000 mW) in the range of 4000-400 cm^{-1} . Relative intensity is given in percent. IR spectra were recorded with a Perkin-Elmer Spectrum BX-FTIR spectrometer coupled with a Smiths ATR DuraSample IRII device. Measurements were recorded in the range of 4000-650 cm^{-1} . All Raman and IR spectra were measured at ambient temperature. NMR spectra were recorded with JEOL Eclipse and Bruker TR 400 MHz spectrometers at 25 °C. Chemical shifts were determined in relation to external standards Me_4Si (^1H , 399.8 MHz); (^{13}C , 100.5 MHz); (^{29}Si , 79.4 MHz) and MeNO_2 (^{14}N , 28.9 MHz; ^{15}N , 40.6 MHz). Mass spectrometric data were determined with a JEOL MStation JMS 700 spectrometer (DEI+, FAB-). Elemental analyses (CHN) were obtained with a Vario EL Elemental Analyzer.

The sensitivity data were acquired by measurements with a BAM drophammer and a BAM friction tester.¹¹ Melting and decomposition points were determined by differential scanning calorimetry (DSC) using a Perkin-Elmer Pyris6 DSC at a heating rate of 5 °C min^{-1} . Measurements were performed in closed aluminum containers against empty containers up to 400 °C via nitrogen flows.

4.5.2 X-ray Crystallography

The crystal structure data were obtained using an Oxford Xcalibur CCD Diffraktometer with a KappaCCD detector at low temperature (173 K, 123 K). Mo- K_{α} radiation ($\lambda = 0.71073 \text{ \AA}$) was delivered by a Spellman generator (voltage 50 kV, current 40 mA). Data collection and reduction were performed using the CRYSTALIS CCD¹⁶ and CRYSTALIS RED¹⁷ software, respectively. The structures were solved by SIR92/SIR97¹⁸ (direct methods) and refined using

the SHELX-97¹⁹ software, both implemented in the program package WinGX22.²⁰ Finally, all structures were checked using the PLATON software.²¹ Structures displayed with ORTEP plots are drawn with thermal ellipsoids at 50 % probability level.

4.5.3 Computational Details

The theoretical calculations were achieved by using the Gaussian 09 program package¹² and were visualized by using GaussView 5.08.²² Optimizations and frequency analyses were performed at the B3LYP level of theory (Becke's B3 three parameter hybrid functional by using the LYP correlation functional) with a cc-pVDZ basis set. After correcting the optimized structures with zero-point vibrational energies, the enthalpies and free energies were calculated on the CBS-4M (complete basis set) level of theory.²³ The detonation parameters were obtained by using the EXPLO5 (V6.02) program package.^{13, 24}

4.5.4 Synthesis

CAUTION! The higher substituted silicon containing nitrocarbamates (**2b**, **3b**, **4b**) are energetic materials and show sensitivities in the range of primary explosives! They should be handled with caution during synthesis or manipulation and additional protective equipment (leather jacket, face shield, ear protection, Kevlar gloves) is strongly recommended.

Carbamoylmethyl trimethylsilane (1a**):** To an ice-cooled solution of trimethylsilyl methanol (1.04 g, 10 mmol) in dry acetonitrile (20 mL), chlorosulfonyl isocyanate CSI (1.56 g, 11 mmol) was added slowly under dry nitrogen atmosphere. After 5 min at 0 °C, the ice bath was removed and the colorless solution was stirred for another hour at ambient temperature. The reaction was cooled again with an ice-bath, water (10 mL) was added carefully and the stirring was continued for 10 min at 0 °C. The organic solvent was removed in vacuo and colorless oil precipitated out of the aqueous phase. After 24 h at 4 °C, the oily residue crystallized and the colorless solid was collected by filtration. Recrystallization in boiling hexane yielded the pure product **1a** as colorless needles (1.45 g, 98%).

¹H NMR (CDCl₃): δ = 4.65 (br, 2H, NH₂), 3.73 (s, 2H, ²J (H, ²⁹Si) = 3.5 Hz, CH₂), 0.07 (s, 9H, ²J (H, ²⁹Si) = 6.8 Hz, CH₃); ¹³C{¹H} NMR (CDCl₃): δ = 158.3 (CO), 58.6 (CH₂), -3.1 (¹J (C, ²⁹Si) = 52.5 Hz, CH₃); ¹⁵N NMR (CDCl₃): δ = -310.5 (NH₂); ²⁹Si NMR (CDCl₃): δ = 0.3. Raman (800 mW): 2961 (40), 2902 (100), 1691 (8), 1440 (2), 1418 (9), 1114 (5), 1074 (10), 907 (10), 703 (10), 604 (77), 510 (5), 317 (12) cm⁻¹. IR: 3439 (w), 3330 (w), 3266 (w), 3209 (w), 2957 (w), 2905 (w), 1741 (w), 1687 (s), 1608 (m), 1436 (w), 1375 (s), 1265 (w), 1250 (m), 1219 (w), 1121 (w), 1061 (s), 904 (w), 841 (s), 785 (m), 719 (w), 701 (w) cm⁻¹. MS (DEI+) [m/z]: 147

$[M+H]^+$. $C_5H_{13}NO_2Si$ (147.25 g mol⁻¹): C 40.78, H 8.90, N 9.51; found C 40.73, H 8.90, N 9.51. Mp.: 67 °C.

Nitrocaramoylmethyl trimethylsilane (1b): Acetic anhydride (10 mL) was slowly mixed with anhydrous nitric acid (>99,5%, 1 mL) at 0 °C and stirred for one hour at that temperature. Carbamoylmethyltrimethylsilane (**1a**, 294.5 mg, 2 mmol) was added in small portions, and the suspension was stirred for another two hours at 0 °C. The clear solution was then poured onto ice/water (200 mL) with heavy stirring. The aqueous solution was extracted three times with ethylacetate (3×50 mL) and the combined organic phases were washed with water (2×100 mL) and brine (80 mL). The organic phase was dried over magnesium sulfate and the solvent was finally removed under reduced pressure. The oily, yellowish crude product was crystallized in boiling hexane, and 46.1 mg (12%) of **1b** was obtained as fine, colorless needles.

¹H NMR (CDCl₃): δ = 10.02 (br, 1H, NH), 3.98 (s, 2H, ²J(H,²⁹Si) = 3.4 Hz, CH₂), 0.12 (s, 9H, ²J(H,²⁹Si) = 6.8 Hz, CH₃); ¹³C{¹H} NMR (CDCl₃): δ = 149.1 (CO), 61.9 (¹J(C,²⁹Si) = 53.3 Hz, CH₂), -3.1 (¹J(C,²⁹Si) = 52.6 Hz, CH₃); ¹⁵N NMR (CDCl₃): δ = -48.8 (NO₂), -190.0 (NH, ¹J(N,H) = 98.1 Hz); ²⁹Si NMR (CDCl₃): δ = 0.6; 0.4 (acetone-D₆). Raman (800 mW): 2963 (41), 2903 (100), 1747 (22), 1615 (8), 1431 (12), 1336 (29), 1283 (13), 1221 (6), 1013 (58), 859 (8), 703 (19), 604 (92), 424 (6), 318 (6), 277 (10), 235 (11) cm⁻¹. IR: 3232 (vs), 3132 (w), 3021 (w), 2960 (w), 2899 (vw), 1770 (w), 1743 (m), 1716 (w), 1612 (s), 1562 (w), 1523 (w), 1447 (m), 1429 (m), 1332 (m), 1283 (m), 1250 (m), 1220 (w), 1176 (s), 1101 (m), 1010 (w), 1001 (w), 935 (m), 842 (vs), 757 (m), 742 (s), 700 (m), 601 (m) cm⁻¹. MS (DEI+) [m/z]: 177.0 [M-CH₃]⁺, 147.0 [C₅H₁₃NO₂Si]⁺. $C_5H_{12}N_2O_4Si$ (192.25 g mol⁻¹): C 31.24, H 6.29, N 14.57; found C 31.31, H 6.22, N 14.69. Mp.: 50 °C. Dec. point: 155 °C. Sensitivities (BAM): impact 35 J; friction 360 N (grain size <100 µm).

Bis(carbamoylmethyl) dimethylsilane (2a): To an ice-cooled solution of bis(hydroxymethyl) dimethylsilane (1.40 g, 11.6 mmol) in dry acetonitrile (30 mL), chlorosulfonyl isocyanate CSI (1.77 g, 12.5 mmol) was added slowly under dry nitrogen atmosphere. After 5 min at 0 °C, the ice bath was removed and the colorless solution was stirred for another hour at ambient temperature. The reaction was cooled again with an ice-bath, water (10 mL) was added carefully and the stirring was continued for 10 min at 0 °C. The organic solvent was removed in vacuo and the aqueous residue started to tarnish. The aqueous phase was extracted with ethyl acetate (3×50 mL) and the combined organic phases were washed with water (50 mL) and brine (50 mL). The organic solution was dried over magnesium sulfate and the solvent was removed under reduced pressure. The solid white product could be further purified by

recrystallization in boiling toluene, yielding 0.9 g (38%) of **2a** as colorless plates. The yield can likely be improved by further concentrating the mother liquor.

¹H NMR (CDCl₃): δ = 4.64 (br, 4H, NH₂), 3.84 (s, 4H, ²J(H,²⁹Si) = 3.4 Hz, CH₂), 0.16 (s, 6H, ²J(H,²⁹Si) = 7.0 Hz, CH₃); ¹³C{¹H} NMR (CDCl₃): δ = 158.0 (CO), 56.2 (¹J(C,²⁹Si) = 58.2 Hz, CH₂), -5.9 (¹J(C,²⁹Si) = 53.1 Hz, CH₃); ¹⁴N NMR (CDCl₃): δ = -152 (NH₂); ²⁹Si NMR (CDCl₃): δ = -1.2. Raman (800 mW): 2973 (51), 2935 (26), 2911 (100), 1665 (17), 1440 (18), 1418 (3), 1262 (9), 1218 (18), 1110 (5), 1088 (9), 1067 (19), 899 (33), 704 (6), 679 (12), 657 (8), 600 (65), 510 (11), 364 (5), 314 (6), 272 (11), 239 (6), 219 (14), 187 (3), 143 (5), 110 (52), 96 (19) cm⁻¹. IR: 3444 (w), 3407 (w), 3290 (w), 3212 (w), 2954 (vw), 2935 (vw), 2914 (vw), 1947 (vw), 1733 (w), 1686 (vs), 1627 (m), 1598 (w), 1430 (m), 1389 (s), 1367 (s), 1283 (w), 1257 (m), 1244 (m), 1217 (w), 1109 (m), 1085 (w), 1053 (vs), 986 (w), 898 (m), 846 (s), 811 (m), 786 (m), 773 (m), 727 (w), 702 (vw), 677 (w), 656 (vw) cm⁻¹. MS (DEI+) [m/z]: 206.1 [M]⁺, 191.1 [C₆H₁₃NO₄Si]⁺, 132.1 [C₅H₁₃NO₂Si]⁺. C₆H₁₄N₂O₄Si (206.27 g mol⁻¹): C 34.94, H 6.84, N 13.58, found C 34.98, H 6.89, N 13.38. Mp.: 95 °C.

Bis(nitrocarbamoylmethyl) dimethylsilane (2b): Anhydrous nitric acid (>99.5%, 3 mL) was slowly dropped into concentrated sulfuric acid (3 mL) at 0 °C. With strong stirring, bis(carbamoylmethyl) dimethylsilane (**2a**, 309 mg, 1.5 mmol) was added in small portions and the suspension was stirred for one hour at 0 °C. The clear solution was then poured onto ice/water (200 mL) with heavy stirring. The aqueous solution was extracted three times with ethylacetate (3×50 mL) and the combined organic phases were washed with water (2×100 mL) and brine (80 mL). The organic phase was dried over magnesium sulfate and the solvent was finally removed under reduced pressure. The yellow, oily crude product was recrystallized in dichloromethane and **2b** was obtained as chunky, colorless crystals (93.3 mg, 21%).

¹H NMR (DMSO-D₆): δ = 3.98 (s, 4H, CH₂), 0.16 (s, 6H, ²J(H,²⁹Si) = 7.0 Hz, CH₃); ¹³C{¹H} NMR (DMSO-D₆): δ = 150.0 (CO), 57.4 (¹J(C,²⁹Si) = 57.4 Hz, CH₂), -6.2 (¹J(C,²⁹Si) = 53.9 Hz, CH₃); ¹⁵N NMR (DMSO-D₆): δ = -41.7 (NO₂), -185.7 (NH); ²⁹Si NMR (DMSO-D₆): δ = -0.6; -0.4 (acetone-D₆). Raman (800 mW): 2970 (29), 2944 (39), 2905 (74), 1735 (38), 1623 (24), 1423 (19), 1382 (36), 1332 (13), 1006 (51), 897 (38), 750 (12), 707 (10), 677 (12), 604 (100), 464 (43), 416 (12), 309 (12), 230 (29) cm⁻¹. IR: 3224 (w), 3171 (w), 3124 (w), 3011 (w), 2819 (vw), 1764 (m), 1726 (s), 1615 (s), 1604 (s), 1554 (w), 1513 (vw), 1446 (m), 1415 (m), 1377 (m), 1321 (m), 1284 (s), 1264 (m), 1240 (s), 1223 (s), 1193 (vs), 1094 (w), 1069 (m), 1002 (s), 937 (m), 894 (m), 859 (m), 834 (s), 811 (m), 758 (m), 742 (m), 719 (w), 674 (vw) cm⁻¹. MS (DEI+) [m/z]: 295.3 [M]⁺, 147.2 [C₅H₁₁O₃Si]⁺. C₆H₁₂N₂O₈Si (296.27 g mol⁻¹): C 24.32, H 4.08, N 18.91;

found C 24.24, H 4.36, N 19.06. Mp.: 100 °C. Dec. point: 142 °C. Sensitivities (BAM): impact 3 J; friction 192 N (grain size 100–500 µm).

Tris(carbamoylmethyl) methylsilane (3a): To an ice-cooled solution of tris(hydroxymethyl)methylsilane (1.00 g, 7.3 mmol) in dry acetonitrile (50 mL), chlorosulfonyl isocyanate CSI (3.54 g, 25.0 mmol) was added slowly under dry nitrogen atmosphere. After 5 min at 0 °C, the ice bath was removed and the colorless solution was stirred for another hour at ambient temperature. The reaction was cooled again with an ice-bath, water (15 mL) was added carefully and the stirring was continued for 10 min at 0 °C. The organic solvent was removed in *vacuo*. The aqueous phase was extracted with ethylacetate (3×50 mL) and the combined organic phases were washed with water (50 mL) and brine (50 mL). The organic solution was dried over magnesium sulfate and the solvent was removed under reduced pressure. The crude product was obtained as colorless oil, which started to crystallize after a short period of time. The recrystallization in a mixture of dichloromethane and dioxane (50:50) yielded 520 mg (27%) of **3a** as colorless crystals.

¹H NMR (DMSO-D₆): δ = 6.45 (br, 6H, NH₂), 3.68 (s, 6H, ²J(H,²⁹Si) = 3.4 Hz, CH₂), 0.10 (s, 3H, ²J(H,²⁹Si) = 6.9 Hz, CH₃); ¹³C{¹H} NMR (DMSO-D₆): δ = 157.9 (CO), 53.7 (CH₂), -7.6 (CH₃); ²⁹Si NMR (DMSO-D₆): δ = -5.5. Raman (800mW): 3261 (3), 3200 (9), 2973 (19), 2954 (3), 2945 (20), 2910 (100), 2861 (8), 1695 (20), 1633 (6), 1633 (6), 1444 (26), 1306 (12), 1265 (8), 1217 (14), 1121 (20), 1083 (10), 1071 (6), 1015 (9), 904 (40), 835 (30), 768 (5), 711 (10), 647 (4), 610 (41), 537 (6), 501 (19), 367 (12), 341 (3), 317 (9), 278 (7), 237 (3), 209 (6) cm⁻¹. IR: 3420 (m), 3332 (m), 3269 (m), 3207 (m), 2943 (vw), 2907 (w), 1779 (w), 1701 (vs), 1615 (s), 1429 (m), 1279 (m), 1246 (m), 1215 (m), 1121 (m), 1063 (vs), 903 (m), 840 (vs), 801 (m), 784 (s), 776 (s), 748 (m), 711 (m), 651 (m), 609 (m) cm⁻¹. MS (DEI+) [m/z]: 250.2 [C₇H₁₄N₂O₆Si]⁺, 191.2 [C₅H₁₁N₂O₄Si]⁺. C₇H₁₅N₃O₆Si (265.30 g mol⁻¹): C 31.69, H 5.70, N 15.84; found C 31.80, H 5.65 N, 15.60. Mp.: 108 °C.

Tris(nitrocarbamoylmethyl) methylsilane (3b): Anhydrous nitric acid (>99.5%, 1 mL) was slowly dropped into concentrated sulfuric acid (1 mL) at 0 °C. With strong stirring, tris(carbamoylmethyl) methylsilane (**3a**, 195 mg, 0.73 mmol) was added in small portions and the suspension was stirred for one hour at 0 °C. The clear solution was then poured onto ice/water (200 mL) with heavy stirring. The aqueous solution was extracted ice-cold three times with ethylacetate (3×50 mL) and the combined organic phases were washed with water (2×100 mL) and brine (80 mL). The organic phase was dried over magnesium sulfate and the solvent was finally removed under reduced pressure. The resulting colorless solid was dissolved in acetonitrile (1 mL) and large amounts of chloroform (50 mL) were added, resulting

in precipitation of a colorless solid containing solvent molecules. The filtrated solid was again dissolved in acetonitrile and the solvent was evaporated with time. After drying under high vacuum, **3b** was obtained as colorless white solid (50 mg, 17%).

¹H NMR (acetone-D₆): δ = 13.31 (br, 3H, NH), 4.21 (s, 6H, ²J (H, ²⁹Si) = 3.5 Hz, CH₂), 0.35 (s, 3H, ²J (H, ²⁹Si) = 7.3 Hz, CH₃); ¹³C{¹H} NMR (acetone-D₆): δ = 150.4 (CO), 56.4 (¹J (C, ²⁹Si) = 60.2 Hz, CH₂), -8.8 (¹J (C, ²⁹Si) = 56.0 Hz, CH₃); ¹⁴N NMR (acetone-D₆): δ = -45 (NO₂); ²⁹Si NMR (acetone-D₆): δ = -3.2. Raman (800 mW): 3180 (6), 2975 (19), 2941 (54), 2910 (13), 1761 (36), 1612 (20), 1433 (18), 1333 (42), 1298 (22), 1234 (10), 1012 (100), 823 (6), 758 (8), 632 (17), 465 (20), 432 (7) cm⁻¹. IR: 3232 (w), 3172 (w), 3028 (vw), 2773 (vw), 1757 (m), 1609 (s), 1445 (m), 1422 (m), 1322 (m), 1286 (m), 1260 (w), 1233 (m), 1201 (m), 1163 (vs), 1091 (m), 1009 (m), 999 (m), 935 (m), 863 (m), 822 (m), 788 (m), 742 (m) cm⁻¹. MS (FAB-) [m/z]: 399.3 [M-H]⁻. C₇H₁₂N₆O₁₂Si (400.29 g mol⁻¹): C 21.00, H 3.02, N 20.99; C 21.01, H 3.08, N 20.69. Mp.: 133 °C. Dec. point: 138 °C. Sensitivities (BAM): impact 5 J; friction 240 N (grain size <100 µm).

Modified Synthesis for Tetrakis(chloromethyl)silane Si(CH₂Cl)₄: Into a stirred mixture consisting of tetrachlorosilane (11.5 g, 67.7 mmol), bromochloromethane (52.4 g, 405 mmol) and THF (150 mL), was added a pre-cooled *n*-butyl lithium solution in *n*-hexane (113 mL, 2.5 M, 283 mmol of *n*-BuLi) within 4 h. The mixture and also the *n*-butyl lithium solution were cooled to -78 °C with an ethanol/dry ice cooling. After the addition was complete, the reaction mixture was stirred at -78 °C for further 5 h and then warmed to 20 °C over night. The mixture was concentrated under reduced pressure, and the resulting precipitate was removed by filtration and washed with *n*-hexane. This procedure was repeated one more time to remove most of the THF, and the concentrated solution was cooled in the refrigerator overnight. A colorless crystalline crude product precipitates, is filtered off and washed with *n*-hexane to yield crude tetrakis(chloromethyl)silane. Recrystallization from small amounts of boiling *n*-hexane yielded 3.95 g (26 %) of the pure Si(CH₂Cl)₄ as fine colorless needles.

Tetrakis(carbamoylmethyl)silane (4a): To an ice-cooled solution of tetrakis(hydroxymethyl) silane (0.17 g, 1.1 mmol) in dry acetonitrile (15 mL), chlorosulfonyl isocyanate CSI (0.68 g, 4.8 mmol) was added slowly under dry nitrogen atmosphere. After 5 min at 0 °C, the ice bath was removed and the colorless solution was stirred for another hour at ambient temperature. The reaction was cooled again with an ice-bath, water (7 mL) was added carefully and the stirring was continued for 10 min at ambient temperature. The organic solvent was removed in vacuo and ice was added to the aqueous phase. With the help of ultrasound, **4a** precipitated out of the cold solution as colorless, pure solid (252 mg, 70%).

¹H NMR (DMSO-D₆): δ = 6.45 (s, 8H, NH₂), 3.70 (s, 8H, CH₂); ¹³C{¹H} NMR (DMSO-D₆): δ = 158.1 (CO), 53.4 (¹J(C, ²⁹Si) = 64.5 Hz, CH₂); ²⁹Si NMR (DMSO-D₆): δ = -15.5. Raman (800 mW): 3331 (12), 3284 (2), 2969 (65), 2940 (100), 2860 (7), 1703 (49), 1593 (10), 1446 (55), 1271 (20), 1235 (19), 1120 (29), 1076 (22), 908 (76), 753 (25), 650 (6), 616 (20), 515 (8), 231 (21) cm⁻¹. IR: 3435 (m), 3334 (w), 3199 (vw), 2933 (vw), 1691 (s), 1592 (m), 1435 (w), 1376 (vs), 1269 (w), 1227 (w), 1120 (w), 1060 (vs), 895 (m), 837 (vw), 816 (m), 780 (s), 674 (vw) cm⁻¹. MS (DEI+) [m/z]: 250.2 [C₆H₁₂N₃O₆Si]⁺. C₈H₁₆N₄O₈Si (324.32 g mol⁻¹): C 29.63, H 4.97, N 17.28; found C 29.34, H 4.96, N 17.05. Mp.: 138 °C.

Tetrakis(nitrocaramoylmethyl)silane (sila-PETNC, 4b): 0.19 g (0.6 mmol) tetrakis(carbamoylmethyl) silane (**4a**) was solved in concentrated sulfuric acid (2 mL) in small portions at 0 °C. With strong stirring, anhydrous acid (>99.5%, 2 mL) was added dropwise with caution to the clear solution. After one hour at 0 °C, the solution was poured onto ice/water (150 mL) with heavy stirring and a colorless precipitate formed. After filtering the colorless solid and washing with cold water, sila-PETNC was obtained as pure product (240 mg, 79%).

¹H NMR (acetone-D₆): δ = 13.40 (br, 4H, NH), 4.31 (s, 8H, ²J(H, ²⁹Si) = 3.5 Hz, CH₂); ¹³C{¹H} NMR (acetone-D₆): δ = 150.7 (CO), 55.6 (¹J(C, ²⁹Si) = 62.3 Hz, CH₂); ¹⁵N NMR (acetone-D₆): δ = -45.3 (NO₂), -190.4 (NH, br); ²⁹Si NMR (acetone-D₆): δ = -9.8. Raman (800 mW): 3178 (5), 2968 (17), 2935 (43), 2844 (3), 1773 (36), 1609 (15), 1433 (15), 1335 (41), 1302 (22), 1228 (13), 1180 (6), 1099 (3), 1014 (100), 952 (4), 853 (3), 822 (9), 748 (5), 489 (2), 646 (10), 469 (20), 432 (9) cm⁻¹. IR: 3236 (w), 3174 (m), 3024 (w), 2934 (vw), 2774 (vw), 1775 (m), 1607 (s), 1445 (m), 1423 (m), 1323 (m), 1291 (s), 1233 (m), 1180 (vs), 1165 (vs), 1014 (m), 1000 (m), 948 (m), 820 (m), 794 (m), 760 (m), 743 (s), 718 (m), 644 (s) cm⁻¹. MS (FAB-) [m/z]: 503.3 [M-H]⁻. C₈H₁₂N₈O₁₆Si (504.31 g mol⁻¹): C 19.05, H 2.40, N 22.22; found C 18.94, H 2.56, N 21.93. Dec. point: 170 °C. Sensitivities (BAM): impact 3 J; friction 240 N (grain size <100 µm).

1,3-Bis(nitrocaramoylmethyl)-1,1,3,3-tetramethylsiloxyane (5): Anhydrous nitric acid (>99.5%, 1 mL) was slowly dropped into concentrated sulfuric acid (1 mL) at 0 °C. With strong stirring, carbamoylmethyltrimethylsilane (**1a**, 147 mg, 1.0 mmol) was added in small portions and the suspension was stirred for one hour at 0 °C. The clear solution was then poured onto ice/water (200 mL) with heavy stirring. The aqueous solution was extracted ice-cold three times with ethyl acetate (3×50 mL) and the combined organic phases were washed with water (3×30 mL) and brine (30 mL). The organic phase was dried over magnesium sulfate and the solvent was finally removed under reduced pressure. The crude, yellow gum was recrystallized

from boiling toluene, and the disiloxane **5** was obtained as fine colorless needles (85 mg, 46%).

¹H NMR (CDCl₃): δ = 10.58 (br, 2H, NH), 3.96 (s, 4H, CH₂), 0.20 (s, 12H, ²J (H, ²⁹Si) = 6.8 Hz, CH₃); ¹³C{¹H} NMR (CDCl₃): δ = 149.3 (CO), 61.2 (¹J (C, ²⁹Si) = 63.9 Hz, CH₂), -1.2 (¹J (C, ²⁹Si) = 62.4 Hz, CH₃); ¹⁵N NMR (CDCl₃): δ = -48.2 (NO₂), -190.1 (NH, ¹J (N,H) = 97.5 Hz); ²⁹Si NMR (CDCl₃): δ = 3.5. Raman (800 mW): 2967 (53), 2933 (30), 2901 (100), 1748 (37), 1620 (10), 1451 (4), 1429 (17), 1415 (4), 1332 (44), 1282 (18), 1230 (8), 1011 (99), 756 (8), 667 (19), 522 (24), 459 (33), 427 (7), 324 (5), 294 (21), 205 (1) cm⁻¹. IR: 3236 (vw), 3154 (w), 3033 (w), 2961 (vw), 2933 (vw), 2771 (vw), 1747 (s), 1606 (s), 1554 (vw), 1449 (m), 1330 (m), 1280 (m), 1261 (m), 1228 (m), 1172 (vs), 1076 (vs), 1009 (m), 937 (m), 846 (m), 798 (vs), 753 (m), 714 (m) cm⁻¹. MS (DEI+): [m/z]: 281.2 [C₈H₂₁N₂O₅Si₂]⁺, 135.1 [C₄H₁₁O₃Si]⁺. C₈H₂₀N₄O₉Si₂ (370.42 g mol⁻¹): C 25.94, H 4.90, N 15.13; found C 26.03, H 4.88, N 15.04. Mp.: 68 °C. Dec. point: 150 °C. Sensitivities (BAM): impact 35 J; friction 360 N (grain size <100 µm).

4.6 References

- [1] (a) Q. J. Axthammer, B. Krumm, T. M. Klapötke, *J. Org. Chem.* **2015**, 6329–6335; (b) Q. J. Axthammer, B. Krumm, T. M. Klapötke, *Eur. J. Org. Chem.* **2015**, 723–729; (c) D. S. Bohle, Z. Chua, *Inorg. Chem.* **2014**, 53, 11160–11172.
- [2] J. Köhler, R. Meyer, A. Homburg, *Explosives*. Wiley-VCH: Weinheim (Germany), **2007**.
- [3] T. M. Klapötke, B. Krumm, R. Ilg, D. Troegel, R. Tacke, *J. Am. Chem. Soc.* **2007**, 129, 6908–6915.
- [4] W.-G. Liu, S. V. Zybin, S. Dasgupta, T. M. Klapötke, W. A. Goddard III, *J. Am. Chem. Soc.* **2009**, 131, 7490–7491.
- [5] C. Evangelisti, T. M. Klapötke, B. Krumm, A. Nieder, R. J. F. Berger, S. A. Hayes, N. W. Mitzel, D. Troegel, R. Tacke, *Inorg. Chem.* **2010**, 49, 4865–4880.
- [6] (a) U.-P. Apfel, D. Troegel, Y. Halpin, S. Tschierlei, U. Uhlemann, H. Goerls, M. Schmitt, J. Popp, P. Dunne, M. Venkatesan, M. Coey, M. Rudolph, J. G. Vos, R. Tacke, W. Weigand, *Inorg. Chem.* **2010**, 49, 10117–10132; (b) D. Troegel, F. Möller, C. Burschka, R. Tacke, *Organometallics* **2009**, 28, 5765–5770; (c) J. O. Daiss, K. A. Barth, C. Burschka, P. Hey, R. Ilg, K. Klemm, I. Richter, S. A. Wagner, R. Tacke, *Organometallics* **2004**, 23, 5193–5197; (d) R. Ilg, D. Troegel, C. Burschka, R. Tacke, *Organometallics* **2006**, 25, 548–551.
- [7] R. J. Fessenden, M. D. Coon, *J. Med. Chem.* **1965**, 8, 604–8.
- [8] G. Socrates, *Infrared and Raman Characteristic Group Frequencies*. John Wiley & Sons Ltd.: Chichester (U.K.), **2001**; Vol. 3, p 366.
- [9] A. Bondi, *J. Phys. Chem.* **1964**, 68, 441–451.
- [10] L. Ascherl, C. Evangelisti, T. M. Klapötke, B. Krumm, J. Nafe, A. Nieder, S. Rest, C. Schütz, M. Suceska, M. Trunk, *Chem. - Eur. J.* **2013**, 19, 9198–9210.
- [11] T. M. Klapötke, *Chemistry of High-Energy Materials*. 3rd ed.; De Gruyter: Berlin, **2015**.
- [12] M. J. Frisch, G. W. Trucks, H. B. Schlegel, G. E. Scuseria, M. A. Robb, J. R. Cheeseman, G. Scalmani, V. Barone, B. Mennucci, G. A. Petersson, H. Nakatsuji, M. Caricato, X. Li, H. P. Hratchian, A. F. Izmaylov, J. Bloino, G. Zheng, J. L. Sonnenberg, M. Hada, M. Ehara, K. Toyota, R. Fukuda, J. Hasegawa, M. Ishida, T. Nakajima, Y. Honda, O. Kitao, H. Nakai, T. Vreven, J. A. Montgomery Jr., J. E. Peralta, F. Ogliaro, M. J. Bearpark, J. Heyd, E. N. Brothers, K. N. Kudin, V. N. Staroverov, R. Kobayashi, J. Normand, K. Raghavachari, A. P. Rendell, J. C. Burant, S. S. Iyengar, J. Tomasi, M. Cossi, N. Rega, N. J. Millam, M. Klene, J. E. Knox, J. B. Cross, V. Bakken, C. Adamo, J. Jaramillo, R. Gomperts, R. E. Stratmann, O. Yazyev, A. J. Austin, R. Cammi, C. Pomelli, J. W. Ochterski, R. L. Martin, K. Morokuma, V. G. Zakrzewski, G. A. Voth, P. Salvador, J. J. Dannenberg, S. Dapprich, A. D. Daniels, Ö. Farkas, J. B. Foresman, J. V. Ortiz, J. Ciosowski, D. J. Fox, Gaussian, Inc., *Gaussian 09*, Wallingford, **2009**.
- [13] M. Suceska, *EXPLO5*, v. 6.02; Brodarski Institute: Zagreb (Croatia), **2013**.
- [14] M. W. Chase, *J. Phys. Chem. Ref. Data, Monogr.* **9** **1998**, 1–1951.
- [15] NIST Chemistry WebBook, NIST Standard Reference Database Number 69, *2016 by the U.S. Secretary of Commerce on behalf of the United States of America*: <http://webbook.nist.gov/chemistry/>.

- [16] *CrysAlis CCD*, 1.171.35.11; Oxford Diffraction Ltd.: Abingdon, Oxford (U.K.), **2011**.
- [17] *CrysAlis RED*, 1.171.35.11; Oxford Diffraction Ltd.: Abingdon, Oxford (U.K.), **2011**.
- [18] A. Altomare, M. C. Burla, M. Camalli, G. L. Cascarano, C. Giacovazzo, A. Gualandi, A. G. G. Moliterni, G. Polidori, R. Spagna, *J. Appl. Crystallogr.* **1999**, *32*, 155–119.
- [19] (a) G. M. Sheldrick, *Programs for Crystal Structure Determination*. University of Göttingen: Germany, **1997**; (b) G. M. Sheldrick, *Acta Crystallogr.* **2008**, *64 A*, 112–122.
- [20] L. Farrugia, *J. Appl. Crystallogr.* **1999**, *32*, 837–838.
- [21] A. Speck, *Acta Crystallogr.* **2009**, *65 D*, 148–155.
- [22] R. D. Dennington, T. A. Keith, J. M. Millam, *GaussView*. v. 5.08, Semicem, Inc.: Wallingford, **2009**.
- [23] J. A. Montgomery, M. J. Frisch, J. W. Ochterski, G. A. Petersson, *J. Chem. Phys.* **2000**, *112*, 6532–6542.
- [24] M. Suceska, *Propellants Explos. Pyrotech.* **1991**, *16*, 197–202.

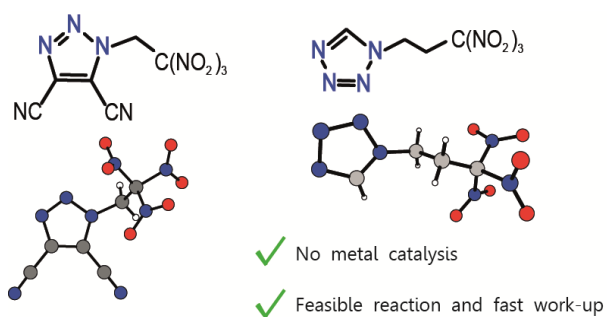
5 *N*-Trinitroalkyl Substituted Azoles

SYNTHETIC ROUTES TO A TRIAZOLE AND TETRAZOLE WITH TRINITROALKYL SUBSTITUTION AT NITROGEN

Thomas M. Klapötke, Burkhard Krumm, Thomas Reith and Cornelia C. Unger

as submitted to

The Journal of Organic Chemistry



5.1 Abstract

Two N-substituted trinitroalkyl azoles, one triazole and one tetrazole, were synthesized and isolated via efficient cyclization reactions. Both materials were thoroughly characterized and their structures were confirmed by X-ray diffraction. The formation of the N-trinitroethyl substituted triazole proceeds unexpectedly via nitrosation of an N-substituted diaminomaleonitrile initially with HNO_3 and subsequently confirmed with HNO_2 . The N-trinitropropyl substituted tetrazole was prepared via a standard cyclization route from trinitropropylammonium chloride with orthoformate and azide.

5.2 Introduction

The trinitromethyl group is an important building block in the research for new energetic materials with good availability of the sources nitroform or trinitroethanol.^{1, 2, 3} In combination with already oxygen-rich energetic materials, many potent replacements for the common but harmful³ oxidizer ammonium perchlorate were investigated, such as trinitroethyl nitrocarbamate (**A**) and bis(trinitroethyl)oxalate (**B**).^{1, 4} In the ongoing research to replace the secondary explosive RDX, the combination of the trinitromethyl moiety with different azoles results in interesting compounds (Figure 1) (**C–F**).^{5–8} In general, either trinitroethanol was reacted with heterocyclic amines to incorporate the trinitromethyl unit^{8, 9} or the exhaustive nitration of activated methylene groups forms the trinitromethyl moiety e.g. in azolylacetic acids.^{6, 7, 10} However, only very sparse information exists about azoles with nitrogen substituted trinitroalkyl units.^{7, 10, 11}

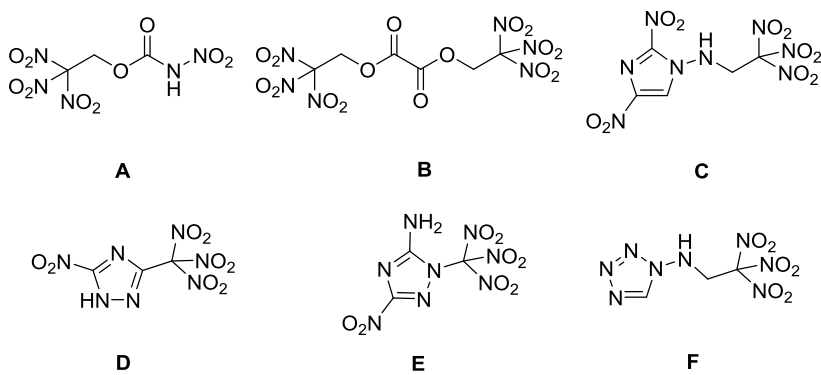


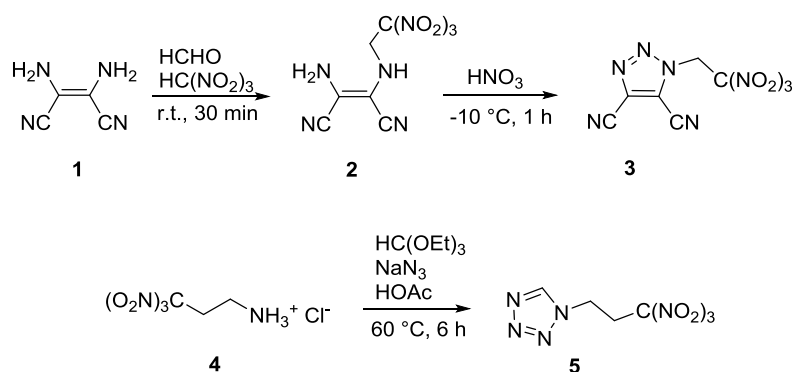
Figure 5.5: Oxygen-rich materials: trinitroethyl nitrocarbamate (**A**), bis(trinitroethyl)oxalate (**B**), 2,4-dinitro-N-(2,2,2-trinitroethyl)-1*H*-imidazol-1-amine (**C**), 5-nitro-3-trinitromethyl-1*H*-1,2,4-triazole (**D**), 3-nitro-1-trinitromethyl-1*H*-1,2,4-triazol-5-amine (**E**) and 1-(2,2,2-trinitroethylamino)tetrazole (**F**).

In those few examples, rather sensitive *N*-trinitromethyl triazoles were obtained either by exhaustive nitration mentioned above, or by nitration of dinitromethyl derivatives with nitronium tetrafluoroborate. The *N*-substitution with longer trinitroalkyl chains, such as trinitroethyl and trinitropropyl units, should provide better thermal and mechanical stability¹², but none described to the best of our knowledge. The low reactivity of deactivated aromatic azoles seems not sufficient enough to react with nitroform or trinitroethanol.¹³⁻¹⁵ At the same time, trinitromethyl containing starting materials tend to be chemically rather labile^{16, 17}, particularly against bases and high temperatures, which prevent many ring closing mechanisms of functional groups.¹⁸

5.3 Results and Discussion

5.3.1 Synthesis

In this contribution, pathways to two polyazoles with *N*-substituted trinitroethyl- and trinitropropyl moieties are reported and their properties examined. In both cases, a trinitromethyl containing precursor was selected to further cyclize to a triazole and a tetrazole (Scheme 1).



Scheme 5.2: Synthesis of 4,5-dicyano-1*N*-(trinitroethyl)-1,2,3-triazole (3) and 1*N*-trinitropropyl tetrazole (5) from the precursors diaminomaleonitrile (1) and trinitropropylammonium chloride (4).

Diaminomaleonitrile (1) was converted quantitatively into amino-(trinitroethyl)amino maleonitrile (2) by reaction with formaldehyde and nitroform in aqueous solution. Without further purification, nitration was performed in white fuming nitric acid. Surprisingly, the originally intended nitration at the NH₂-group of 2 was not observed, but a cyclized product, which was identified as 4,5-dicyano-1*N*-(trinitroethyl)-1,2,3-triazole (3), was isolated. The substituted maleonitrile 2 turns very sensitive upon thorough drying and may deflagrate

5 N-Trinitroalkyl Substituted Azoles

spontaneously without external stimulation, which occurred once in our laboratory during storage. The triazole **3** is still very sensitive towards impact (2 J) and moderately sensitive to friction (216 N), but is stable in air at room temperature for at least several months.

Primary amines undergo heterocyclization with triethyl orthoformate and sodium azide in acetic acid. This facile synthetic route yields *N*-substituted tetrazoles in good yields.¹⁹ Our precursor, 3,3,3-trinitropropyl amine as the HCl-salt (**4**),²⁰ undergoes the cyclization reaction at 60 °C for 6 hours. Simple work-up procedures afforded 1*N*-trinitropropyl tetrazole (**5**) as an orange-colored solid.

5.3.2 NMR Spectroscopy

The substituted maleonitrile **2** starts to decompose quickly in several deuterated solvents. However, reasonable spectra were obtained from acetonitrile CD₃CN. The ¹H NMR spectrum shows three resonances at 5.1 ppm (br), 4.65 ppm (d) and 4.08 ppm (t). In the ¹³C{¹H} NMR spectra the expected six resonances are observed. The ¹⁴N NMR spectrum shows the signal for the nitro groups at -31 ppm. NMR spectroscopy of the triazole **3** in deuterated acetone reveals a singlet at 7.02 ppm in the ¹H NMR spectrum and six resonances in the range between 128.2 and 51.3 ppm in the ¹³C{¹H} NMR spectrum, including the typically broadened signal for the trinitromethyl carbon atom. The ¹⁴N NMR spectrum shows the resonance at -35 ppm for the nitro groups.

The tetrazole **5** shows the acidic tetrazole hydrogen resonance at 9.41 ppm and the methylene resonances at 5.00 and 4.20 ppm in the ¹H NMR spectrum. In the ¹³C{¹H} NMR spectrum the four carbon resonances are in the expected range between 144.4 ppm for the azole carbon atom and 32.3 ppm for the methylene group. In the ¹⁵N NMR spectrum the nitrogen atoms of the tetrazole ring and the trinitro moiety are detected at 12.4 (N4), -14.6 (N2/N3), -29.9 (C(NO₂)₃), -52 (N3/N4) and -147.5 ppm (N1).

5.3.3 Single Crystal Structure Analysis

Suitable single crystals for X-ray diffraction of triazole **3** were obtained from aqueous work up by evaporation at ambient temperature. The 4,5-dicyano-1*N*-(trinitroethyl)-1,2,3-triazole (**3**) crystallizes in the monoclinic space group *P*2₁/n with four molecules per unit cell and a density of 1.72 g cm⁻³ at 173 K (Figure 5.2).

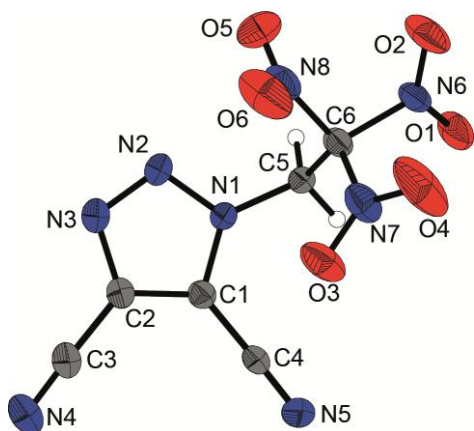


Figure 5.6: X-ray molecular structure of 4,5-dicyano-1*N*-(trinitroethyl)-1,2,3-triazole (**3**). Thermal ellipsoids represent the 50% propability level. Selected atom distances (Å) and angles (deg.): C1–C4 1.419 (3), C4–N5 1.135 (3), C1–C2 1.368 (3), C1–N1 1.337 (3), N1–N2 1.346 (2), N2–N3 1.304 (3), C2–N3 1.362 (3), N1–C5 1.460 (3); C2–C1–C4 130.9 (2), C1–C4–N5 179.2 (2), C1–C2–C3 128.0 (2), C2–C3–N4 178.1 (3), C1–N1–C5 129.6, N2–N1–C5 120.1, N1–C5–C6 114.0 (2); C1–N1–N2–N3 –0.4 (2), N1–N2–N3–C2 0.6 (2), N2–N3–C2–C1 –0.7 (2), N2–N3–C2–C3 –179.5 (2), N2–N1–C1–C4 178.9 (2), C5–N1–N2–N3 –177.4 (2).

In the solid state, the triazole ring forms an almost planar system with the two nitrile substituents (torsion angles along the triazole ring less than 1 °, N2–N3–C2–C3 –179.5 °). The trinitromethyl unit forms the typical propeller-type structure.²¹ The molecule contains no classical proton donor, therefore strong hydrogen bonds are absent. Some weak intermolecular hydrogen bonds can be found between the methylene group as proton donor and neighboring nitro oxygen atoms or nitrile nitrogen atoms as proton acceptors (C5–H2···O4, d(D–H) = 0.94 Å, d(H···A) = 2.49 Å, \angle (D–H···A) = 141.0 °).²²

Suitable single crystals of tetrazole **5** were obtained from ethyl acetate at ambient temperature. The 1*N*-trinitropropyl tetrazole crystallizes as yellow platelets in the monoclinic space group $P2_1/c$ with four formula units per unit cell and a density of 1.75 g cm^{–3} at 143 K (Figure 5.3). The aromatic tetrazole is almost planar as shown by the torsion angles N1–N2–N3–N4 –0.07 ° and N2–N3–N4–C1 –0.12 °. As already mentioned for **3**, the structure of the **5** reveals the typical propeller-type structure of the trinitromethyl unit.²¹ Compared to common C–N bond lengths (1.47 Å),²² the C–N bonds in the trinitromethyl moiety are in the range of 1.53 Å, which is significantly longer. This may result from steric repulsion of the proportionally large nitro groups around the carbon atom C4.

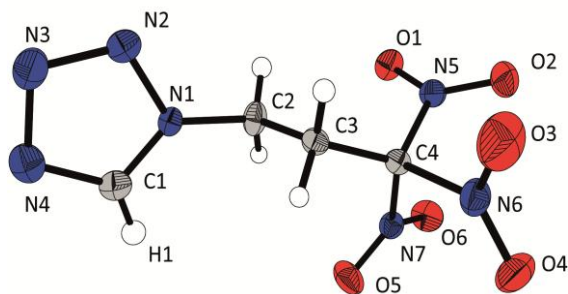


Figure 5.7: X-ray molecular structure of 1N-trinitropropyl tetrazole (5). Thermal ellipsoids represent the 50% probability level. Selected atom distances (Å) and angles (deg.): C2–C3 1.528 (3), C3–C4 1.499 (2), C1–N1 1.327 (3), C1–N4 1.308 (2), C4–N5 1.522 (3), C4–N6 1.535 (2), C4–N7 1.525 (3), N1–N2 1.343 (2), N2–N3 1.291 (2), N3–N4 1.358 (3), N5–O1 1.217 (2), N5–O2 1.214 (2), N6–O3 1.214 (2), N6–O4 1.213 (2), N7–O5 1.210 (3), N7–O6 1.219 (2), N1–C2–C3 108.23 (2), C2–C3–C4 117.34 (2), C3–C4–N5 116.06 (1), C4–N5–O1 115.06 (1), C2–N1–N2 121.14 (2), C2–N1–C1 130.94 (2), N1–C2–C3–C4 165.32 (2), C2–C3–C4–N6 –176.89 (2), N1–N2–N3–N4 –0.07 (2), N2–N3–N4–C1 –0.12 (2), C2–N1–C1–N4 –179.18 (2).

5.3.4 Thermal Stabilities and Energetic Properties

DTA measurements of the heterocycles indicate a decomposition point of 132 °C for triazole **3** and of 125 °C for the tetrazole **5**, which additionally melts at 66 °C. Calculation²³⁻²⁵ of enthalpies on CBS-4M level led to heats of formation of –1117 kJ mol^{–1} (**3**) and 227 kJ mol^{–1} (**5**), which were further used for EXPLO5 calculations^{26, 27} to estimate the detonation parameters. The triazole **3** and the tetrazole **5** show detonation velocities (V_{Det}) of 4557 m s^{–1} and 8388 m s^{–1}, respectively. Furthermore, the detonation pressure (p_{CJ}) was determined ($p_{\text{CJ}} = 55$ kbar (**3**) and $p_{\text{CJ}} = 293$ kbar (**5**)). The energetic parameters of **5** are promising and almost in the range of PETN (pentaerythritol tetranitrate, $V_{\text{Det}} = 8405$ m s^{–1} and $P_{\text{CJ}} = 319$ kbar), a commonly used secondary explosive. In addition the specific impulse I_{sp} , a benchmark for composite propellants in rocket engines, was predicted for **5**. Neat **5** ($I_{\text{sp}} = 278$ s) and mixtures with 15% aluminum and 14% binder ($I_{\text{sp}} = 252$ s) are in an appropriate range. The nitrile units of the triazole **3** reduce the energetic parameters significantly with the tremendous high enthalpy of formation and the unfavorable influence on the oxygen balance. A further derivatization of **3** however could possibly give access to a variety of potential energetic materials.

Since the treatment of **2** with HNO₃ surprisingly yielded a triazole **3**, which could be due to nitrosation, control experiments were carried out by using nitrite in HCl and H₂SO₄. And

indeed, with both systems the formation of the identical triazole **3** was observed, which is reported for other triazoles.²⁸ Therefore we conclude, that in the initial HNO_3 approach sufficient amounts of the nitrosonium cation NO^+ prevail and react with the maleonitrile **2**. The formation of NO^+ in white fuming HNO_3 can be explained by the presence of some nitrogen dioxide NO_2 , which is known to disproportionate to nitrite and nitrate.²⁹ Subsequently, the unstable nitrous acid HNO_2 is the precursor for the nitrosonium cation after water elimination.

5.4 Conclusion

Two hitherto unknown azoles with *N*-substituted trinitroalkyl units have been synthesized in this study. The 4,5-dicyano-1*N*-(trinitroethyl)-1,2,3-triazole (**3**) was formed unexpectedly by nitrosation. The 1*N*-trinitropropyl tetrazole (**5**) was obtained by cyclization of trinitropropylammonium chloride with sodium azide and triethyl orthoformate, leading to the first isolated *N*-substituted trinitroalkyl tetrazole. The energetic properties of **5** are in the range of PETN, a commonly used secondary explosive.

5.5 Experimental Section

5.5.1 General Information

All chemicals were used as received from the suppliers. Raman spectra were recorded with a Bruker MultRAM FT-Raman spectrometer using glass tubes or metal plates. A Nd:YAG laser excitation up to 1000 mW (at 1064 nm) in the range between 400 and 4000 cm^{-1} was used. The intensities are reported as percentages of the most intense peak and are given in parentheses. Infrared (IR) spectra were measured with an ATR device at ambient temperature (20 °C). Transmittance values are qualitatively described as “strong” (s), “medium” (m) and “weak” (w). The NMR spectra were recorded with a 400 MHz instrument and chemical shifts were determined relative to external Me_4Si (^1H , 399.8 MHz, ^{13}C , 100.5 MHz) and MeNO_2 (^{14}N , 28.9 MHz, ^{15}N , 40.6 MHz) at ambient temperature. The melting and decomposition points were measured with an OZM Research DTA 552-Ex with a heating rate of 5 °C min^{-1} in a temperature range of 20 to 400 °C. They were also checked with a Büchi Melting Point B-540 apparatus. Sensitivity data were determined using a BAM drophammer and friction tester.

5.5.2 X-ray Crystallography

Single-crystal X-ray diffraction was performed with an Oxford XCalibur3 diffractometer equipped with a Spellman generator and a KappaCCD detector operating with $\text{Mo}-K_\alpha$ radiation ($\lambda = 0.71073$) at low temperatures. The data collection was realized by using CRYSALISPRO³⁰

software, structures were solved by direct methods (SIR-92 or SIR-97) implemented in the program package WINGX³¹ and finally checked using PLATON.³² All non-hydrogen atoms were refined anisotropically, hydrogen atom positions were located in a difference Fourier map.³³ Crystallographic data for the reported structures in this contribution have been deposited with the Cambridge Crystallographic Data Centre as supplementary publication numbers CCDC 1587493 (**3**) and CCDC 1822024 (**5**).

5.5.3 Synthesis

CAUTION! *These materials are energetic compounds with sensitivity to various stimuli, especially the maleonitrile **2** and the triazole **3** should be treated with caution. While no serious issues in the synthesis and handling of this material were encountered, proper protective measures (face shield, ear protection, body armor, Kevlar gloves and grounded equipment) as well as a plastic spatula, should be used all the time.*

Amino-(trinitroethylamino)maleonitrile (2**):** Diaminomaleonitrile (**1**, 1.08 g, 10 mmol) was added to 40 ml of H₂O. To the slurry 8.31 g of an aqueous nitroform solution (40%, 22 mmol) and 1.8 ml of a formaldehyde solution (37% in water, 22 mmol) were added with stirring. Within 15 minutes the colour of the slurry turns from brown to orange and amino-(trinitroethylamino)maleonitrile (2.7 g, 99%) was obtained in high yield and purity by filtration and repeated washing with cold water. After hours to days exposed to air and humidity the substance will turn red and decompose slowly.

DTA (5 °C min⁻¹): 67 °C (onset dec.); IR (ATR, cm⁻¹): ν = 3362 (w), 3283 (w), 2200 (m), 2170 (m), 1589 (vs), 1488 (w), 1427 (m), 1378 (m), 1305 (s), 1266 (m), 1204 (m), 805 (m), 782 (m), 662 (w), 634 (w), 517 (w); Raman (1064 nm, 800 mW, cm⁻¹): 2957 (6), 2604 (4), 2264 (7), 2232 (48), 2200 (100), 2158 (5), 2137 (6), 2061 (4), 1625 (15), 1592 (46), 1380 (15), 1347 (9), 857 (20), 784 (6), 642 (6), 516 (5), 476 (6), 410 (5), 377 (14), 217 (7); ¹H NMR (400 MHz, CD₃CN, ppm): δ = 5.1 (br, 2H, NH₂), 4.65 (d, 2H, ³J¹H,¹H) = 7.3 Hz, CH₂), 4.08 (t, 1H, ³J¹H,¹H) = 7.4 Hz, NH); ¹³C{¹H} NMR (101 MHz, CD₃CN, ppm): δ = 127 (br, C(NO₂)₃), 122.3/116.1/114.9/102.9 (CN, C=C), 50.8 (CH₂); ¹⁴N NMR (28.9 MHz, CD₃CN, ppm): δ = -31 (NO₂); EA (C₆H₅N₇O₆, 271.15 g mol⁻¹): calc.: C 26.58, H 1.86, N 36.16%; found: C 26.54, H 1.94, N 35.65%. Sensitivity tests unchecked due to extreme sensitivity in dry condition.

4,5-Dicyano-1N-(trinitroethyl)-1,2,3-triazole (3**):** 2-Amino-3-(2,2,2-trinitroethylamino)maleonitrile (**2**, 2.7 g, 10 mmol) was slowly added to 10 mL colourless fuming nitric acid at -10 °C with good stirring, accompanied by a heavy reaction. After one hour the red colored reaction mixture was poured on ice and 4,5-dicyano-1N-(trinitroethyl)-1,2,3-triazole (1.56 g,

55%) precipitated as colorless powder, which was obtained by filtration and washed several times with water.

DTA (5 °C min⁻¹): 132 °C (onset dec.); IR (ATR, cm⁻¹): ν = 3007 (w), 2963 (w), 2267 (w), 1626 (m), 1599 (vs), 1457 (m), 1427 (m), 1380 (w), 1332 (m), 1289 (s), 1255 (m), 1206 (w), 1138 (w), 1071 (w), 871 (m), 857 (w), 816 (m), 789 (s), 780 (s), 719 (w), 603 (w), 543 (s); Raman (1064 nm, 800 mW, cm⁻¹): 3008 (3), 2963 (8), 2265 (100), 1632 (3), 1554 (29), 1457 (3), 1333 (9), 1319 (3), 1256 (11), 1137 (5), 990 (4), 859 (14), 722 (4), 651 (5), 544 (4), 503 (9), 464 (4), 446 (5), 401 (5), 373 (9), 302 (8), 258 (4), 237 (4); ¹H NMR (400 MHz, acetone-D₆, ppm): δ = 7.02 (s, 2H, CH₂); ¹³C{¹H} NMR (101 MHz, acetone-D₆, ppm): δ = 128.2 (C=C), 123.3 (C(NO₂)₃), 122.2 (C=C), 109.4 (CN), 105.9 (CN) 51.3 (CH₂); ¹⁴N NMR (28.9 MHz, acetone-D₆, ppm): δ = -35 (NO₂); EA (C₆H₂N₈O₆, 282.13 g mol⁻¹): calc.: C 25.54, H 0.71, N 39.72%; found: C 25.68, H 0.92, N 39.69%; BAM drophammer: 2 J (<100 µm); friction tester: 216 N (<100 µm).

Additional experiments with NaNO₂/HCl/H₂SO₄.

2-Amino-3-(2,2,2-trinitroethylamino) maleonitrile (**2**, 268 mg, 1 mmol) was slowly added to a mixture of 2.5 mL water and 2.5 mL concentrated HCl or concentrated H₂SO₄ acid with good stirring and ice bath cooling. Sodium nitrite, NaNO₂ (70 mg, 1 mmol), was dissolved in 1 mL water and slowly added. After one hour at 0 °C the slightly orange colored reaction mixture was poured on ice and 4,5-dicyano-1N-(trinitroethyl)-1,2,3-triazole (**3**, 59 mg, 21% for HCl and 64 mg, 22% for H₂SO₄) precipitated as colorless powder, which was obtained by filtration and washed several times with water. Alternatively, the use of concentrated acids to form **3** did not improve the yields. The product was identified by NMR measurements and confirmed the previously obtained data with HNO₃.

1N-Trinitropropyl tetrazole (5): 3,3,3-Trinitropropyl-1-ammonium chloride (**4**, 118 mg, 0.51 mmol) and sodium azide (40 mg, 0.62 mmol) were suspended in triethyl orthoformate (0.5 mL, 3.0 mmol) and concentrated acetic acid (2 mL) was added. After heating up to 60 °C in an oil bath for 6 h, an orange precipitate was formed. The solvent was removed and the orange residue was dried under high vacuum. The residue was portioned between ethyl acetate (15 mL) and water (15 mL). The aqueous phase was extracted with ethyl acetate (2 × 15mL) and the combined organic phases were washed with water (15 mL) and brine (15 mL). After drying with magnesium sulfate, the solvent was removed to obtain an orange oil. The oil was repeatedly treated with toluene and subsequently dried under high vacuum to obtain a red-orange crystalline solid (61.1 mg) in 48% yield.

5 N-Trinitroalkyl Substituted Azoles

DTA (5 °C min⁻¹): 66 °C (onset mp.), 125 °C (onset dec.); IR (ATR, cm⁻¹): ν = 3139 (w), 2985 (w), 2949 (w), 2132 (w), 1737 (w), 1681 (w), 1651 (w), 1591 (vs), 1482 (m), 1427 (w), 1371 (m), 1298 (s), 1242 (m), 1198 (m), 1171 (m), 1129 (m), 1103 (m), 1055 (m), 1014 (w), 963 (w), 856 (w), 801 (s), 707 (w), 649 (m), 546 (w), 475 (w), 475 (w), 416 (w); Raman (1064 nm, 800 mW, cm⁻¹): 3130 (35), 3045 (25), 2996 (82), 2948 (100), 2860 (12), 1616 (31), 1608 (28), 1592 (11), 1484 (15), 1409 (32), 1379 (44), 1352 (14), 1320 (26), 1306 (31), 1279 (37), 1259 (15), 1179 (23), 1136 (7), 1105 (16), 1063 (9), 1022 (33), 1006 (19), 967 (15), 907 (10), 855 (71), 774 (7), 677 (7), 647 (7), 622 (13), 521 (23), 467 (13), 410 (13), 396 (34), 378 (46), 311 (21), 269 (21), 223 (16), 212 (12); ¹H NMR (400 MHz, DMSO-D₆, ppm): δ = 9.41 (s, 1H, CH), 5.00 (t, 2H, ³J¹H, ¹H) = 6.9 Hz, CH₂N), 4.20 (t, 2H, ³J¹H, ¹H) = 6.9 Hz, CH₂C(NO₂)₃); ¹³C{¹H} NMR (101 MHz, DMSO-D₆, ppm): δ = 144.4 (NCN), 129.0 (C(NO₂)₃), 41.5 (CH₂N), 32.3 (CH₂C(NO₂)₃); ¹⁵N NMR (40.6 MHz, DMSO-D₆, ppm): δ = 12.4 (d, ²J(¹⁵N, ¹H) = 2.9 Hz, N4), -14.6 (N2/N3), -29.9 (t, ³J(¹⁵N, ¹H) = 2.9 Hz), C(NO₂)₃), -51.8 (N2/N3), -147.5 (m, N1); EA (C₄H₅N₇O₆, 247.13 g mol⁻¹): calc.: C 19.44, H 2.04, N 39.68%; found: C 21.09, H 2.21, N 38.26%. BAM drop hammer: 25 J (500–1000 µm); friction tester: 360 N (500–1000 µm).

5.6 References

- [1] T. M. Klapötke, B. Krumm, R. Scharf, *Eur. J. Inorg. Chem.* **2016**, 3086–3093.
- [2] M. E. Hill, US Patent 3.306.939, **1967**.
- [3] T. M. Klapötke, *Chemistry of High-Energy Materials*, 4th ed., De Gruyter, Berlin, **2015**.
- [4] Q. J. Axthammer, T. M. Klapötke, B. Krumm, R. Moll, S. F. Rest, *Z. Anorg. Allg. Chem.* **2014**, *640*, 76–83.
- [5] P. Yin, Q. Zhang, J. Zhang, D. A. Parrish, J. M. Shreeve, *J. Mater. Chem. A* **2013**, *1*, 7500–7510.
- [6] V. Thottempudi, J. M. J. Shreeve, *Am. Chem. Soc.* **2011**, *133*, 19982–19992.
- [7] T. P. Kofman, G. Y. Kartseva, E. Y. Glazkova, *Russ. J. Org. Chem.* **2008**, *44*, 870–873.
- [8] T. M. Klapötke, D. G. Piercy, J. Stierstorfer, *Dalton Trans.* **2012**, *41*, 9451–9459.
- [9] I. V. Ovchinnikov, A. S. Kulikov, M. A. Epishina, N. N. Makhova, V. A. Tartakovskiy, *Russ. Chem. Bull.* **2005**, *54*, 1346–1349.
- [10] T. P. Kofman, G. Y. Kartseva, E. Y. Glazkova, K. N. Krasnov, *Russ. J. Org. Chem.* **2005**, *41*, 753–757.
- [11] V. V. Semenov, M. I. Kanischev, S. A. Shevelev, A. S. Kiselyov, *Tetrahedron* **2009**, *65*, 3441–3445.
- [12] Q. J. Axthammer, B. Krumm, T. M. Klapötke, R. Scharf, *Chem. Eur. J.* **2015**, *21*, 16229–16239.
- [13] N. E.-B. Kassimi, R. J. Doerksen, A. J. Thakkar, *J. Phys. Chem.* **1995**, *99*, 12790–12796.
- [14] D. T. Davies, *Aromatic Heterocyclic Chemistry*, Oxford University Press Inc., New York, **1992**.
- [15] Z.-H. Yu, Z.-Q. Xuan, T.-X. Wang, H.-M. Yu, *J. Phys. Chem. A* **2000**, *104*, 1736–1747.
- [16] H. Feuer, T. Kucera, *J. Org. Chem.* **1960**, *25*, 2069–2070.
- [17] M. B. Frankel, *Tetrahedron* **1963**, *19*, 211–213.
- [18] M. Ramanathan, Y.-H. Wang, S.-T. Liu, *Org. Lett.* **2015**, *17*, 5886–5889.
- [19] P. N. Gaponik, V. P. Karavai, Y. V. Grigor'ev, *Chem. Heterocycl. Comd.* **1985**, *21*, 1255–1258.
- [20] Q. J. Axthammer, T. M. Klapötke, B. Krumm, R. Scharf, C. C. Unger, *Dalton Trans.* **2016**, *45*, 18909–18920.
- [21] T. Steiner, *Angew. Chem. Int. Ed.* **2002**, *41*, 48–76.
- [22] A. Bondi, *J. Phys. Chem.* **1964**, *68*, 441–451.
- [23] R. D. Dennington, T. A. Keith, J. M. Millam, *GaussView*, v. 5.08, Semichem, Inc., Wallingford, **2009**.
- [24] M. J. Frisch, G. W. Trucks, H. B. Schlegel, G. E. Scuseria, M. A. Robb, J. R. Cheeseman, G. Scalmani, V. Barone, B. Mennucci, G. A. Petersson, H. Nakatsuji, M. Caricato, X. Li, H. P. Hratchian, A. F. Izmaylov, J. Bloino, G. Zheng, J. L. Sonnenberg, M. Hada, M. Ehara, K. Toyota, R. Fukuda, J. Hasegawa, M. Ishida, T. Nakajima, Y. Honda, O. Kitao, H. Nakai, T. Vreven, J. A. Montgomery Jr., J. E. Peralta, F. Ogliaro, M. J. Bearpark, J. Heyd, E. N. Brothers, K. N. Kudin, V. N. Staroverov, R. Kobayashi, J. Normand, K.

Raghavachari, A. P. Rendell, J. C. Burant, S. S. Iyengar, J. Tomasi, M. Cossi, N. Rega, N. J. Millam, M. Klene, J. E. Knox, J. B. Cross, V. Bakken, C. Adamo, J. Jaramillo, R. Gomperts, R. E. Stratmann, O. Yazyev, A. J. Austin, R. Cammi, C. Pomelli, J. W. Ochterski, R. L. Martin, K. Morokuma, V. G. Zakrzewski, G. A. Voth, P. Salvador, J. J. Dannenberg, S. Dapprich, A. D. Daniels, Ö. Farkas, J. B. Foresman, J. V. Ortiz, J. Cioslowski, D. J. Fox, Gaussian, Inc., *Gaussian 09*, Wallingford, **2009**.

[25] J. A. Montgomery, M. J. Frisch, J. W. Ochterski, G. A. Petersson, *J. Chem. Phys.* **2000**, *112*, 6532–6542.

[26] M. Sućeska, *Propellants, Explos., Pyrotech.* **1991**, *16*, 197–202.

[27] M. Sućeska, *Explor5 program*, 6.03 ed., Zagreb, **2013**.

[28] A. Al-Azmi, P. George, Q. M. E. El-Dusouqui, *Heterocycles* **2007**, *71*, 2183–2201.

[29] On Earth and Life Studies Division *Acute Exposure Guideline Levels for Selected Airborne Chemicals: Volume 14*, National Academies Press (US), Washington (DC), **2013**.

[30] CrysAlisPro; Version 1.171.35.11 (release 16.05.2011 CrysAlis171.net), Agilent Technologies: **2011**.

[31] L. J. Farrugia, *J. Appl. Crystallogr.* **1999**, *32*, 837.

[32] A. L. Spek, *Platon, A Multipurpose Crystallographic Tool*: Utrecht University, Utrecht (NL) **1997**.

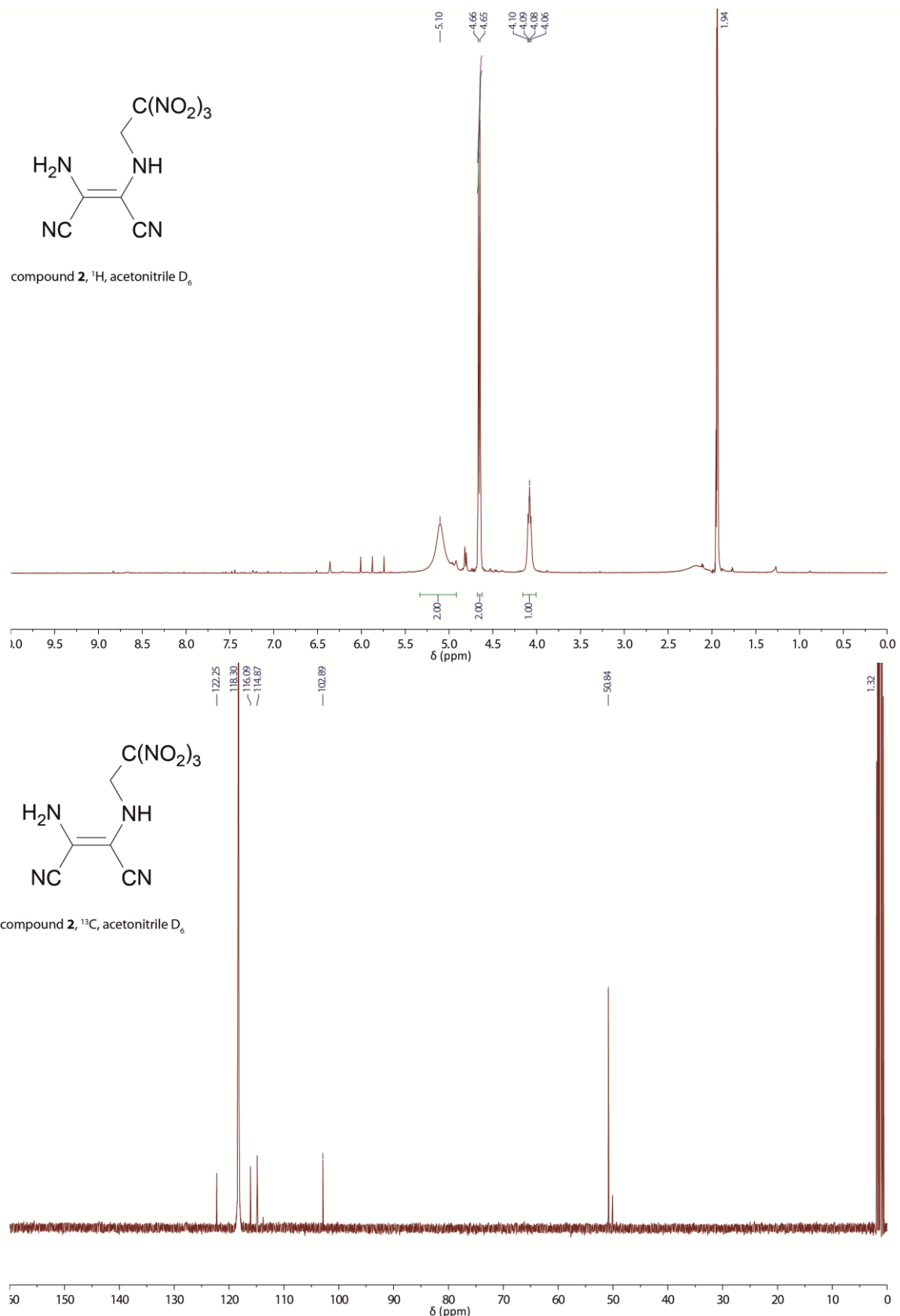
[33] K. Brandenburg; Diamond, 3.2k ed.; Crystal Impact GbR: Berlin, **2014**.

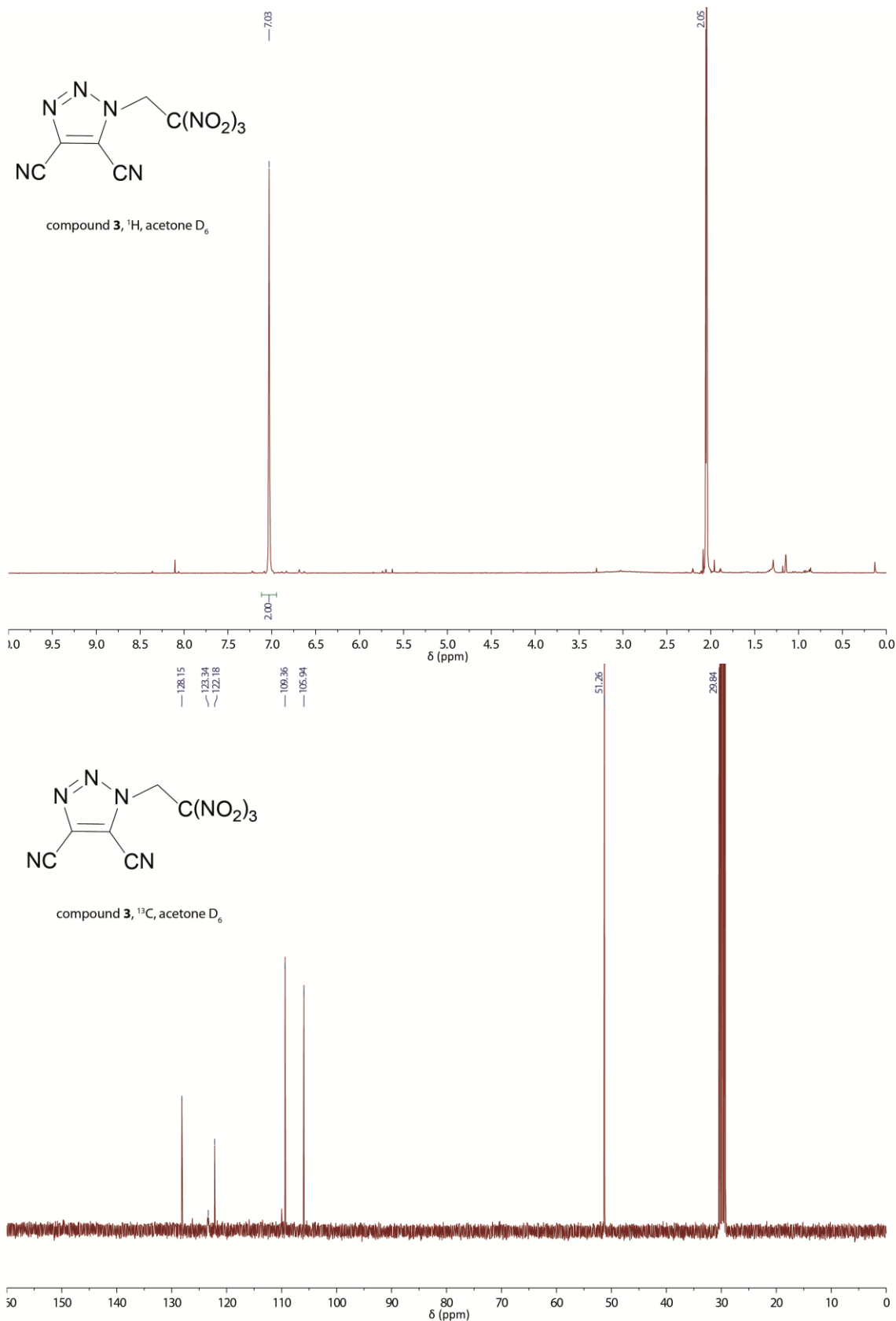
5.7 Supporting Information

- 1 ¹H and ¹³C NMR data of compound **2**
- 2 ¹H and ¹³C NMR data of triazole **3**
- 3 ¹H and ¹³C NMR data of tetrazole **5**
- 4 Crystallographic data of triazole **3**
- 5 Crystallographic data of tetrazole **5**
- 6 Theoretical Calculations
- 7 Calculation details of triazole **3**
- 8 Calculation details of tetrazole **5**
- 9 References

5 N-Trinitroalkyl Substituted Azoles

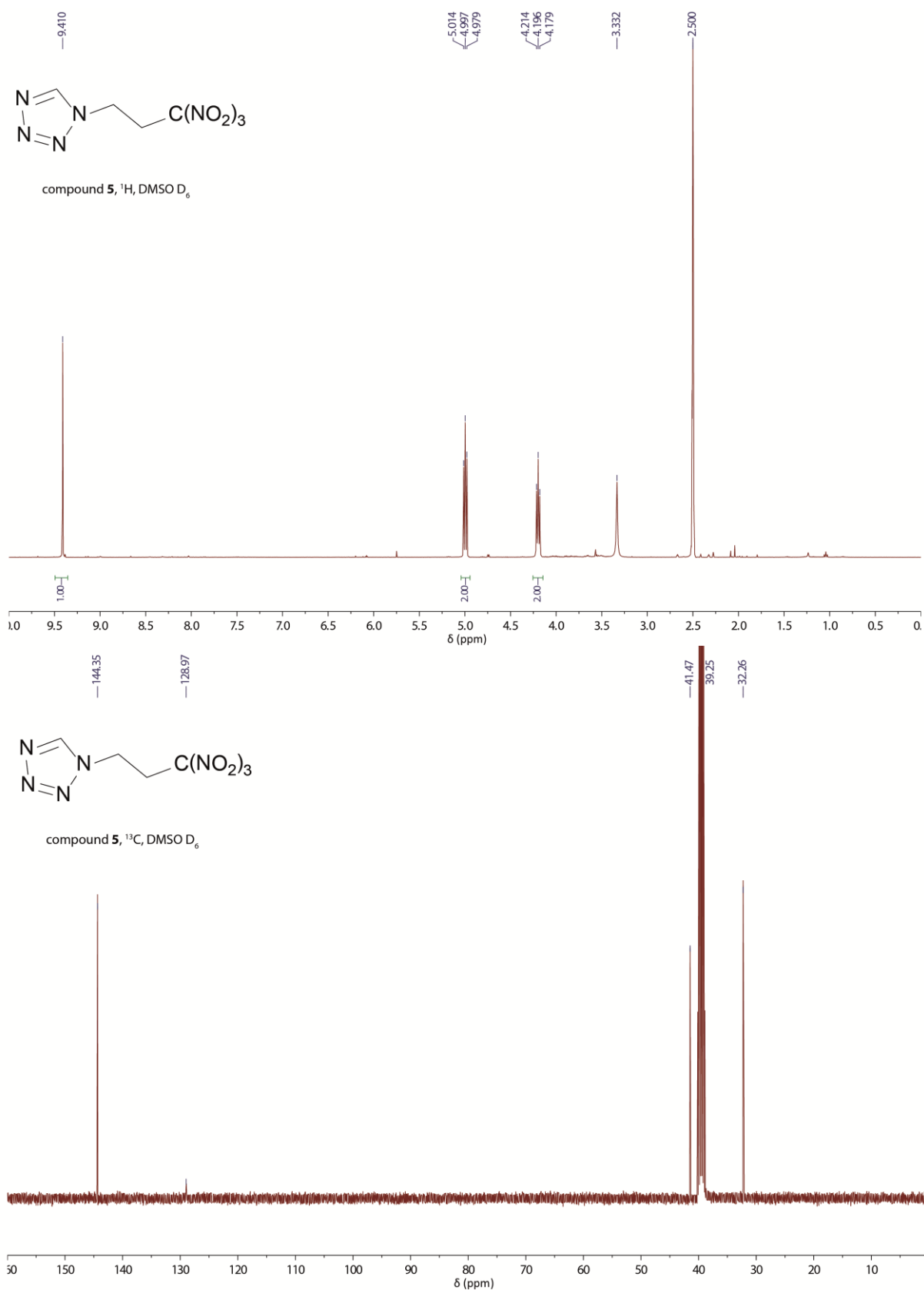
1 ^1H and ^{13}C NMR data of compound 2



2 ¹H and ¹³C NMR data of triazole 3

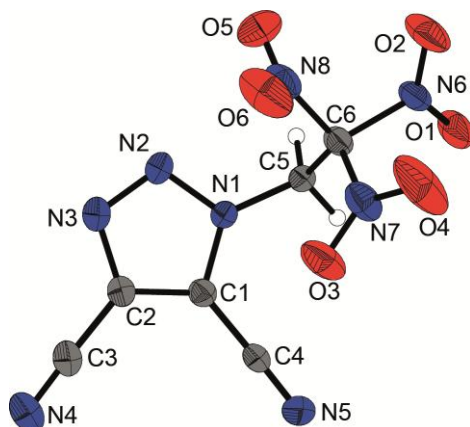
5 N-Trinitroalkyl Substituted Azoles

3 ^1H and ^{13}C NMR data of tetrazole 5



4. Crystallographic data of triazole **3**

3	
formula	C ₆ H ₂ N ₈ O ₆
FW [g mol ⁻¹]	282.13
T [K]	173
λ [Å]	0.71073
crystal system	monoclinic
space group	<i>P</i> 2 ₁ / <i>n</i>
crystal size [mm]	0.37 x 0.04 x 0.04
crystal habit	colorless needle
<i>a</i> [Å]	10.933 (7)
<i>b</i> [Å]	9.353 (5)
<i>c</i> [Å]	11.274 (9)
<i>α</i> , <i>γ</i> [deg]	90
<i>β</i> [deg]	108.6 (8)
<i>V</i> [Å ³]	1092.3 (9)
<i>Z</i>	4
ρ _{calc.} [g cm ⁻³]	1.72
μ	0.155
<i>F</i> (000)	568
2θ range [deg]	4.50 – 27.47
index ranges	$-12 \leq h \leq 13$ $-11 \leq k \leq 11$ $-14 \leq l \leq 14$
reflections collected	8407
reflections unique	2221
parameters	189
Goof	1.023
<i>R</i> ₁ / <i>wR</i> ₂ [<i>I</i> > 2σ(<i>I</i>)]	0.0453 / 0.0773
<i>R</i> ₁ / <i>wR</i> ₂ (all data)	0.0923 / 0.1064
max / min residual electron density [Å ⁻³]	0.367 / -0.321

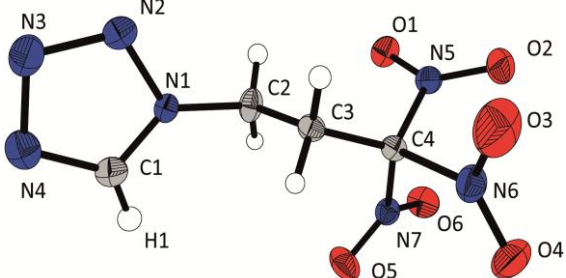


X-ray molecular structure of 4,5-dicyano-1*N*-(trinitroethyl)-1,2,3-triazole (**3**). Thermal ellipsoids represent the 50% probability level.

CCDC: 1587493

5. Crystallographic data of tetrazole 5

5	
formula	C ₄ H ₅ N ₇ O ₆
FW [g mol ⁻¹]	247.13
T [K]	143
λ [Å]	0.71073
crystal system	monoclinic
space group	P2 ₁ /c
crystal size [mm]	0.35 x 0.15 x 0.03
crystal habit	yellow platelet
a [Å]	11.0691 (16)
b [Å]	7.7257 (9)
c [Å]	12.030 (2)
α, γ [deg]	90
β [deg]	114.457 (19)
V [Å ³]	936.5 (3)
Z	4
ρ _{calc.} [g cm ⁻³]	1.75
μ	0.163
F(000)	504
2θ range [deg]	4.20 – 29.34
index ranges	-14 ≤ h ≤ 14 -10 ≤ k ≤ 10 -13 ≤ l ≤ 16
reflections collected	2197
reflections unique	1463
parameters	174
GooF	0.977
R ₁ / wR ₂ [I > 2σ(I)]	0.0449 / 0.0795
R ₁ / wR ₂ (all data)	0.0769 / 0.0911
max / min residual electron density [Å ⁻³]	0.285 / -0.308



X-ray molecular structure of 1N-trinitropropyl tetrazole (5). Thermal ellipsoids represent the 50% probability level.

CCDC: 1822024

6. Computational Details

Enthalpies of formation of all presented compounds were calculated using the CBS-4M quantum chemical method^[1-2] with Gaussian09 A.02^[3]. The CBS (complete basis set) models use the known asymptotic convergence of pair natural orbital expressions to extrapolate from calculations using a finite basis set to the estimated complete basis set limit. In this study we applied the modified CBS-4M method (M referring to the use of Minimal Population localization) which is a re-parameterized version of the original CBS-4 method and also includes some additional empirical corrections. The calculated gas phase enthalpies were transformed to solid state enthalpies by subtraction of sublimation enthalpy calculated by using Trouton's rule^[4].

Detonation parameters were calculated using the EXPLO5 6.03 computer code^[5] with the CBS-4M calculated enthalpies of formation. The program is based on the steady-state model of equilibrium and uses the Becker-Kistiakowsky-Wilson equation of state (BKW EOS.) for gaseous detonation products and the Murnaghan EOS for both solid and liquid products. It is designed to enable the calculation of detonation parameters at the Chapman–Jouguet point (C–J point). The C–J point was found from the Hugoniot curve of the system by its first derivative.^[6] The calculations were performed using the maximum densities at room temperature. The densities at 298 K were either obtained by pycnometer measurement or calculated from the corresponding crystal densities by following equation and the α_v coefficient of volume expansion from the nitramine HMX ($\alpha_v = 1.6 \cdot 10^{-4} \text{ K}^{[7]}$).

$$\rho_{298\text{K}} = \rho_T / (1 + \alpha_v(298 - T))$$

7. Calculation details of triazole **3**Compound **3**

Minimum energy of optimized structure, MP4(SDQ)/6-31 G	-1114.2693144 a.u.
CBS-4M enthalpy, basis for EXPL05 6.03 calculations	-1117.430133 a.u.
CSB-4M energy	-1117.431077 a.u.
CSB-4M free energy	-1117.495594 a.u.
Number of imaginary frequencies	0

Cartesian coordinates

Atom	x	y	z
O	2.68780900	1.54869300	-1.32770500
N	2.80273600	0.51135300	-0.64590100
O	3.81387700	-0.10310200	-0.35292900
C	1.49748900	0.03367500	-0.07749500
N	1.65442700	-1.40693400	0.27369100
C	0.40985900	0.22857200	-1.13125300
N	1.29480100	0.83850400	1.16643700
O	1.95589800	-2.10324800	-0.70163500
O	1.43550400	-1.73519900	1.43298300
N	-0.87095000	-0.27747900	-0.69285200
H	0.33443000	1.27775700	-1.35037800
H	0.71964300	-0.31809400	-2.00608100
O	0.19042500	1.37593400	1.30163800
O	2.26561200	0.88598200	1.91565200
C	-2.00656400	0.37975900	-0.37081100
N	-1.09395900	-1.64310600	-0.62222900
C	-2.15450400	1.77638000	-0.37966500
C	-2.92135800	-0.59094000	-0.09648800
N	-2.31383000	-1.81270600	-0.25850200
N	-2.29004900	2.90633600	-0.39936900
C	-4.26637300	-0.43593000	0.28205700
N	-5.35436900	-0.29614400	0.58649000

8. Calculation details of tetrazole 5

Compound 5			
Minimum energy of optimized structure, MP4(SDQ)/6-31 G		–985.6322218 a.u.	
CBS-4M enthalpy, basis for EXPLO5 6.03 calculations		–988.475794 a.u.	
CSB-4M energy		–988.476738 a.u.	
CSB-4M free energy		–988.537654 a.u.	
Number of imaginary frequencies		0	
Cartesian coordinates			
Atom	x	y	z
N	1.72577700	–0.62568700	1.21272700
O	0.84589700	2.10968400	–0.78089200
N	2.01293300	–0.69509600	–1.18667300
O	1.14065600	–0.17592000	2.21227900
O	2.54166700	1.71967200	0.59715500
N	–2.56799000	0.15800200	0.24925700
N	–3.11557300	–1.11304100	0.26856500
N	1.56761900	1.39347400	–0.06949200
O	2.63820900	–1.43702800	1.16565900
N	–4.31106300	–1.00814700	–0.17538600
O	1.66047900	–1.84169700	–1.47462500
O	2.91589500	–0.02100500	–1.67807600
N	–4.59573900	0.33463100	–0.49957400
C	–1.20438700	0.37416400	0.70529600
C	–0.26171000	–0.31395200	–0.30365800
C	–3.51002300	0.99472800	–0.22567000
C	1.21689200	–0.06475200	–0.07730200
H	–0.48318300	0.06365200	–1.29057900
H	–0.42272000	–1.38049600	–0.29774600
H	–1.02484900	1.43624100	0.72735000
H	–1.09773400	–0.03909300	1.68977400
H	–3.37030600	2.03995800	–0.34875800

9. References

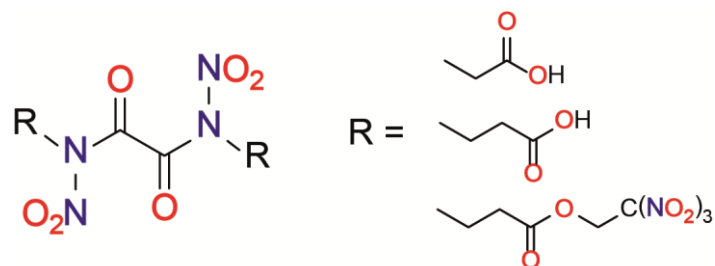
- [1] J. J. A. Montgomery, M. J. Frisch, J. W. Ochterski, G. A. Petersson, *J. Chem. Phys.* **2000**, *112*, 6532–6542.
- [2] J. W. Ochterski, G. A. Petersson, J. J. A. Montgomery, *J. Chem. Phys.* **1996**, *104*, 2598–2619.
- [3] M. J. Frisch, G. W. Trucks, H. B. Schlegel, G. E. Scuseria, M. A. Robb, J. R. Cheeseman, G. Scalmani, V. Barone, B. Mennucci, G. A. Petersson, H. Nakatsuji, M. Caricato, X. Li, H. P. Hratchian, A. F. Izmaylov, J. Bloino, G. Zheng, J. L. Sonnenberg, M. Hada, M. Ehara, K. Toyota, R. Fukuda, J. Hasegawa, M. Ishida, T. Nakajima, Y. Honda, O. Kitao, H. Nakai, T. Vreven, J. A. Montgomery Jr., J. E. Peralta, F. Ogliaro, M. J. Bearpark, J. Heyd, E. N. Brothers, K. N. Kudin, V. N. Staroverov, R. Kobayashi, J. Normand, K. Raghavachari, A. P. Rendell, J. C. Burant, S. S. Iyengar, J. Tomasi, M. Cossi, N. Rega, N. J. Millam, M. Klene, J. E. Knox, J. B. Cross, V. Bakken, C. Adamo, J. Jaramillo, R. Gomperts, R. E. Stratmann, O. Yazyev, A. J. Austin, R. Cammi, C. Pomelli, J. W. Ochterski, R. L. Martin, K. Morokuma, V. G. Zakrzewski, G. A. Voth, P. Salvador, J. J. Dannenberg, S. Dapprich, A. D. Daniels, Ö. Farkas, J. B. Foresman, J. V. Ortiz, J. Cioslowski, D. J. Fox, Gaussian, Inc., *Gaussian 09*, Wallingford, **2009**.
- [4] F. Trouton, *Philos. Mag.* **1884**, *18*, 54–57.
- [5] M. Sućeska, *Explo5* program, 6.03 ed., Zagreb, Croatia, **2015**.
- [6] M. Sućeska, *Propellants, Explos., Pyrotech.* **1991**, *16*, 197–202.
- [7] C. Xue, J. Sun, B. Kang, Y. Liu, X. Liu, G. Song, Q. Xue, *Propellants, Explos., Pyrotech.* **2010**, *35*, 333–338.

6 *N*-Dinitrated Oxamides

N-DINITRATED OXAMIDES: TRINITROETHYL ESTERS AND NITROCARBAMATES

Thomas M. Klapötke, Burkhard Krumm, and Thomas Reith

unpublished results



6.1 Abstract

Several derivates of *N*-nitrated oxamides were derived from the readily available starting materials diethyl oxalate, glycine and β -alanine. Following the initial condensation reactions, the oxamide derivatives were subsequently nitrated to yield the corresponding dinitroxamides. Conversion of the β -alanine based dinitroxamide into the acid chloride was accomplished by the reaction with thionyl chloride. The final reaction with trinitroethanol yielded the energetic target ester in moderate yield and high purity. Additionally, a reaction path starting with diethyl oxalate and ethanolamine gave access to a nitrocarbamate derivative.

6.2 Introduction

In the last decades of energetic materials research, the search for environmental benign alternatives for commonly used compounds is one of the main objectives.¹ Heavy metal-free primary explosives and pyrotechnics, non-toxic secondary explosives and halogen-free oxidizers are still under investigation. “Green” high energy dense oxidizers (HEDOs) are generally developed to replace ammonium perchlorate (AP), which is employed as standard oxidizer in composite propellant mixtures for rocket and missile engines.¹ Ammonium perchlorate has numerous advantages such as its outstanding low price, great availability and favorable oxygen balance.¹ Nonetheless the perchlorate ion is very persistent and causes several environmental problems, mainly as competitor to iodine in the thyroid gland.²⁻³ Additionally upon combustion, large amounts of chlorinated products are formed and set free in the atmosphere. These exhaust gases directly harm the environment and can be detected easily, leading to tactical disadvantages.¹ Several potential halogen-free alternatives have been synthesized over the last decades. Ionic compounds such as ammonium dinitramide and ammonium nitrate appear to be potent replacements.⁴⁻⁵ Covalent structures generally utilize specific oxygen-rich moieties. Some of the most promising alternatives based on the trinitroethyl moiety, such as trinitroethyl nitrocarbamate, bis(trinitroethyl)oxalate and 2,2,2-trinitroethyl formate (Figure 6.1).⁶⁻⁹ Synthetically, this group is conveniently accessible through the precursor trinitroethanol (TNE). Usually the trinitroethyl moiety is combined with an energetic or oxygen-rich backbone, such as nitrocarbamates, oxalates, esters or amides. Introducing trinitroethyl esters has proven to be an effective way to incorporate the oxygen-rich unit.

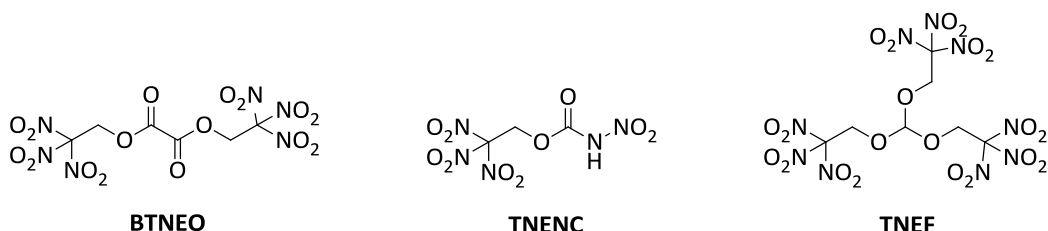
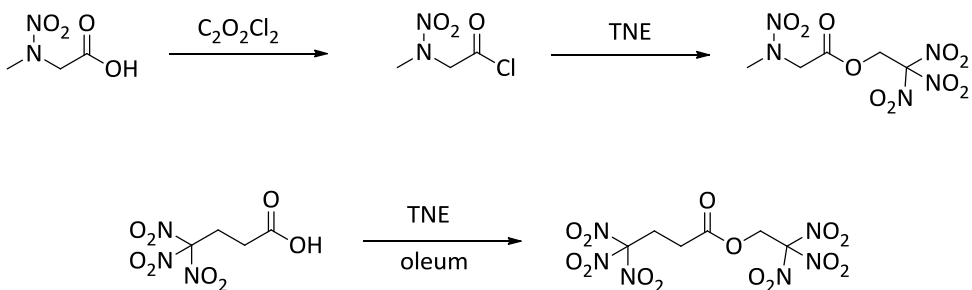


Figure 6.1: Molecular structures of bis(trinitroethyl)oxalate (BTNEO), trinitroethyl nitrocarbamate (TNENC) and 2,2,2-trinitroethyl formate (TNEF).

The synthesis of trinitroethyl esters starting from carbonic acids can be achieved on several pathways. One approved method is to increase the reactivity of the carbonic acid group through the conversion into reactive acid chlorides.^{8, 10-11} Another synthetic route exploits the strong dehydrating characteristic of sulfuric acid or oleum to achieve the direct conversion (Scheme 6.1).¹²



Scheme 6.1: Reaction paths to TNE esters starting from carbonic acids, utilizing acid chloride intermediates (top) and fuming sulfuric acid (bottom).

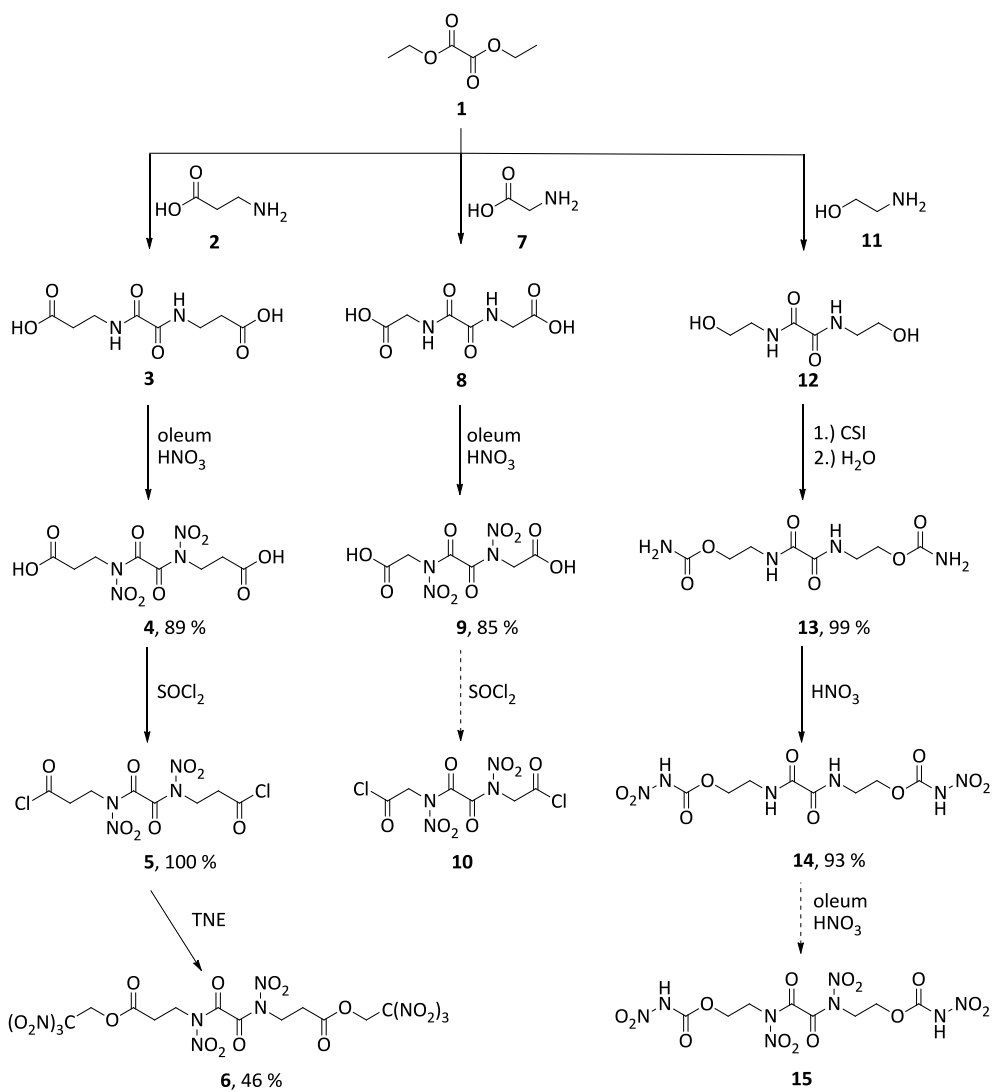
In this study, oxamide precursors were obtained by the reaction of ethyl oxalate with amino acids.^[13] In a nitration mixture composed of oleum and concentrated nitric acid, the oxamides were converted into the corresponding dinitroxamides. In case of the β -alanine based derivative, it was possible to transform the carbonic acid units to acid chlorides. Subsequently, the reaction with trinitroethanol, releasing gaseous HCl in the course, yields the final ester in high purity. Furthermore, one new nitrocarbamate derivative was synthesized originating from the reaction of ethyl oxalate with ethanolamine.¹⁴

6.3 Results and Discussion

6.3.1 Synthesis

The oxamide precursors **3**, **8** and **12** were synthesized from diethyl oxalate (**1**) according to literature by the reaction with β -alanine (**2**), glycine (**7**) and ethanolamine (**11**),

respectively.¹³⁻¹⁴ The oxamides **3** and **8** were nitrated in a mixture of oleum and concentrated nitric acid with gently heating up to 50 °C. The dinitroxamide **4** precipitates from the aqueous work-up, whereas the nitrated glycine derivative **9** needed to be extracted with ethyl acetate. Both dinitroxamides **4** and **9** contain two identical carbonic acid functionalities, and the β -alanine based compound **4** was converted into the corresponding acid chlorides **5a** by the reaction with thionyl chloride. The reaction of the glycine based dinitroxamide with chlorinating agents (SOCl_2 , $\text{C}_2\text{O}_2\text{Cl}_2$, PCl_5) did not yield any isolable product. The final reaction step of the acid chloride **5** with appropriate equivalents of trinitroethanol yielded the TNE-ester **6** in good yield and purity (Scheme 6.2).



Scheme 6.2: Synthesis of the dinitroxamides **4**, **5**, **6** and **9**, the carbamate precursor **13** and the nitrocarbamate **14**.

The oxamide **12**, originating from the reaction of diethyl oxalate **1** with ethanolamine **11**, was transformed into the corresponding biscarbamate **13** utilizing the valuable reagent chlorosulfonyl isocyanate (CSI). A first nitration reaction carried out in pure concentrated nitric acid yielded the bisnitrocarbamate **14** in high yields and purity. A second nitration reaction in fuming sulfuric acid and concentrated nitric acid, converting the amide moieties into nitramides, should be manageable, however the desired compound **15** was not isolable so far.

All synthesized compounds are colorless solids, although the acid chloride **5** might show slightly yellowish residues. All precursors **1–5**, **7–9** and **11–13** were employed after the corresponding work-up without further purification. The final products **6** and **14** are obtained elemental analysis pure from the work-up.

6.3.2 NMR and Vibrational Spectroscopy

All synthesized compounds were characterized by ^1H and ^{13}C NMR spectroscopy; additionally the ^{14}N NMR spectra of the nitroxamides **4**, **5**, **6** and **9** as well as of the nitrocarbamate **14** were recorded. The precursor oxamides **3**, **8** and **12** and the carbamate **13** were dissolved in $[\text{D}_6]\text{DMSO}$, the dinitroxamides **4**, **6**, **9** and the nitrocarbamate **14** were recorded in $[\text{D}_6]\text{acetone}$ and the acid chloride **5** was measured in CDCl_3 .

Regarding the ^1H NMR spectrum of the β -alanine based amide **3**, the twelve hydrogen atoms are detected as four resonances due to the high symmetry. The two acidic COOH protons are recorded at the expected range at 12.3 ppm as broadened singlet. The amide NH signals are located as a triplet at 8.68 ppm due to coupling with the neighboring methylene unit. The two CH_2 groups are found at 3.33 and 2.46 ppm. Both methylene groups form triplets. The CH_2 unit next to the amide NH results in a doublet of triplets with coupling constants of $^3J(^1\text{H}, ^1\text{H}) = 7.1$ Hz and 5.9 Hz. In the ^1H NMR spectrum of the nitrated **4**, only two signals are observed. The acidic COOH protons are not detected, probably due to deuterium exchange with the solvent or distinct broadening. The amide hydrogen atoms of the precursor are substituted with nitro units. The two remaining CH_2 groups are recorded as singlet signal at 4.5 ppm and one triplet at 2.82 ppm. The signal at 4.5 ppm is clearly broadened. After the transformation into the acid chloride **5**, the broadening of the corresponding signal persists, but is observed as two broad signals at 4.5 ppm. The second methylene signal of compound **5** is located at 3.36 ppm, split into a triplet. Further, one CH_2 signal is broadened in the ^1H NMR spectrum of the TNE-ester at 4.6 ppm, while the second methylene unit is found at 3.06 ppm, split into a triplet. Additionally, a new singlet is originating at 5.87 ppm for the methylene unit of the trinitroethyl moiety. In the ^{13}C NMR of the β -alanine based compounds, the precursor **3** starts

6 N-Dinitrated Oxamides

with four signals representing the carboxylic acid carbon (172.7 ppm), the oxamide carbonyl carbon (159.8 ppm) and the two methylene carbons (35.1 and 33.2 ppm). Upon nitration to the dinitroxamide **4**, the signals are found at 171.4, 159.2, 42.5 and 30.8 ppm. The acid chloride **5** shows the four carbon resonances at 171.1, 158.1, 43.1 and 41.1 ppm. The final TNE-ester **6** adds two signals for the trinitroethyl moiety, and the carbon resonances are located at 168.8, 159.0, 124, 61.9, 42.0 and 31.0 ppm. The signal at 124 ppm is only visible as distinctively broadened resonance due to the three neighboring nitro groups. In the ¹⁴N NMR spectra of the dinitroxamides **4**, **5** and **6**, the nitramide CONNO₂ nitrogen signals are observed at around -45 ppm. The TNE-ester **6** shows an additional signal at -31 ppm, which can be assigned to the aliphatic nitro groups.

In the NMR spectra of the glycine-based materials **8** and **9** similar trends with respect to the β -alanine based derivatives are observed. In the ¹H NMR spectrum, three signals are found for the eight hydrogen atoms of the precursor **8**. The acidic protons of the carboxylic acid units are located as broadened signal at 12.5 ppm. The amide NH hydrogen is found as triplet at 8.91 ppm and is coupled to the methylene unit, which is found at 3.81 ppm. Upon nitration, the dinitroxamide **9** shows only two singlet for the carboxylic acid protons at 12.1 ppm and the CH₂ group at 5.10 ppm. In contrast to the corresponding β -alanine based dinitroxamide **4**, the signal for the methylene units next to the nitramide moieties is not broadened. Regarding the ¹³C NMR spectra, the precursor **8** shows the expected three resonances for the carboxylic acid carbon (170.3 ppm), the oxamide carbonyl carbon (159.9 ppm) and the methylene unit (40.9 ppm). After nitration to the dinitroxamide **9**, the signals are only slightly shifted to 166.6, 158.9 and 46.6 ppm. Additionally, the nitramide CONNO₂ groups of **9** are detected in the ¹⁴N NMR spectrum at -46 ppm.

In the ¹H NMR spectrum of precursor **12** four signals are observed at 8.56, 4.73, 3.44 and 3.21 ppm. The signal at 8.56 ppm can be assigned to the amide NH hydrogen and is split into a triplet by the neighboring methylene unit. The hydroxyl hydrogen signal is also split to a triplet at 4.73 ppm. The two CH₂ units are found as multiplets at 3.47–3.42 ppm and 3.23–3.18 ppm. After the reaction with CSI to compound **13**, the hydroxyl hydrogen signal is removed and replaced with the carbamate C(O)NH₂ unit, which is observed as a broad signal at 6.5 ppm. The oxamide NH signal is found at 8.73 ppm and the two methylene units are observed as triplet at 3.99 ppm and multiplet at 3.36–3.32 ppm. After the nitration to the nitrocarbamate **14**, the acidic nitrocarbamate NH proton is shifted distinctly low field to 13.4 ppm. The oxamide NH proton is located at 8.3 ppm and the two methylene units show their signals as multiplets at 4.40–4.37 ppm and 3.65–3.61 ppm. Regarding the ¹³C NMR

spectra, the precursor **12** shows one signal for the carboxylic acid carbon at 160.0 ppm, and two signals at 59.2 and 41.7 ppm representing the methylene units. The carbamate **13** adds one signal for the carbamate carbonyl carbon, and the resonances are observed at 160.0, 156.5, 61.4 and 38.7 ppm. Upon nitration to **14**, the signals are slightly shifted to 161.0, 149.3, 65.7 and 39.1 ppm. Finally, the nitramino NHNO_2 moieties of nitrocarbamate **14** can be observed in the ^{14}N NMR spectrum at -45 ppm.

6.3.3 Single Crystal Structure Analysis

Suitable single crystals for a crystal structure determination of the dinitroxamide **4** were obtained from methanol by slow evaporation at room temperature. Bis(carboxyethyl) dinitroxamide crystallizes in the monoclinic space group $P2_1/c$ with 20 molecules in the unit cell and a density of 1.61 g cm^{-3} at 173 K (Figure 6.2, Table 6.1).

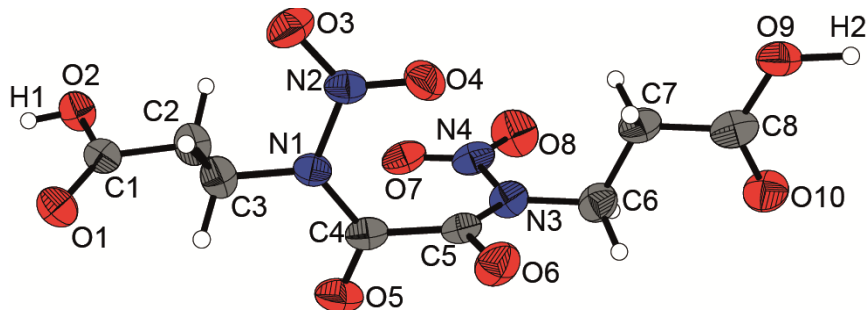


Figure 6.2: X-ray molecular structure of Bis(carboxyethyl) dinitroxamide (**4**). Thermal ellipsoids represent the 50% probability level. Selected atom distances [\AA] and bond angles [deg]: N1–N2 1.410 (6), N1–C4 1.383 (7), C4–C5 1.514 (6), C4–O5 1.188 (6), C5–O6 1.216 (6), C5–N3 1.383 (6), N3–N4 1.398 (6); C1–O2–H1 109.5 (4), C3–N1–C4 122.7 (4), C3–N1–N2 116.5 (4), C4–N1–N2 120.5 (4); C5–C4–N1–N2 15.3 (7), C4–C5–N3–N4 17.1 (7), N1–C4–C5–N3 -98.8 (6), N1–C4–C5–O6 91.1 (6), N2–N1–C4–O5 -173.5 (5), O5–C4–C5–O6 -80.2 (6).

The determination and refinement of compound **4** in space group $P2_1/c$ leads to 20 molecules in the unit cell and rather huge cell dimensions ($V = 6465.4 \text{ \AA}^3$). The platon software coincides with the space group but may detect pseudo translations with a potential higher symmetry. However, refinement in other relevant monoclinic space groups, such as the body-centered $I2/a$, did not yield better refinements of the structure in the solid state.

In the crystalline state, the molecule center of the nitroxamide **4** is heavily twisted as demonstrated by the torsion angles N1–C4–C5–O6 (91.1°), O5–C4–C5–O6 (-80.2°) and O5–C4–C5–N3 (90.0°). The two carbonyl units C(O) in the center align almost perfectly

orthogonal to each other, however span a plane with the neighboring nitramino units (e.g. N2–N1–C4–O59. The intramolecular structure is defined by dimerization due to strong hydrogen bonds between the carboxylic acid moieties (Figure 6.3). As the dinitroxamide bears one carboxylic acid group on each side, the dimerization results in a structure of one dimensional chains.

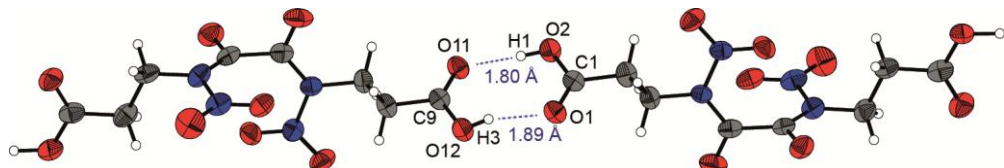


Figure 6.3: Dimers of **4** connected via hydrogen bonds of the carboxyl units.

Table 6.1: Crystal data, details of the structure determinations and refinement of **4**.

	4	4
formula	$C_8H_{10}N_4O_{10}$	$V [\text{\AA}^3]$
$FW [\text{g mol}^{-1}]$	322.19	Z
$T [\text{K}]$	130	$\rho_{\text{calc.}} [\text{g cm}^{-3}]$
$\lambda [\text{\AA}]$	0.71073	μ
crystal system	monoclinic	$F(000)$
space group	$P2_1/c$	2Θ range [deg]
crystal size [mm]	0.40 x 0.28 x 0.21	index ranges $-16 \leq h \leq 17$ $-34 \leq k \leq 35$ $-26 \leq l \leq 24$
crystal habit	colorless block	reflections collected
$a [\text{\AA}]$	12.952 (1)	reflections unique
$b [\text{\AA}]$	26.482 (1)	parameters
$c [\text{\AA}]$	19.471 (1)	GOF
α [deg]	90	$R_1 / wR_2 [I > 2\sigma(I)]$
β [deg]	104.51 (1)	R_1 / wR_2 (all data)
γ [deg]	90	max / min residual electron density [\AA^{-3}]
		-0.289 / 0.639

6.3.4 Thermal Stabilities and Energetic Properties

The physical properties of the nitroxamides **4**, **6** and **9** as well as of nitrocarbamate **14** were determined and summarized in Table 6.2. The thermal stabilities (onset decomposition temperatures) of these compounds were determined by Differential Thermal Analysis (DTA) measurements. The temperature range of 15–400 °C was recorded with a heating rate of 5 °C min⁻¹. The two nitroxamide precursors **4** and **9** do not melt before decomposing at 183 °C (**4**) and 144 °C (**9**). The TNE-ester **6** melts at 118 °C and decomposed in two distinct steps at 159 °C and 203 °C. The nitrocarbamate derivative **14** melts at 108 °C and decomposed at 178 °C.

Table 6.2: Physical and energetic properties of the dinitroxamides **4**, **6** and **9** and the nitrocarbamate **14**.

	4	6	9	14
Formula	C ₈ H ₁₀ N ₄ O ₁₀	C ₁₂ H ₁₂ N ₁₀ O ₂₂	C ₆ H ₆ N ₄ O ₁₀	C ₈ H ₁₂ N ₆ O ₁₀
FW [g mol ⁻¹]	322.19	648.28	294.13	352.22
T _{melt} [°C] ^[a]	-	118	-	108
T _{dec} [°C] ^[a]	183	159	144	178
IS [J] ^[b]	40	6	10	40
FS [N] ^[b]	360	360	360	360
ρ [g cm ⁻³] ^[c]	1.62	1.75	1.74	1.61
O [%] ^[d]	49.7	54.3	54.4	45.4
Ω _{CO} [%] ^[e]	-14.9	9.9	5.4	-18.2
Δ _f H _m ° [kJ mol ⁻¹] ^[f]	-1071.4	-997.8	-956.4	-1030.3
V _{det} [m s ⁻¹] ^[g]	6528	8025	7264	6696
p _{det} [kbar] ^[g]	157	278	211	162
I _{sp} [s] ^[h]	163	243	195	166
I _{sp} [s] (15 % Al) ^[h]	213	255	230	214
I _{sp} [s] (15 % Al, 14% binder) ^[h]	206	228	212	208

[a] Onset melting T_m and decomposition point T_{dec} from DTA measurements, heating rate 5 °C min⁻¹. [b] Sensitivity towards impact IS and friction FS. [c] Density at room temperature determined by pycnometer measurements. [d] Oxygen content. [e] Oxygen balance assuming formation of CO. [f] Energy of formation calculated on the CBS-4M level using Gaussian 09. [g] Predicted detonation velocity and detonation pressure. [h] Specific impulse I_{sp} of the neat compound and compositions with aluminum or aluminum and binder (6 % polybutadiene acrylic acid, 6 % polybutadiene acrylonitrile and 2 % bisphenol A ether) using the EXPLO5 (Version 6.03) program package (70 kbar, isobaric combustion, equilibrium to throat and frozen to exit).

Friction and impact sensitivities were evaluated according to BAM standards. In terms of impact sensitivity, the β-alanine nitroxamide **4** (IS > 40 J) is significantly more stable than the

glycine relative **9** ($IS = 10$ J). Compound **6** shows impact sensitivity values of 6 J. The nitrocarbamate **14** shows no sensitivity to impact ($IS > 40$ J). Concerning the sensitivity towards friction, all compounds are regarded as insensitive ($FS > 360$ N).

The density of compounds **4**, **6**, **9** and **14** were determined via gas pycnometer measurements. The lowest density was measured for the nitrocarbamate derivative **14** with a value of 1.61 g cm^{-3} , while the highest densities were recorded for the glycine-based nitroxamide **9** (1.74 g cm^{-3}) and the TNE-ester **6** (1.75 g cm^{-3}). The oxygen balance Ω_{CO} , assuming the formation of carbon monoxide, is positive for these relatively dense compounds **6** and **9**.

The heat of formation (CBS-4M level) was calculated with the GAUSSIAN program package, and in combination with the experimental density the energetic properties were estimated utilizing the EXPL05 (Version 6.03) computer code. The target molecule, TNE-ester **6**, develops a detonation velocity $V_{det} > 8000\text{ m s}^{-1}$ and a detonation pressure $p_{det} = 278\text{ kbar}$. It reaches a calculated specific impulse of $I_{sp} = 255\text{ s}$ in mixture with aluminum and $I_{sp} = 228\text{ s}$ in mixture with aluminum and binder. The second target molecule, the trinitroethyl ester of the glycine-based dinitroxamide **9**, should develop superior performance data. By comparison of the two precursor dinitroxamides **4** and **9**, the glycine-based **9** shows a higher density (**4**: 1.62 g cm^{-3} , **9**: 1.74 g cm^{-3}), a positive oxygen balance Ω_{CO} (**4**: -14.9 \% , **9**: $+5.4\text{ \%}$) and a lower molecular weight (**4**: 322.19 g mol^{-1} , **9**: 294.13 g mol^{-1}). Those advantages should persist along the synthetic pathway to the corresponding TNE-ester compounds, leaving the glycine-based TNE-ester with promising combustion performances.

6.4 Conclusion

Several new *N*-nitrated oxamides were synthesized and thoroughly characterized in this study. Furthermore, a reaction path starting from diethyl oxalate and ethanolamine yielded a nitrocarbamate derivative. All syntheses start from easily available starting materials, such as diethyl oxalate and the amino acids glycine and β -alanine. The nitration of the amide functionalities was achieved by a mixture of oleum (ca. 25 %) and concentrated nitric acid. Most of the designed materials combine good yields with fast reaction times and a high purity without further purification steps. The first target molecule **6**, the dinitroxamide based on β -alanine in combination with trinitroethyl ester units, develops a detonation velocity of over 8000 m s^{-1} and a moderate specific impulse in composite mixtures. The second target molecule, the glycine derivative combined with TNE, should surpass the performance and develop promising combustion parameters. The synthesis of the third target molecule, the dinitroxamide derivative of the nitrocarbamate **14**, is still under investigation.

6.5 Experimental Section

6.5.1 General Information

Solvents were dried and purified with standard methods. Diethyl oxalate (**1**), β -alanine (**2**), glycine (**7**) and ethanolamine (**11**) are commercially available and were used without further purification. Raman spectra were recorded in glass tube with a Bruker MultiRAM FT-Raman spectrometer with a Klaastech DENICAFC LC-3/40 laser (Nd:YAG, 1064 nm, up to 1000 mW) in the range of 4000–400 cm^{-1} . Relative intensity is given in percent. IR spectra were recorded with a Perkin-Elmer Spectrum BX-FTIR spectrometer coupled with a Smiths ATR DuraSample IRII device. Measurements were recorded in the range of 4000–650 cm^{-1} . All Raman and IR spectra were measured at ambient temperature. NMR spectra were recorded with JEOL Eclipse and Bruker TR 400 MHz spectrometers at 25 °C. Chemical shifts were determined in relation to external standards Me_4Si (^1H , 399.8 MHz); (^{13}C , 100.5 MHz); MeNO_2 (^{14}N , 28.9 MHz). Elemental analyses (CHN) were obtained with a Vario EL Elemental Analyzer.

The sensitivity data were acquired by measurements with a BAM dropammer and a BAM friction tester. Melting and decomposition points were determined by differential thermal calorimetry (DTA) using a OZM Research DTA 552-Ex instrument at a heating rate of 5 °C min^{-1} . Measurements were performed in open glas vessels against a reference material up to 400 °C.

6.5.2 X-ray Crystallography

The crystal structure data were obtained using an Oxford Xcalibur CCD Diffraktometer with a KappaCCD detector at low temperature (173 K, 123 K). Mo-K α radiation ($\lambda = 0.71073 \text{ \AA}$) was delivered by a Spellman generator (voltage 50 kV, current 40 mA). Data collection and reduction were performed using the CRYSTALIS CCD¹⁷ and CRYSTALIS RED¹⁸ software, respectively. The structures were solved by SIR92/SIR97¹⁹ (direct methods) and refined using the SHELX-97²⁰⁻²¹ software, both implemented in the program package WinGX22.²² Finally, all structures were checked using the PLATON software.²³ Structures displayed with ORTEP plots are drawn with thermal ellipsoids at 50 % probability level.

6.5.3 Computational Details

The theoretical calculations were achieved by using the GAUSSIAN09 program package¹⁵ and were visualized by using GAUSSVIEW5.08.²⁴ Optimizations and frequency analyses were performed at the B3LYP level of theory (Becke's B3 three parameter hybrid functional by using

the LYP correlation functional) with a cc-pVDZ basis set. After correcting the optimized structures with zero-point vibrational energies, the enthalpies and free energies were calculated on the CBS-4M (complete basis set) level of theory.²⁵ The detonation parameters were obtained by using the EXPL05 (V6.03) program package.^{16, 26}

6.5.4 Synthesis

CAUTION! The nitrated oxamides **4**, **5**, **6** and **9** and the nitrocarbamate **14** are energetic materials and show sensitivities in the range of secondary explosives! They should be handled with caution during synthesis or manipulation and additional protective equipment (leather jacket, face shield, ear protection, Kevlar gloves) is strongly recommended.

Bis(carboxyethyl) oxamide (3): This compound was synthesized according to literature.¹³

¹H NMR ([D₆]DMSO): δ = 12.3 (br, 2H, COOH), 8.68 (t, 2H, ³J(¹H, ¹H) = 6.0 Hz, NH), 3.33 (dt, 4H, ³J(¹H, ¹H) = 7.1 Hz, 5.9 Hz, NHCH₂), 2.46 (t, 4H, ³J(¹H, ¹H) = 7.1 Hz, CH₂). ¹³C NMR ([D₆]DMSO): δ = 172.7 (COOH), 159.8 (CONH₂), 30.1 (CH₂), 33.2 (CH₂).

Bis(carboxyethyl) dinitroxamide (4): Bis(carboxyethyl) oxamide (**3**, 0.52 g, 2.2 mmol) was added in small portions to a mixture of fuming sulfuric acid (60 %, 1.4 mL), concentrated sulfuric acid (96 %, 2.6 mL) and nitric acid (100 %, 3 mL) under constant cooling with an ice bath. The reaction mixture was stirred at 50 °C for 5 h and afterwards poured onto 150 ml of ice. The precipitated colorless solid was filtered off, washed with cold water and dried under reduced pressure. Bis(carboxyethyl) dinitroxamide (**4**) was obtained as a colorless solid (0.64 g, 89 %).

¹H NMR ([D₆]acetone): δ = 4.5 (br, 4H, NCH₂), 2.82 (t, 4H, ³J(¹H, ¹H) = 7.2 Hz, CH₂). ¹³C NMR ([D₆]acetone): δ = 171.4 (COOH), 159.2 (CONH₂), 42.5 (CH₂), 30.8 (CH₂). ¹⁴N NMR ([D₆]acetone): δ = -45 (NO₂). Raman (800 mW): 3030 (18), 2990 (46), 2972 (24), 2939 (62), 2824 (5), 1732 (100), 1708 (29), 1652 (7), 1606 (15), 1454 (3), 1437 (6), 1416 (38), 1368 (4), 1353 (18), 1321 (8), 1237 (11), 1096 (5), 1051 (32), 960 (10), 924 (59), 900 (22), 837 (57), 772 (19), 742 (14), 694 (4), 666 (6), 619 (7), 596 (7), 510 (48), 487 (11), 392 (6), 368 (13), 355 (6), 288 (10) cm⁻¹. IR: 2889 (w), 2623 (w), 1702 (s), 1588 (s), 1433 (m), 1321 (m), 1306 (m), 1252 (vs), 1225 (s), 1217 (s), 1094 (s), 995 (w), 958 (w), 899 (m), 835 (m), 801 (m), 739 (w), 676 (w), 584 (s), 505 (m) cm⁻¹. C₈H₁₀N₄O₁₀ x H₂O (322.19 g mol⁻¹): C 28.24, H 3.56, N 16.47; found C 28.48, H 3.29, N 16.63. Dec. point: 183 °C. Sensitivities (BAM): impact >40 J; friction >360 N; (grain size 100–500 µm).

Bis(chlorocarbonylethyl) dinitroxamide (5): Thionyl chloride (5.0 mL, 68.9 mmol) was placed in a dry flask equipped with a bubble counter. Bis(carboxyethyl) dinitroxamide (4, 1.24 g, 3.85 mmol) was slowly added. After the gas evolution stopped, the reaction mixture was refluxed at 70 °C for 4 h. Excess thionyl chloride was removed from the clear yellow solution under reduced pressure, and bis(chlorocarbonylethyl) dinitroxamide (5, 1.38 g) was obtained as a yellow solid in quantitative yield.

^1H NMR (CDCl_3): δ = 4.5 (br, 4H, NCH_2), 3.36 (t, 4H, $^3J^{1\text{H}, 1\text{H}} = 7.1$ Hz, CH_2). ^{13}C NMR (CDCl_3): δ = 171.1 (COOH), 158.1 (CONH₂), 43.1 (CH₂), 41.1 (CH₂). ^{14}N NMR (CDCl_3): δ = -47 (NO₂). Raman (800 mW): 2981 (62), 2932 (46), 1789 (25), 1739 (100), 1715 (28), 1596 (12), 1435 (8), 1410 (26), 1374 (11), 1359 (7), 1259 (53), 1232 (4), 1203 (5), 1093 (10), 1049 (14), 956 (18), 902 (8), 849 (53), 796 (9), 763 (13), 747 (13), 729 (20), 702 (14), 612 (6), 582 (7), 509 (10), 487 (10), 464 (90), 429 (13), 363 (18), 348 (3), 237 (9) cm^{-1} . IR: 3025 (w), 2933 (w), 2832 (w), 1780 (s), 1735 (m), 1707 (m), 1568 (s), 1437 (w), 1407 (m), 1354 (w), 1295 (s), 1248 (vs), 1204 (s), 1094 (s), 1047 (s), 973 (s), 950 (s), 903 (w), 785 (s), 760 (m), 729 (m), 698 (s), 611 (m), 580 (s), 509 (w), 483 (w), 458 (m), 418 (m) cm^{-1} . $\text{C}_8\text{H}_8\text{N}_4\text{O}_{10}\text{Cl}_2$ (359.08 g mol⁻¹): C 26.76, H 2.25, N 15.60; found C 26.61, H 2.35, N 15.42. T_{melt} : 65 °C, Dec. point: 157 °C.

Bis(carboxyethyl) dinitroxamide bis(2,2,2-trinitroethyl)ester (6): Bis(chlorocarbonylethyl) dinitroxamide 5 (1.38 g, 3.85 mmol) was dissolved in CHCl_3 (25 mL) at room temperature and 2,2,2-trinitroethanol 6 (1.74 g, 9.61 mmol) was added slowly. To the reaction mixture catalytic amounts of AlCl_3 were added. The pale yellow solution was refluxed for 2 h, using a bubble counter indicating the formation of hydrogen chloride gas. Any solids were filtered off and the remaining filtrate was reduced under reduced pressure. Bis(carboxyethyl) dinitroxamide bis(2,2,2-trinitroethyl)ester (6) was obtained as colorless solid (1.16 g, 46.2 %).

^1H NMR ($[\text{D}_6]\text{acetone}$): δ = 5.87 (s, 4H, CH_2O), 4.6 (br, 4H, NCH_2), 3.06 (t, 4H, $^3J^{1\text{H}, 1\text{H}} = 7.0$ Hz, CH_2). ^{13}C NMR ($[\text{D}_6]\text{acetone}$): δ = 168.8 (COOH), 159.0 (CONH₂), 124 (br, $\text{C}(\text{NO}_2)_3$), 61.6 (CH₂O), 42.0 (CH₂), 31.0 (CH₂). ^{14}N NMR ($[\text{D}_6]\text{acetone}$): δ = -46 (NNO₂), -33 (C(NO₂)₃). Raman (800 mW): 3036 (7), 2986 (19), 2960 (69), 1775 (18), 1741 (47), 1720 (13), 1622 (16), 1610 (10), 1600 (30), 1440 (21), 1425 (13), 1403 (5), 1384 (22), 1357 (35), 1308 (57), 1261 (39), 1245 (6), 1212 (7), 1093 (5), 1074 (15), 1057 (5), 1030 (6), 1003 (11), 952 (25), 942 (3), 919 (8), 884 (10), 857 (100), 829 (41), 803 (10), 784 (11), 758 (2), 749 (9). 719 (7), 649 (11), 619 (7), 563 (8), 533 (12), 499 (23), 406 (44), 371 (66), 342 (6), 313 (19), 284 (13), 265 (8), 243 (5), 228 (12) cm^{-1} . IR: 3011 (w), 2963 (w), 2898 (w), 1772 (m), 1739 (w), 1718 (m), 1578 (vs), 1401 (m), 1401 (m), 1296 (s), 1258 (s), 1213 (m), 1151 (vs), 1089 (s), 1030 (w), 1001 (m), 976 (m), 951 (w), 856 (m), 828 (m), 798 (s), 781 (s), 742 (m), 719 (m), 698 (w), 649 (w), 585 (m),

557 (w), 531 (m), 505 (w) cm^{-1} . $\text{C}_{12}\text{H}_{12}\text{N}_{10}\text{O}_{22}$ (648.28 g mol $^{-1}$): C 22.23, H 1.87, N 21.61; found C 21.93, H 2.02, N 20.92. T_{melt} : 118 °C, Dec. point: 159 °C. Sensitivities (BAM): impact 6 J; friction > 360 N; (grain size 100–500 μm).

Bis(carboxymethyl) oxamide (8): This compound was synthesized according to literature.¹³

^1H NMR ($[\text{D}_6]\text{DMSO}$): δ = 12.5 (br, 2H, COOH), 8.91 (t, 2H, $^3J(^1\text{H}, ^1\text{H})$ = 6.2 Hz, NH), 3.81 (d, 4H, $^3J(^1\text{H}, ^1\text{H})$ = 6.2 Hz, CH_2). ^{13}C NMR ($[\text{D}_6]\text{DMSO}$): δ = 170.3 (COOH), 159.9 (CONH₂), 41.0 (CH_2).

Bis(carboxymethyl) dinitroxamide (9): Bis(carboxymethyl) oxamide (8, 2.0 g, 9.8 mmol) was added in small portions to a mixture of fuming sulfuric acid (60 %, 12 mL), concentrated sulfuric acid (96 %, 4 mL) and nitric acid (100 %, 12 mL) under constant cooling with an ice bath. The reaction mixture was stirred at 50 °C for 5 h and afterwards poured onto 150 mL of ice. The aqueous solution was extracted with ethyl acetate (3 × 100 mL), the combined organic phases were washed with water (100 mL) and brine (100 mL), and finally dried over magnesium sulfate. The organic solvent was removed under reduced pressure, and bis(carboxymethyl) dinitroxamide 9 was obtained as colorless solid (2.5 g, 85 %).

^1H NMR ($[\text{D}_6]\text{acetone}$): δ = 12.1 (br, 2H, COOH), 5.10 (s, 4H, CH_2). ^{13}C NMR ($[\text{D}_6]\text{acetone}$): δ = 166.6 (COOH), 158.9 (CONH₂), 46.6 (CH_2). ^{14}N NMR ($[\text{D}_6]\text{acetone}$): δ = -46 (NO₂). Raman (800 mW): 3012 (26), 2961 (99), 1745 (100), 1400 (19), 1353 (28), 1289 (16), 1265 (32), 907 (48), 774 (19), 761 (7), 748 (10), 638 (12), 506 (34), 491 (7), 423 (14), 362 (11), 263 (15) cm^{-1} . IR: 3002 (w), 1711 (s), 1593 (s), 1435 (w), 1399 (w), 1287 (m), 1226 (vs), 1114 (m), 1080 (s), 953 (m), 910 (s), 828 (w), 763 (m), 743 (m), 675 (w), 641 (w), 591 (vs), 489 (w) cm^{-1} . $\text{C}_6\text{H}_6\text{N}_4\text{O}_{10}$ (294.13 g mol $^{-1}$): C 24.50, H 2.06, N 19.05; found C 24.68, H 2.17, N 18.85. Dec. point: 144 °C. Sensitivities (BAM): impact 10 J; friction > 360 N; (grain size 100–500 μm).

Bis(hydroxyethyl) oxamide (12): This compound was synthesized according to literature.¹⁴

^1H NMR ($[\text{D}_6]\text{DMSO}$): δ = 8.56 (t, 2H, $^3J(^1\text{H}, ^1\text{H})$ = 5.9 Hz, NH), 4.73 (t, 2H, $^3J(^1\text{H}, ^1\text{H})$ = 5.6 Hz, OH), 3.47–3.42 (m, 4H, CH_2), 3.23–3.18 (m, 4H, CH_2). ^{13}C NMR ($[\text{D}_6]\text{DMSO}$): δ = 160.0 (CONH), 59.2 (CH_2O), 41.7 (CH_2).

Bis(carbamoylethyl) oxamide (13): The alcohol precursor bis(hydroxyethyl) oxamide (12, 1.88 g, 10.7 mmol) was added slowly to a ice-cooled solution of chlorosulfonyl isocyanate (CSI, 2.17 g, 25.0 mmol) in dry acetonitrile (30 mL). The ice bath was removed after the complete addition and stirring at room temperature was continued for one hour. The solution was cooled again with an ice bath and cold water (20 mL) was added slowly. After 10 minutes, the

organic solvent was removed under reduced pressure and the precipitated solid was collected by filtration and washed with cold water to obtain the pure bis(carbamoylethyl) oxamide (**13**) (2.77 g, 99 %).

¹H NMR ([D₆]DMSO): δ = 8.73 (t, 2H, ³J¹H, ¹H) = 6.0 Hz, NH), 6.5 (br, 4H, CONH₂) 3.99 (t, 4H, ³J¹H, ¹H) = 5.8 Hz, CH₂OH), 3.36–3.32 (m, 4H, CH₂). ¹³C NMR ([D₆]DMSO): δ = 160.0 (CONH), 156.5 (OCONH₂), 61.4 (CH₂O), 38.7 (CH₂). Raman (800 mW): 3314 (24), 3200 (13) 3018 (31), 2988 (14), 2972 (95), 2949 (2), 2930 (71), 2864 (8), 1684 (81), 1634 (15), 1554 (28), 1443 (40), 1426 (4), 1307 (35), 1279 (100), 1247 (33), 1139 (4), 1131 (34), 1103 (51), 971 (60), 924 (13), 898 (14), 828 (31), 676 (11), 523 (9), 478 (11), 369 (13), 304 (34), 264 (10) cm⁻¹. IR: 3415 (w), 3305 (m), 3273 (w), 3217 (w), 1697 (vs), 1659 (vs), 1619 (m), 1527 (s), 1419 (vs), 1365 (w), 1344 (m), 1292 (w), 1251 (m), 1225 (m), 1130 (s), 1082 (s), 1037 (m), 966 (w), 749 (m), 596 (s), 556 (m), 534 (s) cm⁻¹. C₈H₁₄N₄O₆ (262.22 g mol⁻¹): C 36.64, H 5.38, N 21.37; found C 36.54, H 5.29, N 21.09. T_{melt}: 235 °C.

Bis(nitrocarbamoylethyl) oxamide (14): Bis(carbamoylethyl) oxamide **13** (1.0 g, 3.8 mmol) was slowly added to concentrated nitric acid (100 %, 10 mL) with cooling in an ice bath. The nitration mixture was stirred for 1.5 h with ice cooling, and subsequently poured on ice (150 mL). The precipitated product was filtered off and washed with cold water. Bis(nitrocarbamoylethyl) oxamide **14** was obtained as a colorless solid (1.2 g, 93 %).

¹H NMR ([D₆]acetone): δ = 13.4 (br, 2H, NHNO₂), 8.3 (br, 2H, NH), 4.40–4.37 (m, 4H, CH₂O) 3.65–3.61 (m, 4H, CH₂). ¹³C NMR ([D₆]acetone): δ = 161.0 (CONH), 149.3 (OCONHNO₂), 65.7 (CH₂O), 39.1 (CH₂). ¹⁴N NMR ([D₆]acetone): δ = -45 (NHNO₂). Raman (800 mW): 3015 (5), 3001 (15), 2972 (100), 2938 (5), 2890 (9), 1773 (49), 1694 (21), 1565 (15), 1557 (3), 1454 (12), 1432 (19), 1333 (59), 1306 (29), 1270 (15), 1231 (13), 1119 (10), 1102 (25), 1032 (39), 104 (19), 794 (11), 462 (20), 374 (10), 329 (9) cm⁻¹. IR: 3646 (m), 3361 (m), 3112 (w), 2968 (w), 2790 (w), 1770 (s), 1662 (s), 1618 (s), 1519 (m), 1451 (m), 1430 (m), 1363 (w), 1330 (s), 1283 (w), 1253 (w), 1177 (vs), 1053 (w), 996 (m), 908 (w), 868 (w), 810 (w), 723 (s), 565 (m) cm⁻¹. C₈H₁₂N₆O₁₀ (352.22 g mol⁻¹): C 27.28, H 3.43, N 23.86; found C 27.77, H 3.60, N 22.91. T_{melt}: 108 °C, Dec. point: 178 °C. Sensitivities (BAM): impact > 40 J; friction > 360 N; (grain size 100–500 µm).

6.6 References

- [1] T. M. Klapötke, *Chemistry of High-Energy Materials*, 4th ed., De Gruyter, Berlin, **2015**.
- [2] <https://echa.europa.eu/information-on-chemicals/evaluation/community-rolling-action-plan/corap-table/-/dislist/details/0b0236e1807e9ab1>, **accessed 04.2018**.
- [3] C. M. Steinmaus, *Curr. Environ. Health Rep.* **2016**, *3*, 136–143.
- [4] H. F. R. Schoeyer, A. J. Schnorhk, P. A. O. G. Korting, P. J. van Lit, J. M. Mul, G. M. H. J. L. Gadiot, J. J. Meulenbrugge, *J. Propul. Power* **1995**, *11*, 856869.
- [5] J. C. Bottaro, P. E. Penwell, R. J. Schmitt, *J. Am. Chem. Soc.* **1997**, *119*, 9405–9410.
- [6] Q. J. Axthammer, T. M. Klapötke, B. Krumm, R. Moll, S. F. Rest, *Z. Anorg Allg. Chem.* **2014**, *640*, 76–83.
- [7] Q. J. Axthammer, B. Krumm, T. M. Klapötke, *J. Org. Chem.* **2015**, *80*, 6329–6335.
- [8] T. M. Klapötke, B. Krumm, R. Scharf, *Eur. J. Inorg. Chem.* **2016**, 3086–3093.
- [9] T. M. Klapötke, B. Krumm, R. Moll, S. F. Rest, *Z. Anorg. Allg. Chem.* **2011**, *637*, 2103–2110.
- [10] T. M. Klapötke, B. Krumm, R. Scharf, *Z. Anorg. Allg. Chem.* **2016**, *642*, 887–895.
- [11] T. M. Klapötke, B. Krumm, R. Scharf, *Chem. Asian J.* **2016**, *11*, 3134–3144.
- [12] Q. J. Axthammer, C. Evangelisti, T. M. Klapötke, B. Krumm, R. Scharf, C. C. Unger, *Dalton Trans.* **2016**, *45*, 18909–18920.
- [13] S. Coe, J. J. Kane, T. L. Nguyen, L. M. Toledo, E. Wninger, F. W. Fowler, J. W. Lauher, *J. Am. Chem. Soc.* **1997**, *119*, 86–93.
- [14] M. L. Testa, E. Zaballos, R. J. Zaragozá, *Tetrahedron* **2012**, *68*, 9583–9591.
- [15] M. J. Frisch, G. W. Trucks, H. B. Schlegel, G. E. Scuseria, M. A. Robb, J. R. Cheeseman, G. Scalmani, V. Barone, B. Mennucci, G. A. Petersson, H. Nakatsuji, M. Caricato, X. Li, H. P. Hratchian, A. F. Izmaylov, J. Bloino, G. Zheng, J. L. Sonnenberg, M. Hada, M. Ehara, K. Toyota, R. Fukuda, J. Hasegawa, M. Ishida, T. Nakajima, Y. Honda, O. Kitao, H. Nakai, T. Vreven, J. A. Montgomery Jr., J. E. Peralta, F. Ogliaro, M. J. Bearpark, J. Heyd, E. N. Brothers, K. N. Kudin, V. N. Staroverov, R. Kobayashi, J. Normand, K. Raghavachari, A. P. Rendell, J. C. Burant, S. S. Iyengar, J. Tomasi, M. Cossi, N. Rega, N. J. Millam, M. Klene, J. E. Knox, J. B. Cross, V. Bakken, C. Adamo, J. Jaramillo, R. Gomperts, R. E. Stratmann, O. Yazyev, A. J. Austin, R. Cammi, C. Pomelli, J. W. Ochterski, R. L. Martin, K. Morokuma, V. G. Zakrzewski, G. A. Voth, P. Salvador, J. J. Dannenberg, S. Dapprich, A. D. Daniels, Ö. Farkas, J. B. Foresman, J. V. Ortiz, J. Ciosowski, D. J. Fox, Gaussian, Inc., Wallingford, **2009**.
- [16] M. Suceska, v. 6.03 ed., Zagreb, **2015**.
- [17] 1.171.35.11 ed., Oxford Diffraction Ltd., Abingdon, Oxford (U.K.), **2011**.
- [18] 1.171.35.11 ed., Oxford Diffraction Ltd., Abingdon, Oxford (U.K.), **2011**.
- [19] A. Altomare, M. C. Burla, M. Camalli, G. L. Cascarano, C. Giacovazzo, A. Gualdi, A. G. G. Moliterni, G. Polidori, R. Spagna, *J. Appl. Crystallogr.* **1999**, *32*, 155–119.
- [20] G. M. Sheldrick, *Programs for Crystal Structure Determination*, University of Göttingen, Germany, **1997**.
- [21] G. M. Sheldrick, *Acta Crystallogr.* **2008**, *64 A*, 112–122.

- [22] L. Farrugia, *J. Appl. Crystallogr.* **1999**, *32*, 837–838.
- [23] A. L. Spek, *Acta Crystallogr.* **2009**, *65 D*, 148–155.
- [24] R. D. Dennington, T. A. Keith, J. M. Millam, *GaussView*, v. 5.08, Semicem, Inc., Wallingford, **2009**.
- [25] J. A. Montgomery, M. J. Frisch, J. W. Ochterski, G. A. Petersson, *J. Chem. Phys.* **2000**, *112*, 6532–6542.
- [26] M. Suceska, *Propellants Explos. Pyrotech.* **1991**, *16*, 197–202.

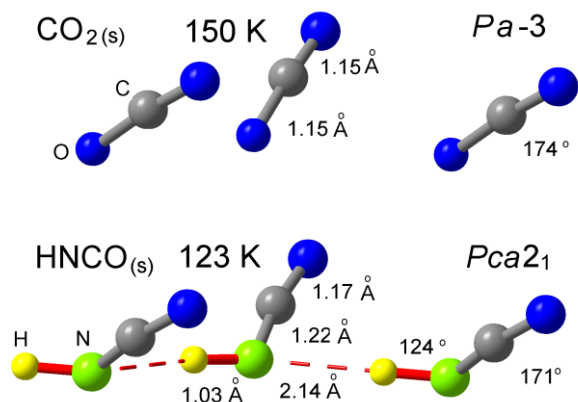
7 Molecular Structure of Isocyanic Acid

MOLECULAR STRUCTURE OF ISOCYANIC ACID HNCO, THE IMIDE OF CARBON DIOXIDE

Jürgen Evers, Burkhard Krumm, Quirin J. Axthammer, Jörn Martens, Peter Blaha, Franz Xaver Steemann, Thomas Reith, Peter Mayer, and Thomas M. Klapötke

as published in

The Journal of Physical Chemistry A **2018**, *122*, 3287–3292



7.1 Abstract

Isocyanic acid HNCO, the imide of carbon dioxide, was prepared by reaction of stearic acid and potassium cyanate (KOCN) at 60 °C in a sealed, thoroughly dried reactor. Interestingly, its crystal structure, solved by X-ray single crystal diffraction at 123(2) K, shows a group–subgroup relation for the NCO⁻ anion to carbon dioxide: (CO₂: cP12, Pa–3, $a = 5.624(2)$ Å, 150 K, C–O 1.151(2) Å; HNCO: oP16, Pca21, $a = 5.6176(9)$, $b = 5.6236(8)$, $c = 5.6231(7)$ Å, 123(2) K). Precise positions of H, N, C and O were determined by DFT calculations with WIEN2k leading to interatomic distances C–O 1.17, C–N 1.22, N–H 1.03, –N–H...N 2.14 Å and the interatomic angle N–C–O 171°.

7.2 Introduction

In 1919 Irving Langmuir pointed out the extraordinary agreement between the physical properties of carbon dioxide (CO₂) and dinitrogen monoxide (N₂O), including e.g. critical temperatures and pressures, densities of the liquids, viscosities and refractive indexes and introduced the principle of isosterism.¹ If compounds with the same number of atoms have also the same total number of electrons, the electrons may arrange themselves in the same manner.¹ In this case the compounds or groups of atoms are said to be isosteric.¹ For CO₂ and N₂O there are three atoms and 22 total or 16 valence electrons (e). Langmuir's concept is extraordinary useful in predicting properties of isosteric molecular species. About 26 isosteric species to CO₂, either neutral or charged, are known today.¹⁻⁷

Both, the three-atomic heterocumulenic cyanate and azide anions possess 22 total e, corresponding to the weak acids isocyanic acid HNCO⁸ and hydrazoic acid HN₃,⁹ respectively. In 1919 Langmuir gave a first indication to their isosterism.¹ Isocyanic acid was first prepared by Liebig and Wöhler¹⁰ in 1830. However, information on the molecular geometry on HNCO was obtained about 100 years later in the decade 1940–1950 by electron diffraction,¹¹ by microwave¹² and by infrared spectroscopy,^{13,14} all performed in the gas phase. As a result from those studies, the C–O, N–C and N–H distances were determined to 1.17, 1.21 and 0.99 Å, respectively, with the hydrogen atom being connected to nitrogen with an H–N–C angle of 128°. More recent studies regarding synthesis and properties of HNCO were reported in our laboratory.¹⁵

In 1955 von Dohlen and Carpenter performed the first X-ray single crystal investigation. In their work, HNCO crystallized at –125 °C in an orthorhombic lattice, probably with space group *Pnma*.¹⁶ The resulting distances C–O and N–C (1.18(2) Å, 2x) are in rough agreement

with the earlier investigations in the gas phase. However, the quality of the crystal was not sufficient to localize the hydrogen atoms by difference Fourier analysis.

Apart from the interests of theoretical and synthetic chemistry for isocyanic acid, a special importance arises now due to its role in urban air pollution and possible toxicity. Cars with gasoline and diesel engines are known to emit HNCO, especially if selective catalytic reduction systems are used to reduce the emission of nitrogen oxides NO_x . In this case an aqueous solution of urea $(\text{NH}_2)_2\text{CO}$ is added to the exhausts of the engine. In the catalytic reduction system, urea is thermally decomposed into ammonia (NH_3) and isocyanic acid (HNCO). The last compound is rapidly decomposed with water on the catalyst surface into ammonia and carbon dioxide. However, there remains emission of HNCO in the range between 30 and 50 mg HNCO/kg fuel,¹⁷ which is found in urban air pollution and could negatively affect human health.

Of special interest is the comparison of the crystal structures of the isosteric acids HNCO and HN_3 . The structure of HN_3 was recently solved by an X-ray single crystal investigation at $100(2)$ K¹⁸ and shows a very interesting two-dimensional net, formed by bifurcated hydrogen bonds, in which tetramers $(\text{HN}_3)_4$ were found in a nearly plane net of 4-, 8- and 16-membered rings. Now, a structural investigation of HNCO in the space group $Pca2_1$ is reported, including refinement of the positional parameters by DFT calculations with the program WIEN2k.¹⁹

7.3 Experimental Section

7.3.1 General Information

Isocyanic acid HNCO was prepared from potassium cyanate KOCN and stearic acid as previously reported.¹⁵ Both starting materials were intensively ground and filled into a Duran reactor, having attached at one side a thin-walled X-ray capillary. The reactor with the starting materials was dried on a high vacuum line while cooling with liquid nitrogen traps.

7.3.2 X-ray Crystallography

After several days of drying, the reactor was sealed from the vacuum line and then slowly heated to 60 °C. Stearic acid melts near this temperature, and then, the formation of gaseous HNCO starts. Isocyanic acid condenses at the capillary, which is cooled with liquid nitrogen and then sealed. From each heating experiment three capillaries filled with HNCO were obtained, and were stored in liquid nitrogen.

Single crystals of HNCO for the structure determination were grown *in situ* in the capillary adjusted to the Oxford Xcalibur diffractometer. Several cooling and heating cycles are required to obtain a single crystal in order to check the diffraction pattern. The structure was determined at 123(2) K. The hkl ranges of the measured reflections were the following: h from -8 to 7, k from -8 to 8, and l from -8 to 8. Within a 24 h cooling and heating procedure from 100(5) to 185(5) K, searching for the orthorhombic phase of von Dohlen and Carpenter¹⁶ was negative. Structural calculations on HNCO ($Pca2_1$) were performed with SHELXL-2014.²⁰ The investigated crystal was disordered and contained two individuals with 55% and 45%. The individuals were rotated against each other with oxygen and nitrogen atoms nearly lying above each other. Therefore, hydrogen atoms could not be detected from a difference Fourier analysis. In addition, with the position derived by SHELXL-2014, unrealistic short C–O and unrealistic long C–N distances had been obtained.

7.3.3 Density Functional Theory (DFT) Calculations

The theoretical calculations are based on density functional theory (DFT) and were performed with the augmented plane wave + local orbital method as implemented in the WIEN2k¹⁹ program. We utilized the generalized gradient approximation of Perdew et al.²¹ and treated the weak but important van der Waals interactions using DFT-D3.²² The atomic sphere radii R_{MT} were chosen as 0.545 Å for C, 0.598 Å for N and O, and 0.333 Å for H. The plane wave cutoff parameter for the wave functions, R^*K_{MAX} , was set to 4 and the charge density and potential was expanded in plane waves up to $G_{MAX} = 20$. For the calculations with $Pca2_1$, a 4x4x4 mesh was used, and for that with $Pnma$, there is a 2x4x8 mesh. We used experimental lattice parameters in all cases, but refined the positional parameters of all atoms until the forces were well below 1 mRy/bohr. Since the positions of the H atoms are unknown in many cases, we started from several educated guesses and refined to the next local minimum. Clearly, the structure with H attached to N and bridging to another N atom has the lowest total energy. The calculations were performed at the mpp2 cluster of the Leibniz–Rechenzentrum, Garching (Bavarian Academy of Science), and the Vienna Scientific Cluster (VSC3).

7.4 Results and Discussion

7.4.1 X-Ray Diffraction Results

The results of a single crystal X-ray structure investigation are summarized in Table 7.1.

Table 7.1: Crystallographic data of solid HNCO, determined at 123(2) K by X-ray single crystal investigation.^a

crystal system	orthorhombic
space group	<i>Pca2</i> ₁
<i>a</i> (Å)	5.6176(9)
<i>b</i> (Å)	5.6236(8)
<i>c</i> (Å)	5.6231(7)
<i>T</i> (K)	123(2)
<i>V</i> (Å ³)	177.64(4)
<i>Z</i>	4
4 H, 4 N, 4 C, 4 O	4 <i>a</i>
ρ_{calc} (g·cm ⁻³)	1.609
reflns measured	1390
reflns unique	339
<i>R</i> (σ)	0.0260
R1	0.0352
wR2	0.0887
GOF	1.175
highest residual electron density (e/ Å ⁻³)	+0.10/ 0.17

^aStructural analysis with the SHELXL-2014²⁰ program showed that the investigated crystal consists of two crystals (1, 55 %; 2, 45 %), stacked above each other. Therefore, hydrogen positions could not be precisely determined by a difference Fourier analysis.

HNCO crystallizes in the orthorhombic acentric space group *Pca2*₁ with 4 formula units in the unit cell. The positional parameters determined from the X-ray diffraction structure analysis by the program SHELXL-2014²⁰ lead to both very short C–O (0.99(1), 1.04(1) Å) and very long C–N (1.30(1) and 1.36(1) Å) distances, since in space group *Pca2*₁ it is difficult to grow polarity pure single crystals.

7.4.2 DFT Results

Therefore, it was decided to perform DFT calculations with the program WIEN2k.¹⁹ In Table 7.2 the calculated positional parameters of solid isocyanic acid HNCO in the polar space group *Pca*2₁ are summarized.

Table 7.2: Positional parameters *x*, *y*, *z* of solid isocyanic acid HNCO in space group *Pca*2₁ derived by DFT calculations with the program WIEN2k.^{19, a}

atom	<i>x</i>	<i>y</i>	<i>z</i>
C	0.0273	0.2699	0.0000
O	0.3329	0.3770	-0.6121
N	0.8733	0.1437	-0.9142
H	0.1755	0.8520	-0.2386

^aThe C-, N- and O-atoms have been all located in Wyckoff position 4a. Starting parameters were those obtained by the program SHELXL-2014.²⁰ These atomic positions were then refined with WIEN2k.¹⁹ The positions of the H-atoms were derived *ab initio*. Details of the calculations are given in the Experimental Section.

7.4.3 Group–Subgroup Relations

Solid carbon dioxide CO₂²³ crystallizes at ambient pressure in the cubic space group *Pa* with four molecules in the unit cell. The lattice parameter is *a* = 5.624(2) Å²³ at 150 K leading to a unit-cell volume *V* = 177.88(20) Å³. Solid isocyanic acid HNCO (Table 7.1) crystallizes in the orthorhombic space group *Pca*2₁ with pseudocubic lattice parameters *a* = 5.6176(9), *b* = 5.6236(8), *c* = 5.6231(7) Å at 123 K. Hence, HNCO easily suggests a structural comparison of CO₂ and HNCO in a groupsubgroup relation^{24–32} (Figure 7.1).³³ Coming from cubic CO₂ (*P*2₁/*a*, No. 205) the first step leads to a *translationengleich*^{24–31} (t) step of index 3 (t3) to the maximal nonisomorphic subgroup *Pcab* (*P* 2₁/*c* 2₁/*a* 2₁/*b*, No. 61). The position 24*d* in No. 205 is here reduced to 8*c* in No. 61 while the axes have to be changed into **c**, **b**, **–a** and the coordinates into *z*, *y*, *–x*. Further symmetry reduction is achieved in a *translationengleich* step of index 2 (t2) and an origin change with (0, *–1/4*, 0) to the maximal nonisomorphic subgroup *Pca*2₁. Here, position 8*c* in No. 61 is changed into twice 4*a* in No. 29 upon changing the coordinates into *x*, *y*+1/4, *z*. In Figure 7.1 the group–subgroup relation is shown.

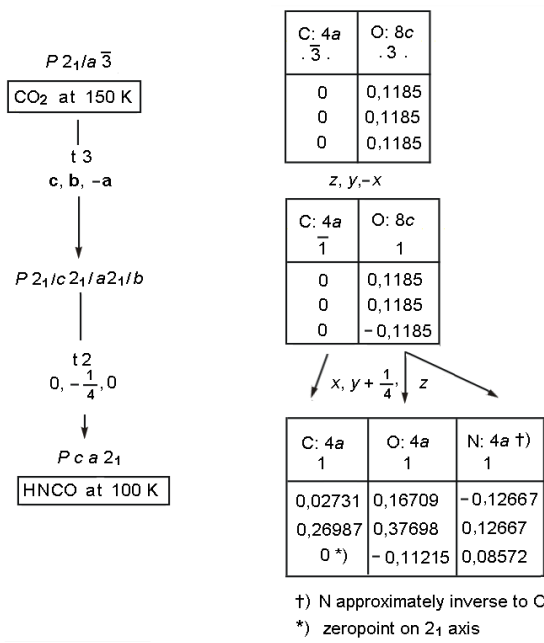


Figure 7.1: Group–subgroup relation^{24–31} showing the symmetry reduction for CO₂ in the centrosymmetric cubic space group $P2_1/a\bar{3}$ (No. 205) to $Pcab$ ($P2_1/c\ 2_1/a\ 2_1/b$, No. 61) and then for HNCO to the acentric polar orthorhombic space group $Pca2_1$ (No. 29).

In CO₂ the coordinates of the C atoms remain in position 4a (0,0,0), whereas the oxygen atoms O are shifted from (0.1185, 0.1185, 0.1185) in $Pa\bar{3}$ to (0.1185, 0.1185, -0.1185) in $P2_1/c\ 2_1/a\ 2_1/b$. For CO₂ in $Pca2_1$ the C atoms have the coordinates (0, 1/4, 0), the O atom (0.1185, 0.3685, -0.1185) and the Oⁱ atom (-0.1185, 0.1315, 0.1185).

The symmetry reduction of $Pa\bar{3}$ via $Pcab$ to $Pca2_1$ (Figure 7.1) leads to two polar structures. The polar structure 1 is obtained with the z parameters (Table 7.2, $z = -0.6121$ and $z = -0.9142$) for the O and the N atom, respectively. In the polar structure 2 the z parameters are inverted to $z = 0.6121$ and $z = 0.9142$ for O and N, respectively. The polar structure 2 is obtained from polar structure 1 by reflection with a mirror.

During the synthesis of HNCO with stearic acid and potassium cyanate (KOCN) and cooling to 100 K, the obtained sample will contain approximately the same number of crystals with polarity 1 and with polarity 2. This could be a reason that the single crystal of HNCO used for the X-ray diffraction investigation was obtained only with low quality. In principle, the absolute configuration of a single crystal in space group $Pca2_1$ with good quality, investigated by X-ray diffraction, could be determined by anomalous dispersion.³² However, for elements with low scattering power such as H, C, N and O, the contribution is low, and therefore, it is not an easy procedure to distinguish between them between such crystals.

In Figure 7.2, a *Diamond view*³³ of the polar HNCO structure is shown with polarity 1 with negative positional parameters z for the N, O and H atoms (Table 7.1).

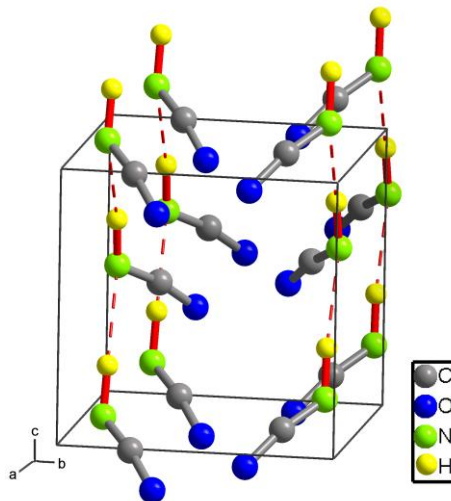


Figure 7.2: *Diamond view*³³ along [100] for the polar structure of HNCO in $Pca2_1$ is shown with polarity 1 (negative positional parameters z for the O, N and H atoms, Table 7.1. The red N–H bonds have the direction “up”. In the structure with polarity 2 (positive positional parameters z for such atoms), the red N–H bonds have the direction “down”. Isotropic displacement spheres of 50 % are shown with $U = 0.0300 \text{ \AA}^2$ for C, O, N and $U = 0.0200 \text{ \AA}^2$ for H. The red N–H distances are 1.026 \AA . The fragmented red N–H···N hydrogen bonds are 2.14 \AA . The chains of N–H···N contacts are zigzag shaped and run along [001]. The carbon atoms with $z = 0$ have the same coordinates.

In this case the N–H bonds with 1.026 \AA in slightly zigzag chains have the direction “up” parallel to c . In the HNCO structure with polarity 2 with positive positional parameters z for the O, N and H atoms, the N–H bonds have the direction “down”. In both polarities the z parameter of the C atoms is fixed to $z = 0$. Interestingly, in HNCO short hydrogen distances of the type N–H···N exist with 2.14 \AA but none exist for N–H···O, although oxygen is more electronegative than nitrogen. The N–H bonds bonds create hydrogen bonds as one-dimensional zigzag shaped chains along [001].

7.4.4 Crystal Chemical Properties

Interatomic distances (\AA) and angles (deg) for HNCO of previous investigations^{10,11,14} and those obtained by this investigation with DFT calculations (WIEN2k¹⁹) are summarized in Table 7.3.

Table 7.3: Interatomic distances (Å) and angles (deg) determined by previous investigations in HNCO by electron diffraction¹¹, microwave and infrared spectroscopy¹² in the gas phase and X-ray diffraction¹⁶ in the solid state and those obtained by DFT calculations with WIEN2k.¹⁹

Experimental Technique	H–N	N–C	C–O	H–N–C	C–N–O	N–H···N	N–H···N / H–N···H
Electron diffraction ¹¹ (gas phase)	1.01(est.)*	1.19	1.19	125 (est.)			
microwave, infra-red ¹² (gas phase)	0.99(1)	1.21(1)	1.17(1)	128(1)			
X-ray diffraction ¹⁶ (solid state)	–	1.18(2)	1.18(2)	–			
this study, DFT, WIEN2k ¹⁹	1.03	1.22	1.17	124	171	2.14	164 / 133

* estimated

The best agreement in Table 7.3 between the previous results and those obtained by DFT calculations is achieved by Jones et al.¹² with microwave and infrared investigations in the gas phase. In the previous X-ray diffraction investigation,¹⁶ the hydrogen atoms could not be detected due to the low crystal quality. Regarding the interatomic distances N–C and C–O, identical values of 1.18(2) Å were obtained for both. However, in this study the C–O distance (1.17 Å) is smaller than the N–C distance (1.22 Å), as also observed by microwave and infrared spectroscopic investigations in the gas phase, 1.17(1) and 1.21(1) Å, respectively, by Jones et al.¹²

In this investigation no evidence of an orthorhombic phase was found, which was observed by von Dohlen and Carpenter.¹⁶ In addition to the structural investigation at 123(2) K (Table 7.1), a search within 24 h for an orthorhombic phase was performed by measurements at 100(5), 120(5), 140(5), 160(5), 165(5), 170(5), 175(5), 180(5), and 185(5) K. In all cases only the slightly varying orthorhombic lattice parameters in the range 5.62– 5.68 Å were obtained. Therefore, it must be concluded that the phase of von Dohlen and Carpenter¹⁶ is metastable, if obtained by depolymerization of cyanuric acid and not by protonation of cyanate by stearic acid. Also, from WIEN2k¹⁹ calculations it is evident that the total energy of the HNCO phase of von Dohlen and Carpenter¹⁶ is a few kJ/mol higher than our HNCO phase related to CO₂. Interestingly, a refinement of von Dohlen's positional parameters¹⁶ by DFT calculations³⁴ with WIEN2k¹⁹ showed that in this phase N–H···O hydrogen bonds are present.

As already mentioned, the anions OCN/NCO[–] and N₃[–] are isosteric, but the crystal structures of HNCO and HN₃¹⁸ differ significantly. In HNCO only one short N–H···N hydrogen bond of 2.14 Å is observed connecting the HNCO molecules to one-dimensional zigzag chains along [001].

7 Molecular Structure of Isocyanic Acid

Hydrazoic acid contains 16 formula units in the unit cell, space group *C1c1*, and four crystallographic independent HN_3 molecules. Here, the $\text{N}-\text{H}\cdots\text{N}$ hydrogen bonds are bifurcated into shorter distances (Table 7.4, $\text{N}-\text{H}\cdots\text{N}_{\text{short}}$ 2.24(20) Å) and longer distances (Table 7.4, $\text{N}-\text{H}\cdots\text{N}_{\text{long}}$ 2.78(20) Å). With this connection a two-dimensional layer structure is created, with 4-, 8- and 16-membered rings formed by $(\text{HN}_3)_4$ tetramers. Displacement ellipsoids show their highest values perpendicular to the layers, indicating only weak van der Waals forces between them. In Table 7.4 the average distances and angles in solid HN_3 are summarized with labeling as $\text{H}-\text{N}_1-\text{N}_2-\text{N}_3$.¹⁸

Table 7.4: Average interatomic distances (Å) in HN_3 for $\text{H}-\text{N}_1$, N_1-N_2 , N_2-N_3 , $\text{N}-\text{H}\cdots\text{N}_{\text{short}}$, $\text{N}-\text{H}\cdots\text{N}_{\text{long}}$ and average angles (deg) $\text{H}-\text{N}_1-\text{N}_2$, $\text{N}_1-\text{N}_2-\text{N}_3$, as determined by X-ray single crystal investigation.¹⁸

$\text{H}-\text{N}_1$ (Å)	N_1-N_2 (Å)	N_2-N_3 (Å)	$\text{H}-\text{N}_1-\text{N}_2$ (deg)	$\text{N}_1-\text{N}_2-\text{N}_3$ (deg)	$\text{N}-\text{H}\cdots\text{N}_{\text{short}}$ (Å)	$\text{N}-\text{H}\cdots\text{N}_{\text{long}}$ (Å)
0.82(20)	1.233(4)	1.121(4)	109(4)	172.8(3)	2.24(20)	2.78(20)

Upon comparison of the H–N interatomic distances in HNCO and HN_3 according Tables 7.3 and 7.4, it is obvious that the N–C distance with 1.22 Å in HNCO is comparable to the N_1-N_2 distance with 1.233(4) Å in HN_3 . However, the C–O distance with 1.17 Å in HNCO is remarkably longer than the N_2-N_3 distance with 1.121(4) Å in HN_3 . The angles N–C–O with 171 ° in HNCO and $\text{N}_1-\text{N}_2-\text{N}_3$ with 172.8(3) ° in HN_3 deviate only by 2 °. The strongest deviation is found for N–H distances. In HNCO it was calculated by DFT to 1.03 Å, but in HN_3 , determined by X-ray diffraction, the averaged distance is 0.82(20) Å which is 0.21 Å smaller than in HNCO. The smaller value results from the fact that the hydrogen atom in HN_3 does not have a core electron.³⁵ Therefore, the determined N–H distance is too short by X-rays.³⁵ A N–H distance of approximately 1.03 Å, as calculated by WIEN2k¹⁹ in HNCO, can also be approximately assumed for HN_3 .

Although HNCO and HN_3 are isosteric acids, there are small, but significant differences for the melting and boiling points, as well as the acid constants $\text{p}K_{\text{a}}$, as displayed in Table 7.5.

Table 5. Melting/boiling points and acid constants $\text{p}K_{\text{a}}$ for HNCO and HN_3 .

	melting point (°C)	boiling point (°C)	acid constant $\text{p}K_{\text{a}}$
HNCO	–86.8, ⁸ –86 ³⁶	23.5 ⁸ , 23 ³⁶	3.9 ⁸ , 3.7 ³⁶
HN_3	~–80, ⁹ –80 ³⁶	35.7 ⁹ , 35.7 ³⁶	4.8 ⁹ , 4.6 ³⁶

The bonding in HNCO is to a small degree slightly weaker than in HN_3 . Therefore, the melting point for the first is approximately 6°C lower (Table 7.5). This tendency holds also for the boiling point of HNCO which is approximately 12°C lower than in HN_3 . The one-dimensional chains in HNCO (Figure 7.2) seem to be slightly weaker than the two-dimensional net in HN_3 with a layer structure formed by bifurcated hydrogen bonds.

These structural facts are also reflected in the acid–base properties of HNCO and HN_3 . The $\text{p}K_{\text{a}}$ acid constant for HNCO is nearly 1 unit of magnitude lower than that in HN_3 , indicating a weaker $\text{N}-\text{H}\cdots\text{N}$ bond and therefore slightly stronger acid properties for HNCO.

Although HNCO has slightly weaker hydrogen-bonding than HN_3 , the cell volume for one formula unit of HNCO at 1 bar (44.35 \AA^3 , $123(2)\text{ K}$) is approximately 11 % lower than that for HN_3 (49.68 \AA^3 , $100(2)\text{ K}$). In this case the sizes of molecules with different composition are compared to each other. However, one N-atom is also present in HNCO, and the sizes of the remaining two atoms C and O with covalent radii r for the $r_{\text{C}} = 0.77\text{ \AA}$ and $r_{\text{O}} = 0.66\text{ \AA}$ (with a sum of $0.77 + 0.66 = 1.43\text{ \AA}$)³⁷ can be approximately substituted by two N-atoms with $r_{\text{N}} = 0.70\text{ \AA}$ (with a sum of $0.70 + 0.70 = 1.40\text{ \AA}$).³⁷ Since the layers in HN_3 containing 4-, 8- and 16-membered rings create large voids, it can be expected that squeezing of HN_3 (with HN_3 structure) could probably lead to a transformation into a more densely packed polymorph with HNCO structure.

However, as our own experimental experience shows, filling a high pressure diamond cell with liquid HN_3 at ambient pressure in a cooling room at $T = -20^\circ\text{C}$ is not an easy experimental task. HN_3 is a strong poison, highly explosive, and has a high vapor pressure. The difference of the boiling temperatures of diethylether (Et_2O) and hydrazoic acid (HN_3) is about 1°C .³⁸ However, one could obtain isotypic structures for HNCO at 1 bar and at -86°C and for HN_3 squeezed in a diamond cell. Then, electrons may arrange themselves in the same manner, thus clearly fulfilling Langmuir's criterion for isosterism¹ also for these solids.

7.5 Conclusion

Isocyanic acid (space group $Pca2_1$), the imide of carbon dioxide, shows strong structural relations to CO_2 ($Pa\bar{3}$). The lattice parameters of orthorhombic HNCO (123 K) are pseudocubic ($Pca2_1$) and deviate only on the second digit from that of cubic CO_2 . In solid CO_2 isolated molecules are bound to each other by only weak van der Waals bonds in a molecular structure.

From a topological projection of the crystal structure of CO_2 on the crystal structure of HNCO without hydrogen atoms, it is shown that the C, N and O atoms are only slightly shifted. The

7 Molecular Structure of Isocyanic Acid

strongest shift is found for the carbon atoms with 0.15 Å, for the oxygen atoms O with 0.27, and for the Oⁱ and N atoms with –0.18 Å, respectively. In HNCO, short N–H···N hydrogen bonds (2.14 Å) connect the molecules to one-dimensional zigzag chains. Due to the polar space group *Pca2*₁, there are two structures for HNCO, e.g. one with the N–H bond showing upward in the chain, and the other one downward.

The comparison of the two isosteric acids shows that HNCO with chains of one-dimensional hydrogen bonds is slightly weaker bonded than HN₃ with bifurcated hydrogen bonds in plane layers, resulting in lower melting and boiling points for the first and also slightly stronger acid–base properties.

7.6 References

- [1] I. Langmuir, *J. Am. Chem. Soc.* **1919**, *41*, 1543–1559.
- [2] J. Goubeau, *Naturwissenschaften* **1948**, *35*, 246–250.
- [3] J. F. Z. Cordes, *Z. Naturforsch.* **1958**, *31*, 622–623.
- [4] P. Pyykkö, Y. Zhao, *J. Phys. Chem.* **1990**, *94*, 7753–7759.
- [5] F. Halet, J.-Y. Saillard, J. Bauer, *J. Less-Common Met.* **1990**, *158*, 239–250.
- [6] T. M. Klapötke, *Angew. Chem., Int. Ed. Engl.* **1994**, *33*, 1575–1576.
- [7] F. Jach, S. I. Brückner, A. Ovchinnikov, A. Isaeva, M. Bobnar, M. F. Groh, E. Brunner, P. Höhn, M. Ruck, *Angew. Chem., Int. Ed.* **2017**, *56*, 2919–2922.
- [8] N. N. Greenwood, A. Earnshaw, *Chemie der Elemente*, VCH Verlagsgesellschaft, **1988**, p 379.
- [9] N. N. Greenwood, A. Earnshaw, *Chemie der Elemente*, VCH Verlagsgesellschaft, **1988**, p 553.
- [10] J. Liebig, F. Wöhler, *Ann. Phys.* **1830**, *20*, 369–400.
- [11] E. E. Eyster, R. H. Gilette, L. O. Brockway, *J. Am. Chem. Soc.* **1940**, *62*, 3236–3240.
- [12] H. Jones, R. G. Shoolery, D. M. Yost, *J. Chem. Phys.* **1950**, *18*, 990–991.
- [13] G. Herzberg, C. Reid, *Discuss. Faraday Soc.* **1950**, *9*, 92–99.
- [14] R. Kewley, K. V. L. N. Sastry, M. Winnewisser, *J. Mol. Spectrosc.* **1963**, *10*, 418–441.
- [15] G. Fischer, J. Geith, T. M. Klapötke, B. Krumm, *Z. Naturforsch. B* **2002**, *57*, 19–24.
- [16] W. von Dohlen, G. B. Carpenter, *Acta Crystallogr.* **1955**, *8*, 646–651.
- [17] S. H. Jathar, C. Heppding, F. M. Link, D. K. Farmer, A. Akherati, M. J. Kleemann, J. A. de Gouw, R. P. Veres, J. M. Roberts, *Chem. Phys.* **2017**, *17*, 8959–8970.
- [18] J. Evers, M. Göbel, B. Krumm, F. Martin, S. Medvedev, G. Oehlinger, F. X. Steemann, I. Troyan, T. M. Klapötke, M. I. Eremets, *J. Am. Chem. Soc.* **2011**, *133*, 12100–12105.
- [19] P. Blaha, K. Schwarz, G. Madsen, D. Kvasnicka, J. Luitz, WIEN2k *An Augmented PlaneWave Plus Local Orbitals Program for Calculating Crystal Properties*, Vienna, Austria.
- [20] G. M. Sheldrick, SHELXL-2014, *Program for Crystal Structure Refinement*, University of Göttingen: Göttingen, Germany, **2014**.
- [21] J. P. Perdew, K. Burke, M. Ernzerhof, *Phys. Rev. Lett.* **1996**, *77*, 3865–3868.
- [22] S. Grimme, J. Antony, S. Ehrlich, H. A. Krieg, *J. Chem. Phys.* **2010**, *132*, 154104-1–154104-19.
- [23] A. Simon, K. Peters, *Acta Crystallogr.* **1980**, *B36*, 2750–2751.
- [24] J. Neubüser, H. Wondratschek, *Krist. Tech.* **1966**, *1*, 529–543.
- [25] H. Bärnighausen, *MATCH, Communications in Mathematical Chemistry*, **1980**, *9*, 139.
- [26] A. Meyer, *Symmetriebeziehungen zwischen Kristallstrukturen des Formeltyps AX, ABX und ABX*. Dissertation, Universität Karlsruhe, **1981**, Vol. I, p 99, and Vol. II, p 76 and 99.

- [27] H. Wondratschek, U. Müller, Symmetry Relations Between Space Groups. *International Tables For Crystallography*, 2nd ed.; Eds.; Wiley: Chichester, U.K., **2010**; Vol. A1.
- [28] U. Müller, *Inorganic Structural Chemistry*; Wiley: Chichester, U.K., **2007**.
- [29] U. Müller, *Symmetry Relationships between Crystal Structures*; Oxford University Press: Oxford, U.K., **2013**.
- [30] U. Müller, *Relaciones de simetria entre estructuras cristalinas*; Sintesis: Madrid, Spain, **2013**.
- [31] U. Müller, *Symmetriebeziehungen zwischen verwandten Kristallstrukturen*; Studienbücher Chemie, Vieweg + Teubner Verlag: Wiesbaden, **2011**; pp 206 and 328.
- [32] L. V. Azároff, *Elements of X-Ray Crystallography*; McGraw-Hill Book Company: New York, **1968**; pp 130, 166 and 294.
- [33] K. Brandenburg, *Visual Crystal Structure Information System, Diamond2*; Crystal Impact GbR: Bonn, **1999**.
- [34] P. Blaha, DFT calculation with WIEN2k for HNCO, unpublished results: *Pnma*, $a = 10.82 \text{ \AA}$, $b = 5.23 \text{ \AA}$, $c = 3.57 \text{ \AA}$, N (0.4301, 1/4, 0.4041), C (0.3259, 1/4, 0.281), O (0.2192, 1/4, 0.2103), H (0.5128, 1/4, 0.2700).
- [35] K. Christe, W. W. Wilson, D. A. Dixon, S. I. Khan, R. Bau, T. Metzenhin, R. Lu, *J. Am. Chem. Soc.* **1993**, *115*, 1836–1842.
- [36] Haynes, D. R. Lide, *CRC Handbook of Chemistry and Physics, A Ready Reference Book of Chemical and Physical Data*, 92nd ed; HEds.; CRC Press, Boca Raton, FL, **2011**; pp 5–92 and 5–94.
- [37] N. Wiberg, *Holleman-Wiberg, Lehrbuch der Anorganischen Chemie*; Walter de Gruyter: Berlin, **2007**; pp 2002–2004.
- [38] H. Beyer, *Lehrbuch der Organischen Chemie*; S. Hirzel Verlag: Leipzig, **1967**; pp 112. The boiling temperature of Et₂O is 34.6 °C compared to 35.7 °C for HN₃ (Table 7.5).

IV Appendix

Bibliography

Peer-reviewed Publications

Thomas M. Klapötke, Burkhard Krumm, Thomas Reith and Cornelia C. Unger
Synthetic Routes to a Triazole and Tetrazole with Trinitroalkyl Substitution at Nitrogen
J. Org. Chem., *in press*.

Thomas M. Klapötke, Burkhard Krumm, and Thomas Reith
Dihydrazinium Nitrates Derived from Malonic and Iminodiacetic Acid
Propellants, Explos., Pyrotech. **2018**, *43*, 685–693.

Jürgen Evers, Burkhard Krumm, Quirin J. Axthammer, Jörn Martens, Peter Blaha, Franz Xaver Steemann, Thomas Reith, Peter Mayer, and Thomas M. Klapötke
Molecular Structure of Isocyanic Acid HNCO, the Imide of Carbon Dioxide
J. Phys. Chem. A **2018**, *122*, 3287–3292.

Thomas M. Klapötke, Burkhard Krumm, and Thomas Reith
Polynitrocaramates Derived from Nitromethane
Z. Anorg. Allg. Chem. **2017**, *643*, 1474–1481.

Thomas M. Klapötke, Burkhard Krumm, and Thomas Reith
Polyfunctional Energetic Nitrates Derived from Tris(hydroxymethyl)aminomethane (Tris)
Eur. J. Org. Chem. **2017**, 3666–3673.

Quirin J. Axthammer, Thomas M. Klapötke, Burkhard Krumm, and Thomas Reith
Energetic Sila-Nitrocaramates: Silicon Analogues of Neo-Pentane Derivatives
Inorg. Chem. **2016**, *55*, 4683–4692.

Conference Posters

Thomas M. Klapötke, Burkhard Krumm, and Thomas Reith

“Energetic Nitrate Esters based on Tris(hydroxymethyl)aminomethane (TRIS)”

20th New Trends in Research of Energetic Materials, Proceedings of the Seminar, Pardubice, Czech Republic, **2017**, 950–959.

Quirin J. Axthammer, Thomas M. Klapötke, Burkhard Krumm, and Thomas Reith

“Synthesis and Properties of a Silicon Containing Nitrocarbamate Based on Pentaerythritol”

21th New Trends in Research of Energetic Materials, Proceedings of the Seminar, Pardubice, Czech Republic, **2016**, 861–868.

Conference Talks

Thomas M. Klapötke, Burkhard Krumm, Cornelia C. Unger and Thomas Reith

“Recent Developments on the Research of Energetic Materials: Nitrates, Nitrocarbamates and Polynitro Compounds”

New Energetics Workshop (NEW), Stockholm, Schweden, **2018**.

Thomas M. Klapötke, Burkhard Krumm, and Thomas Reith

“Dinitrates of Malonyl and Nitraminodiacetyl Hydrazides”

21th New Trends in Research of Energetic Materials, Proceedings of the Seminar, Pardubice, Czech Republic, **2018**.

